Declassified in Part - Sanitized Copy Approved for Release @ 50-Yr 2014/06/09 : CIA-RDP81-01043R003000180001-4

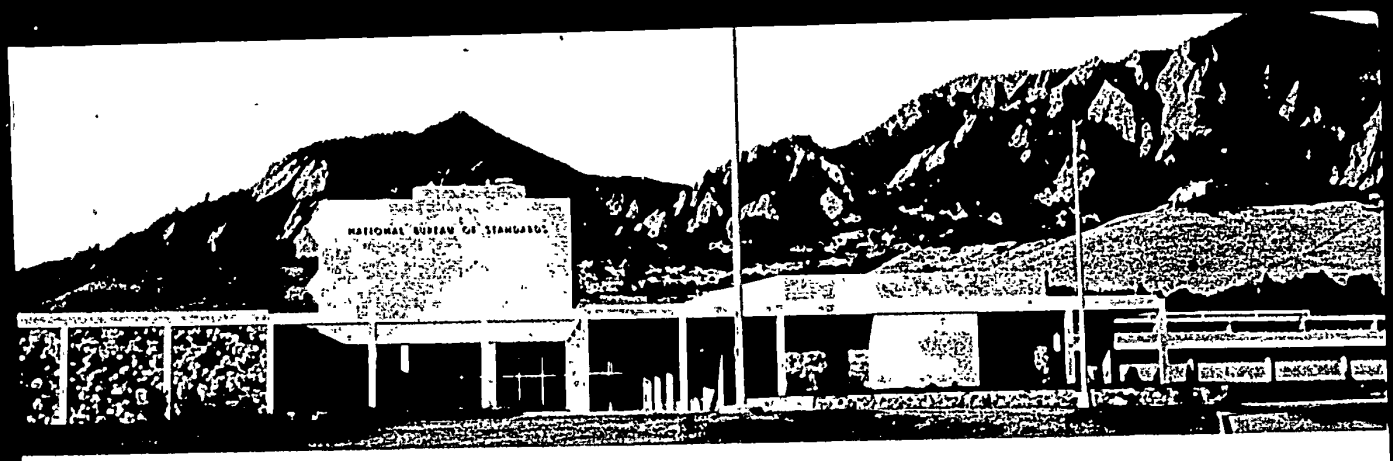

NBS REPORT

6014

THIRD REPORT

ON

REGULAR VHF IONOSPHERIC PROPAGATION OBSERVABLE OVER LONG DISTANCES

Edited
by

R. C. Kirby
R. M. Davis, Jr.

STAT

FINAL REPORT ON SIGNAL CORPS INTERDEPARTMENTAL PROCUREMENTS
No. 821-PHIBP-51-04, R54-73-SC-91 and R56-0002-SC-91

Covering work carried out from
March 1951 to June 1958

NBS

U. S. DEPARTMENT OF COMMERCE
NATIONAL BUREAU OF STANDARDS
BOULDER LABORATORIES
Boulder, Colorado

STAT

Declassified in Part - Sanitized Copy Approved for Release @ 50-Yr 2014/06/09 : CIA-RDP81-01043R003000180001-4

Declassified in Part - Sanitized Copy Approved for Release @ 50-Yr 2014/06/09 : CIA-RDP81-01043R003000180001-4

THE NATIONAL BUREAU OF STANDARDS

Functions and Activities

The functions of the National Bureau of Standards are set forth in the Act of Congress, March 3, 1901, as amended by Congress in Public Law 619, 1950. These include the development and maintenance of the national standards of measurement and the provision of means and methods for making measurements consistent with these standards: the determination of physical constants and properties of materials; the development of methods and instruments for testing materials, devices, and structures; advisory services to Government Agencies on scientific and technical problems; invention and development of devices to serve special needs of the Government; and the development of standard practices, codes and specifications. The work includes basic and applied research, development, engineering, instrumentation, testing, evaluation, calibration services, and various consultation and information services. A major portion of the Bureau's work is performed for other Government Agencies, particularly the Department of Defense and the Atomic Energy Commission. The scope of activities is suggested by the listing of divisions and sections on the inside back cover.

Reports and Publications

The results of the Bureau's work take the form of either actual equipment and devices or published papers and reports. Reports are issued to the sponsoring agency of a particular project or program. Published papers appear either in the Bureau's own series of publications or in the journals of professional and scientific societies. The Bureau itself publishes three monthly periodicals, available from the Government Printing Office: The Journal of Research, which presents complete papers reporting technical investigations; the Technical News Bulletin, which presents summary and preliminary reports on work in progress; and Basic Radio Propagation Predictions, which provides data for determining the best frequencies to use for radio communications throughout the world. There are also five series of nonperiodical publications: The Applied Mathematics Series, Circulars, Handbooks, Building Materials and Structures Reports, and Miscellaneous Publications.

Declassified in Part - Sanitized Copy Approved for Release @ 50-Yr 2014/06/09 : CIA-RDP81-01043R003000180001-4

Declassified in Part - Sanitized Copy Approved for Release @ 50-Yr 2014/06/09 : CIA-RDP81-01043R003000180001-4

NATIONAL BUREAU OF STANDARDS REPORT

NBS PROJECT 8200-10-8725 September 26, 1958 **NBS REPORT** 6014

THIRD REPORT

ON

REGULAR VHF IONOSPHERIC PROPAGATION OBSERVABLE OVER LONG DISTANCES

Edited
by

R. C. Kirby
R. M. Davis, Jr.

FINAL REPORT ON SIGNAL CORPS INTERDEPARTMENTAL PROCUREMENTS
No. 821-PHIBP-51-04, R54-73-SC-91 and R56-0002-SC-91

Covering work carried out from
March 1951 to June 1958

U. S. DEPARTMENT OF COMMERCE
NATIONAL BUREAU OF STANDARDS
BOULDER LABORATORIES
Boulder, Colorado

Declassified in Part - Sanitized Copy Approved for Release @ 50-Yr 2014/06/09 : CIA-RDP81-01043R003000180001-4

Declassified in Part - Sanitized Copy Approved for Release @ 50-Yr 2014/06/09 : CIA-RDP81-01043R003000180001-4

IMPORTANT NOTICE

NATIONAL BUREAU OF STANDARDS REPORTS are usually preliminary or progress accounting documents intended for use within the Government. Before material in the reports is formally published it is subjected to additional evaluation and review. For this reason, the publication, reprinting, reproduction, or open-literature listing of this Report, either in whole or in part, is not authorized unless permission is obtained in writing from the Office of the Director, National Bureau of Standards, Washington 25, D. C. Such permission is not needed, however, by the Government agency for which the Report has been specifically prepared if that agency wishes to reproduce additional copies for its own use.

Declassified in Part - Sanitized Copy Approved for Release @ 50-Yr 2014/06/09 : CIA-RDP81-01043R003000180001-4

Declassified in Part - Sanitized Copy Approved for Release @ 50-Yr 2014/06/09 : CIA-RDP81-01043R003000180001-4

UNITED STATES ARMY SIGNAL RESEARCH AND DEVELOPMENT LABORATORY

CONTRACT NOS R54-73-SC-91
R56-0002-SC-91

DISTRIBUTION LIST

THIRD AND FINAL REPORT

CHIEF OF RESEARCH & DEVELOPMENT
OCS, DEPARTMENT OF THE ARMY
WASHINGTON 25, D.C. 1

CHIEF SIGNAL OFFICER
DEPARTMENT OF THE ARMY
WASHINGTON 25, D.C.
ATTN: SIGRD 1
SIGRD-6-f 1

DIRECTOR
US NAVAL RESEARCH LABORATORY
WASHINGTON 25, D.C.
ATTN: CODE 2027 1
3407 1

COMMANDING OFFICER & DIRECTOR
US NAVY ELECTRONICS LAB
SAN DIEGO 52, CALIFORNIA
ATTN: LIBRARY 1

COMMANDER
WRIGHT AIR DEVELOPMENT CTR
WRIGHT PATTERSON AFB, OHIO
ATTN: WCOSI-3 2
DR. PAUL L. TAYLOR 1

COMMANDER
AIR FORCE CAMBRIDGE RES CTR
L.G. HANSCOM FIELD
BEDFORD, MASSACHUSETTS
ATTN: CROTLR-2 1

COMMANDER
ROME AIR DEVELOPMENT CENTER
GRIFFISS AFB, NEW YORK
ATTN: RCSSLD 1
MR. L. COLIN 1

DIRECTOR OF COMMUNICATIONS
HQS, USAF
WASHINGTON 25, D.C.
ATTN: AFOAC 1

COMMANDER
USAF SECURITY SERVICE
SAN ANTONIO, TEXAS
ATTN: S-DC 1

CHIEF BUREAU OF SHIPS
CODE 835
DEPARTMENT OF THE NAVY
WASHINGTON 25, D.C.
ATTN: MR. R.S. BALDWIN 1

COMMANDER
ARMED SERV TECH INFO AGCY
ARLINGTON HALL STATION
ARLINGTON 12, VIRGINIA 10

COMMANDING GENERAL
US ARMY ELECTRONIC PROV GR
FORT HUACHUCA, ARIZONA
ATTN: SIGPG-SCGP-1 3

COMMANDING OFFICER
US ARMY SIG EQUIP SPT AGCY
FORT MONMOUTH, NEW JERSEY
ATTN: SIGFM/ES-ASA 1

US NAVY LIAISON OFFICER
DEPARTMENT OF THE NAVY
USASRDL
FORT MONMOUTH, NEW JERSEY 1

COMMANDING OFFICER
AIR R&D COMMAND, USASRDL
FORT MONMOUTH, NEW JERSEY 1

COMMANDING OFFICER
US MARINE CORPS LIAISON OFF
CODE AO-4C USASRDL
FORT MONMOUTH, NEW JERSEY 1

CHIEF SIGNAL OFFICER
COMBAT DEV & OP DIVISION
DEPARTMENT OF THE ARMY
WASHINGTON 25, D.C.
ATTN: SIGCO 1

CHIEF SIGNAL OFFICER
PLANS & PROGRAMS DIV
DEPARTMENT OF THE ARMY
WASHINGTON 25, D.C.
ATTN: SIGPL 1

COMMANDER
AIR R&D COMMAND
PO BOX 1395
BALTIMORE, MARYLAND
ATTN: MAJOR A.L. BAKER 2

DEPUTY CHIEF OF STAFF,
INTELLIGENCE
HQS, TACTICAL AIR COMM
LANGLEY AFB, VIRGINIA 2

DIRECTOR, NAVAL ORDNANCE LAB
WHITE OAK
SILVER SPRINGS, MARYLAND
ATTN: LIBRARIAN RM1-327 1

CHIEF SIGNAL OFFICER
ARMY COMM SERV DIVISION
DEPARTMENT OF THE ARMY
WASHINGTON 25, D.C. 2

COMMANDING OFFICER
ARMY SIG COMM ENGRG AGCY
DEPARTMENT OF THE ARMY
WASHINGTON 25, D.C.
ATTN: MR. J.N.CRAVER 1

COMMANDING OFFICER
HQS, ALASKAN AIR COMMAND
DEPT OF COMM & ELECTRONICS
APO 942, c/o POSTMASTER
SEATTLE, WASHINGTON 1

COMMANDING OFFICER
ALASKA COMM SYSTEM
550 FEDERAL OFFICE BLDG
SEATTLE 4, WASHINGTON 1

PRESIDENT, BOARD #5
CONTINENTAL ARMY COMMAND
FORT BRAGG, NO. CAROLINA 1

SIG C LIAISON OFFICER
MIT, LINCOLN LAB, PO BOX 73
LEXINGTON, MASSACHUSETTS 1
ATTN: MR. W.G. ABEL, LIBRARIAN

DIRECTOR COMM-ELECTRONICS
JOINT CHIEF OF STAFF
WASHINGTON 25, D.C. 1

COMMANDER
AIR FORCE MISSILE TEST CTR
PATRICK AFB, FLORIDA
ATTN: TECH LIBRARY 1

DIRECTOR
ARMANENT LABORATORY
WRIGHT PATTERSON AFB, OHIO
ATTN: MCREZGD 1

COMMANDING GENERAL
NORTHEAST AIR COMMAND
PEPPERREL AFB, APO 862
c/o POSTMASTER, NEW YORK N.Y. 1

US NAVAL INSPECTOR OF ORDNANCE
APPLIED PHYSICS LABORATORY
JOHN HOPKINS UNIVERSITY
SILVER SPRINGS, MARYLAND 2

Declassified in Part - Sanitized Copy Approved for Release @ 50-Yr 2014/06/09 : CIA-RDP81-01043R003000180001-4

Declassified in Part - Sanitized Copy Approved for Release @ 50-Yr 2014/06/09 : CIA-RDP81-01043R003000180001-4

UNITED STATES ARMY SIGNAL RESEARCH AND DEVELOPMENT LABORATORY
CONTRACT NOS R54-73-SC-91 and R56-0002-SC-91
DISTRIBUTION LIST
THIRD AND FINAL REPORT (Cont'd)

ELECTRONICS RESEARCH LAB
STANFORD UNIVERSITY
STANFORD, CALIFORNIA
ATTN: ASSOCIATE DIRECTOR 1

DIRECTOR, OFFICE OF NAVAL RES
DEPARTMENT OF THE NAVY
1000 GEARY STREET
SAN FRANCISCO, CALIFORNIA 1

DIRECTOR, CENTRAL INTELLIGENCE AGENCY
2430 E STREET N.W.
WASHINGTON, D.C. 1

DIRECTOR, NATIONAL SECURITY AGCY
WASHINGTON 25, D.C. 1

ASSISTANT SECRETARY OF DEFENSE
R&D INFORMATION DIVISION
LIBRARY BR, PENTAGON 3D-1041
WASHINGTON 25, D.C. 1

FEDERAL COMM COMMISSION
WASHINGTON 25, D.C.
ATTN: CH, ENGRG TECH RES DIV 1

DIRECTOR REFERENCE DEPARTMENT
TECH INFO DIV, LIBRARY OF CONGRESS
WASHINGTON 25, D.C. 3

CORNELL UNIVERSITY
SCHOOL OF ELECTRICAL ENGRG
ITHACA, NEW YORK
ATTN: DR. H.G. BOOKER 1

USCONARC LIAISON OFFICER
USASRDL
FORT MONMOUTH, NEW JERSEY 1

UNIVERSITY OF ALASKA
COLLEGE, ALASKA
ATTN: DR. C.T. ELVERY, DIR 1

DEPARTMENT OF STATE
WASHINGTON 25, D.C.
ATTN: MR. F.C. deWOLFE
CH, TELECOMM DIV 1

DIRECTOR US INFO AGENCY
VOICE OF AMERICA
330 INDEPENDENCE AVE S.W.
WASHINGTON 25, D.C.
ATTN: MR. GEORGE JACOBS 1

SIG C LIAISON OFFICER
OPERATIONS RESEARCH OFFICE
JOHN HOPKINS UNIVERSITY
SILVER SPRINGS, MARYLAND 1

COMMANDING OFFICER
USA SIG C RADIO PROP AGCY
DEPARTMENT OF THE ARMY
FORT MONMOUTH, NEW JERSEY 2

COMMANDING OFFICER
US ARMY SIGNAL R&D LABORATORY
FORT MONMOUTH, NEW JERSEY
ATTN:
DIRECTOR OF RESEARCH 1
TECH DOC CENTER, EVANS 1
TECH INFO DIV 5
EXPLOR DIV, FILE UNIT 6
BLDG 37a EVANS 1
DIR, EXPLOR RES DIV "S" 5
DIR, COMM DEPT ATTN MR BROWN 1
EXPLOR RES DIV "C" 1
DIR COMM DEPT 1
DIR, COUNTERMEASURES DIV 1
DIR, RADAR DIV 1
ATTN: MR. WOODYARD
DIR, APP PHYS DIV 1
TECH DOC CTR, HEX 9

This contract is supervised by Exloratory Research "S" Division, Surveillance Department, US Army Signal Research and Development Laboratory, Fort Monmouth, New Jersey. For further information contact Mr. Arthur Harris, Project Engineer. Telephone: LIberty 2-4000, Extension 61344.

Declassified in Part - Sanitized Copy Approved for Release @ 50-Yr 2014/06/09 : CIA-RDP81-01043R003000180001-4

Declassified in Part - Sanitized Copy Approved for Release @ 50-Yr 2014/06/09 : CIA-RDP81-01043R003000180001-4

CONTENTS

	PAGE
FOREWORD	vii
1. Introduction - Scope of Report	1
2. The Program	1
2.1 Variations with Season, Geographical Position and Solar Activity	1
2.2 Frequency Dependence	3
2.3 Scattering Heights, Dependence of Transmission Loss on Path Geometry	3
2.4 Sporadic-E Observation	3
2.5 Development of Low-Power Narrow Band Recording Equipment	3
3. Results in Detail	4
3.1 Routine Recording Program	4
3.11 Cedar Rapids to Sterling Test Path - 49.8 Mc/s	4
3.12 Fargo to Churchill Test Path - 49.7 Mc/s	5
3.13 Anchorage to Barrow Test Path - 48.87 Mc/s	5
3.14 Routine Recording at Other Frequencies	5
a. Anchorage to Barrow - 24.325 Mc/s	5
b. Cedar Rapids to Sterling - 27.775 Mc/s	5
c. Cedar Rapids to Sterling - 107.8 Mc/s	6
3.15 Seasonal Variation of Signal Intensity	6
3.16 Annual Variation of Signal Intensity; Correlation with Geomagnetic Observations and Ionospheric Conditions Observed at High Frequencies	6
3.17 Sporadic-E Propagation	7
3.2 Experimental and Developmental Phases of the Program	7
3.21 Frequency Dependence	7
3.22 Scattering Heights, Dependence of Transmission Loss on Path Geometry	8
3.23 Signal Fading Characteristics	9
3.24 Doppler-Shifted Meteor Echoes	9
3.25 Development of Low-Power Narrow Band Recording Equipment for Routine Observations	10
4. Discussion and Conclusions	10
4.1 General	10

Declassified in Part - Sanitized Copy Approved for Release @ 50-Yr 2014/06/09 : CIA-RDP81-01043R003000180001-4

Declassified in Part - Sanitized Copy Approved for Release @ 50-Yr 2014/06/09 : CIA-RDP81-01043R003000180001-4

		PAGE
4.2	New Results	11
	a. Scattering Heights	11
	b. Solar Cycle Dependence	11
	c. Useful Range of Frequencies	12
	d. Meteoric Contribution	13
	e. Sporadic-E Propagation	13
4.3	Outstanding Problems	13
	a. Frequency Dependence	14
	b. Optimum Antenna Design, Including Beam Slewing	14
	c. Modulation Studies	15
	d. Geographical Dependence	16
ACKNOWLEDGEMENTS		17
REFERENCES		18

FIGURES 1 through 40 . . . .

APPENDICES

I.	Part I	Experimental Study of Frequency Dependence -- R. C. Kirby and R. M. Davis, Jr.
	Part II	Determination of Frequency Dependence Exponent by True Power Measurement -- G. E. Boggs and N. C. Hekimian
II.	Part I	Experimental Investigations of Ionospheric Forward Scattering at VHF using Pulse Techniques -- V. C. Pineo
	Part II	Summer Heights of VHF Scattering -- V. C. Pineo
	Part III	Scattering Angle Dependence Tests -- V. C. Pineo
III.	Part I	Correlation of VHF Signal Intensities with Magnetic K-Indices -- H. I. Leighton
	Part II	Correlation of VHF Scatter Intensities with H'F Records -- R. M. Davis, Jr.
IV.		Oblique-Incidence VHF Sporadic E Observations -- R. M. Davis, Jr.
V.		Meteor Whistles on the Cedar Rapids to Sterling Path -- E. K. Smith
VI.	Part I	Off-Path Measurements of Azimuth of Arrival of 49.8 Mc/s Signal -- V. C. Pineo
	Part II	Experimental Observations of the Contribution of Meteoric Ionization to the Propagation of VHF Radio Waves by Ionospheric Forward Scatter -- V. C. Pineo
VII.		A Narrow-Band Recording Receiver -- G. F. Montgomery
VIII.		Three Kilowatt VHF Transmitter for Radio Propagation Studies -- W. B. Harding and D. C. Whittaker
IX.		Stable Frequency Control for Narrow-Band Recording Receiver and Transmitter -- P. G. Sulzer
	Part I	One-Megacycle High Stability Oscillator
	Part II	Filter-Type Exciter

Declassified in Part - Sanitized Copy Approved for Release @ 50-Yr 2014/06/09 : CIA-RDP81-01043R003000180001-4

Declassified in Part - Sanitized Copy Approved for Release @ 50-Yr 2014/06/09 : CIA-RDP81-01043R003000180001-4

IX. Part III Phase-Locked-Oscillator Exciter

Part IV Direct Multiplier Exciter

X. Solar Cycle Influence on the Lower Ionosphere and on VHF Forward Scatter -- C. D. Ellyett and H. I. Leighton

XI. Tabulated Monthly Median and Decile Values of Hourly Median Signal Intensity Recorded in the Routine Recording Programs

XII. Summary Technical Paper, D. K. Bailey, R. Bateman and R. C. Kirby, "Radio Transmission at VHF by Scattering and other Processes in the Lower Ionosphere," reprinted (by permission) from Proc. I.R.E., 43, October 1955.

FOREWORD

This is the third and final of a series of reports in which the results of studies of regular VHF ionospheric propagation (scattering) are presented; it is prepared in fulfillment of the requirement for a final report on a program of work covered by Signal Corps Interdepartmental Procurement Numbers 821-PHIBP-51-04, R54-73-SC-91, R56-0002-SC-91, and associated amendments, representing financial support from the Departments of the Army, Air Force and Navy.

The principal additional data obtained from the routine recording program during the period September, 1952, to December, 1955 are contained herein, together with results of the experimental and developmental phases of the program before their termination in February, 1956, under the support of the subject MIPR's; work carried out after that time under the MIPR's was in connection with analysis and reporting of data. (Beginning in July, 1954, the National Bureau of Standards had begun direct support of a continuing basic research program on VHF ionospheric scattering, which continues to the present time.)

A summary of most of the important results of the program was published as a technical paper in the October, 1955, "Scatter Propagation" issue of the Proceedings of the I.R.E.; to avoid the necessity for repetition or paraphrasing much of the material contained in that paper, it has been referred to frequently throughout, and reprints have been included as Appendix XII in a limited number of copies of this report. The scope of the present report, therefore, is largely to supplement that summary paper with detailed technical data which was not included, as well as to report on the results obtained in limited experimental work subsequently.

As indicated in previous reports, emphasis throughout the program was toward obtaining information directly useful for assessing communication possibilities of the propagation mechanism. It is believed that the data presented in this and the preceding reports are sufficient, from the propagation point of view, to provide a basis for system engineering in temperate and high latitudes. Although the principal phenomena associated with ionospheric scatter propagation are now well-known, many questions still remain unanswered, and the nature of some of these is suggested in the text.

Consistent with downgrading of the classification of the earlier two reports of the series, by authority of letter from U. S. Army Signal Supply Agency, February 3, 1958, signed by the Contracting Officer, and approvals for publication in technical journals of summaries of material contained herein, the security classification of this report is UNCLASSIFIED.

Declassified in Part - Sanitized Copy Approved for Release @ 50-Yr 2014/06/09 : CIA-RDP81-01043R003000180001-4

Declassified in Part - Sanitized Copy Approved for Release @ 50-Yr 2014/06/09 : CIA-RDP81-01043R003000180001-4

THIRD REPORT
ON
REGULAR VHF IONOSPHERIC PROPAGATION
OBSERVABLE OVER LONG DISTANCES

Edited
by

R. C. Kirby
R. M. Davis, Jr.

1. Introduction - Scope of Report

The purpose of this report is to provide a formal final report in connection with the financial support of the work extended by the various military departments.*

A summary of most of the important results of the program through July, 1955, has already been published as a technical paper[1] and is referred to frequently throughout this report. Two earlier NBS Reports[2,3] gave detailed data obtained from the program through September, 1952.

The present report contains the principal additional detailed data obtained from the routine recording program during the period September, 1952, to December, 1955, as well as further results of the experimental and developmental phases of the program before their termination in February, 1956. The latter are reported in the various appendices.

2. The Program

Emphasis throughout the program was on obtaining information applicable to the design of communication systems; it was also intended to obtain the kind of results necessary for an understanding and development of the theory of the physical conditions and processes giving rise to the observed propagation. The program may be described under the following headings:

2.1 Variations with Season, Geographical Position and Solar Activity

Table 1 should be studied in connection with the program in general and this aspect in particular. Work under this topic required the regular operation of three experimental paths at just below 50 Mc/s: Cedar Rapids to Sterling at 49.8 Mc/s, Fargo to Churchill at 49.7 Mc/s, and Anchorage to Barrow at 48.87 Mc/s. The frequency and transmitter power were substantially the same for these three paths. The antenna systems were all long rhombic antennas (25 wavelengths on each leg), of the same nominal design. Probable effects of departures from ideal siting, and

*See foreword.

Declassified in Part - Sanitized Copy Approved for Release @ 50-Yr 2014/06/09 : CIA-RDP81-01043R003000180001-4

Declassified in Part - Sanitized Copy Approved for Release @ 50-Yr 2014/06/09 : CIA-RDP81-01043R003000180001-4

TABLE 1

Details of Experimental Paths Comprising Routine Recording Program

	Cedar Rapids-Sterling			Anchorage-Barrow			Fargo-Churchill
Frequency, Mc/s	49.800[1]	107.800	27.775	48.870	48.870	24.325	49.700
Date of commencement	January 23, 1951	December 4, 1951	May 6, 1953	August 28, 1951	March 2, 1953	February 16, 1953	August 29, 1951
Date of termination	June 30, 1958	January 31, 1953	February 29, 1956	June 30, 1953	June 30, 1953	June 30, 1953	March 31, 1953
Transmitter location coordinates of site	Cedar Rapids, Iowa 41°52'N; 91°41'W	Same	Same	Anchorage, Alaska 61°17'N; 149°42'W	Same	Same	Fargo, North Dakota 46°55'N; 96°46'W
Receiver location coordinates of site	Sterling, Virginia 38°59'N; 77°29'W	Same	Same	Barrow, Alaska 71°18'N; 156°45'W	Same	Same	Churchill Manitoba 58°44'N; 94°05'W
Surface path length (great circle)	1,243 km. 773 st. mi.	Same	Same	1,156 km. 718 st. mi.	Same	Same	1,326 km. 824 st. mi.
Geographic coordinates of path midpoint	40°39'N; 84°26'W	Same	Same	66°20'N; 152°31'W	Same	Same	52°50'N; 95°36'W
Geomagnetic latitude of path midpoint	51°38'N	Same	Same	65°02'N	Same	Same	62°42'N
True azimuth of transmitter from receiver	289°30'	Same	Same	160°55'	Same	Same	188°56'
True azimuth of receiver from transmitter	100°17'	Same	Same	347°24'	Same	Same	6°47'
Type of antennas	Rhombic-Rhombic	Same	Same	Same	Yagi-Yagi	Same	Rhombic-Rhombic
Elevation of maximum of main lobe, degrees	7.0	Same	Same	5.7[2]	6.4[2]	6.4[2]	5.4
Height, feet	41	19	73	50	45	90	52
Leg length, feet	500	230	897	500	--	--	500
Estimated plane-wave gain, relative to dipole at same height, decibels	18	18	18	18	9	9	18
Horizontal beamwidth, degrees	6	6	6	60	60	60	6
1.0 microvolt received[3] signal intensity on graphs for 30 Kw antenna power, represents							
Attenuation relative to inverse distance (perfect reflection in ionosphere) db	122	115	127	123	105	111	122
Transmission loss, db	199	199	199	199	199	199	199

[1] 49.600 Mc/s used from January 17, 1952 through March 31, 1952.

[2] Includes effect of sloping site at Anchorage.

[3] Received open-circuit antenna voltage measured at 600 ohms impedance (-154 dbw). Reference power to transmitting antenna is 30 Kw.

the somewhat lower heights of the antennas used on the original installations at Cedar Rapids and Sterling, are discussed.

2.2 Frequency Dependence

This part of the program involved operation of the Cedar Rapids to Sterling test path at 107.8 Mc/s to January 31, 1953, followed by operation at 27.775 Mc/s to February 29, 1956. From March through June, 1953, variation of signal intensity with frequency was also investigated for the arctic path from Anchorage to Barrow by provision of test transmissions at 24.325 Mc/s.

2.3 Scattering Heights, Dependence of Transmission Loss on Path Geometry

Heights of scattering from the lower ionosphere were deduced initially from one-way measurements of the relative transit times of the tropospheric component and the ionospheric component of a pulse signal at 49.7 Mc/s. The observed scattering heights were compared with simultaneous observations of virtual heights of low frequency reflections near the midpoint of the path.

For path lengths up to about 1,000 Km the scattering angle is fairly large ($> 20^{\circ}$) and depends on path length. The extent to which the transmission loss depends upon this angle was investigated. Round-trip pulse delay measurements were made finally to obtain heights of ionospheric and tropospheric scattering.

To obtain information about the possibilities of off-path interference in VHF propagation, the signal intensities of the Cedar Rapids transmissions at 49.8 Mc/s beamed toward Sterling were received at off-path receiving sites and compared with the signal intensities observed simultaneously at Sterling. Off-path observations were also made to investigate experimentally the contribution of meteoric ionization to the observed propagation.

2.4 Sporadic-E Observation

During the early phases of the program occurrences of sporadic-E propagation at 50 Mc/s were observed and reported. The program was expanded to include regular observation and analysis of the occurrence of sporadic-E on all the paths and at all the frequencies used.

2.5 Development of Low-Power Narrow Band Recording Equipment

In order to reduce the power requirement for routine observations of transmission loss, development of a narrow band recording receiver was undertaken along with the necessary stable frequency control for a recording receiver and transmitter; a 3 kilowatt VHF transmitter was developed for unattended operation.

Declassified in Part - Sanitized Copy Approved for Release @ 50-Yr 2014/06/09 : CIA-RDP81-01043R003000180001-4

Declassified in Part - Sanitized Copy Approved for Release @ 50-Yr 2014/06/09 : CIA-RDP81-01043R003000180001-4

3. Results in Detail

3.1 Routine Recording Program

Table 1 supplies many details of the various test paths, and frequent reference to it will be found useful in connection with the following results. Appendix XX of the second report[3] gave details of the measurements and methods for reporting the data from the field stations, and indicates how and why various corrections were made. Appendix VIII of the first report[2] described the complete recording setup, and Appendix XV of the second report[3] described a new type of gain-stable converter which was developed and placed in service. The newly developed narrow band recording systems were not used for the routine recording program during the period covered by this report.

Throughout the present report, except where otherwise indicated, signal-intensity data are given in decibels above one microvolt received open-circuit antenna voltage for 600 ohms terminal impedance. Corrections have been made for any transmission line losses, and all hourly values have been normalized to the estimated antenna power shown. Available power at the receiving antenna is $E^2/4R$, so that one microvolt (zero decibel level) corresponds to an available power of -154 dbw. For the data given in Figures 1 to 40 in the main text and the tables in Appendix XI, the reference antenna power is 30 kilowatts; the reference power is specified in the various appendices where it may differ from the standard reference power. One microvolt (zero decibels) corresponds to a transmission loss of 199 decibels, or to the values of attenuation relative to inverse distance (perfect reflection in the ionosphere) given in Table 1; these values depend on path length.

The signal-intensity results are given in plots and tables showing for each hourly period the signal levels equalled or exceeded 10%, 50% (the monthly median), and 90% of the days for each month. These may be regarded as final results. The previous report[3] gave corresponding data for the period September, 1951, through September, 1952.

The frequency and path length were substantially the same for the Cedar Rapids-Sterling, Fargo-Churchill and Anchorage-Barrow paths; the differences observed in diurnal and seasonal variation of transmission loss therefore represent mainly geographical dependence. There are probably residual differences of up to 6 db which are attributable to departures from ideal siting; furthermore, the Cedar Rapids-Sterling antennas were designed to aim the first lobe at 110 Km in the initial existence test, and their heights remained unchanged throughout the program. The antennas for the other two paths were designed to aim the main lobes at the 85 Km scattering height.

3.11 Cedar Rapids to Sterling Test Path - 49.8 Mc/s

Forty months of data are presented covering completely the period from September, 1952, through December, 1955, in Figures 1-10 and in the tables of Appendix XI.

The cumulative distribution of hourly median values of signal intensity, by season, are given in Figures 23 through 27. Because of their direct usefulness in evaluating communication performance, these distributions have also been expressed in terms of transmission loss and loss relative to inverse distance transmission (that is, relative to perfect reflection in the ionosphere). Such a distribution for a complete year of data has been published as Figure 10 of Reference 1.

3.12 Fargo to Churchill Test Path - 49.7 Mc/s

Seven months of data, for September, 1952, through March, 1953, are given in Figures 11 and 12 and in the tables of Appendix XI.

Cumulative distributions of the hourly values of signal intensity, by season, for the complete observing period on the Fargo-Churchill path, September, 1951 through March, 1953, are given in Figures 30 and 31.

3.13 Anchorage to Barrow Test Path - 48.87 Mc/s

Ten months of data, September, 1952, through June, 1953, are presented in Figures 13 through 15 and in the tables of Appendix XI. Cumulative distributions of the hourly median values of signal intensity, by season, are given in Figures 28 and 29 for the complete observing period on this path, September, 1951, through June, 1953.

3.14 Routine Recording at Other Frequencies

a. Anchorage to Barrow - 24.325 Mc/s

Four months of data, March, 1953, through June, 1953, representing diurnal variation of hourly median signal intensity using Yagi transmitting and receiving antennas, are given in Figure 16 and in the tables of Appendix XI. The cumulative distributions of the hourly median values for two spring months and two summer months are given in Figure 35.

b. Cedar Rapids to Sterling - 27.775 Mc/s

A total of 18 months of data, covering the periods April, 1954, through January, 1955, and May, 1955, through December, 1955, are given in Figures 17 through 21 and in the tables of Appendix XI. Other requirements for the Cedar Rapids transmissions caused interruption of the observations from February through April, 1955. (Transmissions from May, 1953, through April, 1954, were recorded, but questions regarding transmitter power and antenna adjustment made the data unreliable.) Cumulative distributions of the hourly median values, by season, are given in Figures 33 and 34. Rhombic antennas, scaled relative to the 49.8 Mc/s antenna, were used at 27.775 Mc/s.

Declassified in Part - Sanitized Copy Approved for Release @ 50-Yr 2014/06/09 : CIA-RDP81-01043R003000180001-4

Declassified in Part - Sanitized Copy Approved for Release @ 50-Yr 2014/06/09 : CIA-RDP81-01043R003000180001-4

c. Cedar Rapids to Sterling - 107.8 Mc/s

Four additional months of data are given in Figure 22 and in tables of Appendix XI for the period October, 1952, through January, 1953. The previous report[3] gave corresponding data for the months January through September, 1952. The cumulative distribution of the hourly median values, by season, from March, 1952, through January, 1953, is given in Figure 32.

3.15 Seasonal Variation of Signal Intensity

A discussion of the important seasonal variation of signal intensity was given in Reference 1, p. 1188. Figures 36 and 37 herein show running plots of monthly median values of signal intensities for three-hour periods centered at 00, 06, 12, and 18 hours local time at the path midpoint, as well as a running plot of the level exceeded 95% of the hours during each month. The daytime signal (noon) for the temperate latitude path from Cedar Rapids to Sterling (Figure 36) shows clear semiannual maxima during summer and winter with equinoctial minima; these are observed at all three frequencies. At 18 hours, the winter maximum is somewhat suppressed but still in evidence; the summer maximum remains distinct. The summer maximum is evident day and night.

For the arctic and subarctic paths from Anchorage to Barrow and Fargo to Churchill respectively (Figure 37) very strong summer maxima are observed. For the Fargo-Churchill path it is interesting that during the daytime, both at 12 and 18 hours, a secondary winter maximum appears nearly as strong as the summer maximum.

3.16 Annual Variation of Signal Intensity; Correlation with Geomagnetic Observations and Ionospheric Conditions Observed at High Frequencies

Figures 38 and 39 show a comparison of five years of observations of signal intensity during the months of March, June, September and December. These data should be considered in connection with the more comprehensive discussion of solar cycle dependence given in Appendix X. Appendix III summarizes the study of correlation of the observed VHF propagation with geomagnetic indices and with ionospheric propagation conditions observed at high frequencies by vertical incidence sounders.

The long-term variation of signal intensity was also observed by plotting twelve-month running means of monthly medians of received signal intensity (Figure 40) for three-hour periods centered at 00, 06, 12 and 18 hours, and of the level exceeded 95% of the hours during the month (See also Reference 4). It was interesting to observe whether the long-term variation of signal intensity was different for noon values, for example, when a dominant solar influence might be expected, as contrasted to the values observed during early morning (at 06 hours) when meteoric influence is presumed to be predominant. The variation of the noon value

was found indeed to have a greater long-term variation than the early morning values, and to correspond more closely with the twelve-month smoothed index of magnetic activity than directly with smoothed relative sunspot number. A strong long-term variation also appears at 18 hours and tends to influence the levels of the weakest signals observed, as indicated by Figure 40 (e); the weakest signals are usually observed in the early evening hours. Appendix X discusses in greater detail the physical significance of the kind of data presented in Figure 40.

3.17 Sporadic-E Propagation

Reference 1 (pp. 1200-1204) discusses the interpretation of the very strong signals observed in the records, considered to be a result of sporadic-E propagation; a brief statistical summary of the observations of sporadic E to 1954 is given in the Figures 25 and 26 of Reference 1. Appendix IV of the present report gives a detailed summary of the data from 1951 through 1955. A more comprehensive report of the sporadic-E observations on the Cedar Rapids to Sterling path, and their interpretation relative to vertical incidence ionosphere soundings, has also already been published separately.[5]

Cumulative distributions of the signal intensities due to sporadic-E propagation are presented in Reference 5 for various time intervals. Evidence is presented that the occurrence of sporadic E is associated with geomagnetic activity. During the observing period 1952 through 1954 at least twice as many hours of oblique incidence sporadic-E propagation occurred on the five magnetically quiet days per month as occurred on the five disturbed days. The preference for quiet days was weaker in 1951 and disappeared in 1955. The dependence of received power on frequency during the periods of sporadic-E propagation is strikingly different from that observed during conditions of normal scatter propagation. The ratio of signal intensities observed at 49.8 and 27.775 Mc/s during conditions of Es propagation corresponded to a median frequency exponent for received power in the neighborhood of 12, although the spread of values was very great. This is noted in Appendix I, in connection with analysis of the frequency dependence of ionospheric scattering.

3.2 Experimental and Developmental Phases of the Program

3.21 Frequency Dependence

The results of the observations of frequency dependence, using transmissions at 107.8, 49.8 and 27.775 Mc/s are discussed in Reference 1 (pp. 1196-1199). The only additional point to mention is that certain limitations of the present program prevented obtaining the data under the very desirable conditions of (a) simultaneous observations at all frequencies, (b) an adequate number of frequencies to establish the curvature of frequency dependence law if it genuinely departs from a constant exponential, (c) ideal sites at transmitter and receiver to assure uniform

Declassified in Part - Sanitized Copy Approved for Release @ 50-Yr 2014/06/09 : CIA-RDP81-01043R003000180001-4

Declassified in Part - Sanitized Copy Approved for Release @ 50-Yr 2014/06/09 : CIA-RDP81-01043R003000180001-4

and identical illumination of the scattering volume at each frequency, (d) frequency stability and receiving bandwidth appropriate for reliable observations at low values of signal-to-noise ratio, especially encountered at the higher frequencies, and to permit studies of the fading structure at each frequency.

Appendix I gives detailed data of frequency dependence not reported earlier, including the results of true power measurements in comparing the 107.8 and 49.8 Mc/s transmissions.

3.22 Scattering Heights, Dependence of Transmission Loss on Path Geometry

The results of experimental investigations of scattering at VHF using pulse techniques are reported in Appendix II. Under this topic scattering heights and dependence of transmission loss on scattering angle in the plane of the great circle path were investigated; observed scattering heights were compared with simultaneous observations of virtual heights of 460 Kc/s reflections observed near the midpoint of the path. Reference 1 summarizes the results obtained from the early measurements of heights of scattering, from one-way measurements of relative transit times of the tropospheric component and the ionospheric component (pp. 1194-1195), as well as the angle dependence results (pp. 1195-1196).

The most important additional contribution included in the present report involved the use of round-trip techniques to obtain the heights for ionospheric and tropospheric scattering. Observations were made during December, 1954, and October, 1955, at 49.8 Mc/s over a 624 Km path, in a cooperative experiment between the National Bureau of Standards and Lincoln Laboratories of the Massachusetts Institute of Technology. In this experiment it was concluded that the scattering heights were slightly higher than had been deduced from the earlier observations relative to the tropospheric component. The hourly median values of equivalent ionospheric heights based on round-trip delays were, during December (1955), 86 Km during midday (12 to 14 hours) and 90 Km at 10 and 17 hours (see Figure 10 of Appendix II). There were not enough data to calculate medians for the other hours of the day. The median value of all measured daytime delays gave an equivalent midpoint height of 87 Km. The median value of all the daytime observations during October was also 87 Km. Effective midpoint heights for tropospheric scattering as high as 29 Km were observed; the hourly median values for December varied between 20 and 28 Km, with the median of all observations equal to 24 Km. The observed effective heights in this experiment were undoubtedly influenced by the radiation patterns of the antennas which were designed to illuminate the ionospheric scattering volume at 90 Km, so that the intensity of illumination in the troposphere increased very rapidly with height. As these were substantially the conditions for the earlier one-way pulse transmission experiments in which ionospheric transmission delays were referred to the tropospheric delays, it was concluded that the effective tropospheric heights used in the earlier models had been underestimated; this would have had the effect of giving ionospheric scattering heights which were several Km below actual heights.

To obtain information about the possibilities of off-path interference, signal intensities of the Cedar Rapids transmissions at 49.8 Mc/s, beamed towards Sterling, were received at off-path receiving sites and compared with signal intensities observed simultaneously at Sterling.

An interesting and probably significant correspondence was observed between the diurnal variations of the effective midpoint ionospheric scattering height and the virtual height of reflections observed at 460 Kc/s (see Appendix II, Figure 2), even though the actual heights observed differed by a few Km.

By use of narrow beam receiving antennas at off-path receiving sites, directed at the midpoint of the Cedar Rapids to Sterling path, an experimental study was made of the contribution of aspect-sensitive meteor reflections in the total signal observed as ionospheric scattering. A summary of early results with a single off-path receiving location was reported in Reference 1. Appendix VI, Part 2, gives a complete report on this study using two off-path receiving locations; the results confirmed that there are two principal modes involved in ionospheric scatter propagation. The dominant mode during the daylight hours is apparently mainly of solar control, and is most effectively utilized by employing antennas directed along the great circle path between the transmitter and receiver. The dominant mode during the nighttime hours is attributed to meteoric ionization, and received signal intensities can be enhanced by the use of off-path transmission. It is worth emphasizing that the results given in Appendix VI are representative of wintertime conditions and an east-west path; results reported earlier in Reference 1 from a summertime experiment, using only one off-path recording station, with the same geometry, showed the off-path transmission to be dominant for fewer hours of the day. The fading of the off-path signal is more rapid than for great circle transmission; further experiments are necessary to determine whether the fading distribution is as favorable as great circle transmission, in relation to error rates in binary systems. Further experimental work is also necessary to determine the optimum azimuth for the total scatter signal, which varies with time of day and season of the year; observations of the aspect of the larger meteor bursts are not necessarily directly applicable.

3.23 Signal Fading Characteristics

Summaries of the studies of short-term fluctuations of the observed signal are given in Reference 1, pp. 1186-1188 and pp. 1207-1211, as well as in Reference 4 and a paper by Sugar.[6]

3.24 Doppler-Shifted Meteor Echoes

Observations of the rate of occurrence of Doppler components (meteor whistles) differing from the carrier frequency by at least 200 cps were made at Sterling during 1954 and 1955. As an example of the results, the

Declassified in Part - Sanitized Copy Approved for Release @ 50-Yr 2014/06/09 : CIA-RDP81-01043R003000180001-4

Declassified in Part - Sanitized Copy Approved for Release @ 50-Yr 2014/06/09 : CIA-RDP81-01043R003000180001-4

average rates for the month of April, 1955, were given in Reference 1, Figure 57. Appendix V summarizes the observations for the complete period, giving diurnal and seasonal variation of the rate of observation of meteor whistles.

3.25 Development of Low-Power Narrow Band Recording Equipment for Routine Observations

In order to reduce the power requirement for routine observations of transmission loss, development of a narrow band recording receiver was undertaken along with the necessary stable frequency control for a recording receiver and transmitter; a 3 kilowatt VHF transmitter was developed for unattended operation. Appendix VII describes the fixed-frequency narrow band receiver; direct heterodyning of the VHF signal down to 1,000 cps intermediate frequency allows simple plug-in filters to be used. The receiver image response is eliminated by a twin-mixing process with phase shifting and sensing networks. A stable frequency control for the receiver and the transmitter is described in Appendix IX; a 1 Mc/s high stability frequency standard is described, as well as additional units to derive frequencies which are not multiples of 1 Mc/s but which have the frequency stability of a 1 Mc/s reference oscillator. The three exciter units described are of the filter type, the phase-locked oscillator type, and the direct multiplier type. The last one, for applications where the operating frequency can be made a direct multiple of the crystal frequency, has proven the most satisfactory for field use, and crystals having the proper characteristics are now readily obtainable at sub-multiples of arbitrary operating frequencies.

The 3 KW transmitter, described in Appendix VIII, was designed to operate at fixed frequencies in the range 30 to 75 Mc/s, and is capable of unattended operation for long periods. Compactness compatible with ease of servicing was an important objective, since many of the transmitters would be installed in small field laboratory buildings or trailers. The prototype unit was placed in operation at Cedar Rapids in March, 1956, upon termination of the high-power transmissions furnished by the Lincoln Laboratories' contract with Collins Radio Company; the unit remained in substantially continuous service until termination of regular observations on this path June 30, 1958. Subsequently, the number of additional units have been built and operated in connection with other projects.

4. DISCUSSION AND CONCLUSIONS

4.1 General

The comprehensive summary to 1955 of the important features of transmission by VHF scattering has been published in References 1 and 4 and will not be repeated here. The physical processes and ionizing agents operating in the lower ionosphere giving rise to the observed propagation are discussed; short and long-term characteristics of the observed signals are

described as well as the results of experiments with spaced and other antenna arrangements. Dependence of the strength of the signals on path length, frequency, scattering angle, and geographical position of the transmission path are summarized. Results of the measurements of realized gain of directive antenna systems are interpreted in relation to parameters of the scattering geometry, the influence of meteoric ionization, and the existence of large-scale inhomogeneities in the ionosphere. Application of VHF propagation to communication systems operating over distances from about 1,000 to 2,300 kilometers is discussed. Design considerations are given for antenna systems, including siting, choice of polarization, and space diversity. The useful range of frequencies and certain modulation techniques are discussed, as well as multipath effects associated with the scattering process and with the presence of meteoric and auroral ionization. Reliability of performance of typical systems is estimated.

Attention is also drawn to a paper[7] reporting studies in the extreme distance range for transmission by scattering.

4.2 New Results

a. Scattering Heights

The round-trip pulse observations have indicated scattering heights of about 87 Km, a few Km higher than deduced from earlier one-way pulse observations; the lower heights, in the range 70 to 80 Km, as observed during the earlier tests, were not observed either during October or December during the round-trip tests. The reason is not entirely understood but may indicate a somewhat greater angle dependence associated with scattering from the lower heights, making transmission loss over the very short (624 Km path) too great for observability of the low-lying strata. Further observations should be carried out over paths longer than 1,000 kilometers, with a systematic program for observation of diurnal and seasonal variation of scattering heights and contributions from the various strata.

b. Solar Cycle Dependence

Noon values of signal intensity, after smoothing to remove effect of seasonal variations, exhibit a long-term variation of received power, of the order of 6 db, which tends to follow more closely the index of magnetic activity than direct smoothed relative sunspot number. Values at 18 hours show a similar though slightly smaller variation, while the nighttime values and early morning values, which presumably include the effects of meteoric ionization, show substantially less long-term variation.

As a practical matter, it was of interest to learn whether the higher transmission losses which could be expected with the use of higher frequencies in the VHF range during times of maximum solar activity to avoid

Declassified in Part - Sanitized Copy Approved for Release @ 50-Yr 2014/06/09 : CIA-RDP81-01043R003000180001-4

Declassified in Part - Sanitized Copy Approved for Release @ 50-Yr 2014/06/09 : CIA-RDP81-01043R003000180001-4

long-distance F2 propagation, might be offset to some extent by increased signal intensities due to solar dependence of the VHF scatter signal. One must conclude that the rise in signal intensity is not enough to compensate for losses involved in the use of the higher frequencies. Only 1 or 2 decibels increase in signal intensity was observed during the periods of weakest signal intensity, that is the level exceeded 95% of the hours during the month. Furthermore, the time lag between the rise in signal intensity and the rise in sunspot number, which leads to the use of higher frequencies, is such that the practical advantage is reduced.

c. Useful Range of Frequencies

The data given in Reference 1 on frequency dependence of scattered signal intensity and the background galactic radio noise suffices to indicate how required power varies with frequency, for a given required signal-to-noise ratio. It is recommended that the data for scaled antennas be used. In practice, because of the failure to realize gain in proportion to increased directivity, antenna apertures will generally be scaled in proportion to frequency. In the frequency range 30 to 50 Mc/s, approximately $4\frac{1}{2}$ db increase in transmitter power is required for 10 Mc/s increase in operating frequency.

A slightly lower exponent for frequency dependence may be deduced from the cumulative distribution of transmission loss at various frequencies, as given in figures. However, the difference from the median value (Appendix I) obtained by comparing simultaneous hours of transmission is small and should be regarded with caution. The cumulative distribution of signal intensity does not necessarily involve simultaneous observations for all hours at the various frequencies.

In spite of the greater signal-to-noise ratio realized at the lower frequencies of this range, applications requiring the highest order of reliability will need to use, at times, frequencies in the higher part of the range. On rare occasions intense absorption in arctic regions can cause effective blackout at the lower frequencies in the range, say near 30 Mc/s or below; no such occurrences have been observed at 50 Mc/s. It is unlikely, even at lower frequencies in the range, that such circuit interruptions would occur on more than a few occasions during a solar cycle.

In the absence of suitable international frequency allocations and assignment plans at VHF, designed to avoid mutual interference from long-distance F2 propagation, operation at frequencies above the F2 maximum usable frequency (MUF) must be considered to avoid long range interference.

As far as the effects of ground backscatter propagated by F2 are concerned, as a source of self-interference to high speed telegraph systems, development of suitable modulation techniques and/or antenna characteristics

gives definite promise of alleviating the difficulties.[8,9] It can be noted, therefore, that civil circuits, or any which can tolerate the rare interruptions mentioned above, could quite satisfactorily use frequencies below the F2 MUF down to as low as 30 Mc/s, or perhaps a bit lower. There is certainly a valid question as to the wisest frequency allocation policy, involving considerations which are beyond the scope of this report.

Reference 10 gives world-wide contour maps of frequencies which exceed the F2 MUF for long-distance propagation 1% and 10% of the hours during the various seasons of the year, for conditions of maximum and minimum solar activity.

d. Meteoric Contribution

The off-path transmission studies have shown that hourly median transmission losses may be reduced during the night hours (and during the evening hours of weakest signal intensity) by slewing the antenna beams to one side or the other of the great circle path, to take advantage of specular reflections from meteor trails. The advantage would appear to be greater during the winter when the hours of sunlight on the path are fewest; the advantage is realized during only a few night hours during the summer months. Further studies need to be made of the diurnal and seasonal variation of (a) the gain obtainable from off-path transmission, (b) the optimum angles for beam slewing, and (c) the multipath structure and characteristic short-term fading of the off-path signal as these may affect utility of modulation techniques. It is known that the observed fading rates are much higher for off-path transmission than for great circle transmission, and it may well be that the amplitude distribution of the short-term fading is less favorable for conventional continuous modulation systems.

e. Sporadic-E Propagation

This report includes a comprehensive statistical summary of diurnal, seasonal, and annual variations of occurrence of sporadic-E propagation for the temperate latitude and arctic paths. From the point of view of mutual interference with other services, it is evident that terminals of scatter services must be separated from other services by greater than one hop sporadic-E distances, i.e. > ~2000 Km. During the summer months June and July at temperate latitudes 30 to 40 hours per month of sporadic-E propagation are typically observed at 50 Mc/s, during May and August somewhat less than 20, and during other months of the year only a few hours per month. It is important to note that the transmission loss associated with sporadic-E propagation varies over a wide range and is typically much greater (by at least 30 decibels) than that corresponding to a perfect reflection in the ionosphere.

4.3 Outstanding Problems

During the course of the work the need has become evident for additional investigations, or expansion and refinement of studies reported herein, to obtain data which will provide a better basis for optimizing performance of systems.

Declassified in Part - Sanitized Copy Approved for Release @ 50-Yr 2014/06/09 : CIA-RDP81-01043R003000180001-4

Declassified in Part - Sanitized Copy Approved for Release @ 50-Yr 2014/06/09 : CIA-RDP81-01043R003000180001-4

a. Frequency Dependence

The conclusions relative to frequency dependence of ionospheric scattering have not been left in an entirely satisfactory condition based on the data obtained in this program (See Reference 1 and Appendix I of this report). It was possible to compare only two frequencies at one time; the data showed a curvature in the frequency dependence law, but it is now believed the data may have been inadequate to assure genuineness of the curvature. Neither the transmitting or receiving site (but especially the transmitting site) was ideal enough to assure uniform illumination of the scattering volume at all the frequencies. The background galactic noise observed at 27 Mc/s was about 3 decibels below the level expected based on frequency dependence measurements of other observers; this led to considerable investigation of the losses in the receiving antenna, with no satisfactory explanation resulting. The question is left whether the signal intensities observed at 27 Mc/s were also somewhat lower than should have been observed.

Wheelon[11,12] has indicated the very important requirement for simultaneous observations at a number of frequencies, say five, with careful attention to uniform illumination of the ionosphere at all the frequencies; he has shown that a genuine curvature in the frequency dependence data can be expected on the basis of the theory of scattering from a spectrum of turbulent irregularities, and that the general slope and curvature of the frequency dependence law can be used to deduce important meteorological parameters of the scattering region. A comparison of characteristics of envelope and phase fluctuation in fading at the various frequencies can also yield important information on the physical structure and motions in the scattering volume; it is also important to know how the short-term fluctuation of signal varies with frequency in order to specify limitations on modulation techniques, or even required power versus frequency.

Another project has been undertaken[13] along these lines, using transmissions over the Long Branch, Illinois to Boulder, Colorado path at frequencies near 30, 40, 50, 74, and 108 Mc/s.

b. Optimum Antenna Design, Including Beam Slewing

Further propagation studies, at least throughout one full year, are required to learn the real extent of any advantages of beam slewing to utilize off-path meteor reflections during hours when transmission loss may be less by this mechanism than by great circle transmission. The diurnal and seasonal variation of optimum directions of transmission should be studied, as well as an explicit investigation made of the multipath and fading characteristics of received signals as a function of direction of transmission and beam width of the antennas. Earlier observations have shown that during night hours use of low-gain broad beam antennas does not increase the average transmission loss, relative to high-gain narrow beam antennas, by anything like what might be expected from actual plane wave gains of the antennas. The broad beam antennas, of course, make greater use of the off-path contributions of scattering from irregularities and

aspect-sensitive meteor trails. The fading rate is higher for the off-path contributions to the signal than for the great circle transmission and the amplitude distribution of the total signal, which contains the effect of many bursts, may not be as favorable for continuous transmission systems as great circle transmission.

In connection with another project, theoretical computations of optimum antenna height for scatter propagation in the lower ionosphere have been made[14,15] by integrating over the scattering volume, taking into account the radiation pattern of the antennas and the effect of scattering angle. These results indicate that the optimum antenna height is lower than the height which aligns the first lobe at the path midpoint of a symmetrical path, and that there is a considerable range of lower heights which show a gain over the lobe alignment height. The important conclusion is that the transmission loss is a very broad function of the height of the transmitting and receiving antennas and that substantial compromises may be tolerated below lobe alignment height. Experimental verification of this theoretical result should be obtained by establishing a pair of fixed symmetrical antennas as a reference and a pair of adjustable antennas over a given path at two slightly different frequencies; verification of the theoretical height gain curves could lead to significant savings in the cost of ionospheric scatter systems and allow the use of a broad range of heights in compromised situations.

Further work should be done to improve the design of antennas with respect to suppression of radiation outside the main lobe, an important avenue of attack on the multipath problem. Suppression of radiation outside the main lobe by at least 40 decibels relative to the maximum seems a desirable design goal for high speed telegraph systems, and considerable progress has already been made along this line in another project.[10]

c. Modulation Studies

Further modulation studies need to be made not only to define the transmission capacity using conventional techniques in ionospheric scatter propagation, but also to develop more efficient techniques making effective use of the special characteristics of the signal including the bursts; effort should be made to eliminate the difficulties imposed by Doppler-shifted meteor echoes and long-delayed backscatter propagated via the F2 layer during times of high level of solar activity.

Matters such as correlation of envelope and phase over a frequency bandwidth deserve further investigation in relation to limitations imposed on modulation. A limited amount of work has already been undertaken along these lines.[16]

Detailed study of the fading and multipath characteristics of received signals as a function of frequency may alter the idea that the transmission capacity via ionospheric scattering varies with frequency in the same way as the average transmission loss varies with frequency.

Declassified in Part - Sanitized Copy Approved for Release @ 50-Yr 2014/06/09 : CIA-RDP81-01043R003000180001-4

Declassified in Part - Sanitized Copy Approved for Release @ 50-Yr 2014/06/09 : CIA-RDP81-01043R003000180001-4

d. Geographical Dependence

Experiments presently being conducted are expected to yield valuable information on ionospheric scattering observed in equatorial regions.[17] Observations in other parts of the world at temperate latitudes are also required to determine whether the weakest signal intensities encountered are universally about the same (within a few decibels), at least at 50 Mc/s where the rare occurrences of intense anomalous absorption have practically no effect. (Published results[18] showing much greater transmission loss observed over a European path at 48 Mc/s, from Gibraltar to the United Kingdom, are difficult to understand in the light of other measurements and the basic ideas of the ionospheric properties giving rise to regular VHF propagation. It is virtually certain that experimental difficulties, especially the effects of the transmitting antenna arrangement at Gibraltar, can account for the very unsatisfactory results observed on this path.)

The scope of understanding of the physical mechanisms important in ionospheric scattering can be enhanced by observing clear relationships to other measurable ionospheric parameters. Early attempts to relate the data observed on the Cedar Rapids-Sterling path to critical frequencies of the E region were unsuccessful; it was expected that day-to-day fluctuations in transmission loss might be more closely related to absorption observations at HF over the same path, but attempts to correlate VHF signal variations with day-to-day absorption on a path from Ohio to Virginia gave no clear-cut correlation. Nor did a study of stratification at low ionospheric heights recorded by sweep frequency observations from 100 Kc/s to 2 Mc/s at Sterling, Virginia, give any clear-cut correlation. It is felt, however, that all of these efforts to relate the VHF signal to other observable ionospheric characteristics were limited by not observing the ionospheric characteristics in the same geographical location as that in which the scattering takes place. Observations should definitely be undertaken near the midpoint of a scattering path. In New Zealand, Gregory[19] has shown that low-lying strata are observable at vertical incidence at 2 Mc/s, and he believes these to be closely related to or, in fact, to represent the same propagation mechanism as observed at VHF at oblique incidence. He has studied diurnal and seasonal variation and solar cycle dependence and finds striking correspondence with the VHF results.

ACKNOWLEDGEMENTS

Acknowledgement is made to each of the organizations and individual members (and former members) of the staff of the National Bureau of Standards listed below, for substantial help in furthering the research and/or preparation of this report:

Contractors to the National Bureau of Standards

Collins Radio Company

Engineering Experiment Station
North Dakota Agricultural College

Page, Creutz, Garrison, and Waldschmitt
Consulting Radio Engineers

Other Organizations and Government Agencies

Lincoln Laboratories, Massachusetts Institute of Technology
U. S. Army Signal Corps
U. S. Navy (Pet. 4)
U. S. Air Force
Military District of Washington
Federal Communications Commission
Civil Aeronautics Administration

Personnel of the National Bureau of Standards

D. K. Bailey
R. Bateman
Catherine M. Bell
E. L. Berger
G. E. Boggs
H. G. Booker (consultant)
K. L. Bowles
W. H. Daniels
V. R. Eshleman (consultant)
J. Feinstein
R. S. Gillespie
W. S. Gorbaczewski
W. B. Harding
N. C. Hekimian
Adeline N. Kinchloe
Ann C. McCartney
G. F. Montgomery
W. I. Nodine
R. C. Peck
V. C. Pineo
Anita F. Reisig
C. C. Smith
E. K. Smith
J. L. Spindle
G. R. Sugar
K. W. Sullivan
P. G. Sulzer
Gloria W. Sutton
Joan E. Tveten
M. C. Weeg
A. D. Wheelon (consultant
D. C. Whittaker
Laura F. Williams

Declassified in Part - Sanitized Copy Approved for Release @ 50-Yr 2014/06/09 : CIA-RDP81-01043R003000180001-4

Declassified in Part - Sanitized Copy Approved for Release @ 50-Yr 2014/06/09 : CIA-RDP81-01043R003000180001-4

REFERENCES

1. D. K. Bailey, R. Bateman, R. C. Kirby, "Radio Transmission at VHF by Scattering and Other Processes in the Lower Ionosphere," Proc. I.R.E., vol. 43, pp. 1181-1230, October, 1955. (Reprints are included as Appendix XII in a limited number of copies of this report, furnished to Contracting Officer, USASEL; copies were also furnished earlier to the Contracting Officer as NBS Report 3563.)

2. D. K. Bailey, R. Bateman, R. C. Kirby, "First Report on Regular VHF Ionospheric Propagation Observable Over Long Distances," NBS Report No. 8All1, June 30, 1952, (Interim Technical Report on MIPR No. 821-PHIEP-51-04).

3. D. K. Bailey, R. Bateman, R. C. Kirby, "Second Report on Regular VHF Ionospheric Propagation Observable Over Long Distances," NBS Report No. 8All7, June 30, 1953, (Interim Technical Report on MIPR No. 821-PHIEP-51-04).

4. R. C. Kirby, "VHF Propagation by Ionospheric Scattering - A Survey of Experimental Results," Trans. I.R.E., CS-4, 1955.

5. R. M. Davis and E. K. Smith, "The Effect of Sporadic E on VHF Transmission in the U. S.," NBS Report No. 5547, Jan. 28, 1958.

6. G. R. Sugar, "Some Fading Characteristics of Regular VHF Propagation," Proc. I.R.E., vol. 43, pp. 1432-1436, October, 1955.

7. R. C. Kirby, "Extreme Useful Range of VHF Transmission by Scattering from the Lower Ionosphere," I.R.E. National Conventional Record, Part 1, pp. 112-115, March, 1958.

8. H. V. Cottony, A. C. Wilson, "High Gain Low Side-Lobe VHF Antennas for Ionospheric Scatter Communication," NBS Report in preparation.

9. "Backscatter Multipath Elimination Program," Page Communication Engineers Report PCE-R-4681, August, 1957.

10. R. M. Davis and J. W. Finney, "Interference Effects of F2 Propagation," NBS Report No. 6004.

11. A. D. Wheelon, private communication, December, 1955.

12. A. D. Wheelon, "Radio Frequency and Scattering Angle Dependence of Ionospheric Scatter Propagation at VHF," Jour. Geophys. Res., vol 62, pp. 93-112, March, 1957.

13. "Quarterly Progress Report on Engineering Studies in VHF Ionospheric Scattering," NBS Report No. 5554, February, 1958.

14. R. G. Merrill, "Radiation Patterns in the Lower Ionosphere and Fresnel Zones for Elevated Antennas over Spherical Earth," NBS Report in preparation.

15. R. G. Merrill, "Optimum Antenna Height for Ionospheric Scatter Propagation," NBS Report in preparation.

16. J. W. Koch, "Modulation Studies for VHF Ionospheric Scattering," NBS Report in preparation.

17. K. L. Bowles, R. Cohen, "N.B.S. Equatorial Region VHF Scatter Research Program for the I.G.Y.," QST, pp. 11-15, August, 1957.

18. G. A. Isted, "Analysis of Gibraltar - United Kingdom Ionospheric Scatter Signal Recordings," Jour. I.E.E., vol. 104, Part B, R2523, Jan., 1958.

19. J. Gregory, "The Relation of Forward Scattering of VHF Radio Waves to Partial Reflections of MF Waves at Vertical Incidence," Jour. Geophys. Res., vol. 61, pp. 165-169, 1956.

Declassified in Part - Sanitized Copy Approved for Release @ 50-Yr 2014/06/09 : CIA-RDP81-01043R003000180001-4

Declassified in Part - Sanitized Copy Approved for Release @ 50-Yr 2014/06/09 : CIA-RDP81-01043R003000180001-4

CEDAR RAPIDS TO STERLING — 49.8 Mc/s

PATH LENGTH: 1243 km

DISTRIBUTION OF HOURLY MEDIAN OBSERVATIONS OF
RECEIVED OPEN-CIRCUIT ANTENNA VOLTAGE — 600 Ω ANTENNA

REFERENCE POWER INPUT TO TRANSMITTER FINAL AMPLIFIER 40KW; ESTIMATED ANTENNA POWER 30KW

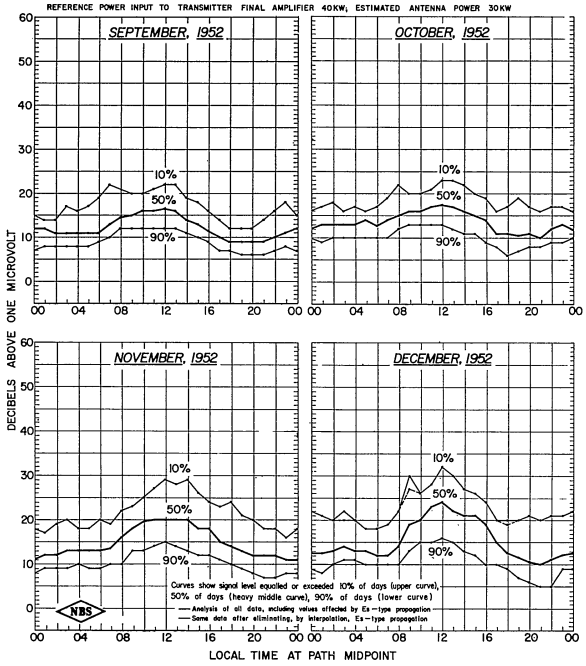

FIG. 1

Declassified in Part - Sanitized Copy Approved for Release @ 50-Yr 2014/06/09 : CIA-RDP81-01043R003000180001-4

Declassified in Part - Sanitized Copy Approved for Release @ 50-Yr 2014/06/09 : CIA-RDP81-01043R003000180001-4

CEDAR RAPIDS TO STERLING — 49.8 Mc/s

PATH LENGTH: 1243 km

DISTRIBUTION OF HOURLY MEDIAN OBSERVATIONS OF
RECEIVED OPEN-CIRCUIT ANTENNA VOLTAGE — 600 Ω ANTENNA

REFERENCE POWER INPUT TO TRANSMITTER FINAL AMPLIFIER 40 KW; ESTIMATED ANTENNA POWER 30 KW

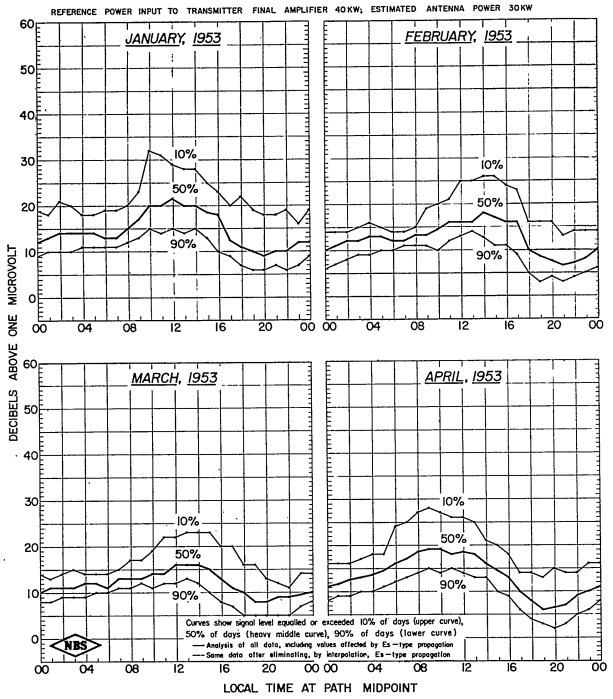

FIG. 2

CEDAR RAPIDS TO STERLING — 49.8 Mc/s

PATH LENGTH: 1243 km

DISTRIBUTION OF HOURLY MEDIAN OBSERVATIONS OF
RECEIVED OPEN-CIRCUIT ANTENNA VOLTAGE — 600 Ω ANTENNA

REFERENCE POWER INPUT TO TRANSMITTER FINAL AMPLIFIER 40 KW; ESTIMATED ANTENNA POWER 30 KW

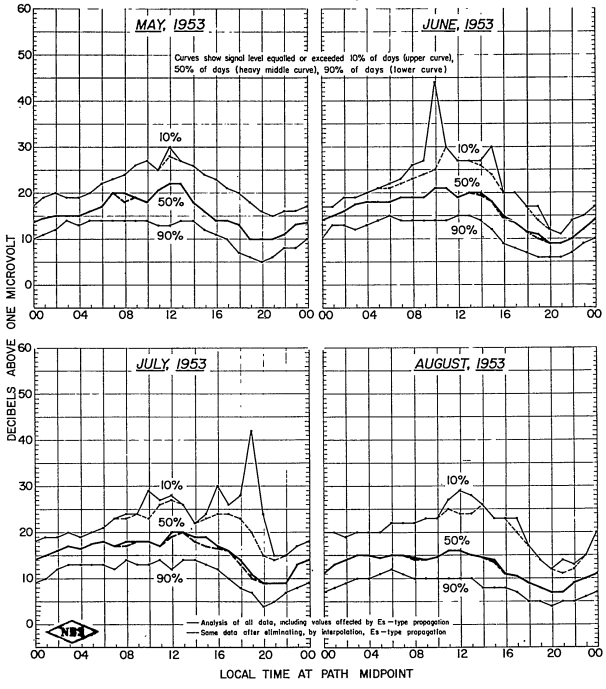

FIG. 3

Declassified in Part - Sanitized Copy Approved for Release @ 50-Yr 2014/06/09 : CIA-RDP81-01043R003000180001-4

Declassified in Part - Sanitized Copy Approved for Release @ 50-Yr 2014/06/09 : CIA-RDP81-01043R003000180001-4

CEDAR RAPIDS TO STERLING — 49.8 Mc/s

PATH LENGTH: 1243 km

DISTRIBUTION OF HOURLY MEDIAN OBSERVATIONS OF
RECEIVED OPEN-CIRCUIT ANTENNA VOLTAGE — 600 Ω ANTENNA

REFERENCE POWER INPUT TO TRANSMITTER FINAL AMPLIFIER 40 KW; ESTIMATED ANTENNA POWER 30 KW

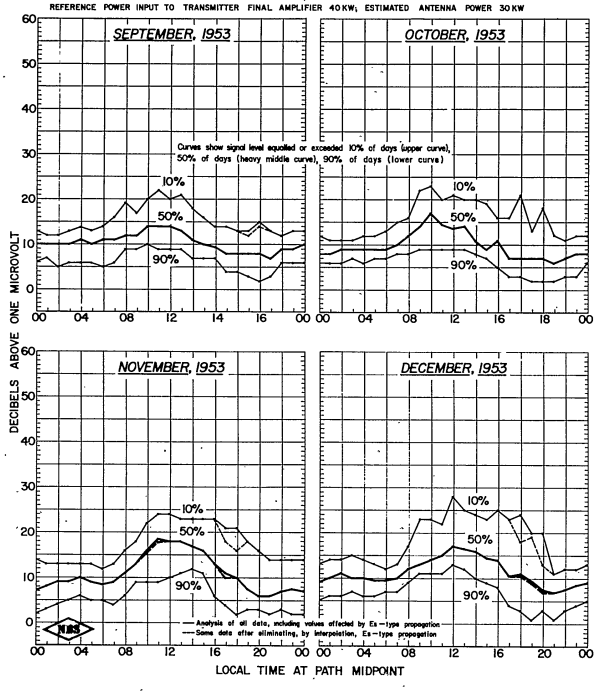
SEPTEMBER, 1953
OCTOBER, 1953
NOVEMBER, 1953
DECEMBER, 1953
Curves show signal level equalled or exceeded 10% of days (upper curve), 50% of days (heavy middle curve), 90% of days (lower curve)
10%
50%
90%
DECIBELS ABOVE ONE MICROVOLT
LOCAL TIME AT PATH MIDPOINT
NBS
— Analysis of all data, including values affected by Es-type propagation
— Same data after eliminating, by interpolation, Es-type propagation

FIG. 4

CEDAR RAPIDS TO STERLING — 49.8 Mc/s

PATH LENGTH: 1243 km

DISTRIBUTION OF HOURLY MEDIAN OBSERVATIONS OF
RECEIVED OPEN-CIRCUIT ANTENNA VOLTAGE — 600 Ω ANTENNA

REFERENCE POWER INPUT TO TRANSMITTER FINAL AMPLFIER 40 KW; ESTIMATED ANTENNA POWER 30 KW

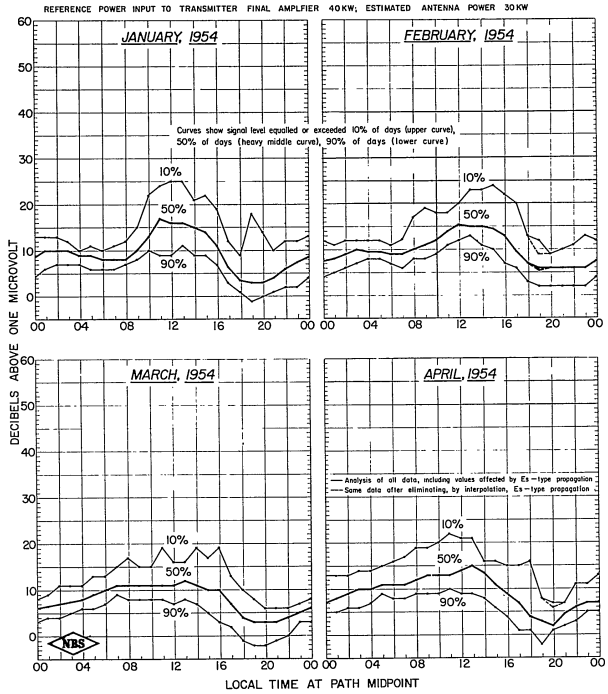
JANUARY, 1954
FEBRUARY, 1954
MARCH, 1954
APRIL, 1954
Curves show signal level equalled or exceeded 10% of days (upper curve), 50% of days (heavy middle curve), 90% of days (lower curve)
10%
50%
90%
DECIBELS ABOVE ONE MICROVOLT
LOCAL TIME AT PATH MIDPOINT
NBS
— Analysis of all data, including values affected by Es-type propagation
— Same data after eliminating, by interpolation, Es-type propagation

FIG. 5

Declassified in Part - Sanitized Copy Approved for Release @ 50-Yr 2014/06/09 : CIA-RDP81-01043R003000180001-4

Declassified in Part - Sanitized Copy Approved for Release @ 50-Yr 2014/06/09 : CIA-RDP81-01043R003000180001-4

CEDAR RAPIDS TO STERLING — 49.8 Mc/s

PATH LENGTH: 1243 km

DISTRIBUTION OF HOURLY MEDIAN OBSERVATIONS OF
RECEIVED OPEN-CIRCUIT ANTENNA VOLTAGE — 600 Ω ANTENNA

REFERENCE POWER INPUT TO TRANSMITTER FINAL AMPLIFIER 40KW; ESTIMATED ANTENNA POWER 30KW

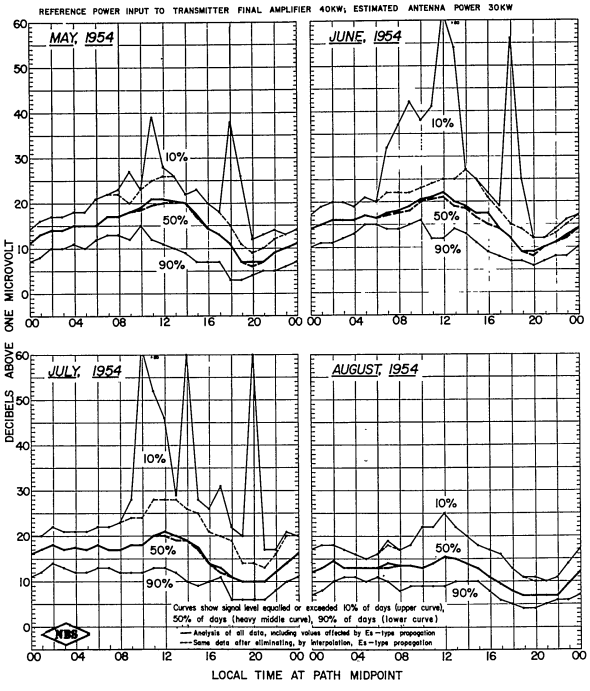

FIG. 6

CEDAR RAPIDS TO STERLING — 49.8 Mc/s

PATH LENGTH: 1243 km

DISTRIBUTION OF HOURLY MEDIAN OBSERVATIONS OF
RECEIVED OPEN-CIRCUIT ANTENNA VOLTAGE — 600 Ω ANTENNA

REFERENCE POWER INPUT TO TRANSMITTER FINAL AMPLIFIER 40KW; ESTIMATED ANTENNA POWER 30KW

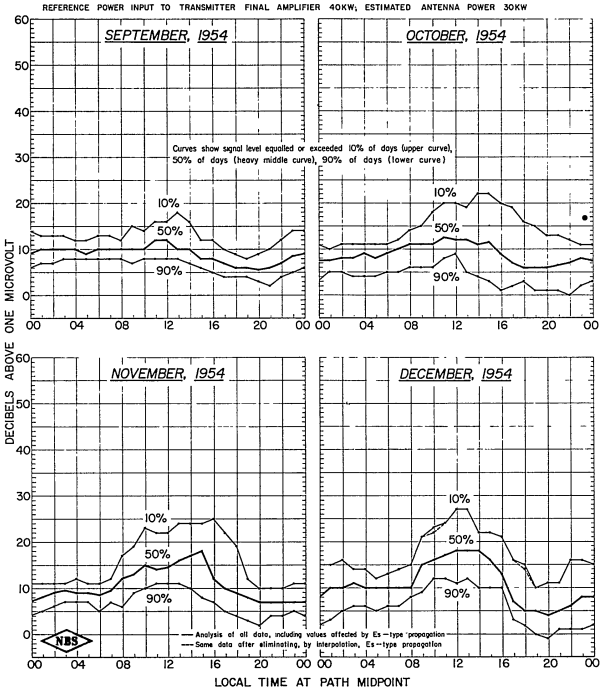

FIG. 7

Declassified in Part - Sanitized Copy Approved for Release @ 50-Yr 2014/06/09 : CIA-RDP81-01043R003000180001-4

Declassified in Part - Sanitized Copy Approved for Release @ 50-Yr 2014/06/09 : CIA-RDP81-01043R003000180001-4

CEDAR RAPIDS TO STERLING — 49.8 Mc/s

PATH LENGTH: 1243 km

DISTRIBUTION OF HOURLY MEDIAN OBSERVATIONS OF
RECEIVED OPEN-CIRCUIT ANTENNA VOLTAGE — 600 Ω ANTENNA

REFERENCE POWER INPUT TO TRANSMITTER FINAL AMPLIFIER 40 KW; ESTIMATED ANTENNA POWER 30 KW

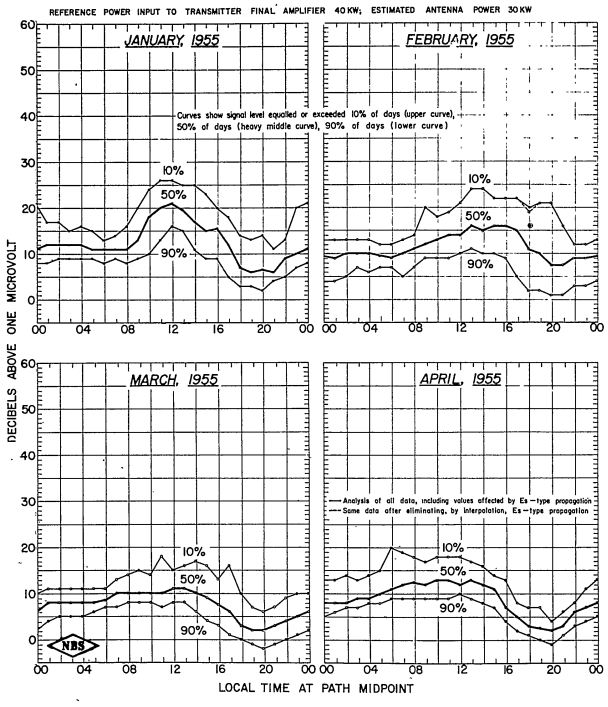
JANUARY, 1955
FEBRUARY, 1955
MARCH, 1955
APRIL, 1955
Curves show signal level equalled or exceeded 10% of days (upper curve), 50% of days (heavy middle curve), 90% of days (lower curve)
10%
50%
90%
DECIBELS ABOVE ONE MICROVOLT
LOCAL TIME AT PATH MIDPOINT
NBS
Analysis of all data, including values effected by Es-type propagation
Same data after eliminating, by interpolation, Es-type propagation

FIG. 8

CEDAR RAPIDS TO STERLING — 49.8 Mc/s

PATH LENGTH: 1243 km

DISTRIBUTION OF HOURLY MEDIAN OBSERVATIONS OF
RECEIVED OPEN-CIRCUIT ANTENNA VOLTAGE — 600 Ω ANTENNA

REFERENCE POWER INPUT TO TRANSMITTER FINAL AMPLIFIER 40 KW; ESTIMATED ANTENNA POWER 30 KW

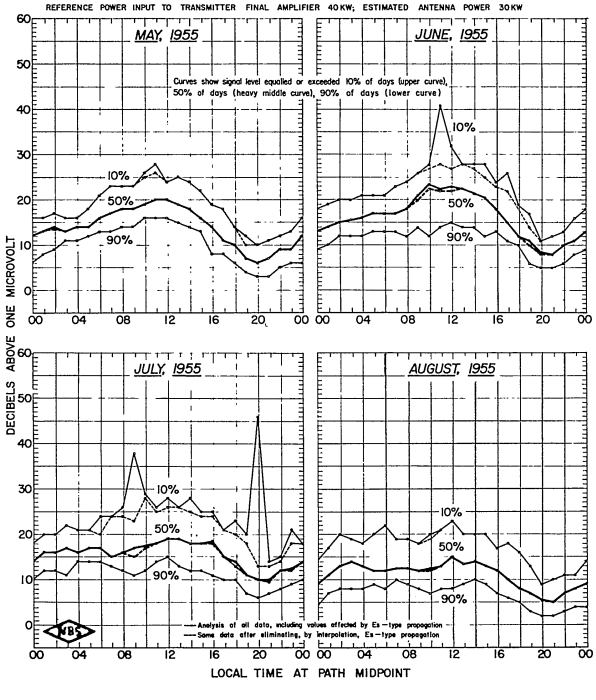
MAY, 1955
JUNE, 1955
JULY, 1955
AUGUST, 1955
Curves show signal level equalled or exceeded 10% of days (upper curve), 50% of days (heavy middle curve), 90% of days (lower curve)
10%
50%
90%
DECIBELS ABOVE ONE MICROVOLT
LOCAL TIME AT PATH MIDPOINT
NBS
Analysis of all data, including values effected by Es-type propagation
Same data after eliminating, by interpolation, Es-type propagation

FIG. 9

Declassified in Part - Sanitized Copy Approved for Release @ 50-Yr 2014/06/09 : CIA-RDP81-01043R003000180001-4

Declassified in Part - Sanitized Copy Approved for Release @ 50-Yr 2014/06/09 : CIA-RDP81-01043R003000180001-4

CEDAR RAPIDS TO STERLING — 49.8 Mc/s

PATH LENGTH: 1243 km

DISTRIBUTION OF HOURLY MEDIAN OBSERVATIONS OF
RECEIVED OPEN-CIRCUIT ANTENNA VOLTAGE — 600 Ω ANTENNA

REFERENCE POWER INPUT TO TRANSMITTER FINAL AMPLIFIER 40 KW; ESTIMATED ANTENNA POWER 30 KW

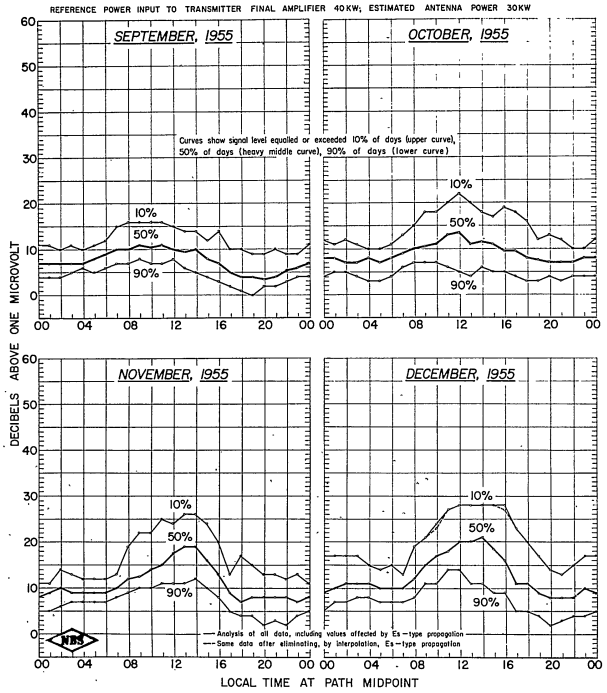

FIG. 10

FARGO TO CHURCHILL — 49.7 Mc/s

PATH LENGTH: 1326 km

DISTRIBUTION OF HOURLY MEDIAN OBSERVATIONS OF
RECEIVED OPEN-CIRCUIT ANTENNA VOLTAGE — 600 Ω ANTENNA

REFERENCE POWER INPUT TO TRANSMITTER FINAL AMPLIFIER 40 KW; ESTIMATED ANTENNA POWER 30 KW

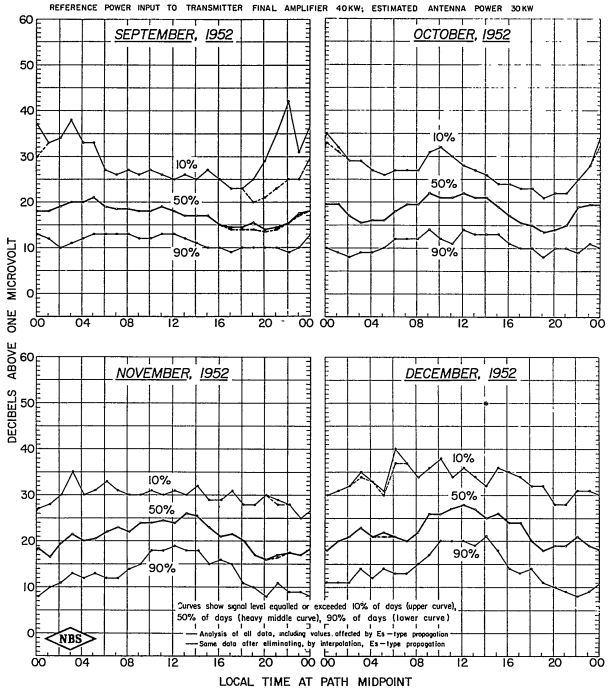

FIG. 11

Declassified in Part - Sanitized Copy Approved for Release @ 50-Yr 2014/06/09 : CIA-RDP81-01043R003000180001-4

Declassified in Part - Sanitized Copy Approved for Release @ 50-Yr 2014/06/09 : CIA-RDP81-01043R003000180001-4

FARGO TO CHURCHILL — 49.7 Mc/s

PATH LENGTH: 1326 km

DISTRIBUTION OF HOURLY MEDIAN OBSERVATIONS OF
RECEIVED OPEN-CIRCUIT ANTENNA VOLTAGE — 600 Ω ANTENNA

REFERENCE POWER INPUT TO TRANSMITTER FINAL AMPLIFIER 40 KW; ESTIMATED ANTENNA POWER 30 KW

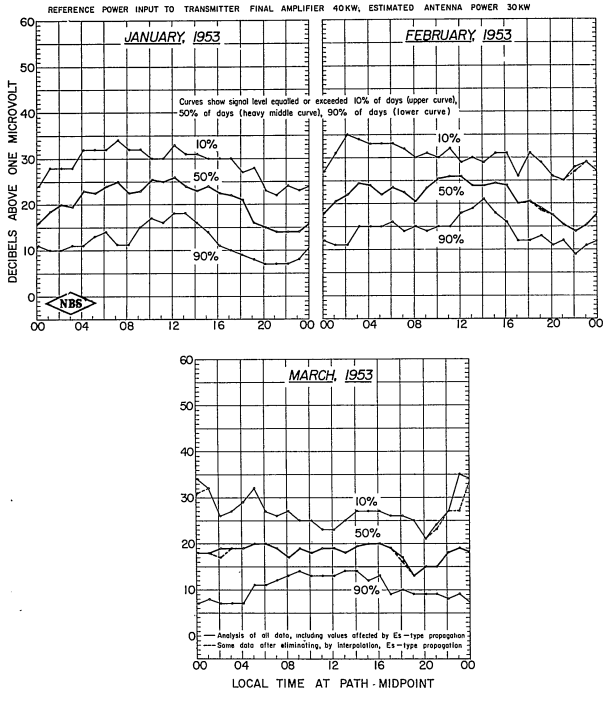
JANUARY, 1953
FEBRUARY, 1953
MARCH, 1953
Curves show signal level equalled or exceeded 10% of days (upper curve), 50% of days (heavy middle curve), 90% of days (lower curve)
10%
50%
90%
NBS
DECIBELS ABOVE ONE MICROVOLT
00 04 08 12 16 20 00
— Analysis of all data, including values affected by Es-type propagation
--- Same data after eliminating, by interpolation, Es-type propagation
LOCAL TIME AT PATH - MIDPOINT

FIG. 12

ANCHORAGE TO BARROW — 48.87 Mc/s

PATH LENGTH: 1156 km

DISTRIBUTION OF HOURLY MEDIAN OBSERVATIONS OF
RECEIVED OPEN-CIRCUIT ANTENNA VOLTAGE — 600 Ω ANTENNA

REFERENCE POWER INPUT TO TRANSMITTER FINAL AMPLIFIER 40 KW; ESTIMATED ANTENNA POWER 30 KW

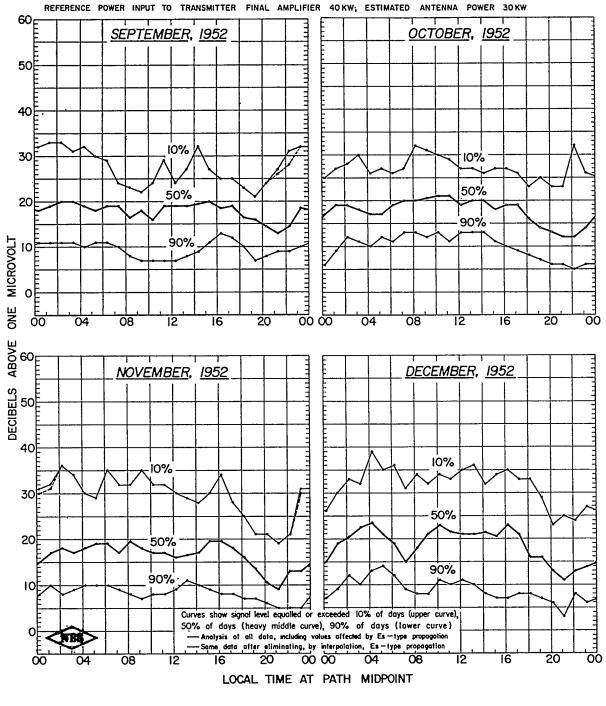
SEPTEMBER, 1952
OCTOBER, 1952
NOVEMBER, 1952
DECEMBER, 1952
10%
50%
90%
NBS
Curves show signal level equalled or exceeded 10% of days (upper curve), 50% of days (heavy middle curve), 90% of days (lower curve)
— Analysis of all data, including values affected by Es-type propagation
--- Same data after eliminating, by interpolation, Es-type propagation
DECIBELS ABOVE ONE MICROVOLT
00 04 08 12 16 20 00
LOCAL TIME AT PATH MIDPOINT

FIG. 13

Declassified in Part - Sanitized Copy Approved for Release @ 50-Yr 2014/06/09 : CIA-RDP81-01043R003000180001-4

Declassified in Part - Sanitized Copy Approved for Release @ 50-Yr 2014/06/09 : CIA-RDP81-01043R003000180001-4

ANCHORAGE TO BARROW — 48.87 Mc/s

PATH LENGTH: 1156 km

DISTRIBUTION OF HOURLY MEDIAN OBSERVATIONS OF
RECEIVED OPEN-CIRCUIT ANTENNA VOLTAGE — 600 Ω ANTENNA

REFERENCE POWER INPUT TO TRANSMITTER FINAL AMPLIFIER 40 KW; ESTIMATED ANTENNA POWER 30 KW

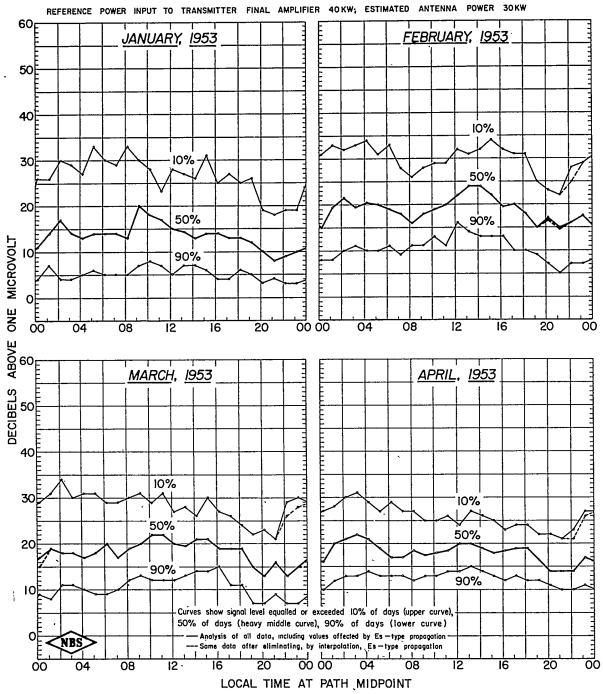

FIG. 14

ANCHORAGE TO BARROW — 48.87 Mc/s

PATH LENGTH: 1156 km

DISTRIBUTION OF HOURLY MEDIAN OBSERVATIONS OF
RECEIVED OPEN-CIRCUIT ANTENNA VOLTAGE — 600 Ω ANTENNA

REFERENCE POWER INPUT TO TRANSMITTER FINAL AMPLIFIER 40 KW; ESTIMATED ANTENNA POWER 30 KW

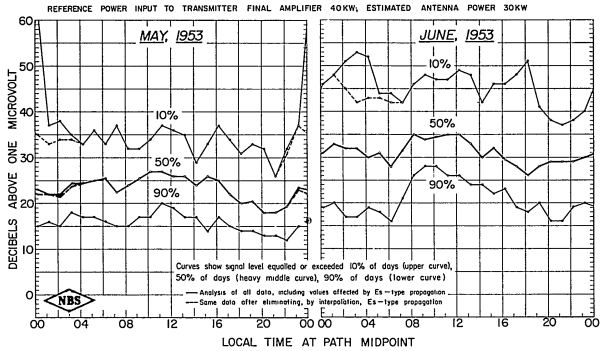

FIG. 15

Declassified in Part - Sanitized Copy Approved for Release @ 50-Yr 2014/06/09 : CIA-RDP81-01043R003000180001-4

Declassified in Part - Sanitized Copy Approved for Release @ 50-Yr 2014/06/09 : CIA-RDP81-01043R003000180001-4

ANCHORAGE TO BARROW — 24.325 Mc/s

PATH LENGTH: 1156 km

DISTRIBUTION OF HOURLY MEDIAN OBSERVATIONS OF
RECEIVED OPEN-CIRCUIT ANTENNA VOLTAGE — 600 Ω ANTENNA

REFERENCE POWER INPUT TO TRANSMITTER FINAL AMPLIFIER 40 KW; ESTIMATED ANTENNA POWER 30 KW
FIVE-ELEMENT YAGI TRANSMITTING AND RECEIVING ANTENNAS USED HAVING COHERENT-PLANE-WAVE GAIN
OF APPROXIMATELY 9 DECIBELS RELATIVE TO HALF-WAVE DIPOLE

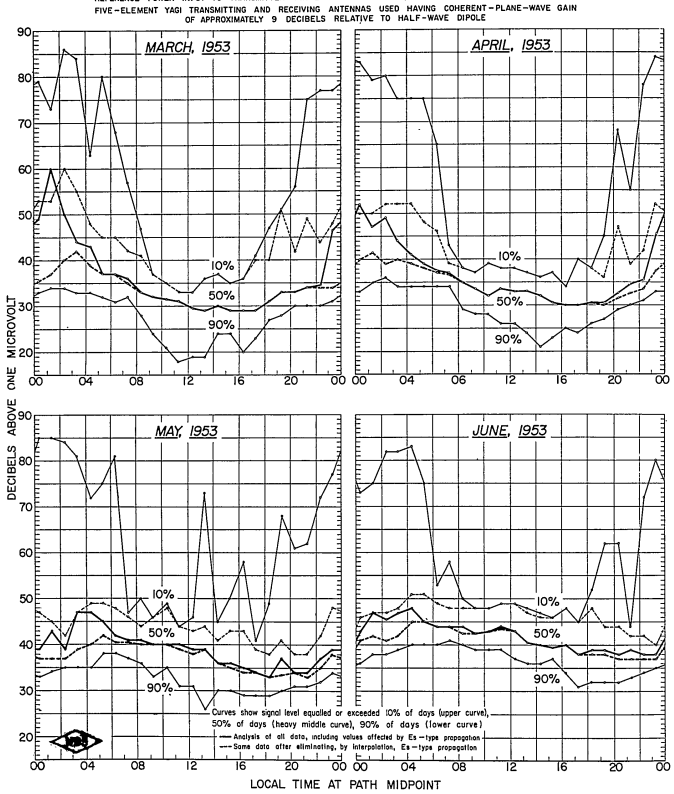
MARCH, 1953
APRIL, 1953
MAY, 1953
JUNE, 1953
10%
50%
90%
DECIBELS ABOVE ONE MICROVOLT
LOCAL TIME AT PATH MIDPOINT
Curves show signal level equalled or exceeded 10% of days (upper curve), 50% of days (heavy middle curve), 90% of days (lower curve)
— Analysis of all data, including values affected by Es-type propagation
--- Same data after eliminating, by interpolation, Es-type propagation

FIG. 16

CEDAR RAPIDS TO STERLING — 27.775 Mc/s

PATH LENGTH: 1243 km

DISTRIBUTION OF HOURLY MEDIAN OBSERVATIONS OF
RECEIVED OPEN-CIRCUIT ANTENNA VOLTAGE — 600 Ω ANTENNA

REFERENCE POWER INPUT TO TRANSMITTER FINAL AMPLIFIER 40 KW; ESTIMATED ANTENNA POWER 30 KW

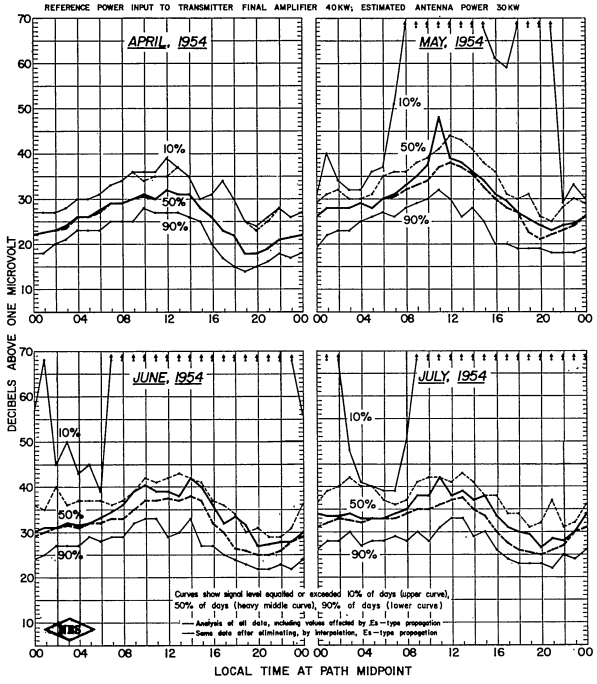
APRIL, 1954
MAY, 1954
JUNE, 1954
JULY, 1954
10%
50%
90%
DECIBELS ABOVE ONE MICROVOLT
LOCAL TIME AT PATH MIDPOINT
Curves show signal level equalled or exceeded 10% of days (upper curve), 50% of days (heavy middle curve), 90% of days (lower curve)
— Analysis of all data, including values affected by Es-type propagation
--- Same data after eliminating, by interpolation, Es-type propagation

FIG. 17

Declassified in Part - Sanitized Copy Approved for Release @ 50-Yr 2014/06/09 : CIA-RDP81-01043R003000180001-4

Declassified in Part - Sanitized Copy Approved for Release @ 50-Yr 2014/06/09 : CIA-RDP81-01043R003000180001-4

CEDAR RAPIDS TO STERLING — 27.775Mc/s

PATH LENGTH: 1243 km

DISTRIBUTION OF HOURLY MEDIAN OBSERVATIONS OF
RECEIVED OPEN-CIRCUIT ANTENNA VOLTAGE — 600 Ω ANTENNA

REFERENCE POWER INPUT TO TRANSMITTER FINAL AMPLIFIER 40KW, ESTIMATED ANTENNA POWER 30KW

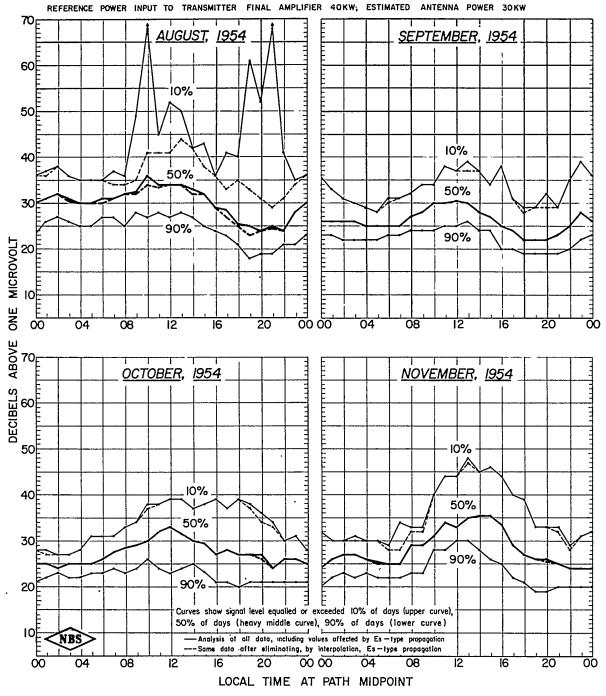

FIG. 18

CEDAR RAPIDS TO STERLING — 27.775Mc/s

PATH LENGTH: 1243 km

DISTRIBUTION OF HOURLY MEDIAN OBSERVATIONS OF
RECEIVED OPEN-CIRCUIT ANTENNA VOLTAGE — 600 Ω ANTENNA

REFERENCE POWER INPUT TO TRANSMITTER FINAL AMPLIFIER 40KW, ESTIMATED ANTENNA POWER 30KW

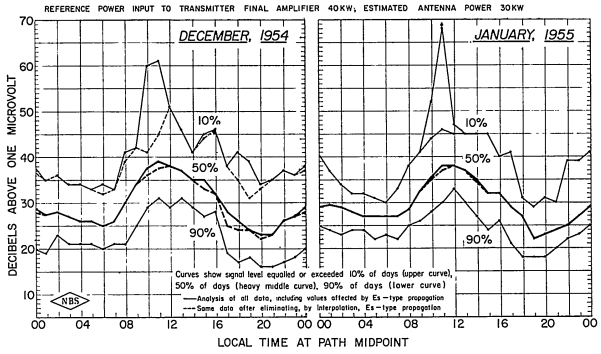

FIG. 19

Declassified in Part - Sanitized Copy Approved for Release @ 50-Yr 2014/06/09 : CIA-RDP81-01043R003000180001-4

Declassified in Part - Sanitized Copy Approved for Release @ 50-Yr 2014/06/09 : CIA-RDP81-01043R003000180001-4

CEDAR RAPIDS TO STERLING — 27.775 Mc/s

PATH LENGTH: 1243 km

DISTRIBUTION OF HOURLY MEDIAN OBSERVATIONS OF
RECEIVED OPEN-CIRCUIT ANTENNA VOLTAGE — 600 Ω ANTENNA

REFERENCE POWER INPUT TO TRANSMITTER FINAL AMPLIFIER 40 KW; ESTIMATED ANTENNA POWER 30 KW

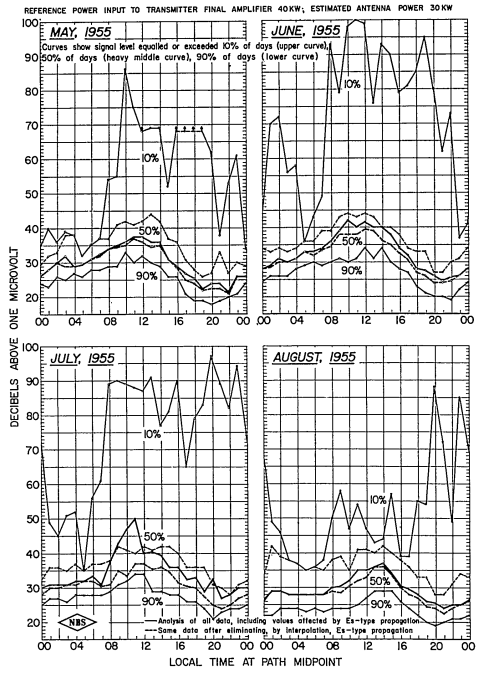

FIG. 20

CEDAR RAPIDS TO STERLING — 27.775 Mc/s

PATH LENGTH: 1243 km

DISTRIBUTION OF HOURLY MEDIAN OBSERVATIONS OF
RECEIVED OPEN-CIRCUIT ANTENNA VOLTAGE — 600 Ω ANTENNA

REFERENCE POWER INPUT TO TRANSMITTER FINAL AMPLIFIER 40 KW; ESTIMATED ANTENNA POWER 30 KW

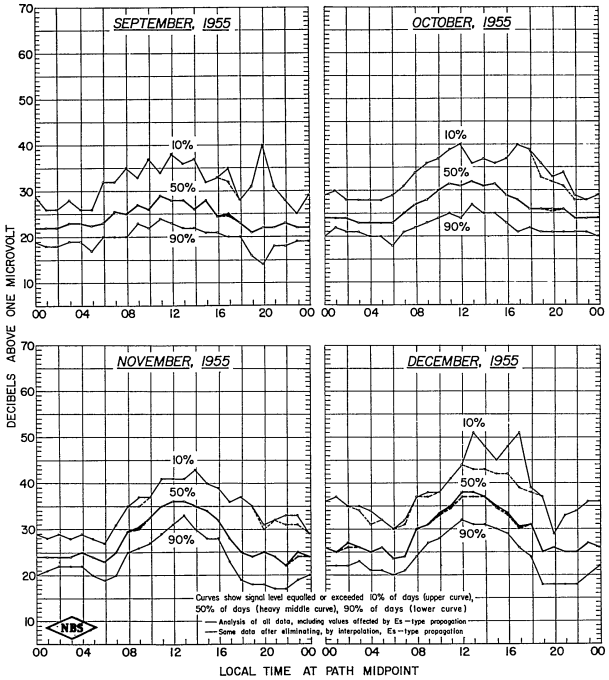

FIG. 21

Declassified in Part - Sanitized Copy Approved for Release @ 50-Yr 2014/06/09 : CIA-RDP81-01043R003000180001-4

Declassified in Part - Sanitized Copy Approved for Release @ 50-Yr 2014/06/09 : CIA-RDP81-01043R003000180001-4

CEDAR RAPIDS TO STERLING — 107.8 Mc/s

PATH LENGTH: 1243 km

DISTRIBUTION OF HOURLY MEDIAN OBSERVATIONS OF
RECEIVED OPEN-CIRCUIT ANTENNA VOLTAGE — 600 Ω ANTENNA

REFERENCE TRANSMITTER POWER TO ANTENNA 30 KW

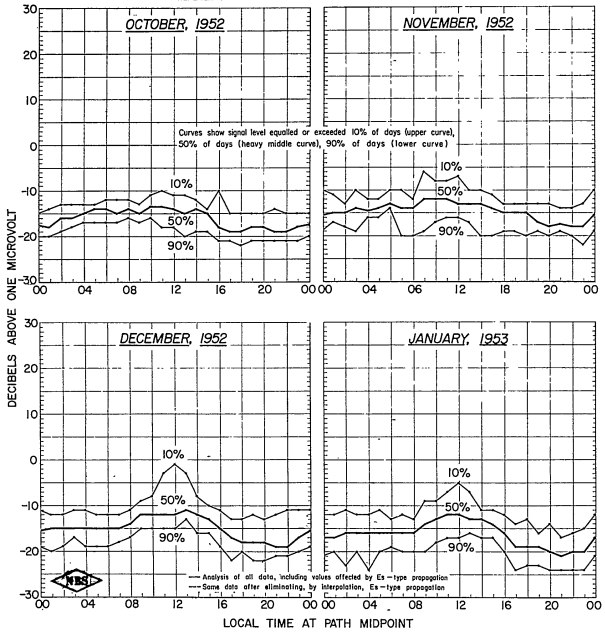

FIG. 22

CEDAR RAPIDS TO STERLING — 49.8 Mc/s

CUMULATIVE DISTRIBUTION OF HOURLY MEDIAN VALUES OF SIGNAL INTENSITY

—— ALL VALUES, INCLUDING VALUES AFFECTED BY Es - TYPE PROPAGATION
--- INTERPOLATED VALUES USED DURING HOURS WITH Es - TYPE PROPAGATION

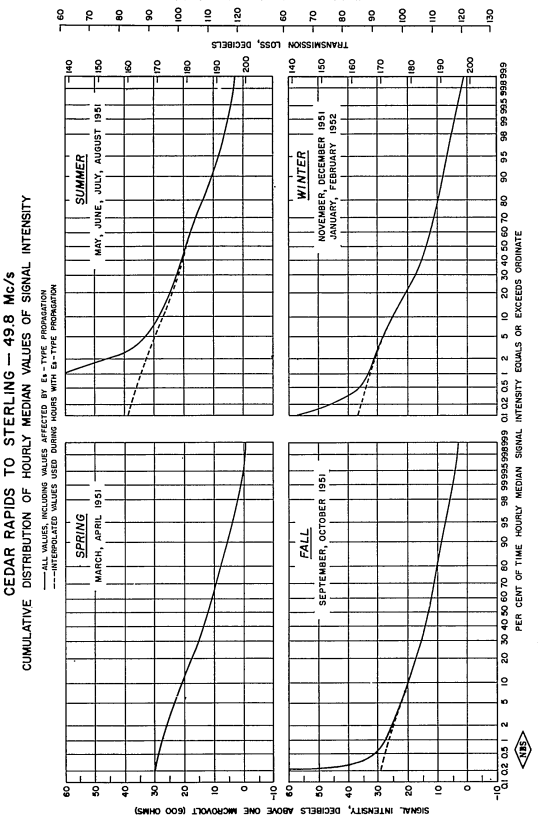
LOSS RELATIVE TO INVERSE-DISTANCE-SQUARED, DECIBELS
60 70 80 90 100 110 120 60 70 80 90 100 110 120 130
TRANSMISSION LOSS, DECIBELS
140 150 160 170 180 190 200 140 150 160 170 180 190 200
SUMMER
MAY, JUNE, JULY, AUGUST 1951
WINTER
NOVEMBER, DECEMBER 1951
JANUARY, FEBRUARY 1952
SPRING
MARCH, APRIL 1951
FALL
SEPTEMBER, OCTOBER 1951
SIGNAL INTENSITY, DECIBELS ABOVE ONE MICROVOLT (600 OHMS)
60 50 40 30 20 10 0 -10 60 50 40 30 20 10 0 -10
PER CENT OF TIME HOURLY MEDIAN SIGNAL INTENSITY EQUALS OR EXCEEDS ORDINATE
0.1 0.2 0.5 1 2 5 10 20 30 40 50 60 70 80 90 95 98 99 99.5 99.8 99.9
NBS

FIG. 23

Declassified in Part - Sanitized Copy Approved for Release @ 50-Yr 2014/06/09 : CIA-RDP81-01043R003000180001-4

CEDAR RAPIDS TO STERLING — 49.8 Mc/s

CUMULATIVE DISTRIBUTION OF HOURLY MEDIAN VALUES OF SIGNAL INTENSITY

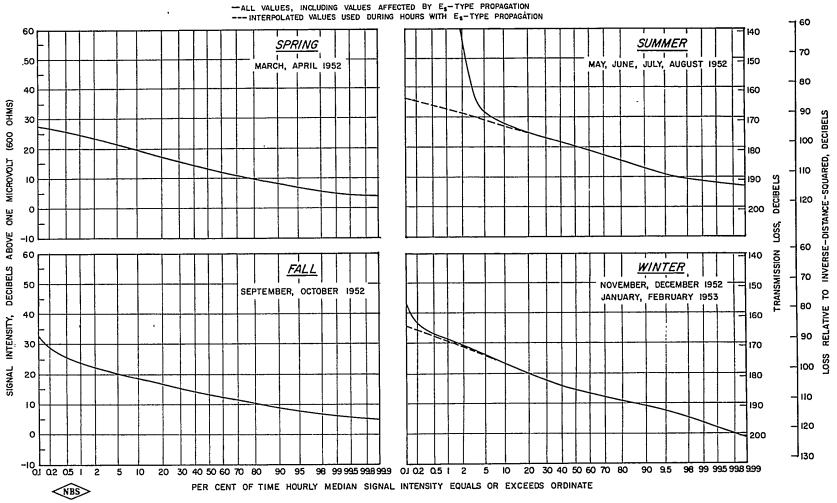
—ALL VALUES, INCLUDING VALUES AFFECTED BY E_s-TYPE PROPAGATION
---INTERPOLATED VALUES USED DURING HOURS WITH E_s-TYPE PROPAGATION
SPRING
MARCH, APRIL 1952
SUMMER
MAY, JUNE, JULY, AUGUST 1952
FALL
SEPTEMBER, OCTOBER 1952
WINTER
NOVEMBER, DECEMBER 1952
JANUARY, FEBRUARY 1953
SIGNAL INTENSITY, DECIBELS ABOVE ONE MICROVOLT (600 OHMS)
TRANSMISSION LOSS, DECIBELS
LOSS RELATIVE TO INVERSE-DISTANCE-SQUARED, DECIBELS
PER CENT OF TIME HOURLY MEDIAN SIGNAL INTENSITY EQUALS OR EXCEEDS ORDINATE
NBS

FIG. 24

CEDAR RAPIDS TO STERLING — 49.8 Mc/s

CUMULATIVE DISTRIBUTION OF HOURLY MEDIAN VALUES OF SIGNAL INTENSITY

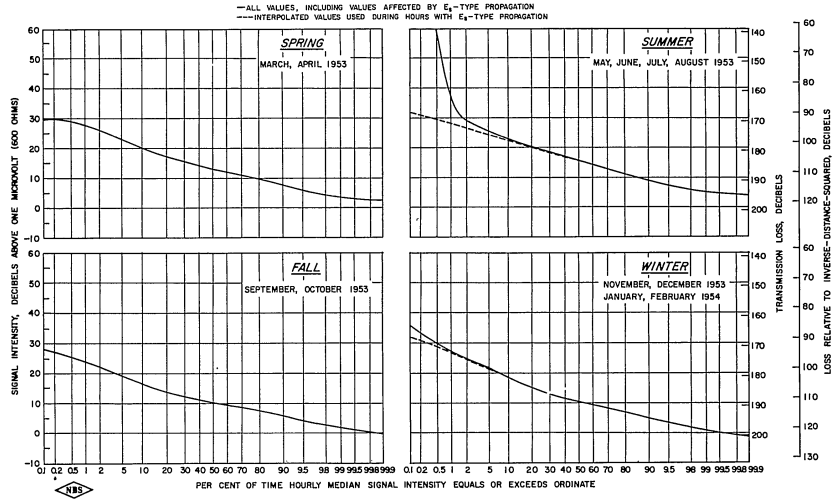
—ALL VALUES, INCLUDING VALUES AFFECTED BY E_s-TYPE PROPAGATION
---INTERPOLATED VALUES USED DURING HOURS WITH E_s-TYPE PROPAGATION
SPRING
MARCH, APRIL 1953
SUMMER
MAY, JUNE, JULY, AUGUST 1953
FALL
SEPTEMBER, OCTOBER 1953
WINTER
NOVEMBER, DECEMBER 1953
JANUARY, FEBRUARY 1954
SIGNAL INTENSITY, DECIBELS ABOVE ONE MICROVOLT (600 OHMS)
TRANSMISSION LOSS, DECIBELS
LOSS RELATIVE TO INVERSE-DISTANCE-SQUARED, DECIBELS
PER CENT OF TIME HOURLY MEDIAN SIGNAL INTENSITY EQUALS OR EXCEEDS ORDINATE
NBS

FIG. 25

Declassified in Part - Sanitized Copy Approved for Release @ 50-Yr 2014/06/09 : CIA-RDP81-01043R003000180001-4
Declassified in Part - Sanitized Copy Approved for Release @ 50-Yr 2014/06/09 : CIA-RDP81-01043R003000180001-4

CEDAR RAPIDS TO STERLING — 49.8 Mc/s

CUMULATIVE DISTRIBUTION OF HOURLY MEDIAN VALUES OF SIGNAL INTENSITY

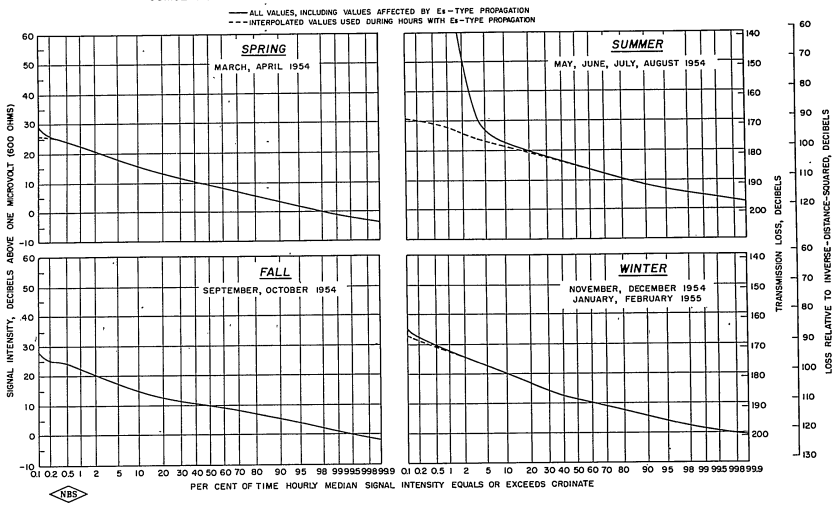
—— ALL VALUES, INCLUDING VALUES AFFECTED BY Es-TYPE PROPAGATION
- - - INTERPOLATED VALUES USED DURING HOURS WITH Es-TYPE PROPAGATION
SPRING
MARCH, APRIL 1954
SUMMER
MAY, JUNE, JULY, AUGUST 1954
FALL
SEPTEMBER, OCTOBER 1954
WINTER
NOVEMBER, DECEMBER 1954
JANUARY, FEBRUARY 1955
SIGNAL INTENSITY, DECIBELS ABOVE ONE MICROVOLT (600 OHMS)
TRANSMISSION LOSS, DECIBELS
LOSS RELATIVE TO INVERSE-DISTANCE-SQUARED, DECIBELS
0.1 0.2 0.5 1 2 5 10 20 30 40 50 60 70 80 90 95 98 99 99.5 99.8 99.9
PER CENT OF TIME HOURLY MEDIAN SIGNAL INTENSITY EQUALS OR EXCEEDS ORDINATE
NBS

FIG. 26

CEDAR RAPIDS TO STERLING — 49.8 Mc/s

CUMULATIVE DISTRIBUTION OF HOURLY MEDIAN VALUES OF SIGNAL INTENSITY

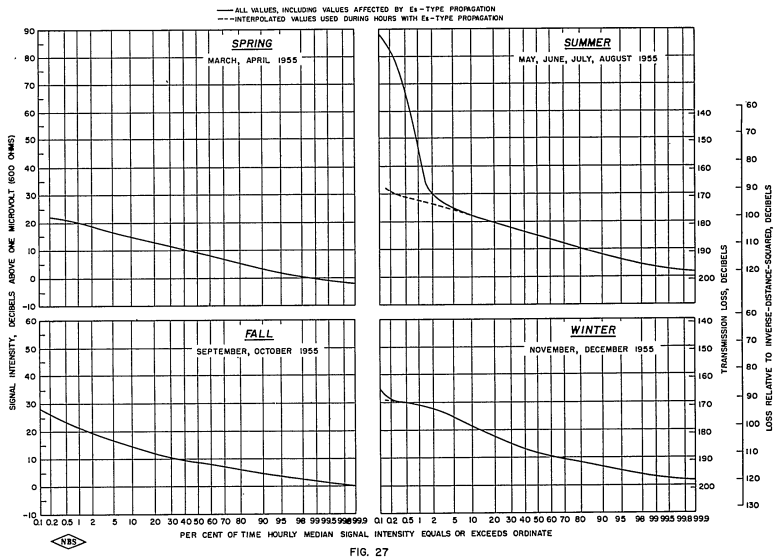
—— ALL VALUES, INCLUDING VALUES AFFECTED BY Es-TYPE PROPAGATION
- - - INTERPOLATED VALUES USED DURING HOURS WITH Es-TYPE PROPAGATION
SPRING
MARCH, APRIL 1955
SUMMER
MAY, JUNE, JULY, AUGUST 1955
FALL
SEPTEMBER, OCTOBER 1955
WINTER
NOVEMBER, DECEMBER 1955
SIGNAL INTENSITY, DECIBELS ABOVE ONE MICROVOLT (600 OHMS)
TRANSMISSION LOSS, DECIBELS
LOSS RELATIVE TO INVERSE-DISTANCE-SQUARED, DECIBELS
0.1 0.2 0.5 1 2 5 10 20 30 40 50 60 70 80 90 95 98 99 99.5 99.8 99.9
PER CENT OF TIME HOURLY MEDIAN SIGNAL INTENSITY EQUALS OR EXCEEDS ORDINATE
NBS

FIG. 27

Declassified in Part - Sanitized Copy Approved for Release @ 50-Yr 2014/06/09 : CIA-RDP81-01043R003000180001-4
Declassified in Part - Sanitized Copy Approved for Release @ 50-Yr 2014/06/09 : CIA-RDP81-01043R003000180001-4

ANCHORAGE TO BARROW — 48.87 Mc/s

CUMULATIVE DISTRIBUTION OF HOURLY MEDIAN VALUES OF SIGNAL INTENSITY

—ALL VALUES, INCLUDING VALUES AFFECTED BY E_s-TYPE PROPAGATION
– – –INTERPOLATED VALUES USED DURING HOURS WITH E_s-TYPE PROPAGATION

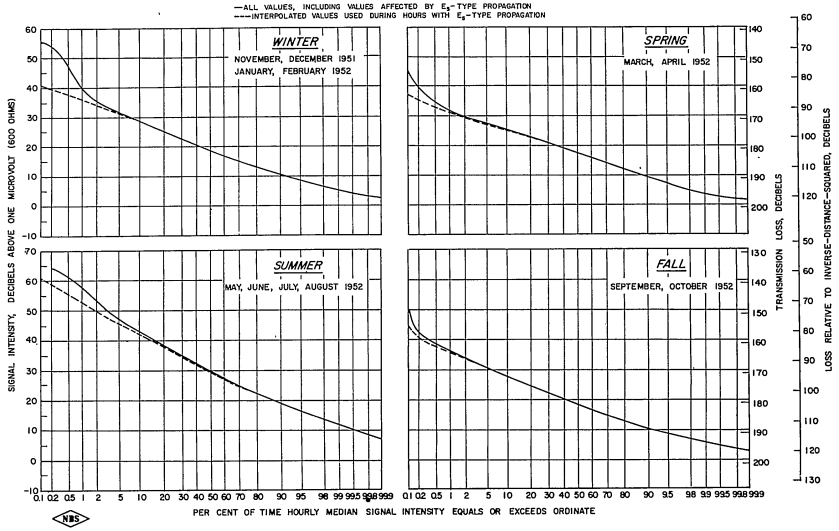
WINTER
NOVEMBER, DECEMBER 1951
JANUARY, FEBRUARY 1952
SPRING
MARCH, APRIL 1952
SUMMER
MAY, JUNE, JULY, AUGUST 1952
FALL
SEPTEMBER, OCTOBER 1952
SIGNAL INTENSITY, DECIBELS ABOVE ONE MICROVOLT (600 OHMS)
TRANSMISSION LOSS, DECIBELS
LOSS RELATIVE TO INVERSE-DISTANCE-SQUARED, DECIBELS
0.1 0.2 0.5 1 2 5 10 20 30 40 50 60 70 80 90 95 98 99 99.5 99.8 99.9
PER CENT OF TIME HOURLY MEDIAN SIGNAL INTENSITY EQUALS OR EXCEEDS ORDINATE
NBS

FIG. 28

ANCHORAGE TO BARROW — 48.87 Mc/s

CUMULATIVE DISTRIBUTION OF HOURLY MEDIAN VALUES OF SIGNAL INTENSITY

—ALL VALUES, INCLUDING VALUES AFFECTED BY E_s-TYPE PROPAGATION
– – –INTERPOLATED VALUES USED DURING HOURS WITH E_s-TYPE PROPAGATION

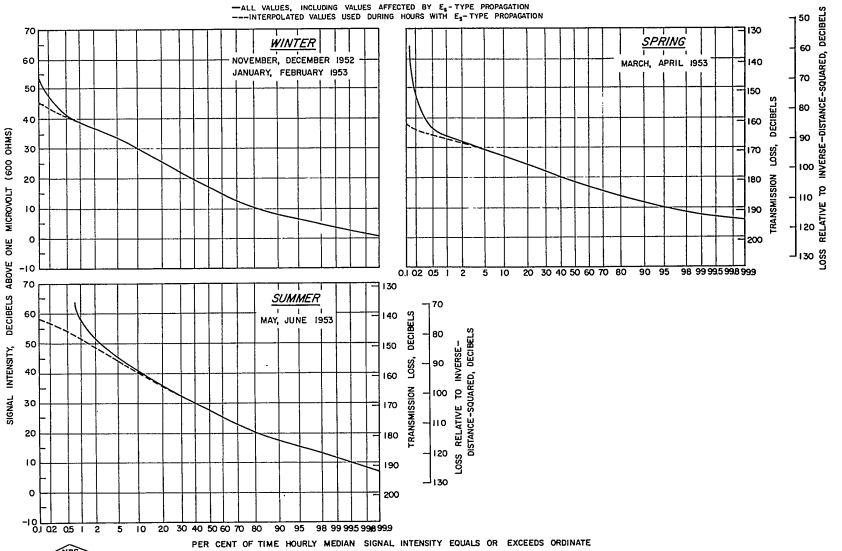
WINTER
NOVEMBER, DECEMBER 1952
JANUARY, FEBRUARY 1953
SPRING
MARCH, APRIL 1953
SUMMER
MAY, JUNE 1953
SIGNAL INTENSITY, DECIBELS ABOVE ONE MICROVOLT (600 OHMS)
TRANSMISSION LOSS, DECIBELS
LOSS RELATIVE TO INVERSE-DISTANCE-SQUARED, DECIBELS
0.1 0.2 0.5 1 2 5 10 20 30 40 50 60 70 80 90 95 98 99 99.5 99.8 99.9
PER CENT OF TIME HOURLY MEDIAN SIGNAL INTENSITY EQUALS OR EXCEEDS ORDINATE
NBS

FIG. 29

Declassified in Part - Sanitized Copy Approved for Release @ 50-Yr 2014/06/09 : CIA-RDP81-01043R003000180001-4
Declassified in Part - Sanitized Copy Approved for Release @ 50-Yr 2014/06/09 : CIA-RDP81-01043R003000180001-4

FARGO TO CHURCHILL — 49.7 Mc/s

CUMULATIVE DISTRIBUTION OF HOURLY MEDIAN VALUES OF SIGNAL INTENSITY

— ALL VALUES, INCLUDING VALUES AFFECTED BY E_s - TYPE PROPAGATION
---- INTERPOLATED VALUES USED DURING HOURS WITH E_s - TYPE PROPAGATION

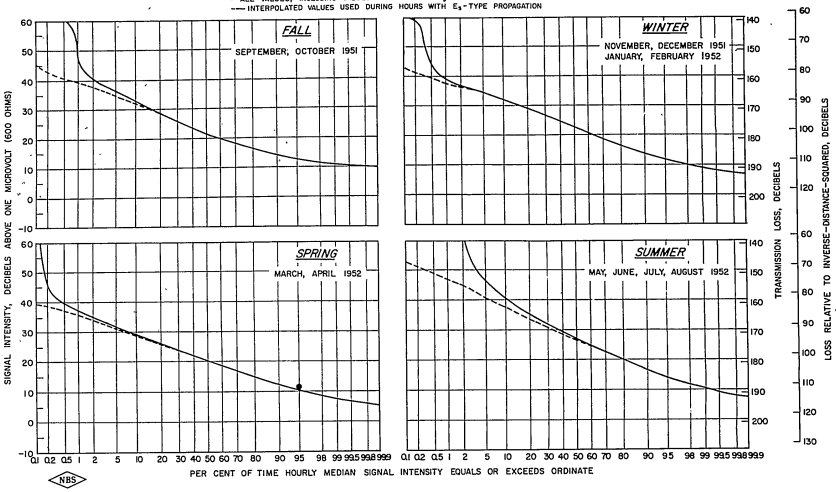

FIG. 30

FARGO TO CHURCHILL — 49.7 Mc/s

CUMULATIVE DISTRIBUTION OF HOURLY MEDIAN VALUES OF SIGNAL INTENSITY

— ALL VALUES, INCLUDING VALUES AFFECTED BY E_s - TYPE PROPAGATION
---- INTERPOLATED VALUES USED DURING HOURS WITH E_s - TYPE PROPAGATION

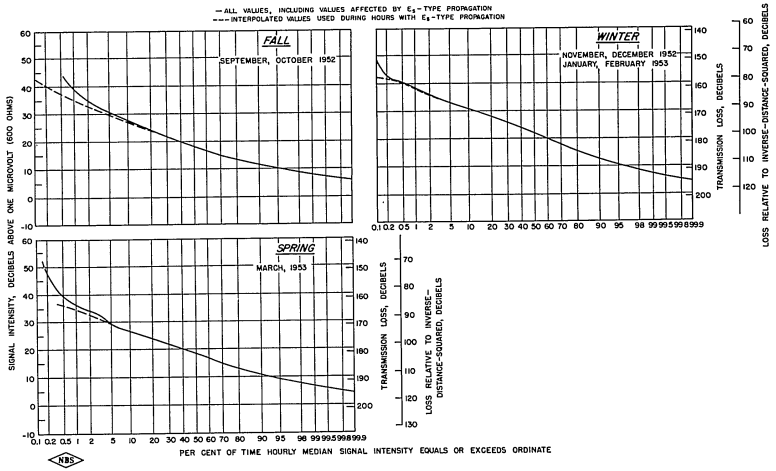

FIG. 31

Declassified in Part - Sanitized Copy Approved for Release @ 50-Yr 2014/06/09 : CIA-RDP81-01043R003000180001-4
Declassified in Part - Sanitized Copy Approved for Release @ 50-Yr 2014/06/09 : CIA-RDP81-01043R003000180001-4

CEDAR RAPIDS TO STERLING — 107.8 Mc/s

CUMULATIVE DISTRIBUTION OF HOURLY MEDIAN VALUES OF SIGNAL INTENSITY

ALL VALUES, INCLUDING VALUES AFFECTED BY E_s-TYPE PROPAGATION
INTERPOLATED VALUES USED DURING HOURS WITH E_s-TYPE PROPAGATION

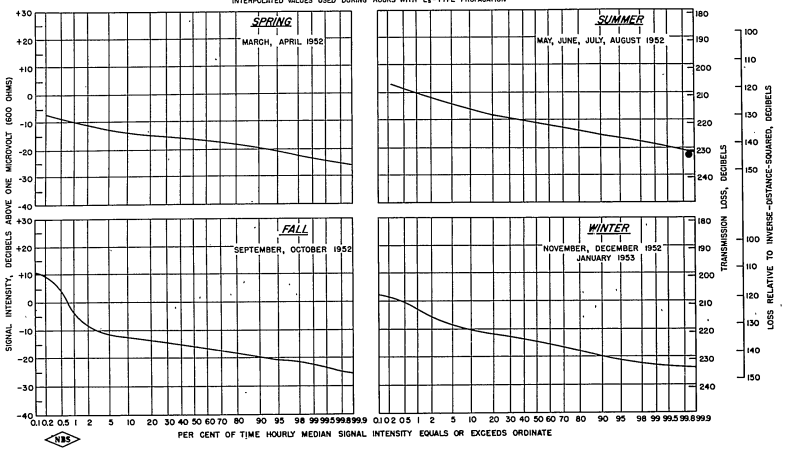

FIG. 32

CEDAR RAPIDS TO STERLING — 27.775 Mc/s

CUMULATIVE DISTRIBUTION OF HOURLY MEDIAN VALUES OF SIGNAL INTENSITY

——ALL VALUES, INCLUDING VALUES AFFECTED BY E_s-TYPE PROPAGATION
- - - INTERPOLATED VALUES USED DURING HOURS WITH E_s-TYPE PROPAGATION

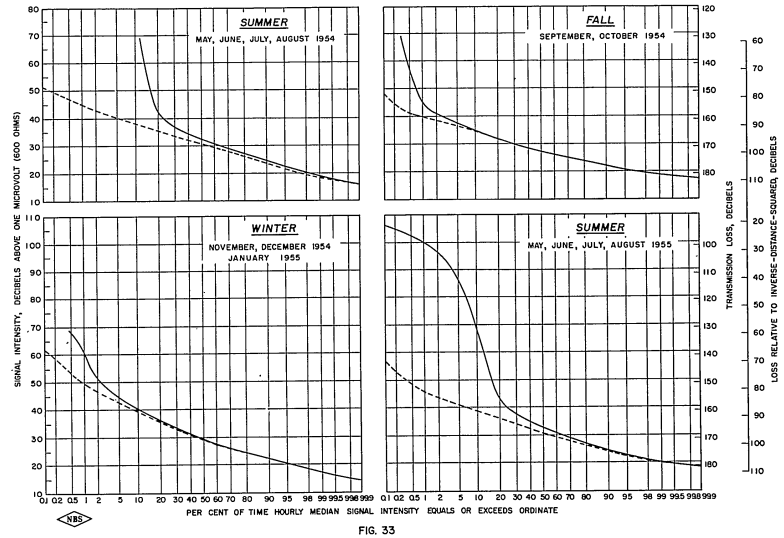

FIG. 33

Declassified in Part - Sanitized Copy Approved for Release @ 50-Yr 2014/06/09 : CIA-RDP81-01043R003000180001-4
Declassified in Part - Sanitized Copy Approved for Release @ 50-Yr 2014/06/09 : CIA-RDP81-01043R003000180001-4

CEDAR RAPIDS TO STERLING — 27.775 Mc/s

CUMULATIVE DISTRIBUTION OF HOURLY MEDIAN VALUES OF SIGNAL INTENSITY

— ALL VALUES, INCLUDING VALUES AFFECTED BY E_s-TYPE PROPAGATION
– – – INTERPOLATED VALUES USED DURING HOURS WITH E_s-TYPE PROPAGATION

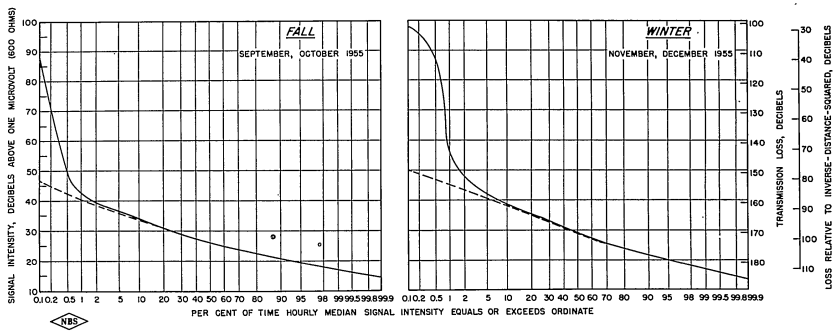
FALL
SEPTEMBER, OCTOBER 1955
WINTER
NOVEMBER, DECEMBER 1955
SIGNAL INTENSITY, DECIBELS ABOVE ONE MICROVOLT (600 OHMS)
TRANSMISSION LOSS, DECIBELS
LOSS RELATIVE TO INVERSE-DISTANCE-SQUARED, DECIBELS
0.1 0.2 0.5 1 2 5 10 20 30 40 50 60 70 80 90 95 98 99 99.5 99.8 99.9
NBS
PER CENT OF TIME HOURLY MEDIAN SIGNAL INTENSITY EQUALS OR EXCEEDS ORDINATE

FIG. 34

ANCHORAGE TO BARROW — 24.325 Mc/s

CUMULATIVE DISTRIBUTION OF HOURLY MEDIAN VALUES OF SIGNAL INTENSITY

— ALL VALUES, INCLUDING VALUES AFFECTED BY E_s-TYPE PROPAGATION
– – – INTERPOLATED VALUES USED DURING HOURS WITH E_s-TYPE PROPAGATION

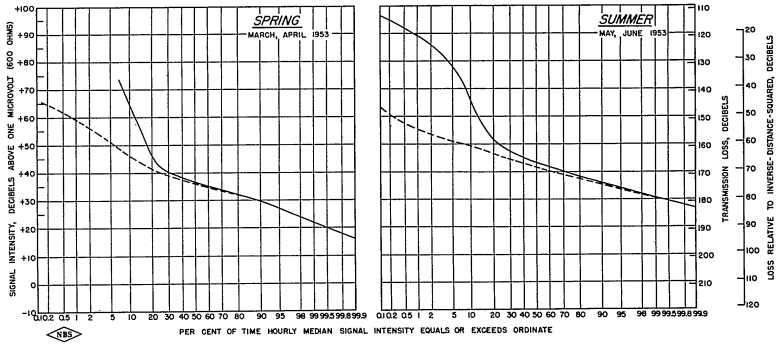
SPRING
MARCH, APRIL 1953
SUMMER
MAY, JUNE 1953
SIGNAL INTENSITY, DECIBELS ABOVE ONE MICROVOLT (600 OHMS)
TRANSMISSION LOSS, DECIBELS
LOSS RELATIVE TO INVERSE-DISTANCE-SQUARED, DECIBELS
0.1 0.2 0.5 1 2 5 10 20 30 40 50 60 70 80 90 95 98 99 99.5 99.8 99.9
NBS
PER CENT OF TIME HOURLY MEDIAN SIGNAL INTENSITY EQUALS OR EXCEEDS ORDINATE

FIG. 35

Declassified in Part - Sanitized Copy Approved for Release @ 50-Yr 2014/06/09 : CIA-RDP81-01043R003000180001-4
Declassified in Part - Sanitized Copy Approved for Release @ 50-Yr 2014/06/09 : CIA-RDP81-01043R003000180001-4

Declassified in Part - Sanitized Copy Approved for Release @ 50-Yr 2014/06/09 : CIA-RDP81-01043R003000180001-4

SEASONAL VARIATION OF SIGNAL INTENSITY

MONTHLY MEDIAN VALUES OF SIGNAL INTENSITY FOR THREE-HOUR PERIODS CENTERED AT 00, 06, 12, AND 18 HOURS, LOCAL TIME AT PATH MIDPOINT, AND LEVEL EXCEEDED 95% OF HOURS DURING MONTH

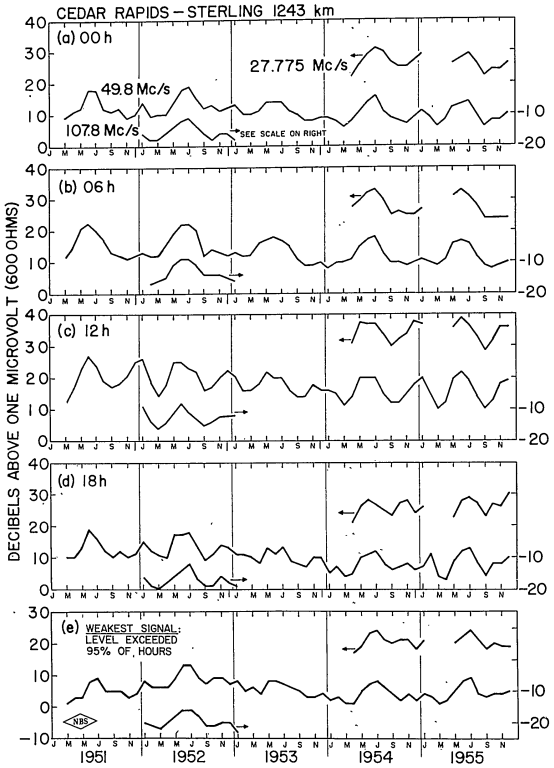

FIG. 36

SEASONAL VARIATION OF SIGNAL INTENSITY

MONTHLY MEDIAN VALUES OF SIGNAL INTENSITY FOR THREE-HOUR PERIODS CENTERED AT 00, 06, 12, AND 18 HOURS, LOCAL TIME AT PATH MIDPOINT, AND LEVEL EXCEEDED 95% OF HOURS DURING MONTH

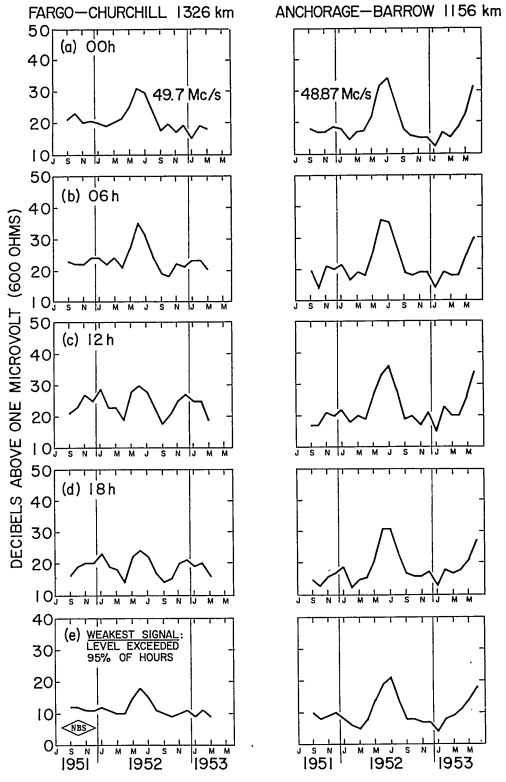

FIG. 37

Declassified in Part - Sanitized Copy Approved for Release @ 50-Yr 2014/06/09 : CIA-RDP81-01043R003000180001-4

Declassified in Part - Sanitized Copy Approved for Release @ 50-Yr 2014/06/09 : CIA-RDP81-01043R003000180001-4

COMPARISON OF FIVE YEARS OF OBSERVATIONS OF SIGNAL INTENSITY

CEDAR RAPIDS TO STERLING – 49.8 Mc/s

MONTHLY MEDIANS OF HOURLY MEDIAN VALUES OF
RECEIVED OPEN-CIRCUIT ANTENNA VOLTAGE – 600 Ω ANTENNA

REFERENCE POWER INPUT TO TRANSMITTER FINAL AMPLIFIER 40 KW; ESTIMATED ANTENNA POWER 30 KW

OBSERVATIONS AFFECTED BY Es-TYPE PROPAGATION OMITTED;
INTERPOLATED VALUES USED WHEN AVAILABLE

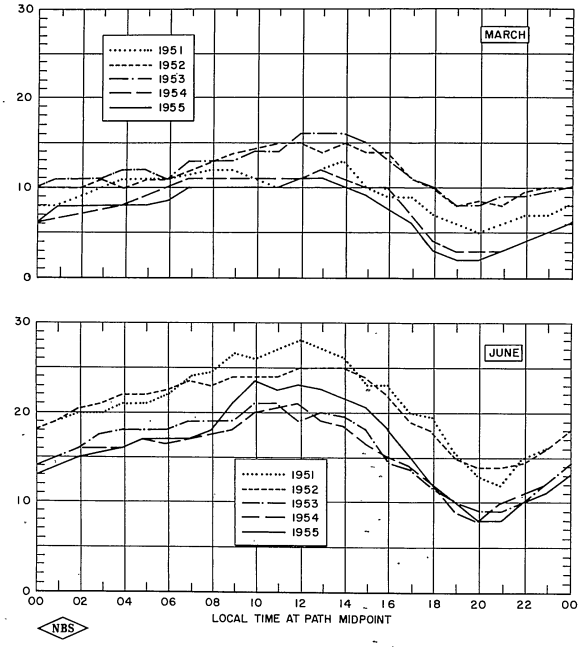

FIG. 38

COMPARISON OF FIVE YEARS OF OBSERVATIONS OF SIGNAL INTENSITY

CEDAR RAPIDS TO STERLING – 49.8 Mc/s

MONTHLY MEDIANS OF HOURLY MEDIAN VALUES OF
RECEIVED OPEN-CIRCUIT ANTENNA VOLTAGE – 600 Ω ANTENNA

REFERENCE POWER INPUT TO TRANSMITTER FINAL AMPLIFIER 40 KW; ESTIMATED ANTENNA POWER 30 KW

OBSERVATIONS AFFECTED BY Es-TYPE PROPAGATION OMITTED;
INTERPOLATED VALUES USED WHEN AVAILABLE

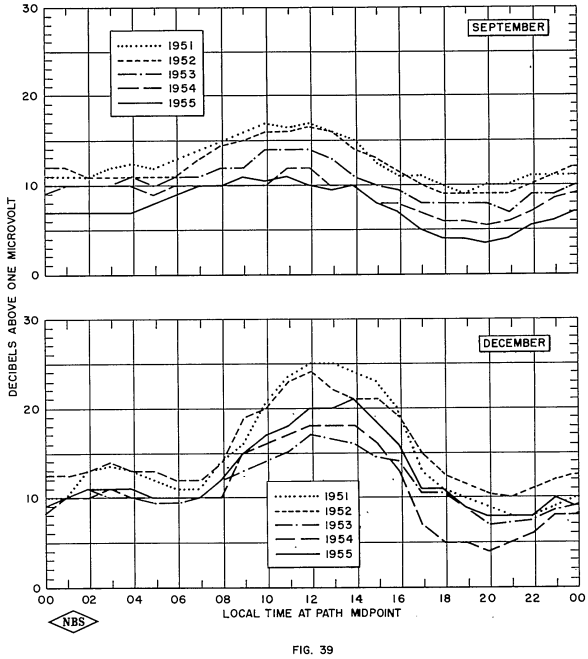

FIG. 39

Declassified in Part - Sanitized Copy Approved for Release @ 50-Yr 2014/06/09 : CIA-RDP81-01043R003000180001-4

Declassified in Part - Sanitized Copy Approved for Release @ 50-Yr 2014/06/09 : CIA-RDP81-01043R003000180001-4

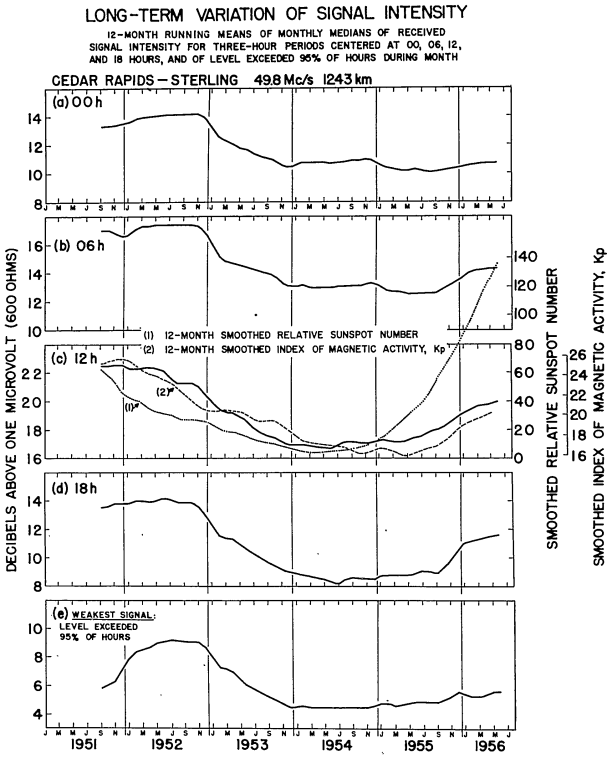
LONG-TERM VARIATION OF SIGNAL INTENSITY
12-MONTH RUNNING MEANS OF MONTHLY MEDIANS OF RECEIVED SIGNAL INTENSITY FOR THREE-HOUR PERIODS CENTERED AT 00, 06, 12, AND 18 HOURS, AND OF LEVEL EXCEEDED 95% OF HOURS DURING MONTH
CEDAR RAPIDS — STERLING 49.8 Mc/s 1243 km
(a) 00 h
(b) 06 h
(c) 12 h
(d) 18 h
(e) WEAKEST SIGNAL: LEVEL EXCEEDED 95% OF HOURS
(1) 12-MONTH SMOOTHED RELATIVE SUNSPOT NUMBER
(2) 12-MONTH SMOOTHED INDEX OF MAGNETIC ACTIVITY, Kp
DECIBELS ABOVE ONE MICROVOLT (600 OHMS)
SMOOTHED RELATIVE SUNSPOT NUMBER
SMOOTHED INDEX OF MAGNETIC ACTIVITY, Kp
1951
1952
1953
1954
1955
1956

FIG. 40

APPENDICES

Declassified in Part - Sanitized Copy Approved for Release @ 50-Yr 2014/06/09 : CIA-RDP81-01043R003000180001-4

Declassified in Part - Sanitized Copy Approved for Release @ 50-Yr 2014/06/09 : CIA-RDP81-01043R003000180001-4

APPENDIX I

MEASUREMENTS OF FREQUENCY DEPENDENCE

PART I - REGULAR PROGRAM OF VOLTAGE RECORDING

R. M. Davis, Jr.
R. C. Kirby

1. INTRODUCTION

The various theories of the scattering of VHF radio waves give expressions for transmission loss in which received power is inversely proportional to some exponent of the transmission frequency.[1,2] The previous reports[3,4,5] and general summary[1] have given earlier experimental data on the value of this exponent n under particular circumstances. This report gives the results of further measurements and indicates the possible sources of error and limitations of the experiment.

The earlier studies showed that the exponent n, representing the ratio of received powers at the two frequencies 49.8 Mc/s and 107.8 Mc/s, varied from about 4 to 12. The median value of the exponent over an extended period was 7. Under conditions of strong signal intensity at 49.8 Mc/s the frequency exponent was higher, in the vicinity of 8. While several factors, such as sporadic-E and tropospheric propagation, could account for many values in the wings of the distribution of n, it was concluded that there was some genuine variation of the exponent with changing conditions in the propagation medium.

2. EXPERIMENTAL PROGRAM

The experimental details of the program have been described in the previous reports.[1,2] During the observing period to be reported here the same methods of frequency dependence observation were followed. Transmitting and receiving antennas were scaled in proportion to their wavelengths so that the geometrical factors were identical for each pair of frequencies. The aperture of the receiving antenna at the higher frequency is smaller than that of the lower by a factor equal to the square of the frequency ratio. An adjustment for "constant aperture" was made; the ratio of the antenna apertures (in decibels) was subtracted from the observed ratio of signal intensities for scaled antennas.

Each ratio of signal intensity for a pair of frequencies was found by comparing the median intensities recorded during simultaneous periods of an hour. The values for such periods were adjusted to insure that they applied to equal radiated power, equal transmission line losses, and equal receiving antenna impedances. Thus adjusted, the decibel ratio of two signal intensities can be interpreted as a ratio of available powers, provided the signal voltages measured are effective root mean square values. A test of this last assumption is made in Part II of this appendix.

Declassified in Part - Sanitized Copy Approved for Release @ 50-Yr 2014/06/09 : CIA-RDP81-01043R003000180001-4

Declassified in Part - Sanitized Copy Approved for Release @ 50-Yr 2014/06/09 : CIA-RDP81-01043R003000180001-4

3. RESULTS

3.1 Observed Frequency Exponents

Figure I-1 incorporates in summary form all of the observations of frequency dependence previously unreported. In each panel the histogram shows the distribution of signal intensity ratios and frequency exponents found when signal intensities at the indicated frequencies were compared. In the top row all of the observations for each pair of frequencies are included. In the middle row of panels only cases of true scatter propagation are retained, unadulterated by sporadic E or other recognizable anomalous conditions. The influence of sporadic E is eliminated by discarding both the hours of recognized Es occurrence and the adjacent hours. Hours of abnormally high absorption, affecting different frequencies by different amounts, are also discarded, as are hours when auroral, or "sputter," propagation was present. Finally in the bottom row of panels attention is confined to the five hours centered approximately on local noon at the path midpoint. These are the hours of typically strongest signals and presumably little influence of aspect-sensitive meteor reflections; only hours uncontaminated by sporadic E or abnormal absorption are used in these distributions. The special circumstances of the frequency-dependence recording of each circuit will now be mentioned.

a. Cedar Rapids to Sterling, 107.8 Mc/s vs. 49.8 Mc/s, rhombic to rhombic

This is a continuation for the four months, October, 1952 through January, 1953, of the study reported previously, which covered January through September, 1952. It will be noted that the shape of the distribution of all observations (top panel), the median frequency exponent of 6.9, and the range of exponents is quite similar to the earlier data. The character of the distribution is affected very little where sporadic-E hours are excluded in the middle panel. At the bottom, however, the distribution is shifted to the right and a higher median exponent, 7.8, results when the smaller sample of data for the five hours around noon is considered.

Operation of the scatter transmission equipment at 107.8 Mc/s presented special difficulties; the frequency stability and recording bandwidth were inadequate for reliable recordings at low signal levels. For the period reported in Figure I-1, however, the experimental data are felt to be of comparable quality with those at 49.8 Mc/s.

b. Cedar Rapids to Sterling, 49.8 Mc/s vs. 27.775 Mc/s, rhombic to rhombic

The middle column of histograms of Figure I-1 presents the frequency dependence found by comparing the signals received at these two frequencies. Again all system parameters have been adjusted to equal values for the two frequencies. Signal intensity ratios for scaled antennas at the two frequencies are shown on the bottom scale, and the corresponding frequency exponents, after adjustment to unit aperture of the receiving antenna, are shown along the top scale.

The histograms show that systematically lower values of frequency exponent result from the comparison of intensities 27.775/49.8 than from 49.8/107.8. Where a median of 6.9 is applied to the higher pair of frequencies, the median exponent is 4.7 for the lower pair. This is true whether all observations are considered, as in the top panel, or only those free of sporadic E and high absorption hours, as in the middle panel. When midday hours with their generally strong signals are the basis of comparison, a slightly higher value of exponent, 5.1, is observed. If allowance is made for the relatively high absorption at 28 Mc/s, a value of n as high as 6 to 6.5 for the 27.775/49.8 comparison may be in order for the scattering process.

No definite source of error in the experimental arrangements has yet been found sufficient to prove that the observed variation is not genuine. Two factors, however, tend in this direction. First, the available power from background galactic noise at 27.775 Mc/s was as much as 3 db less than expected on the basis of other observations. Second, the antenna siting was not ideal, as is presupposed in the comparison of signal intensities.

It is felt on the whole that caution should be used in accepting the variation of exponent with frequency. Recent preliminary results from a more elaborate experiment indicate that a single value of frequency exponent may actually hold over a wide range of frequencies.

c. Anchorage to Barrow, 48.87 Mc/s vs. 24.325 Mc/s, Yagi to Yagi

The last column of histograms in Figure I-1 shows the frequency dependence results of four months of simultaneous recording of Yagi-to-Yagi transmissions over an arctic path at 48.87 Mc/s and 24.325 Mc/s. For this recording period wide dynamic range recorders were in operation, so that all the sporadic-E signal intensities fell within the limits of the recorder. The wide range of ratios that resulted from complete Es recording are shown in the top panel. They will be discussed later in connection with Figure I-9.

The shaded portion of the Anchorage to Barrow histograms indicates ratios for hours when high absorption was in effect, as deduced from a comparison of cosmic noise levels at the two frequencies and from ionospheric sounder records. It was believed that non-deviative absorption, affecting the lower frequency more than the higher, would reduce the frequency exponent. The figure does indeed indicate that hours of unusually high absorption are associated with relatively low ratios. The middle panel shows, however, that when the low ratios for absorption hours are discarded, as well as the ratios for hours of Es and sputter, the resulting median ratio is the same as for all observations, 5.3.

In the bottom panel is shown the distribution of ratios from the five hours centered on local noon. In this case the median ratio is again 5.3. Unlike the noontime signals on the temperate zone path, Anchorage to Barrow signals do not in general reach a maximum around noon. Thus noontime ratios are not above the average for the 24 hours.

Declassified in Part - Sanitized Copy Approved for Release @ 50-Yr 2014/06/09 : CIA-RDP81-01043R003000180001-4

Declassified in Part - Sanitized Copy Approved for Release @ 50-Yr 2014/06/09 : CIA-RDP81-01043R003000180001-4

3.2 Correlation of Signal Intensities at Various Frequencies

In the next three figures, I-2, I-3, and I-4, the diurnal variation of the median signal intensity is compared for the two frequencies in use on a given path. Each comparison is based on a single month's data, the month of June in each case, though the data were obtained in three different years. The lower panel of each figure is a histogram of ratios of signal intensity for the two frequencies in question. Values in the histogram represent all hours where both frequencies were in operation, except those when sporadic E was in control and no interpolated value for the scatter level could be obtained.

It will be noted in Figures I-2 through I-4 that frequency exponents varying over a range of 4 or more were recorded in substantial numbers of cases. This does not mean that signal intensities occurring at the two frequencies were unrelated. The medians of these signal intensities follow the same general diurnal patterns in each of the three comparisons. The Cedar Rapids to Sterling comparison of 49.8 Mc/s with 27.775 Mc/s (Figure I-3) shows the closest agreement of diurnal patterns of signal intensity. For this case the median value of n was 4.3 with a range of 5.9 to 3.1 from the 10% to 90% value. Anchorage to Barrow, 48.87 vs. 24.325 Mc/s (Figure I-4) with a weaker diurnal agreement has a median exponent of 5.0 and a 10% to 90% range of 6.3 to 3.3. Finally the comparison of 107.8 with 49.8 Mc/s intensities on Cedar Rapids to Sterling (Figure I-2) gives a median exponent of 7.2 and a 10% to 90% range of 8.4 to 6.0.

3.3 Diurnal and Seasonal Variation of Frequency Exponents

Figures I-5 through I-8 portray the dependence on local time of the frequency exponent under selected conditions. Data from the 107.8 vs. 49.8 Mc/s Cedar Rapids to Sterling experiment are shown in Figure I-5. The diurnal variation of signal intensity ratio and frequency exponent n are given for two summer months, June and July, 1952, and two winter months, December, 1952, and January, 1953. It will be seen that the diurnal variation of n bears some resemblance to the variation of the median signal intensity itself. There is the same maximum around midday and the same tendency toward low values around 2000. As already mentioned, generally high values of signal intensity tend to result in high values of frequency exponent. Another possible tendency that seems to be borne out in Figure I-5 is the occurrence of higher values of exponent in winter than in summer months. In this small amount of data the tendency is not striking. But more hours are marked by exponents of 8 and above in December and January than in June and July. The range of observed median exponents is greater in winter than in summer, 7 db in ratio as opposed to 5.

Figures I-6 and I-7 present curves of diurnal variation of the median frequency exponent for each month from June, 1954, through January, 1955, Cedar Rapids to Sterling, 49.8 vs. 27.775 Mc/s. All possible effects of Es propagation are eliminated from the data. The exponent undergoes an increase about 0800 local time. In June through September it decreases

during the afternoon or early evening. In subsequent months the exponent maintains a fairly high level, or may even increase, during the evening. There is some evidence of a seasonal variation in the exponent. From a median value of 4.2 in June the exponent increases to 5.2 in October. It remains high in November and December and slips back to a medium value of 4.7 in January. While the data in this sample is scarcely sufficient for strong conclusions, it does support the possibility of a seasonal dependence of frequency exponent, with a minimum in the summer months. In the 49.8/27.775 Mc/s results the effect is undoubtedly partly due to differential absorption effects.

Figure I-8 shows the diurnal variation of the frequency exponent for the Anchorage to Barrow path in the equinox period of March-April and the summer months May-June. Only data uncontaminated by sporadic E and unaffected by absorption or sputter are included in the curves. The diurnal pattern for this arctic path is basically unlike the temperate zone curves of Figures I-5 through I-7. The midday maximum is lacking and there is evidence of a midnight and early morning peak. This distribution may be accounted for by two factors. First, the intense daytime absorption in the Arctic with its greater effect at lower frequencies would tend to suppress a midday maximum in frequency exponent. Observations associated with high absorption are omitted from the curves of Figure I-8, but the same tendency may be residual in the remaining observations. Second, occurrences of sporadic E too weak to be identified and removed would principally affect the nighttime hours 1800 to 0600. This would raise the level of the 24 Mc/s signals relative to those at 49 Mc/s and would tend to produce a nighttime maximum in the frequency exponent.

An additional tendency shown in Figure I-8 is the low general level of frequency exponent in May-June. The median ratio of signal intensity ratios is 23 in March-April compared to 22 in May-June.

3.4 Frequency Dependence During Periods of Sporadic E and Sputter

The histograms of Figure I-9 provide an indication of the dependence of signal intensity on frequency during the recognized contamination of the signal by sporadic-E and sputter propagation. The two displays serve as an enlargement of the corresponding histograms of Figure I-1.

In the upper panel ratios of signal intensity and corresponding frequency exponents are displayed for the four months of simultaneous recording at 48.87 and 24.325 Mc/s on the Anchorage to Barrow path. At the top is shown the distribution of exponents during the reflection from auroras referred to as "sputter." The distribution is broader than that for simple scatter propagation in Figure I-1, and the median exponent is 6.3 compared to 5.3 for scatter. Still, exponents during sputter are not systematically different from those observed during normal scatter conditions.

The upper panel of Figure I-9 also shows the frequency exponents derived during known sporadic E. These are shown in solid black. For the period of the recording program a wide dynamic range recorder was in use at Barrow. It permitted the registering of the entire range of intensities

Declassified in Part - Sanitized Copy Approved for Release @ 50-Yr 2014/06/09 : CIA-RDP81-01043R003000180001-4

Declassified in Part - Sanitized Copy Approved for Release @ 50-Yr 2014/06/09 : CIA-RDP81-01043R003000180001-4

in effect during Es. Thus the black columns represent the array of actual ratios that prevailed when one or both frequencies were affected by sporadic E. Many of the values are for hours when Es was present on 24 Mc/s but not on 49 Mc/s. For this reason, the Anchorage to Barrow histogram does not strictly represent the frequency dependence of sporadic-E signal intensities, although it is a good approximation.

The distribution of Es frequency exponents for the arctic path reveals a large, systematic increase over the values measured for normal scatter. With sporadic E present on one or both of the frequencies the median exponent is 13.2 compared to the scatter value of 5.3. Another study of the Anchorage-Barrow data at 48.87 and 24.325 Mc/s confirmed the Es frequency exponent of roughly 13. Simultaneous five-minute periods when sporadic E was recognizable at both frequencies were compared. A median frequency exponent of 12.9 was calculated, based on all available periods from March through June, 1953.

Figure I-9 also contains a histogram of signal intensity ratios for sporadic-E and adjacent hours for the Cedar Rapids to Sterling comparisons of June, 1954, through January, 1955. Values shown are generally too low because the recorders were incapable of registering the full Es signal intensity in many cases. Such saturation occurred much more often at 28 Mc/s than at 50 Mc/s, so that the true ratios were equal or greater than those shown. Under these conditions the median frequency exponent per unit aperture of the receiving antenna is found to be 11.8 during sporadic E. (A more comprehensive study of frequency dependence during sporadic-E propagation observed at 49.8 and 27.775 Mc/s on the Cedar Rapids-Sterling path has been published.[6])

4. CONCLUSIONS

The frequency dependence of received power appears to depart from a constant exponential relationship on the basis of the data reported. A median frequency exponent of 6.9 was found for the 107.8 to 49.8 Mc/s comparison in the U. S., against a value of 4.7 for the 49.8 to 27.775 Mc/s comparison. In the Arctic the corresponding exponent for 48.87 vs. 24.325 Mc/s was 5.3. Despite this evidence, it is felt that the indicated variation in the frequency exponent should not be accepted without further confirmation. Certain possible sources of error in the experiment may be responsible for the observed curvature of the frequency exponent.

The frequency exponent undergoes a diurnal variation and appears to be lower in summer than at other seasons. A comparison of signal intensities during sporadic-E propagation reveals exponent values very much higher than those pertaining to normal scatter. These exponents cover a wide range of values.

APPENDIX I

PART II - DETERMINATION OF FREQUENCY DEPENDENCE EXPONENT BY TRUE POWER MEASUREMENT

G. E. Boggs and N. C. Hekimian

1. INTRODUCTION

In experimental measurements of frequency-dependence, as reported in Part I and in the previous reports,[3,4] the question has arisen as to the validity of interpretation of average-voltage measurements in terms of ratios of received power at the two observed frequencies. In an effort to determine the experimentally correct value, the tests described in this report were initiated.

To understand the basic differences between the usual averaged voltage recording and a true power average recording, it is well to digress at this point to illustrate the differences encountered in a simple idealized ensemble of three numbers. Consider the set (1, 2, 3). The average is 2 and the root average square is 2.16. Now consider a second set (2, 1, 2). The average is 1.67 and the root average square is 1.73. It should be observed that in both cases the root average square is greater than the average. Indeed this is always the case with any sequence of values averaged in these fashions where all of the values averaged are not identical. The order of the inequality can never reverse and is only an identity when all values are the same in the set being analyzed. The greater the range of values, in general, the greater is the discrepancy. Applied to field intensity recording this shows that power and voltage recording will differ greatest with widely fluctuating signals or noisy signals so long as the fluctuations considered occur within the averaging interval of the recorder.

In a practical sense average power recording can be accomplished by squaring the recorded signal prior to averaging. Since in general a rather large range of signal level is anticipated, some compressed system of recording is preferable, one popular method being a logarithmic scale. Where AGC systems are used to obtain this type of characteristic, it must be controlled by the averaged output which, as stated before, must follow the squaring device. This determines the sequence of devices in the block diagram. The averaging circuit is conventionally a simple RC low-pass filter and the averaging interval is usually considered to be RC seconds. Thus, the interval during which variations in signal level will cause differences between root average square recordings and averaged voltage recording is RC seconds and variations of slower rate should cause no discrepancy.

The basis of the experiment was the measurement signals at 49.8 and 107.8 Mc/s on a time-sharing multiplexing system into a true power recorder while simultaneously making continuous voltage recordings of the signals

Declassified in Part - Sanitized Copy Approved for Release @ 50-Yr 2014/06/09 : CIA-RDP81-01043R003000180001-4

Declassified in Part - Sanitized Copy Approved for Release @ 50-Yr 2014/06/09 : CIA-RDP81-01043R003000180001-4

in separate channels. The recording intervals were taken as 20 minutes on each channel. The higher frequency transmitter was run with an off period of several minutes every half-hour included for noise level determination. Because of the consistent high level of the lower frequency signal, noise level determination was unnecessary.

The experiment was conducted during the month of January, 1953. The recording site was Sterling, Virginia, and the transmitter was located at Cedar Rapids, Iowa. This experiment was part of the "Variations with Frequency" portion of the program outlined in NBS Report 8A111, pp. 4-5, and was mentioned in Appendix I of that report.

In addition to the basic purpose of the experiment, it was felt that the tests would serve to check the validity of simple voltage recording as a basis for power measurement at either frequency, and comparisons were made toward this end.

2. RESULTS

The recorded data was scaled for 20-minute interval median values in conventional fashion. Data for periods of unscalable level or prevalent interference or equipment trouble at either site were discarded. Insofar as possible, meteor bursts were disregarded in the scaling. Due to the time multiplexing, comparisons had to be made for periods where one or the other frequency was recorded but not both. To improve the comparison, when a value was needed for an interval when the signal was not recorded, the averaged decibel level for periods immediately prior and following was used. Intervals where either the prior or following periods were not recorded or usable were discarded. For example, if the 49.8 Mc/s signal was recorded from 1100 to 1120 and 1140 to 1200 and the 107.8 Mc/s signal from 1120 to 1140, the averaged values of the first and third intervals were used for the 49.8 Mc/s reading and comparison was made to the second interval, 107.8 Mc/s, signal. If the first interval was subject to error, it was discarded and a comparison centered on the third interval would be used if good data were available for the fourth period, and so on. Several voltage recordings of both signals were scaled in the same fashion. Calibration for 107.8 Mc/s was made with 20 db IF attenuation added to mask converter noise in the signal range. Correction was made to this reading. Noise levels during the transmitter off periods were scaled for the 107.8 Mc/s signal and the averaging process applied to them as with the other signals. True signal level for the 107.8 Mc/s signal was obtained by converting the decibel level to equivalent microvolts squared and subtracting the noise voltage squared from the recorded signal and noise. The net equivalent microvolts squared were then reconverted to signal level in decibels. Correction for actual radiated power, transmission line impedances, line losses, etc., totaling 18 decibels was subtracted from the 49.8 Mc/s signal relative to the 107.8 signal, and the difference between the corrected 49.8 Mc/s signal and the true 107.8 Mc/s level was divided by 10 $\log_{10}$ (107.8/49.8) to convert to exponent of the frequency ratio, 2.16. The accuracy of the method is contingent upon the signal and noise of the 107.8 Mc/s signal adding in the

square as well as validity of the averages used for the signal missing during the comparison periods. Further, it is assumed in this signal extraction technique that the noise is adequately masked in calibration and that the converter is linear from noise level to the upper calibration level.

The effect of power recording is evident in the pen records by the unusually large range of signal swing. Although this causes some extra difficulty in arriving at a satisfactory median in scaling, the records are still readily scaled. There were no other significant differences noted between voltage and power recordings.

The statistics of the experiment are summarized as follows:

Number of exponent determinations:		115
Over-all average of exponent	:	7.51(3)
Average deviation from average	:	0.46(3) or 1.56 db
Median exponent	:	7.58
Greatest recorded exponent	:	10.15 (date: January 20, 1953)
Least recorded exponent	:	4.74 (date: January 20, 1953)

Figure I-10 presents a bar graph showing the distribution of recorded exponent values for the entire test. Comparison should be made to Figure 53 of NBS Report 8A111 (or Figure I-1 of this appendix) which was based on conventional voltage recording. Figure I-11 presents the averaged daily exponent and the range of values together with the number of observations for each day of the experiment. Figure I-12 shows 20-minute median values for a typical day.

Comparison between voltage and power recording for the strong 49.8 Mc/s signal showed less average difference than the estimated accuracy of the data, and it is assumed that the two systems are essentially in agreement for this type of signal. However, comparisons of the 107.8 Mc/s data almost always showed about 2 db difference in favor of the power recording system. Since the compared data was scaled in the same fashion by the same personnel and calibrations were made on both systems by the same operators, it is assumed that there may be an inherent difference in the response of the average voltage vs power recording systems for signals of this type. Since the 107.8 Mc/s signal is well within the noise level, it is subject to much greater "small detail" fluctuations and as seen in the introduction, the root average square will tend to exceed the average as the spread and fine structure of the test specimen is increased. The 107.8 Mc/s true signal level is shown in Figure I-13 for both voltage and power recording during a typical day. Other usable days were substantially the same.

3. CONCLUSIONS

A median value of $7\frac{1}{2}$ for the frequency dependency exponent was obtained for the period of the observations, all taken near midday. Further, the validity of voltage recording as a basis for power calculations seems

Declassified in Part - Sanitized Copy Approved for Release @ 50-Yr 2014/06/09 : CIA-RDP81-01043R003000180001-4

Declassified in Part - Sanitized Copy Approved for Release @ 50-Yr 2014/06/09 : CIA-RDP81-01043R003000180001-4

verified, especially where the signal recorded does not have high level fine structure during the averaging interval of the recorder. In the case of noisy or wide signal level excursions during the averaging interval, there may be first order errors introduced.

4. DESCRIPTION OF EQUIPMENT

The block diagram for the recording systems is shown in Figure 1-14 and is conventional except in the squaring amplifier in the second IF chain of the power recorder and in the time multiplexer. The squaring amplifier circuit is based on a design of J. R. Johler of the Central Radio Propagation Laboratory. It employs a push-push plate, push-pull grid arrangement wherein the plate circuit is tuned to the second harmonic of the input. Squaring is excellent over at least 40 db input range.

The power recorder bandwidth was 6 Kc/s compared to about 2.5 Kc/s for the voltage recording channels. This caused the apparent recorded 107.8 Mc/s signal in noise and noise levels to differ considerably in actual use; however, signal extraction eliminates this effect.

The cathode follower was included to prevent switching effects in multiplexing from disturbing the voltage recording channels. Sufficient padding was left in the 0-70 db attenuators to cause no disturbance in the voltage recorder chains.

The GS-3 receiver and power supply were highly gain stabilized units developed by the authors at the Central Radio Propagation Laboratory.

REFERENCES

1. D. K. Bailey, R. Bateman, R. C. Kirby, "Radio Transmission at VHF by Scattering and Other Processes in the Lower Ionosphere," Proc. I.R.E., vol. 43, pp. 1181-1230, October, 1955. (Reprints are included as Appendix XII in a limited number of copies of this report, furnished to Contracting Officer, USASEL; copies were also furnished earlier to the Contracting Officer as NBS Report 3563.)

2. A. D. Wheelon, "Radio Frequency and Scattering Angle Dependence of Ionospheric Scatter Propagation at VHF," Jour. Geophys. Res., vol. 62, pp. 93-112, March, 1957.

3. D. K. Bailey, R. Bateman, R. C. Kirby, "First Report on Regular VHF Ionospheric Propagation Observable Over Long Distances," NBS Report No. 8All1, June 30, 1952, (Interim Technical Report on MIPR No. 821-PHIBP-51-04).

4. D. K. Bailey, R. Bateman, R. C. Kirby, "Second Report on Regular VHF Ionospheric Propagation Observable Over Long Distances," NBS Report No. 8All7, June 30, 1953, (Interim Technical Report on MIPR No. 821-PHIBP-51-04).

5. R. C. Kirby, "VHF Propagation by Ionospheric Scattering - A Survey of Experimental Results," Trans. I.R.E., CS-4, 1955.

6. R. M. Davis and E. K. Smith, "The Effect of Sporadic E on VHF Transmission in the U. S.," NBS Report No. 5547, Jan. 28, 1958.

Declassified in Part - Sanitized Copy Approved for Release @ 50-Yr 2014/06/09 : CIA-RDP81-01043R003000180001-4

Declassified in Part - Sanitized Copy Approved for Release @ 50-Yr 2014/06/09 : CIA-RDP81-01043R003000180001-4

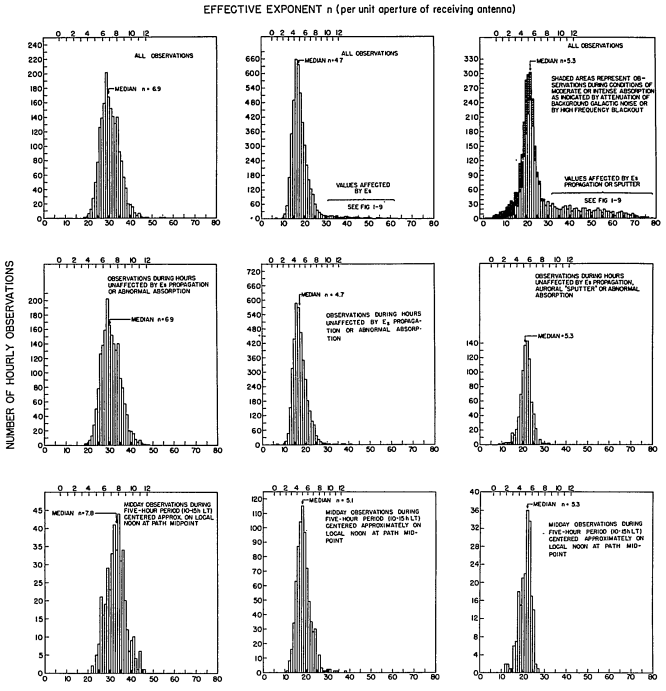
EFFECTIVE EXPONENT n (per unit aperture of receiving antenna)
NUMBER OF HOURLY OBSERVATIONS
ALL OBSERVATIONS
MEDIAN n = 6.9
MEDIAN n=4.7
VALUES AFFECTED BY Es
SEE FIG 1-9
MEDIAN n=5.3
SHADED AREAS REPRESENT OBSERVATIONS DURING CONDITIONS OF MODERATE OR INTENSE ABSORPTION AS INDICATED BY ATTENUATION OF BACKGROUND GALACTIC NOISE, OR BY HIGH FREQUENCY BLACKOUT
VALUES AFFECTED BY Es PROPAGATION OR SPUTTER
OBSERVATIONS DURING HOURS UNAFFECTED BY Es PROPAGATION OR ABNORMAL ABSORPTION
OBSERVATIONS DURING HOURS UNAFFECTED BY Es PROPAGATION, AURORAL "SPUTTER" OR ABNORMAL ABSORPTION
MEDIAN n=7.8
MIDDAY OBSERVATIONS DURING FIVE-HOUR PERIOD (10-15h LT) CENTERED APPROX. ON LOCAL NOON AT PATH MIDPOINT
MEDIAN n = 5.1
MIDDAY OBSERVATIONS DURING FIVE-HOUR PERIOD (10-15h LT) CENTERED APPROXIMATELY ON LOCAL NOON AT PATH MIDPOINT
RATIO OF RECEIVED SIGNAL INTENSITIES (SCALED ANTENNAS) DECIBELS

10.7.80 Mc/s vs 49.80 Mc/s
CEDAR RAPIDS-STERLING
OCT 52 THROUGH JAN. 53

27.775 Mc/s vs 49.80 Mc/s
CEDAR RAPIDS-STERLING
JUNE 54 THROUGH JAN. 55

24.325 Mc/s vs 48.87 Mc/s
ANCHORAGE-BARROW
MARCH 53 THROUGH JUNE 53

FIGURE I-1

Declassified in Part - Sanitized Copy Approved for Release @ 50-Yr 2014/06/09 : CIA-RDP81-01043R003000180001-4

Declassified in Part - Sanitized Copy Approved for Release @ 50-Yr 2014/06/09 : CIA-RDP81-01043R003000180001-4

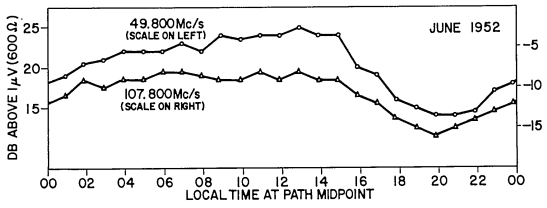

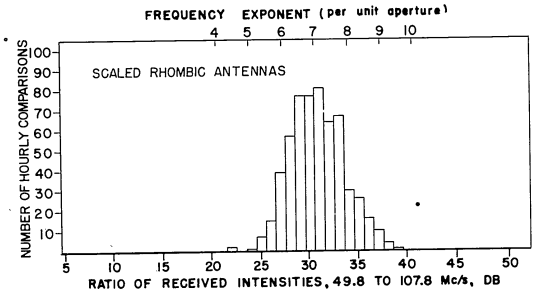
FREQUENCY EXPONENT (per unit aperture)
SCALED RHOMBIC ANTENNAS
NUMBER OF HOURLY COMPARISONS
RATIO OF RECEIVED INTENSITIES, 49.8 TO 107.8 Mc/s, DB

COMPARISON OF SIGNAL INTENSITIES, 107.8 vs. 49.8 Mc/s
Cedar Rapids to Sterling

FIGURE 1 – 2

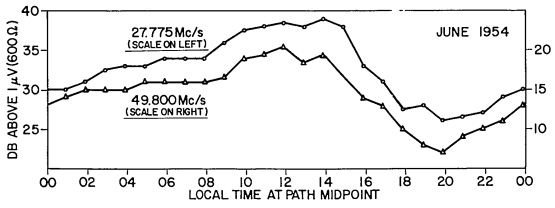

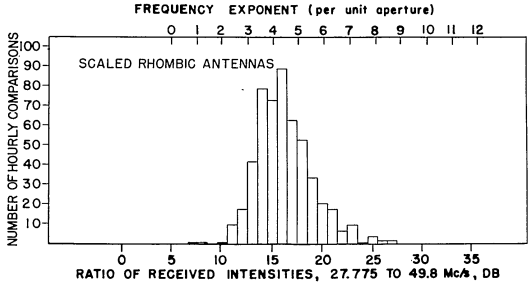
FREQUENCY EXPONENT (per unit aperture)
SCALED RHOMBIC ANTENNAS
NUMBER OF HOURLY COMPARISONS
RATIO OF RECEIVED INTENSITIES, 27.775 TO 49.8 Mc/s, DB

COMPARISON OF SIGNAL INTENSITIES, 49.8 vs. 27.775 Mc/s
Cedar Rapids to Sterling

FIGURE 1 – 3

Declassified in Part - Sanitized Copy Approved for Release @ 50-Yr 2014/06/09 : CIA-RDP81-01043R003000180001-4

Declassified in Part - Sanitized Copy Approved for Release @ 50-Yr 2014/06/09 : CIA-RDP81-01043R003000180001-4

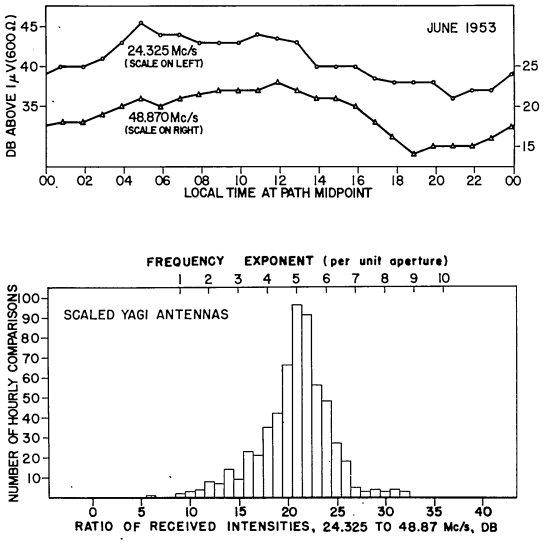

COMPARISON OF SIGNAL INTENSITIES, 48.87 vs. 24.325 Mc/s
Anchorage to Barrow

FIGURE 1 – 4

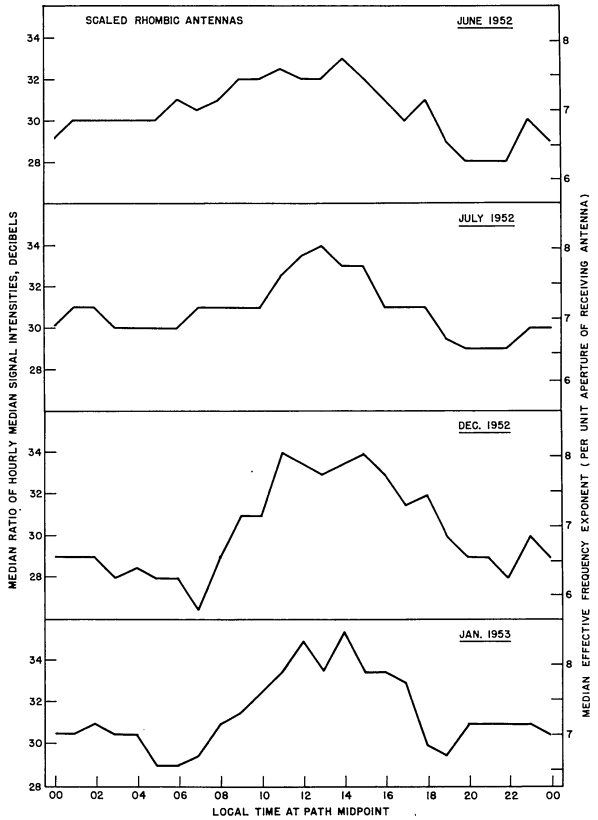

DIURNAL VARIATION OF FREQUENCY DEPENDENCE 107.8 vs 49.8 Mc,
CEDAR RAPIDS TO STERLING, JUNE 1952 – JAN 1953, INCL.

FIGURE 1–5

Declassified in Part - Sanitized Copy Approved for Release @ 50-Yr 2014/06/09 : CIA-RDP81-01043R003000180001-4

Declassified in Part - Sanitized Copy Approved for Release @ 50-Yr 2014/06/09 : CIA-RDP81-01043R003000180001-4

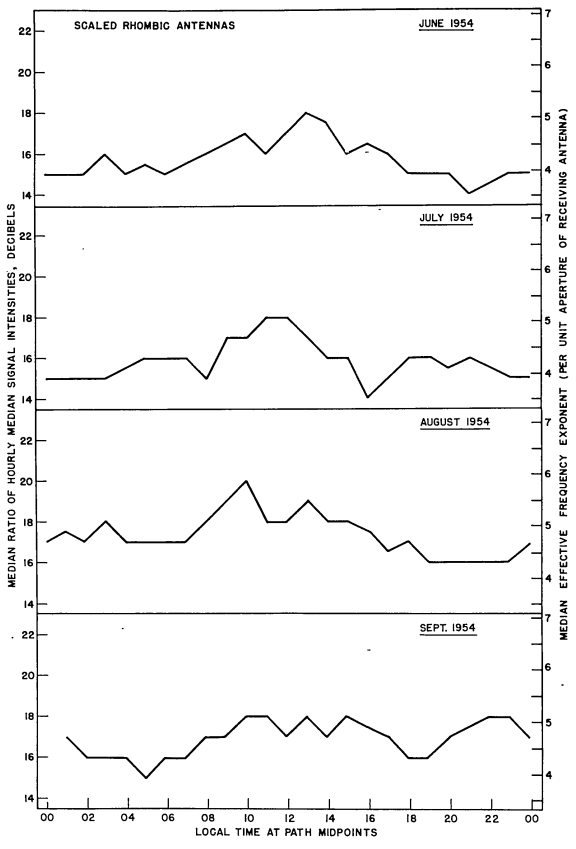
SCALED RHOMBIC ANTENNAS
JUNE 1954
JULY 1954
AUGUST 1954
SEPT. 1954
MEDIAN RATIO OF HOURLY MEDIAN SIGNAL INTENSITIES, DECIBELS
MEDIAN EFFECTIVE FREQUENCY EXPONENT (PER UNIT APERTURE OF RECEIVING ANTENNA)
LOCAL TIME AT PATH MIDPOINTS

DIURNAL VARIATION OF FREQUENCY DEPENDENCE 49.8 vs 27.775 Mc,
CEDAR RAPIDS TO STERLING, JUNE—SEPT. 1954, INCL.

FIGURE 1—6

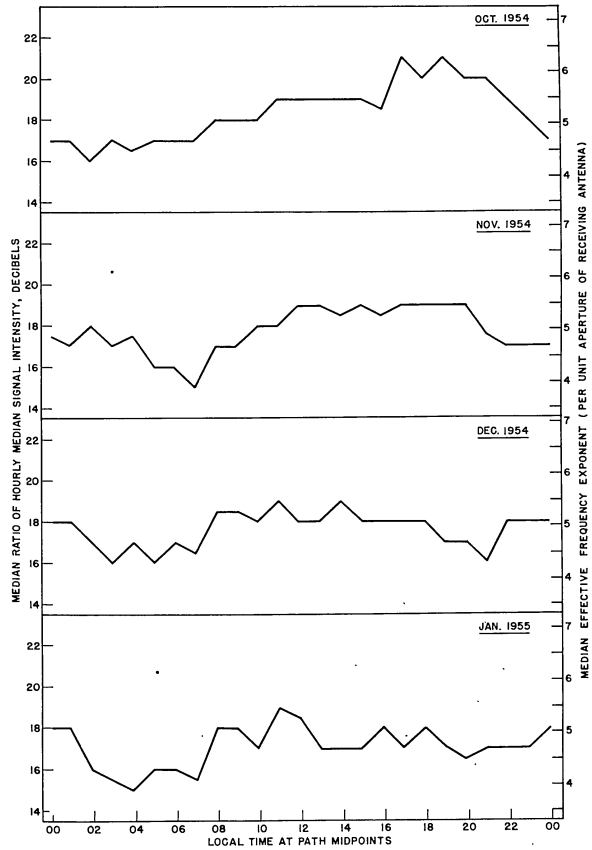
OCT. 1954
NOV. 1954
DEC. 1954
JAN. 1955
MEDIAN RATIO OF HOURLY MEDIAN SIGNAL INTENSITY, DECIBELS
MEDIAN EFFECTIVE FREQUENCY EXPONENT (PER UNIT APERTURE OF RECEIVING ANTENNA)
LOCAL TIME AT PATH MIDPOINTS

DIURNAL VARIATION OF FREQUENCY DEPENDENCE 49.8 vs 27.775 Mc,
CEDAR RAPIDS TO STERLING, OCT. 1954—JAN. 1955, INCL.

FIGURE 1—7

Declassified in Part - Sanitized Copy Approved for Release @ 50-Yr 2014/06/09 : CIA-RDP81-01043R003000180001-4

Declassified in Part - Sanitized Copy Approved for Release @ 50-Yr 2014/06/09 : CIA-RDP81-01043R003000180001-4

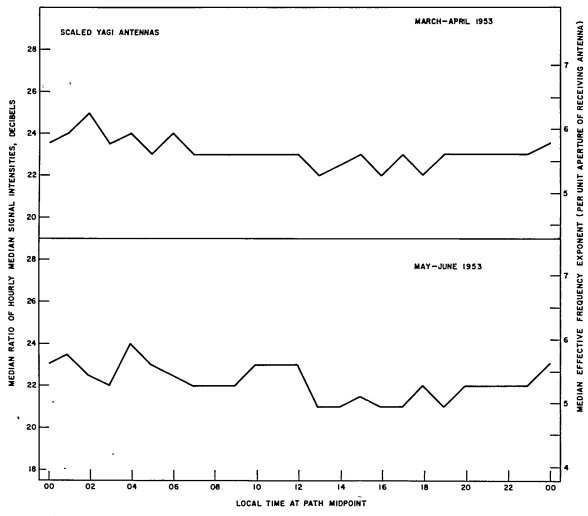
SCALED YAGI ANTENNAS
MARCH–APRIL 1953
MAY–JUNE 1953
MEDIAN RATIO OF HOURLY MEDIAN SIGNAL INTENSITIES, DECIBELS
MEDIAN EFFECTIVE FREQUENCY EXPONENT (PER UNIT APERTURE OF RECEIVING ANTENNA)
LOCAL TIME AT PATH MIDPOINT

DIURNAL VARIATION OF FREQUENCY DEPENDENCE 48.87 vs 24.325 Mc, ANCHORAGE TO BARROW, MARCH–JUNE 1953, INCL.

FIGURE I-8

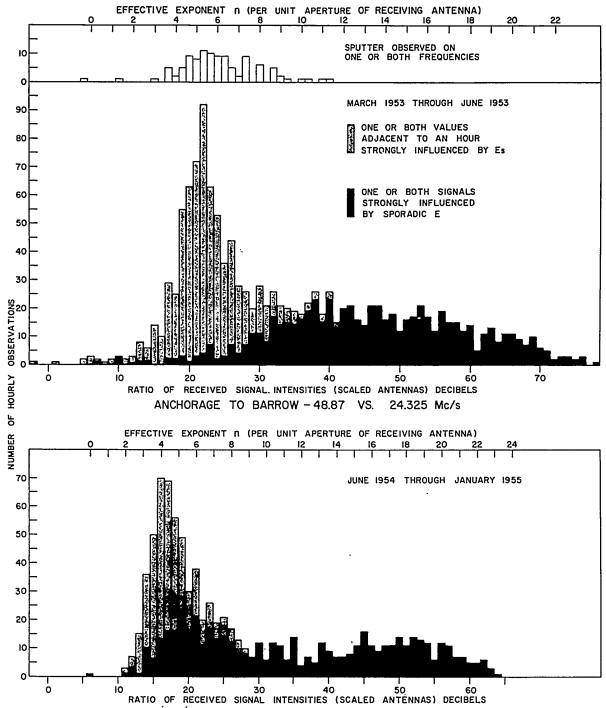
EFFECTIVE EXPONENT n (PER UNIT APERTURE OF RECEIVING ANTENNA)
SPUTTER OBSERVED ON ONE OR BOTH FREQUENCIES
MARCH 1953 THROUGH JUNE 1953
ONE OR BOTH VALUES ADJACENT TO AN HOUR STRONGLY INFLUENCED BY Es
ONE OR BOTH SIGNALS STRONGLY INFLUENCED BY SPORADIC E
NUMBER OF HOURLY OBSERVATIONS
RATIO OF RECEIVED SIGNAL INTENSITIES (SCALED ANTENNAS) DECIBELS
ANCHORAGE TO BARROW – 48.87 VS. 24.325 Mc/s
EFFECTIVE EXPONENT n (PER UNIT APERTURE OF RECEIVING ANTENNA)
JUNE 1954 THROUGH JANUARY 1955
RATIO OF RECEIVED SIGNAL INTENSITIES (SCALED ANTENNAS) DECIBELS
CEDAR RAPIDS TO STERLING – 49.8 VS. 27.775 Mc/s

FIGURE I-9

Declassified in Part - Sanitized Copy Approved for Release @ 50-Yr 2014/06/09 : CIA-RDP81-01043R003000180001-4

Declassified in Part - Sanitized Copy Approved for Release @ 50-Yr 2014/06/09 : CIA-RDP81-01043R003000180001-4

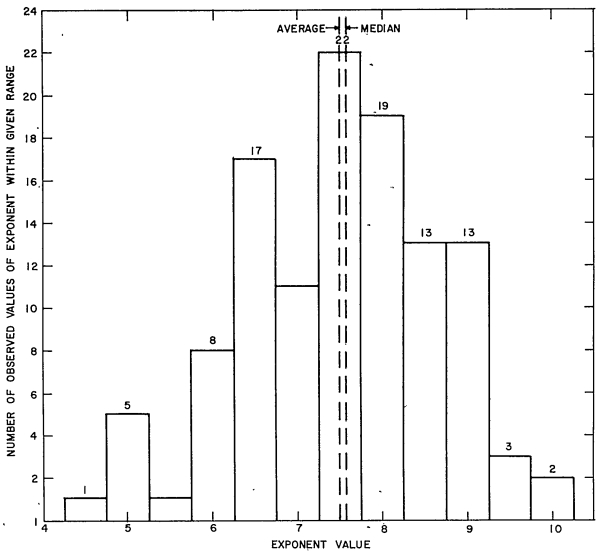

DISPERSION OF RECORDED MEDIAN VALUES OF EXPONENT OF FREQUENCY RATIO (1/2:16)

FIGURE I-10

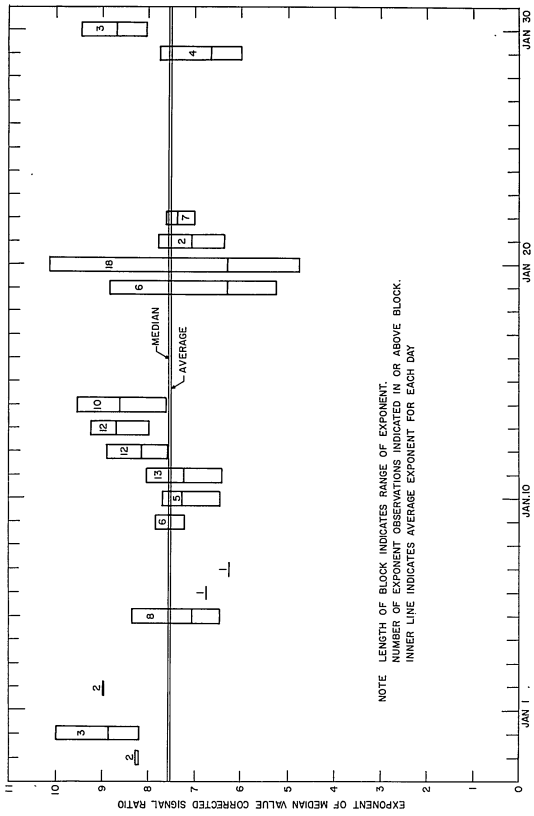

RANGES OF RECORDED MEDIAN VALUES OF EXPONENT FOR ENTIRE TEST

FIGURE I-11

Declassified in Part - Sanitized Copy Approved for Release @ 50-Yr 2014/06/09 : CIA-RDP81-01043R003000180001-4

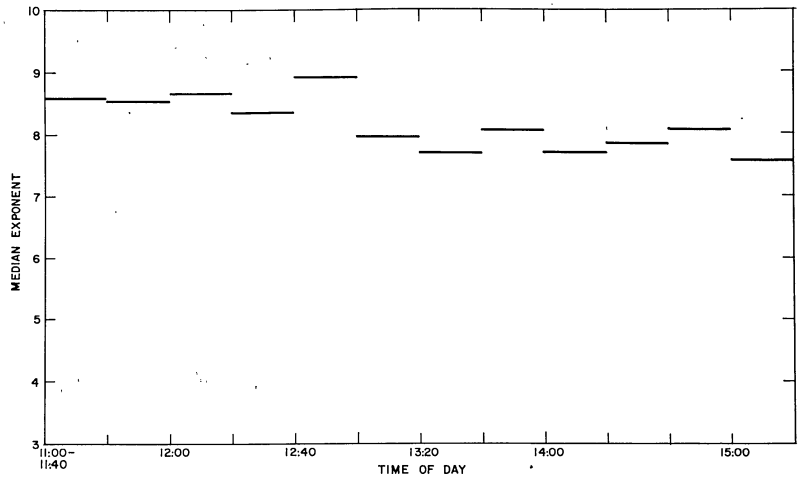

VARIATION OF MEDIAN EXPONENT DURING A TYPICAL DAY, JANUARY 12, 1953

FIGURE 1–12

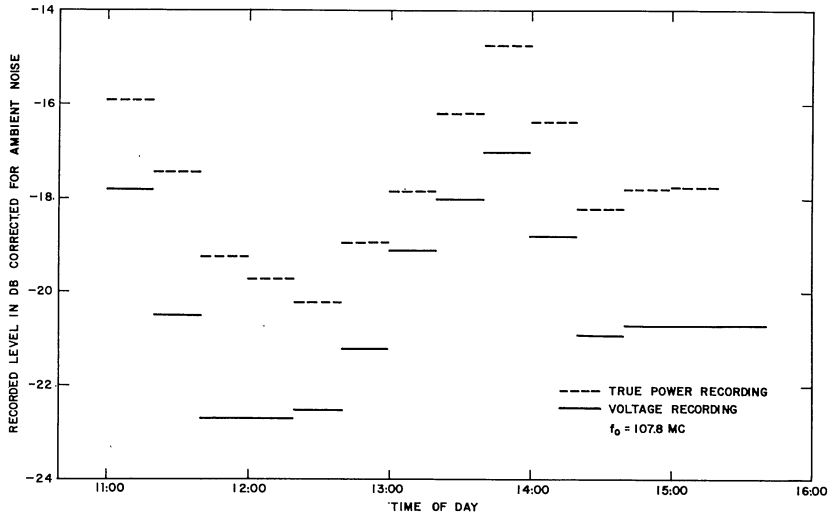

COMPARISON OF VOLTAGE AND POWER RECORDING FOR A TYPICAL DAY, JANUARY 13, 1953

FIGURE 1–13

Declassified in Part - Sanitized Copy Approved for Release @ 50-Yr 2014/06/09 : CIA-RDP81-01043R003000180001-4
Declassified in Part - Sanitized Copy Approved for Release @ 50-Yr 2014/06/09 : CIA-RDP81-01043R003000180001-4

Declassified in Part - Sanitized Copy Approved for Release @ 50-Yr 2014/06/09 : CIA-RDP81-01043R003000180001-4

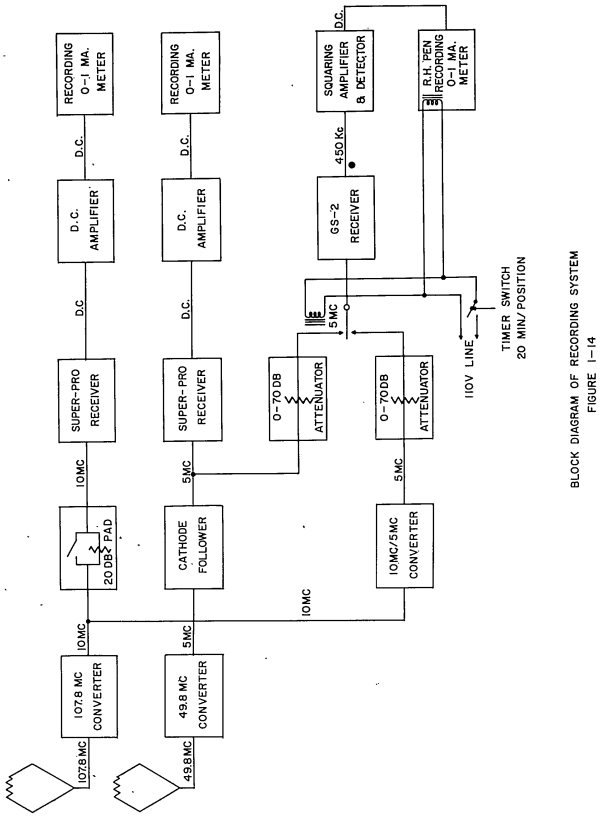

BLOCK DIAGRAM OF RECORDING SYSTEM
FIGURE I-14

APPENDIX II

EXPERIMENTAL INVESTIGATIONS OF IONOSPHERIC FORWARD SCATTERING AT VHF USING PULSE TECHNIQUES

V. C. Pineo

This report is in four parts. Part I describes the results of an experiment performed during the winter of 1954. In this experiment heights of ionospheric forward scattering were deduced from one-way measurements of the relative transit times of the tropospheric component and the ionospheric component of a pulsed signal received at 49.7 Mc/s at a distance of 793 Km from the transmitter. These deduced heights were compared with virtual heights observed simultaneously at 460 Kc/s near the midpoint of the path. Part II describes the results of one-way transit time measurements made during June 1954 at 49.7 Mc/s over a path length of 810 Km. Part III gives results of oblique incidence pulse measurements as a function of path length to determine dependence on scattering angle. Part IV gives experimental results on heights of ionospheric and tropospheric scattering determined from round-trip pulse delay measurements.

PART I - CORRELATION WITH OBSERVED HEIGHTS AT LF

1. INTRODUCTION

The purpose of this experiment was to determine if a correlation exists between the heights of ionospheric forward scattering observed at VHF and the ionospheric heights observed at vertical incidence at LF.

VHF ionospheric scatter heights ranging from about 70 Km to about 90 Km were obtained in earlier experiments by this laboratory.[1,2] Heights within this same range have been observed consistently at LF.[3,4] Thus the possibility is suggested that the propagation of LF radio waves by ionospheric refraction and the propagation of VHF radio waves by ionospheric forward scattering are both due to the same ionization mechanisms. If so, both phenomena might be expected to have similar diurnal variations in height.

In order to test for such a correlation, heights of ionospheric forward scattering observed at 49.7 Mc/s over a 793 Km path length were compared with virtual heights observed simultaneously at 460 Kc/s at vertical incidence at Sterling, Virginia. The VHF path was chosen to place the NBS Sterling, Virginia, laboratory near the midpoint.

The VHF scatter heights were deduced from measurements of the differences in transit time between pulses propagated by tropospheric forward scattering and pulses propagated by ionospheric forward scattering. For convenience, this difference in transit time is called the sky-wave delay.

Declassified in Part - Sanitized Copy Approved for Release @ 50-Yr 2014/06/09 : CIA-RDP81-01043R003000180001-4

Declassified in Part - Sanitized Copy Approved for Release @ 50-Yr 2014/06/09 : CIA-RDP81-01043R003000180001-4

2. EXPERIMENTAL DETAILS

The height observations at 460 Kc/s were made with the NBS vertical-incidence LF ionosphere sounder at Sterling.

The NBS mobile high-powered VHF pulse transmitter[5] was set up at Montgomery, New York, on an unused airfield belonging to the U.S. Air Force. The receiving equipment for the sky-wave delay measurements was located near Dobson, North Carolina.

The width of the transmitted pulse was 30 microseconds. The pulse repetition frequency was 50 pulses per second. The peak power input to the transmitting antenna was about 500 Kw. Rhombic antennas were used for transmitting and receiving.

The VHF receiving equipment at Dobson was housed in a box-body truck. The receiving equipment consisted of a receiver, an oscilloscope-camera recorder, a monitor oscilloscope and associated timing and synchronizing equipment.

The VHF sky-wave delay measurements and the LF virtual height measurements were both obtained with the use of automatically recording cameras. In each case an intensity modulated range-time display on the screen of a cathode-ray oscilloscope was recorded on continuously moving 35 mm film. The rates of film travel in the recording cameras were 3 inches per hour and 8 inches per hour respectively in the VHF and the LF recorders.

Data from which sky-wave delays could be obtained were recorded at 49.7 Mc/s at Dobson during the period January 11, 1954, to February 4, 1954. During this period the 49.7 Mc/s pulse transmitter at Montgomery was operated daily, except for Saturdays and Sundays, during the daylight hours. There were also several 24-hour runs during the period and operations were extended as often as possible to include the hours around sunrise and sunset.

The LF equipment was operated continuously during most of the period without regard to the operating schedule of the VHF equipment. However, some time was lost from the LF height recording program when it was learned that harmonics of the 460 Kc/s operating frequency were interfering with other radio services. The transmitter was shut down for one day while filters were installed to reduce the radiation of harmonics.

The tropospheric component of the pulse signal at Dobson was usually very weak and often could not be received at all. This weakness of the tropospheric pulse limited the amount of sky-wave delay data available for comparison with the virtual heights observed at Sterling.

Because of these and other difficulties, simultaneous recordings at 49.7 Mc/s and at 460 Kc/s were not obtained until January 20.

Typical examples of the photographic records obtained simultaneously at Dobson and at Sterling are shown in Figure II-1.

3. ANALYSIS OF THE DATA

For the purposes of this report the following data were reduced from the records: (1) the median hourly values of the virtual heights of the lowest ionospheric stratum observed at 460 Kc/s at Sterling and, (2) the median hourly values of the sky-wave delays observed at 49.7 Mc/s at Dobson.

The values of the virtual heights obtained at 460 Kc/s are thought to be close to those of the actual heights since there is very little group retardation at frequencies well below the critical frequency of the layer.

The sky-wave delays obtained at 49.7 Mc/s were converted into equivalent midpoint heights using the following equation:

$$\Delta t = \frac{1}{c}\left[2\sqrt{\left(R \sin \frac{\theta}{2}\right)^2 + \left(H + R\left[1 - \cos \frac{\theta}{2}\right]\right)^2} - 2R \tan \frac{\theta}{2}\right] \quad (1)$$

where Δt = sky-wave delay in seconds

$c = 3 \times 10^5$ km/sec.

$\theta = D/R$

D = surface arc distance in kilometers

R = mean radius of the earth = 6368 Km

H = midpoint height in kilometers

$2R \tan \theta/2$ = tropospheric ray-path length determined by the intersection of the horizon planes of the transmitter and the receiver on the Great Circle path.

The arguments for the two tangents model of Equation 1 were discussed in a previous report.[2]

In Figure II-2 the diurnal variations of the hourly median values of midpoint scatter heights obtained from the sky-wave delay observations at 49.7 Mc/s at Dobson are compared with the virtual heights observed simultaneously at 460 Kc/s at Sterling during the period January 20, 1954, through February 3, 1954.

Declassified in Part - Sanitized Copy Approved for Release @ 50-Yr 2014/06/09 : CIA-RDP81-01043R003000180001-4

Declassified in Part - Sanitized Copy Approved for Release @ 50-Yr 2014/06/09 : CIA-RDP81-01043R003000180001-4

Figure II-3 shows the diurnal variations in hourly median values of heights obtained from simultaneous observations at 460 Kc/s and at 49.7 Mc/s during two typical January days.

4. RESULTS

Statistically significant amounts of data were obtained for only the hours 0600 to 1900 inclusive, 75 degrees West time. During these hours there was a pronounced similarity between the diurnal variations of the midpoint heights calculated from the sky-wave delays observed at 49.7 Mc/s and the diurnal variations of the virtual heights observed simultaneously at 460 Kc/s near the midpoint of the VHF path. The virtual heights at 460 Kc/s varied from about 80 Km around midday to about 100 Km around sunrise and sunset. The calculated scatter heights at 49.7 Mc/s varied from about 75 Km during the midday hours to about 90 Km around sunrise and sunset. Thus the midpoint scatter heights obtained from the sky-wave delays at 49.7 Mc/s were from 5 Km to 10 Km lower than the virtual heights observed at 460 Kc/s. It should be noted, however, that these calculated scatter heights will be lower than the actual heights if the transit time of the tropospheric pulse is greater than that of the two tangents model of Equation 1.

In a later experiment (described in Part IV), round-trip pulse techniques were used to measure the transit times over a surface path length of 624 Km of both tropospherically propagated pulses and ionospherically propagated pulses. The equivalent tropospheric scatter heights obtained from these round-trip measurements were between 20 Km and 30 Km above the earth at the midpoint of the path instead of a height of 7.6 Km predicted by the two tangents model. This result was attributed to the radiation patterns of the antennas used in the experiment. These antennas were designed to illuminate a region about 90 Km above the earth at the midpoint of the path. Thus the intensity of illumination over the midpoint of the path increased very rapidly with height, thereby partly offsetting the loss in scattering efficiency with increasing height in the troposphere.

The radiation patterns of the antennas used in the experiment described in this report were similar to those used in the round-trip experiment (Part IV) in that the main lobes were directed at a region in the ionosphere over the midpoint of the 793 Km path. The height of intersection of the tangent rays of the transmitter and receiver over the midpoint of the 793 Km surface path is about 12 Km. However, the actual height of maximum tropospheric scattering was probably greater than 12 Km and could have been between 20 Km and 30 Km. A tropospheric height of 25 Km used in calculating the reference transit time results in calculated ionospheric heights about 5 Km greater than given by Equation 1. Thus, in this experiment, the actual heights of ionospheric scattering at 49.7 Mc/s may have been in better agreement with the virtual heights observed at 460 Kc/s than are indicated in Figures II-2 and II-3.

5. ACCURACY OF THE MEASUREMENTS

The virtual height records from the low frequency ionosphere sounder had height markers at intervals of 20 Km. Virtual heights were read to the nearest kilometer. The estimated reading error was $\pm$ 3 Km.

The sky-wave delay records from the VHF equipment had time-delay markers at intervals of 100 microseconds. Sky-wave delays were obtained by measuring the distance on the record from the leading edge of the tropospheric trace to the leading edge of the ionospheric trace. This distance was then converted into microseconds of delay. The estimated reading error was $\pm$ 5 microseconds of delay or approximately $\pm$ 4 Km in the calculated midpoint height.

There were no known instrumental errors in the low frequency measurements of virtual heights.

The only significant instrumental error in the VHF sky-wave delay measurements was due to the rise time of the transmitted pulse. This rise-time effect caused the received pulse to broaden in the direction of the leading edge with increasing signal intensity. The maximum error from this effect was about 5 microseconds, and occurred at times when the intensity of one component of the signal was very weak and that of the other component was near the saturation level of the receiver. During this experiment the intensity of the tropospheric component of the received signal was always very weak and the intensity of the ionospheric component was usually well below the saturation level of the receiver. Errors in the hourly median values of sky-wave delay due to rise-time effects were estimated to be not more than minus 3 microseconds and the resulting error in calculated height to be no more than minus 2 Km. The maximum errors from this rise-time effect probably occurred most often during the midday hours for this was the time during which the intensity of the ionospheric pulse signal reached its diurnal maximum.

6. CONCLUSIONS

The differences between the values of the virtual heights obtained at 460 Kc/s at Sterling and the calculated height obtained from the sky-wave delays observed at 49.7 Mc/s at Dobson are probably smaller than indicated in Figures II-2 and II-3 because the actual tropospheric delay is almost certain to have been greater than that of the two tangents model of Equation 1. Also, any correction of the measured sky-wave delays for errors due to pulse rise-time effects would result in slightly greater values for the calculated heights. Furthermore, the values of the virtual heights obtained at 460 Kc/s must be slightly greater than the real heights despite the small effect of group retardation at this frequency.

Thus, during the daylight hours, the ionospheric forward scattering of VHF radio waves and the refraction of vertically incident LF radio waves seem to occur at about the same height.

Declassified in Part - Sanitized Copy Approved for Release @ 50-Yr 2014/06/09 : CIA-RDP81-01043R003000180001-4

Declassified in Part - Sanitized Copy Approved for Release @ 50-Yr 2014/06/09 : CIA-RDP81-01043R003000180001-4

The most significant result of the experiment, however, is the similarity in the diurnal variations of the heights obtained at the two experimental frequencies. This result is tentatively interpreted as indicating that the ionospheric refraction of LF radio waves and the ionospheric scattering of VHF radio waves are both due to the same region of ionization.

PART II - SUMMER HEIGHTS OF VHF SCATTERING

1. INTRODUCTION

The purpose of this experiment was to obtain summertime values of sky-wave delays for the 810 Km path from Sterling, Virginia, to Bluffton, South Carolina, to supplement similar data obtained for the same path during the fall of 1952 and during the winter of 1953.[2]

2. EXPERIMENTAL DETAILS

The equipment and the techniques used in this experiment were the same as those that were used for the VHF time-delay measurements described in Part I of this Appendix. The pulse transmitter was located at Sterling, Virginia, and operated at a radio frequency of 49.7 Mc/s. The pulse width was 40 microseconds and the pulse repetition frequency was 50 pulses per second. The receiving and recording equipment was located near Bluffton, South Carolina. Sky-wave delays were obtained during the period from June 18 through June 27, 1954.

The 49.7 Mc/s transmitter at Sterling was normally operated from about 0500 hours to 1900 hours, 75 degrees West time and, on one occasion, it was operated continuously for 48 hours. Unfortunately, intermittent failures of the electric power generator and the recording camera at Bluffton during the 48-hour run caused an aggregate loss of 9½ hours from the recording program. The durations of these interruptions ranged from less than ½ hour to 5½ hours. Equipment failures also occurred occasionally on other days during the experiment. These failures, oddly, occurred most often during the hours around sunset.

3. ANALYSIS AND RESULTS

For purposes of analysis the photographic records were divided into half-hour periods beginning on the hour and the half hour. The median value of the sky-wave delay in microseconds for each half-hour period was read from the records to the nearest 5 microseconds with an estimated reading error of ± 5 microseconds.

These individual half-hour median values of sky-wave delays and of the calculated equivalent midpoint heights are shown in the mass plot of Figure II-4. The diurnal variation of the median value of these half-hourly medians is also shown in Figure 4.

Equivalent midpoint heights calculated from the observed sky-wave delays varied from 67 Km during the midday to 87 Km at night. The half-hourly median values of calculated equivalent midpoint heights for the period of the experiment varied from 71 Km during midday to between 80 Km and 85 Km during the night.

The values of equivalent midpoint height shown in Figure II-4 were calculated using Equation 1 which is discussed in Part I of this Appendix. There it is pointed out that use of Equation 1 leads to values of midpoint heights which are likely to be lower than the actual heights. Thus, for reasons given previously, the calculated heights shown in Figure II-4 are probably about 5 Km lower than the actual heights.

4. DISCUSSION OF THE RESULTS

The median values of the sky-wave delays obtained in this experiment were approximately the same values as those that were obtained for the same path in November, 1952, and in January, 1953.[2] There is, however, one notable difference between the records obtained in this experiment and the records obtained in the earlier experiment. The records from the earlier experiments frequently showed a split sky-wave trace during the daylight hours which seemed to indicate the existence of two scattering stratum, one at a height of about 70 Km and the other at a height of about 85 Km.

Tentative conclusions drawn from these earlier results were that the higher stratum accounted for most of the nighttime scatter and tended to endure weakly throughout the day, and that the lower stratum, which was detected during the daylight hours, accounted for the comparatively high daytime signal intensities.

The signal intensities of pulses received via the lower stratum during the midday hours were roughly 10 db to 25 db greater than either the daytime or nighttime signal intensities of pulses received via the higher stratum.

The separation between the leading edges of the dual sky-wave traces was approximately the same as the width of the transmitted pulse and could only be resolved at times when the signal intensities of the pulses received via the lower stratum were relatively weak. During periods of high signal intensities the two traces overlapped to produce a single trace roughly twice the width of the transmitted pulse.

This splitting of the sky-wave trace is not evident in June, 1954, records, but it is suggested by a pronounced widening of the sky-wave trace during the midday hours.

The difference, with respect to split traces, between these records and the records from the earlier experiments is attributed to one important difference between the experiments in the manner in which the photographic records were made. This difference was in the rate of film travel

Declassified in Part - Sanitized Copy Approved for Release @ 50-Yr 2014/06/09 : CIA-RDP81-01043R003000180001-4

Declassified in Part - Sanitized Copy Approved for Release @ 50-Yr 2014/06/09 : CIA-RDP81-01043R003000180001-4

in the recording camera. A film travel rate of 3 inches per hour was used during the June, 1954, experiment. But a rate of about 1 inch per minute was used in the earlier experiments.

The intensities of two groups of received pulses propagated by different modes have independent fading rates. Under certain conditions this independent fading characteristic makes it possible to distinguish between separate pulse groups even if the difference in transit time is less than the duration of the transmitted pulse. The transit-time difference can be resolved if the intensities at the camera of pulses propagated by the earlier mode are well below the saturation level of the film and if the film is moving at a fast enough rate. Resolution is impossible if the intensities of the pulses due to the earlier mode saturate the film or if the film travel rate is very slow relative to the fading rate of the pulses. In such cases the pulses for the two modes overlap and produce a widened trace having a time-width w = 2d - s

where d = duration of transmitted pulse

s = difference in transit time between the trailing edge of the pulse due to the earlier mode and the leading edge of the pulse due to the later mode.

Widened sky-wave traces were obtained frequently during the June, 1954, observations. The effect of this widening was to decrease the separation between the leading edge of the reference tropospheric trace and the leading edge of the sky-wave trace. Widening of the trace usually became noticeable some time after sunrise and disappeared by sunset.

The width of the received tropospheric pulse was approximately the same as that of the transmitted pulse.

A good example of the difference in width between the sky-wave traces obtained in the morning and those obtained around midday is shown in Figure II-5. In the morning record the sky-wave trace has about the same width as that of the tropospheric trace, and the relative delay between the leading edges of the two traces is about 75 microseconds. In the midday record the sky-wave trace is about 25 microseconds wider than it was in the morning, and its delay relative to the tropospheric trace is about 55 microseconds. But in both the morning and the evening records, the relative delays between the leading edges of the tropospheric traces and the trailing edges of the sky-wave traces are between 130 microseconds and 135 microseconds.

5. CONCLUSIONS

The widening of the sky-wave trace during the daytime can be considered to be the result of simultaneous scattering from two strata at different heights above the earth. The upper stratum is probably an enduring phenomenon. The lower stratum seems to be a phenomenon of the daylight hours only and its scattering efficiency is usually much better than that of the upper stratum.

With the foregoing considerations in mind, the results of the June, 1954, sky-wave delay observations discussed herein are interpreted as supporting evidence obtained in other experiments that the propagation of VHF radio waves by ionospheric scattering is the result of at least two principal propagation modes. The mode associated with the lower scattering stratum is probably the result of solar influence.

PART III - SCATTERING ANGLE DEPENDENCE TESTS

1. INTRODUCTION

This experiment was performed in July, 1953, at a radio frequency of 49.8 Mc/s for the purpose of determining the dependence of the received signal intensity on the forward scatter angle of a VHF radio wave propagated by ionospheric scattering.

A preliminary transmission equation for propagation by ionospheric scattering is given in a paper on long-distance VHF propagation by Bailey, et al.[8] This equation was based on a simplified model for which all the transmitted power is passed through a scattering volume in which the scattering parameters are assumed to be constant and equivalent to those at the path midpoint. Since these conditions will not be realized in practice, this formulation should be regarded only as providing a useful estimate of received signal levels and as a guide for future theoretical and experimental work. A simplified form of this equation is:

$$\frac{P_r}{P_t} \doteq Kq \qquad (1)$$

where K includes all the terms relating to ionospheric structure, wavelength, antenna gains, etc., q is a purely geometric factor and P_r/P_t is the ratio of received power to transmitted power. If the scattering volume is located above the midpoint of the Great Circle path between the transmitter and receiver, q can be expressed as follows:

$$q \doteq \frac{1}{\ell^2 \sin^n \frac{\gamma}{2}} \qquad (2)$$

where: ℓ = length of the ray path

$\frac{\gamma}{2}$ = the angle at which the transmitted ray passes through the scattering layer.

n is the angle-dependence exponent.

Declassified in Part - Sanitized Copy Approved for Release @ 50-Yr 2014/06/09 : CIA-RDP81-01043R003000180001-4

Declassified in Part - Sanitized Copy Approved for Release @ 50-Yr 2014/06/09 : CIA-RDP81-01043R003000180001-4

In the paper by Bailey, et al,[6] n is given a value of 5. Theoretical work by Feinstein and Salzberg[7] yields a value of n = 7 and by Eckersley[8] a value of n = 9. The values of n attributed to Feinstein and Eckersley were not developed in the papers by these authors but result from extending their analyses to the transmission equation.

Experimental values for the angle-dependence exponent, n, were obtained by comparing signal intensities received nearly simultaneously during the daytime at distances of 491 Km, 592 Km and 811 Km from the transmitter which was located at Sterling, Virginia.

2. DESIGN OF THE EXPERIMENTAL SYSTEM

An ideal system for making an experimental determination of the angle-dependence factor would consist of at least three identical transmitter receiver combinations having a common midpoint but different path lengths along the same great-circle path. Signal intensity measurements could then be made simultaneously at each of the receiving points. The differences in received power could be attributed to differences in distances and scattering angles. Such an ideal system would be very expensive. For this reason it was decided to set up an experiment using a single transmitter and three receiving sites along the same great-circle path appropriately spaced to provide the greatest sensitivity to differences in the scatter angle. The effect of the angle dependence in the geometric factor is to cause the received signal power to increase with distance. This effect is greatest for path lengths under 1000 Km.

There were two other requirements governing the choice of the receiving sites. These were (1) low noise levels and uniformity with respect to flatness of the ground and freedom from objects capable of affecting the radiation patterns of the antennas, and (2) location as nearly as possible on the meridian of Sterling so that the differences in local time at the midpoints of the paths would be small. Consideration of these requirements led to the choice of a path running in the approximate direction of Savannah, Georgia, from Sterling. The choice of the shortest path length for the experiment was based on a compromise between desired angle sensitivity and required transmitter power.

Pulse techniques were required to isolate the ionospheric component of the signal from the tropospheric component. The minimum difference in time of arrival between tropospheric and ionospheric pulses anticipated at the most distant site established the maximum pulse width and consequently the bandwidth of the system. A pulse transmitter with useful peak power output in excess of 500 Kw was available at Sterling.

The existence of a large amount of signal-intensity data taken at 49.8 Mc/s over the 1243 KM Cedar Rapids - Sterling path provided a means of estimating signal intensities expected for other paths. As a result of these considerations, approximate path lengths of 500 Km, 600 Km and 800 Km were regarded as suitable. Three receiving sites were located

along this path at distances of 491 Km, 592 Km and 811 Km from the Sterling, Virginia, transmitter. The locations and geographic coordinates are given in Table I.

TABLE I

GEOGRAPHIC DETAILS OF THE SITES

Function	Location	Coordinates	Distance to Transmitter
Transmitting	Sterling, Va.	38°59'N, 77°28'W	---
Receiving	Hamlet, N. C.	34°53'N, 79°34'W	491 Km
Receiving	Florence, S. C.	34°12'N, 79°54'W	592 Km
Receiving	Bluffton, S. C.	32°17'N, 80°51'W	811 Km

Rhombic antennas were used for transmitting and receiving. Each antenna system was designed to align the main lobes to the vertical angle of departure corresponding to a midpoint scatter height of 70 Km. The assumption of a scatter height of 70 Km was based on oblique-incidence measurements[2] made in November 1952 and January 1953. During these experiments the daytime heights observed were usually less than 80 Km and the strongest signal strengths tended to occur when the height was around 70 Km. In no case was the height of the scattering stratum observed to be greater than 90 Km.

3. THE EFFECT OF ANTENNA GAINS ON THE DATA

In the analysis of the data obtained in an experiment such as this one, it is necessary to take account of differences between the antenna gains of the three systems.

It was assumed that the gain due to the antennas for each one of the experimental systems was directly proportional to the product of the plane-wave gains of its transmitting and receiving antennas. This assumption was originally justified on the grounds that the use of peak-reading signal voltage recorders and the operation of the q factor (Equation 1) would result in recorded values of received signal intensities closely related to the field intensities prevailing at the exact midpoints of the paths. Consequently the received signal intensity for any one of the paths would change approximately in direct proportion to changes in illumination of this point resulting from changes in directivity of the antennas. Further support for this assumption is found in the discussion of realized antenna gains in the paper by Bailey, Bateman and Kirby,[9] which shows that the gain realized from a practical antenna system used in propagation by ionospheric forward scatter is directly proportional to the product of the plane-wave gains of its transmitting and receiving antennas, when the beamwidths of the antennas are larger than the beamwidth of the effective scattering volume.

Declassified in Part - Sanitized Copy Approved for Release @ 50-Yr 2014/06/09 : CIA-RDP81-01043R003000180001-4

Declassified in Part - Sanitized Copy Approved for Release @ 50-Yr 2014/06/09 : CIA-RDP81-01043R003000180001-4

It should be noted that the neglecting of differences in antenna gains in the analysis of the signal intensity data will result in deduced values for the angle dependence exponent somewhat larger than they would be if the data were normalized to equal antenna-systems gain.

Since it is necessary to take into account any differences between the gains of the three antenna systems it is desirable that these differences be kept to a minimum.

4. DESIGN OF THE ANTENNA

The effect on the gain of a rhombic antenna resulting from adjusting the tilt angle and leg length to obtain the desired lobe alignment is such that the gain increases as the required vertical angle of departure for which the antenna is designed decreases. This effect on the relative gains of several rhombic antennas with main lobes designed to have different vertical angles of departure can be minimized by using the same leg lengths for all of the antennas and achieving the required lobe alignments by adjusting only the tilt angles and the heights above the ground. This is called the reduced-leg-length compromise design method[12] and was the method used in the design of the rhombic antennas employed in this experiment.

The antennas for the shortest path length (491 Km) were designed to have the maximum gain consistent with correct alignment of the main lobe. The antennas for the longer paths were designed with the same leg lengths as those for the 491 Km path and the heights and tilt angles were adjusted to obtain the desired alignments of the main lobes. Even with this antenna design there are differences in gain which cannot be neglected. Furthermore, the differences in gain between installed antenna systems such as these do not remain constant with changing midpoint scatter height. This sensitivity to variations of the midpoint height affects the relationship between the signal intensities observed at the different path lengths. For this reason provisions for making height measurements were included in the plans for the experiment.

5. DETAILS OF THE EXPERIMENT

The pulse transmitter located at Sterling, Virginia, was operated at a peak pulse power of approximately 500 kilowatts. The pulse duration was approximately 50 microseconds and the repetition frequency was 50 pulses per second. The transmitter was provided with three antennas, each electrically identical to that at the receiving site toward which it was directed.

The equipments at two of the receiving sites were housed in small transportable buildings. A box-body truck was used at the other site. Air conditioners with thermostatic controls were installed at each site. Each receiving site was provided with a pulse-type signal intensity recorder consisting of a gated receiver and a peak-reading recording

voltmeter. The response of the recorder was essentially independent of pulse duration for pulse durations greater than 20 microseconds. A variation in pulse width from 20 to 200 microseconds produced a change of less than $\frac{1}{2}$ db in the record. The recording time-constant was 5 seconds. The gated feature in the receiving equipment was required to prevent contamination of the signal intensity record by the tropospheric component of the signal. The time duration of the receiver gate was approximately 400 microseconds. Synchronization of the receiver gating pulses with the transmitter repetition frequency was accomplished through the use of identical 100 Kc/s crystal-controlled oscillators at the transmitter and receivers. Each receiving site was also provided with equipment for making automatic range-time recordings from which the difference in transit time between the ionospheric and the tropospheric components of the signal could be obtained. Approximate values of midpoint ionospheric heights could be deduced from these range-time measurements.

The range-time recording equipment consisted of a receiver, a cathode-ray oscilloscope and a recording camera.

A block diagram of a complete receiver-recorder installation is shown in Figure II-6.

The output from the pulse transmitter was alternately switched between the three transmitting antennas in accordance with a prearranged schedule. At the outset of the experiment the schedule called for 15 minutes operation on each antenna during the hour with a 5-minute silent period at the end of each transmission. The first transmission of the day started at 0855 hours EST and the last one at 1435 hours EST. This schedule was maintained from July 2 through July 16, Saturdays and Sundays excluded. The level of cosmic and other noise was recorded at the receiving sites during the silent periods. Interference from the Cedar Rapids transmitter, which was operating on the same frequency, was encountered occasionally. In order to avoid loss of records from this source, the Cedar Rapids transmitter was put on a time-sharing schedule with the Sterling pulse transmitter. Under this arrangement the Cedar Rapids transmitter operated for 15 minutes during the hour and the Sterling transmitter was operated during the remaining 45 minutes in three 12-minute intervals, each of which was followed by a 3-minute silent period. This schedule was maintained from 0900 hours to 1357 hours each day from July 17 until the conclusion of the experiment on July 31 at 1112 hours. Each of the signal intensity recorders was calibrated at least twice daily. Identical pulsed signal generators were used at each site for calibration. The signal generators were cross-checked against each other at the beginning and end of the experiment. The maximum difference in output between any two of the signal generators at any attenuator setting was less than half a decibel. The receivers were first calibrated in terms of open-circuit antenna voltage. Immediately following this, another calibration was made with the antenna connected to the receiver input and the signal generator loosely coupled to the antenna. The signal generator output attenuator was then adjusted to produce full-scale deflection of the recorder pen and the

Declassified in Part - Sanitized Copy Approved for Release @ 50-Yr 2014/06/09 : CIA-RDP81-01043R003000180001-4

Declassified in Part - Sanitized Copy Approved for Release @ 50-Yr 2014/06/09 : CIA-RDP81-01043R003000180001-4

attenuator reading noted on the record. The signal generator output was then reduced in convenient steps until the antenna noise level was reached. The attenuator setting for each step was noted on the record. This second calibration was called "signal plus noise calibration" since it provided a means of obtaining a quantitative evaluation of the effect of noise on the recorded value of weak signals. The output from the gated receiver was displayed on a monitor oscilloscope. The operator could adjust the receiver gate delay at will with a continuous 360° phase shifter provided for the purpose. At the start of a recording period, the operator could quickly bring the pulse signal into position on the oscilloscope screen by putting the receiver in the ungated condition and at the same time holding down a "drift" switch which allowed the timing oscillator to run free. The pulse signal would drift onto the screen immediately and could be locked in at once by releasing the "drift" switch. The receiver gate was then turned on and the gate delay adjusted to reject the tropospheric component of the received pulse signal. The operator watched the monitor oscilloscope continuously and adjusted the gate delay whenever necessary to compensate for any frequency drift in the timing oscillators.

The power input to the final amplifier during each transmission was recorded in the transmitter log book. A further check on the stability of the transmitter power was provided by a small dipole using a crystal rectifier and a dc milliammeter. The dipole was kept in a fixed position with respect to the transmitting antennas. The dipole current was read and recorded in the log book once each hour.

Log books were also kept at each of the receiving sites. In these logs, the operators recorded information which would be of use in evaluating the signal strength records.

An example of the pulse photographs is shown in Figure II-7.

6. ANALYSIS OF THE DATA

The signal intensity data were corrected for the effects of noise and variations in transmitter power. Differences in antenna gains were taken into account approximately by normalizing the data to the gain of the antenna system for the 811 Km path. The calculated gain in decibels of each antenna system relative to that for the 811 Km path for ionospheric scatter heights of 70 Km, 80 Km and 90 Km are shown in Table II.

TABLE II

RELATIVE GAINS OF THE ANTENNA SYSTEMS

Path Length in Kilometers	Relative Gain in Db, Height of Ionospheric Scattering		
	70 Km	80 Km	90 Km
811	0	0	0
592	2	2½	3
491	5	6	10

It is to be noted that the antenna system gain at 592 Km relative to that at 811 Km is not appreciably affected by changes in scatter heights within the range of 70 Km to 90 Km.

Two noise correction curves were prepared. One of these curves utilized the noise calibrations made at the receiver sites. The other curve was calculated using the equation:

$$E_s^2 = E_{s+n}^2 - E_n^2 \qquad (3)$$

where E_s = actual signal voltage

E_{s+n} = combined signal and noise voltage, observed

E_n = random noise voltage.

In each of these curves the ratios in decibels of apparent (observed) signal intensities to noise intensities are plotted as abscissae against the correction factors in decibels as ordinates. The apparent signal intensities are the unadjusted values scaled from the signal intensity records and include the effects of noise. Noise intensities were recorded during the scheduled interruptions in transmission. The correction factor is the amount by which the apparent signal intensity exceeds the actual signal intensity. Both correction curves are shown in Figure II-8. The lack of agreement at small differences between signal and noise levels is attributed in part to the difference between the condition of a continuous wave signal mixed with purely random noise assumed in Equation 3 and the conditions of the experimental curve, i.e., a 50-microsecond pulse signal in a 400-microsecond receiver gate with some contamination by nonrandom noise, and in part to variation of the detector characteristic with signal strength. The signal-to-noise ratios encountered during the times that signals were recorded at more than one site were such that the differences in results between the two noise correction curves were small. At 811 Km the difference ranged from 0 to 1 db with a median difference of ½ db. At 592 Km the range was 0 to 2 db with a median of ½ db. At 491 Km the range was 0 to 2 db with a median of 1 db. The difference between the two noise correction curves is even smaller when applied to the differences between the signal intensities observed at 592 Km and 491 Km and those observed at 811 Km. As a practical matter, in order to present a clear picture of the results without undue elaboration, noise corrections lying halfway between those on the observed and calculated curves were chosen. Midday median scatter heights of about 80 Km were obtained in a later experiment performed in June 1954 at the same frequency over the 811 Km path. For this reason the data were normalized to the antenna systems gains for an 80 Km scatter height, except for the hours 09 to 11, July 15, when simultaneous time-delay measurements indicated a height of 90 Km.

Declassified in Part - Sanitized Copy Approved for Release @ 50-Yr 2014/06/09 : CIA-RDP81-01043R003000180001-4

Declassified in Part - Sanitized Copy Approved for Release @ 50-Yr 2014/06/09 : CIA-RDP81-01043R003000180001-4

The records from each site were scaled and the signal intensity and noise level in db above 1 microvolt open-circuit antenna voltage, 600 ohms reference impedance, tabulated for each period during which the pulse transmission was directed towards the site. Graphs of signal intensity vs time, using linear interpolation between consecutive coordinate points, were drawn for each site. The median signal intensity for each hour which presumably would have been recorded at the site if the transmission had been continuous was then obtained from these graphs.

7. RESULTS

Nearly simultaneous records of sky-wave signal intensities were obtained for 10 hours at all three receiving sites and for 25 hours at the 811 Km site and at the 592 Km site. Signal intensity records were obtained at both 592 Km and 491 Km on four occasions during which the records at 811 Km were obliterated by interference.

The automatic time-delay recording part of the program could not be carried out because of corona troubles which developed in the recording oscilloscopes after their installation at the receiving sites. However, some measurements of sky-wave vs tropospheric-wave delay time were obtained manually with the monitor oscilloscope at the 592 Km site between 10 hours and 11 hours, 75°W time on July 15. A midpoint ionospheric height of about 90 Km was calculated from these measurements. This was the only occasion on which height data were obtained while signal intensities were being recorded at all three sites. In addition to these measurements, a series of single-frame photographs of a cathode-ray oscilloscope "A"-type presentation were made on the same day at the 491 Km site between 0900 and 1000 Est. A dual-beam cathode-ray oscilloscope was used. (A sample of the record obtained is shown in Figure II-7.) The output from the ungated IF amplifier is presented on the lower trace. The output from the gated IF amplifier containing only the sky-wave pulse is shown on the upper trace. Both tropospheric and sky-wave pulses together with 100-microsecond markers are seen on the lower trace. The tropospheric pulse is first from the left followed after a delay of 110 microseconds by the sky-wave pulse. The equivalent midpoint ionospheric height is 88 Km. On the basis of these measurements it was assumed that a scatter height of approximately 90 Km prevailed from 0900 hours to 1100 hours on this particular day.

The signal intensities obtained at 811 Km were compared with those obtained at 592 Km and at 491 Km. The results of these comparisons are shown in Figure II-9. Curve (a) in Figure II-9 shows the comparisons for the hour 10 to 11 on July 15. Curve (b) shows the comparisons of the median values of all of the other interpolated hourly signal intensities obtained in the experiment. Two curves showing q as a function of distance calculated for exponents of 5 and 10 for a midpoint height of 80 Km are shown for reference. These comparisons indicate values for the angle-dependence exponent between approximately 8 and 11.

Reference is again made to Table II which shows the effects of variations in midpoint height on the relative gains of the antenna systems. It is seen that within the height range of 70 Km to 90 Km the change in relative signal intensity resulting from such height-related variations in antenna gains is 1 decibel at 592 Km, and is 5 decibels at 491 Km, with 4 decibels of this change occurring in the height range of 80 Km to 90 Km. Consequently the median relative signal intensity at 592 Km will be within $\frac{1}{2}$ decibel of the value shown in Figure II-9(b) regardless of which height within the range of 70 Km to 90 Km is assumed in normalizing the data to equal antenna systems gain. The corresponding results for the 491 Km path are considerably different. Here the use of antenna gains for a 90 Km midpoint height in normalizing the signal-intensity data used in Figure II-9(b) yields an apparent signal intensity at 491 Km slightly greater than that at 592 Km. This is inconsistent with the other results. The smooth curve of Figure II-9(b) resulting from assuming a midpoint height of 80 Km in normalizing the signal intensity data to equal antenna systems gain indicates that the prevailing ionospheric scatter height was about 80 Km during the experiment. This is in agreement with the median midday value of 80 Km obtained a year later over the 811 Km path from measurements of the differences between the transit times of ionospherically-propagated pulses and tropospherically-propagated pulses.

The possibility that the experimentally-determined values of n might be a function of general propagation conditions was investigated by comparing the ratio of the signal intensities observed at 811 Km to those observed at 592 Km with the signal intensities observed at 811 Km; no correlation was apparent.

8. SUMMARY AND DISCUSSION OF THE RESULTS

Received signal intensities increase rapidly as the forward scatter angle at the ionosphere becomes smaller, or, stated differently, the signal intensity increases with increasing distance over the range of distances used in this experiment. A daytime value between 8 and 11 for the angle-dependence exponent, n, in the q factor was indicated.

The values obtained for n did not appear to be correlated with general propagation conditions.

These values for n were deduced by comparing signal intensities which had been normalized to equal antenna systems gains taken to be proportional to the product of the computed plane-wave gains of the transmitting and receiving antenna for each of the test paths.

A qualitative consideration of the relationship of realized antenna systems gains to the beamwidths of the antennas and the beamwidths of the common volumes would indicate the use of normalizing factors slightly smaller than the ones that were used but not as small as those that would result from considering only the gains of the receiving antennas.

Declassified in Part - Sanitized Copy Approved for Release @ 50-Yr 2014/06/09 : CIA-RDP81-01043R003000180001-4

Declassified in Part - Sanitized Copy Approved for Release @ 50-Yr 2014/06/09 : CIA-RDP81-01043R003000180001-4

Any errors due to the use of too large normalizing factors for the antenna gains are partially offset by the tendency of the effective common volume to decrease with distance.[10]

It should be noted that the use of smaller normalizing factors results in larger deduced values for n. Consequently the values obtained for n are considered to be about the minimum values actually existing for the experimental paths during the observation periods.

PART IV - HEIGHTS OF IONOSPHERIC AND TROPOSPHERIC SCATTERING DETERMINED FROM ROUND-TRIP PULSE DELAY MEASUREMENTS

1. INTRODUCTION

Round-trip pulse techniques were used to obtain the heights at which ionospheric and tropospheric scattering of VHF radio waves occurs. Round-trip delay observations were made during the periods December 1 through December 31, 1954, and September 28 through October 14, 1955, at a radio frequency of 49.8 Mc/s over a 624 Km path.

The results given by this part represent an extension of work described in Parts I and II, and earlier,[4] in which height of ionospheric scattering was deduced from measurements of transit time of ionosphere pulses relative to troposphere pulses. The experiment was conducted jointly by the National Bureau of Standards and Lincoln Laboratories of the Massachusetts Institute of Technology. Results have been given in separate presentations,[10,11] but are included here for the sake of completeness of the present appendix.

2. EXPERIMENTAL ARRANGEMENT

Two pulse transmitting and receiving systems were used. One was located at Lincoln Laboratory's Round-Hill, Massachusetts, field station, and the other was located at the NBS Sterling, Virginia, laboratory. Synchronization of the two systems was achieved by using identical 100 Kc/s crystal-controlled timing oscillators at each site. The pulse repetition frequency was 50 pulses per second. Pulse widths of about 20 microseconds were used during the December, 1954, observations. During the 1955 fall observations, the pulse widths were 40 microseconds and 50 microseconds respectively for the Round Hill and the Sterling transmissions. The peak power output of the Round Hill transmitter was about 300 Kw. The peak power output of the Sterling transmitter was 300 Kw during the Dec. 1954, observations and about 900 Kw during the 1955 fall observations. The full rise time of the pulse transmitted from Round Hill was 4 microseconds. The rise time of the pulse transmitted from Sterling was 8 microseconds during the December, 1954, experiment and 14 microseconds during the 1955 fall experiment. Failure of the pulse modulator in the Sterling transmitter at the start of the fall experiment forced a last minute substitution of a pulsing unit having a slower rise time. Separate rhombic antennas were used for transmitting and receiving at each

site. These antennas were electrically identical. The elevation angle of the main lobes was 12 degrees. The bandwidth of the Sterling receiver was 100 Kc/s; that of the Round Hill receiver was 300 Kc/s. The noise figure of each receiver was about 3.

The output of the receiver at each site, containing the local transmitter pulse and the pulses received from the other site, were displayed on a monitor cathode-ray oscilloscope. A fixed delay of about 8 milliseconds was inserted at Sterling between the local Sterling pulse and the first pulse received from Round Hill. This delay was inserted in order to separate the backscattered echoes of each local transmitter from the forward scattered pulses received from the other site. An expanded portion of an intensity-modulated sweep containing only the received forward scattered pulses was displayed on the screen of a recording cathode-ray oscilloscope. Reference markers of known delay relative to the locally transmitted pulse were included in the display. This display was photographed on 35 mm. film moving continuously at about 6 inches per hour in the recording camera.

During the December, 1954, observations, the transmitters were usually operated during alternate half-hour periods from 0915 hours to 1645 hours. Whenever nighttime observations were made the transmitter operated continuously. During the 1955 fall observations the transmitters were operated continuously from 0900 through 1600 hours.

Photographic records were made simultaneously at each station. These records indicate two principal modes of propagation, both of which were continuous over long periods of time. The first mode in time of arrival is attributed to tropospheric scattering and the second mode to ionospheric scattering. The pulses received by these two modes were very weak. In the "A" display of the monitor oscilloscope their apparent amplitudes were seldom much above that of the cosmic noise. There were also numerous random bursts lasting up to a minute or so having various time delays from zero to several hundred microseconds relative to the second mode. These random bursts were probably due to reflections from ionized meteor trails.

Each record was scaled to obtain the delays of the received pulses relative to the locally transmitted pulse. The round-trip propagation time is the sum of the delays measured simultaneously at each of the two sites minus the inserted delay. The delays of the ionospheric component of the signal relative to that of the tropospheric component were also reduced from the records at each site.

Equivalent midpoint heights were calculated from the round-trip data using the following equation:

$$H = \sqrt{\left(\frac{ct}{4}\right)^2 - \left(R \sin \frac{D}{2R}\right)^2} - R\left(1 - R \cos \frac{D}{2R}\right) \qquad (1)$$

Declassified in Part - Sanitized Copy Approved for Release @ 50-Yr 2014/06/09 : CIA-RDP81-01043R003000180001-4

Declassified in Part - Sanitized Copy Approved for Release @ 50-Yr 2014/06/09 : CIA-RDP81-01043R003000180001-4

where H = midpoint height in Km

t = round-trip propagation time in seconds

c = 3×10^5 Km/sec.

D = surface path length in Km

R = radius of curvature of the earth for the path

3. RESULTS

Mass plots of all the ionospheric and tropospheric round-trip delays as read from the photographic records at approximately 15-minute intervals and the equivalent heights are shown in Figures II-10 and II-11 for Dec., 1954, and in Figures II-12 and II-13 for September - October 1955. Each dot in these mass plots represents a single observation at about the indicated time. A slight displacement timewise was occasionally necessary to avoid superposition of the dots.

The hourly median values of equivalent ionospheric heights calculated from the December round-trip data varied between 93 Km at 1000 hours and 1700 hours and 89 Km from 1200 hours to 1400 hours. There were not enough data to calculate the medians for the other hours of the day. The median value of all the measured round-trip ionospheric delays was 4358 microseconds. The equivalent midpoint height is 90 Km.

The equivalent hourly median values of midpoint ionospheric heights calculated from the September - October, 1955, observations ranged from 87 Km at 1230 hours to 97 Km at 1430 hours. The median value of all the heights was 92 Km.

In December the hourly median values of equivalent midpoint tropospheric heights varied from about 30 Km to about 35 Km. The lower heights were observed most frequently during the daylight hours. However, there was no pronounced diurnal variation in the tropospheric height. The median value of all the round-trip tropospheric delays measured during Dec. was 4193 microseconds. The equivalent midpoint height is 32 Km.

The median value of all the tropospheric round-trip delays measured during September - October 1955 was 4206 microseconds. The equivalent midpoint height was 39 Km.

Equivalent midpoint ionospheric scatter heights were also calculated from the relative delays between the ionospheric component and the tropospheric component of the signal measured at each of the two sites. This relative delay is related to the midpoint ionospheric scatter height by the following equation:

$$\Delta t = \frac{1}{c}\left[2\sqrt{\left(R \sin \frac{D}{2R}\right)^2 + \left(H + R\left[1 - \cos \frac{D}{2R}\right]\right)^2} - La\right] \qquad (2)$$

where Δt = relative delay in seconds

La = tropospheric ray-path length in Km.

The smallest value for La consistent with the forward scatter mode of propagation is $2R \tan \frac{D}{2R}$. This two-tangent model is also in accordance with Gordon's analysis[2] which shows that the optimum height for tropospheric forward scattering is at the intersection of the horizon planes of the transmitter and the receiver on the great-circle path.

The hourly median values of ionospheric heights derived from the relative delays observed at Sterling during December, 1954, and the heights derived from simultaneous round-trip observations are compared in Figure II-14. The heights obtained by the round-trip method averaged about 8 Km greater than those obtained by the relative-delay method. The median value of all the heights obtained from the relative-delay measurements at Sterling during December, 1954, was 85 Km. The relative delay data obtained in September - October, 1955, have not been examined.

4. DISCUSSION OF RESULTS AND SOURCES OF ERROR

There are three sources of error which affect the results obtained with either one of these two methods of height determination. They are: (1) errors in computing the surface distance between the two sites, (2) reading errors by persons reducing the data from the recordings, and (3) instrumental errors.

The surface distance for this experiment was computed by the Coast and Geodetic Survey Office of the Department of Commerce.

The approximate magnitude of the reading errors was obtained by comparing the individual numbers read from the Sterling record by NBS personnel with the corresponding numbers read from the same record by Lincoln personnel. This comparison indicated reading errors of about plus or minus 6 microseconds for the tropospheric delays and about plus or minus 13 microseconds for ionospheric delays.

A check for possible instrumental errors was made by taking a low-powered pulse transmitter and a receiver-recorder to each of the two sites in turn and measuring the round-trip delay time over a 2-mile path. With full output from the low-powered transmitter the median value of the measured delays was within 2 microseconds of the calculated delay. Departures from the median were less than ± 5 microseconds. However, when the output of the low-powered transmitter was reduced to the point where the amplitude of the signal received by the opposite receiver was just above the threshold of recordability, the measured delay increased by an amount almost exactly equal to the full rise time of the transmitter

Declassified in Part - Sanitized Copy Approved for Release @ 50-Yr 2014/06/09 : CIA-RDP81-01043R003000180001-4

Declassified in Part - Sanitized Copy Approved for Release @ 50-Yr 2014/06/09 : CIA-RDP81-01043R003000180001-4

pulse. This weak-signal test simulated the actual condition which prevailed at both sites throughout the round-trip delay experiments.

It is evident from the above discussion that the greatest errors in the measured round-trip delays are due to this pulse rise time effect. The relative delay measurements were less sensitive to this effect because the tropospheric and ionospheric components of the received signal were about the same amplitude. The round-trip delays and corresponding equivalent heights shown in the figures do not take account of this effect and therefore are larger than the actual delays. The probable lower limit for the actual round-trip delays can be obtained by subtracting the rise times of both of the transmitted pulses from the measured delays. The total time to be subtracted from the round-trip delays measured in December is 12 microseconds and is 18 microseconds from those measured in October. The hourly median values of equivalent ionospheric heights corresponding to these lower-limit values of the round-trip delays obtained from the December, 1954, observations were 86 Km from 1200 hours to 1400 hours and 90 Km at 1000 hours and 1700 hours. The lower-limit median value of all the equivalent ionospheric heights for December was 87 Km. Similarly, the lower limit of the hourly median values of equivalent tropospheric height for December varied between 20 Km and 28 Km. The lower limit of the median value of all the equivalent tropospheric heights for December was 24 Km. A similar adjustment of the September - October, 1955, data gives lower-limit values of 87 Km for the equivalent ionospheric height and 29 Km for the equivalent tropospheric height.

The tropospheric heights obtained in this experiment were several times greater than the optimum height predicted by Gordon's model.[12] This result could be due to the radiation patterns of the antennas which were designed to illuminate a region about 90 Km above the earth at the midpoint of the path. Thus the intensity of illumination over the midpoint of the path increased very rapidly with height. The loss in scattering efficiency with height in the troposphere could have been partly offset by increased antenna gains at the greater heights.

The diurnal variations in the observed round-trip delays could have been due to variations in pulse rise-time effects with changes in signal levels.

The ionospheric heights obtained in this experiment are valid only for propagation paths similar to the experimental path in length and geographic position. An average height of about 90 Km is indicated.

Tropospheric heights between 20 Km and 30 Km are consistent with tropospheric propagation over distances of 600 miles or so reported by other observers.[13]

More round-trip pulse measurements should be made over longer paths. Shorter pulses with better rise-time characteristics should be used. The

experiments should be designed to discover possible seasonal and geographic effects on ionospheric scatter heights.*

*Note: Since completion of this report and work under the Signal Corps MIPR, an experimental set-up has been established for such measurements between Havana, Illinois, and Boulder, Colorado, and a preliminary report issued.[14]

REFERENCES

1. V. C. Pineo, "Oblique-Incidence Pulse Experiments at 49.8 Mc," NBS Report 4627, April 10, 1956.

2. V. C. Pineo, "Oblique-Incidence Measurements of the Heights at which Ionospheric Scattering of VHF Radio Waves Occurs," Jour. of Geophys. Res., 61, No. 2, June 1956.

3. J. N. Brown and J. M. Watts, "Ionospheric Observations at 50 Kc," Jour. of Geophys. Res., 55, No. 2, June 1950.

4. J. M. Watts, "Oblique-Incidence Propagation at 300 Kc using the Pulse Technique," NBS Report 1674, May 19, 1952.

5. W. H. Martin and P. G. Sulzer, "50 Megacycle Pulse Transmitter," NBS Report 8A117, Appendix XVI.

6. D. K. Bailey, R. Bateman, L. V. Berkner, H. G. Booker, G. F. Montgomery, E. M. Purcell, W. W. Salisbury, J. B. Wiesner, "A New Kind of Radio Propagation at Very High Frequencies Observable over Long Distances," Phys. Rev., 86, pp. 141-145, 1952.

7. J. Feinstein, C. Salzberg, "Ionospheric Reflection of VHF Radio Waves," NBS Report 1812, July 22, 1952.

8. T. L. Eckersley, "Studies in Radio Transmission," J.I.E.E., 71, pp. 405-459, 1932 (see pp. 439-443).

9. D. K. Bailey, R. Bateman, R. C. Kirby, "Radio Transmission at VHF by Scattering in the Lower Ionosphere," Proc. I.R.E., 43, pp. 1181-1230, October 1955. (See pp. 1217-1218.)

10. W. G. Abel and V. C. Pineo, "Scatter Heights Determined from VHF Pulse Experiments," given orally December 15, 1955, at URSI Fall Meeting, Gainesville, Florida.

11. V. C. Pineo, "Heights of Ionospheric and Tropospheric Scattering Determined from VHF Pulse Measurements," NBS Report 3570, February 10, 1956.

Declassified in Part - Sanitized Copy Approved for Release @ 50-Yr 2014/06/09 : CIA-RDP81-01043R003000180001-4

Declassified in Part - Sanitized Copy Approved for Release @ 50-Yr 2014/06/09 : CIA-RDP81-01043R003000180001-4

12. W. E. Gordon, "Radio Scattering in the Troposphere," Proc. I.R.E., 43, pp. 23-28, January 1955.

13. K. A. Norton, P. L. Rice and L. E. Vogler, "Use of Angular Distance in Estimating Transmission Loss," Subtitle No. IV, Proc. I.R.E., p. 1494, October 1955.

14. V. C. Pineo, "An Exploratory Investigation, using Pulse Techniques, of Ionospheric Forward Scatter Propagation at VHF over the 1295 Km Path between Havana, Illinois, and Boulder, Colorado," NBS Report 5532, October 29, 1957.

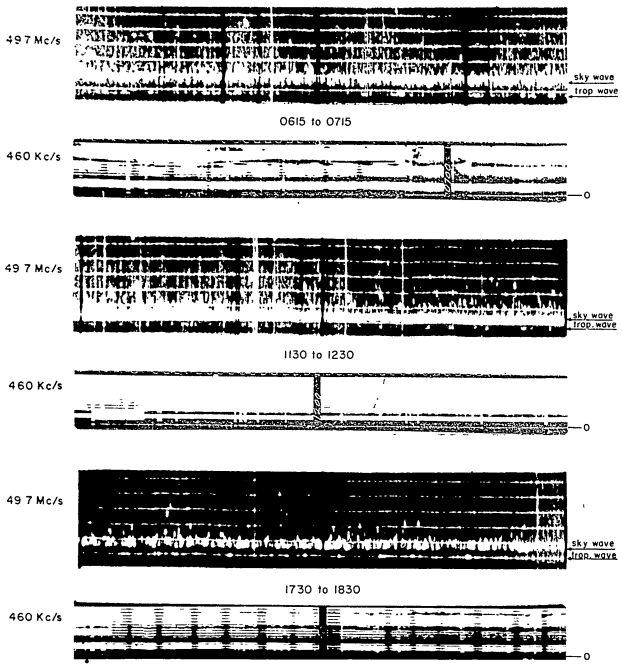

EXAMPLES OF OSCILLOGRAMS OBTAINED SIMULTANEOUSLY AT STERLING, VA. AND DOBSON, N.C. ON FEBRUARY 2, 1954.

FIGURE II-1

Declassified in Part - Sanitized Copy Approved for Release @ 50-Yr 2014/06/09 : CIA-RDP81-01043R003000180001-4

Declassified in Part - Sanitized Copy Approved for Release @ 50-Yr 2014/06/09 : CIA-RDP81-01043R003000180001-4

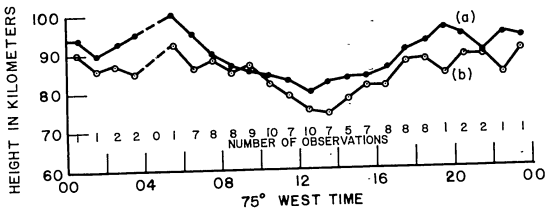

DIURNAL VARIATION OF HOURLY MEDIAN VALUES OF (a) VIRTUAL HEIGHTS OBSERVED AT 460 Kc/s AT STERLING, VA. AND (b) EQUIVALENT MIDPOINT HEIGHTS CALCULATED FROM SKY-WAVE DELAYS OBSERVED SIMULTANEOUSLY AT 49.7 Mc/s AT DOBSON N. C., 793 KM FROM THE MONTGOMERY, N. Y. TRANSMITTER.

FIGURE II-2

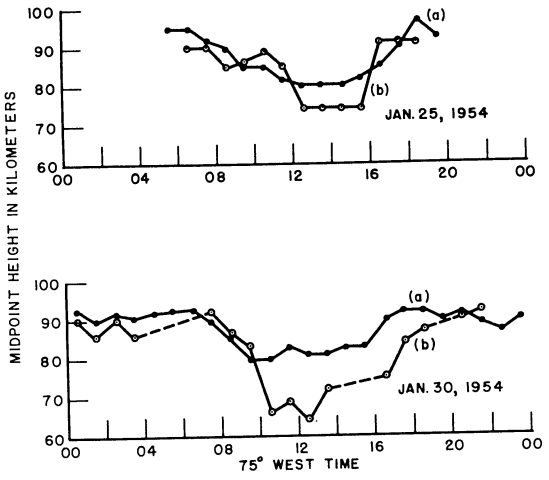

(a) VIRTUAL HEIGHTS OBSERVED DURING TWO TYPICAL DAYS IN JAN., 1954 AT 460 Kc/s AT STERLING, VA. AND (b) EQUIVALENT, MIDPOINT HEIGHTS CALCULATED FROM SKY-WAVE DELAYS OBSERVED SIMULTANEOUSLY AT 49.7 Mc/s AT DOBSON, N.C.

FIGURE II-3

Declassified in Part - Sanitized Copy Approved for Release @ 50-Yr 2014/06/09 : CIA-RDP81-01043R003000180001-4

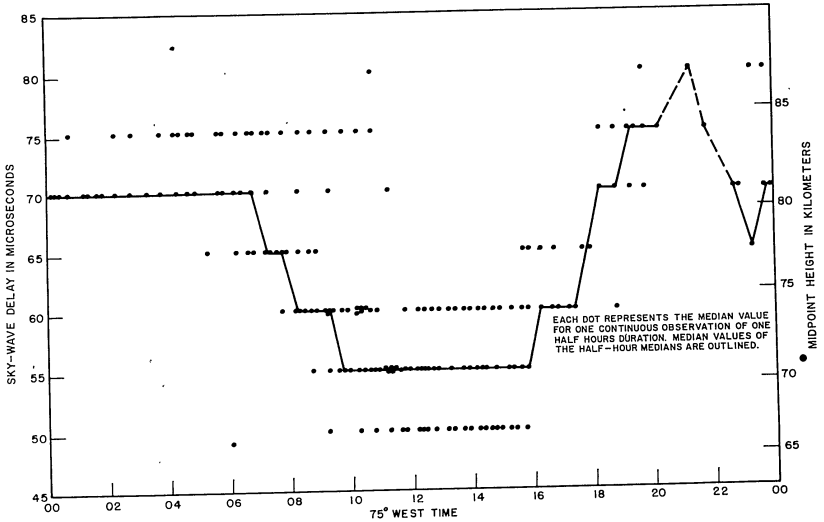
SKY-WAVE DELAY IN MICROSECONDS
MIDPOINT HEIGHT IN KILOMETERS
EACH DOT REPRESENTS THE MEDIAN VALUE FOR ONE CONTINUOUS OBSERVATION OF ONE HALF HOURS DURATION. MEDIAN VALUES OF THE HALF-HOUR MEDIANS ARE OUTLINED.
75° WEST TIME

SKY-WAVE DELAYS AND EQUIVALENT MIDPOINT HEIGHTS OBSERVED DURING THE PERIOD JUNE 18 TO JUNE 27, 1954 AT 49.7 Mc/s FOR THE STERLING, VA. TO BLUFFTON, S C PATH, 810 KM.

FIGURE 11-4

T IS TROPOSPHERIC SIGNAL AND I IS IONOSPHERIC SIGNAL WITH DELAYS RELATIVE TO THE TROPOSPHERIC PULSES CORRESPONDING TO HEIGHTS OF 85 KM and 75 KM RESPECTIVELY AT 0630 HRS AND 1200 HRS. TIME-DELAY MARKERS ARE AT 100 MICROSECOND INTERVALS. DURATION OF TRANSMITTED PULSE IS ABOUT 40 MICROSECONDS. THE PRF IS 50 PULSES PER SECOND. DRIFTING OF TRACES RELATIVE TO TIME-DELAY MARKERS CAUSED BY DIFFERENCE IN FREQUENCY BETWEEN THE TIMING OSCILLATORS FOR THE TRANSMITTER AND RECEIVER. UPPER OSCILLOGRAM SHOWS COMPENSATING ADJUSTMENT AT 0622 HRS.

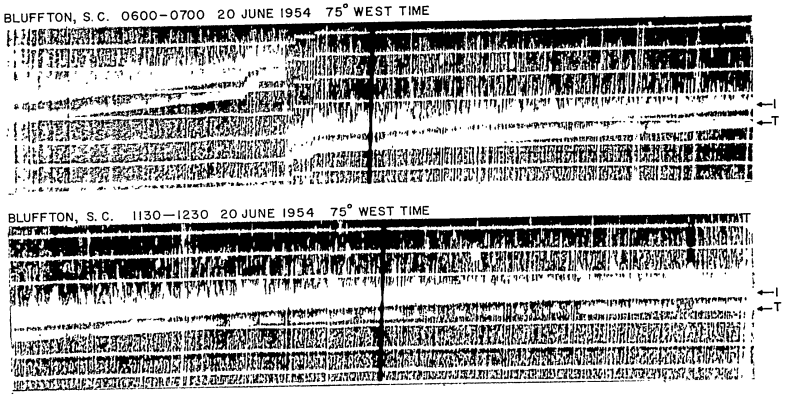

EXAMPLES OF OSCILLOGRAMS OF RECEIVED PULSE SIGNALS AT 49.7 Mc/s ON THE STERLING TO BLUFFTON PATH, 810 KM. SHOWING CHARACTERISTIC DIFFERENCES BETWEEN MORNING AND MIDDAY IN WIDTH OF IONOSPHERIC TRACES.

FIGURE 11-5

Declassified in Part - Sanitized Copy Approved for Release @ 50-Yr 2014/06/09 : CIA-RDP81-01043R003000180001-4
Declassified in Part - Sanitized Copy Approved for Release @ 50-Yr 2014/06/09 : CIA-RDP81-01043R003000180001-4

Declassified in Part - Sanitized Copy Approved for Release @ 50-Yr 2014/06/09 : CIA-RDP81-01043R003000180001-4

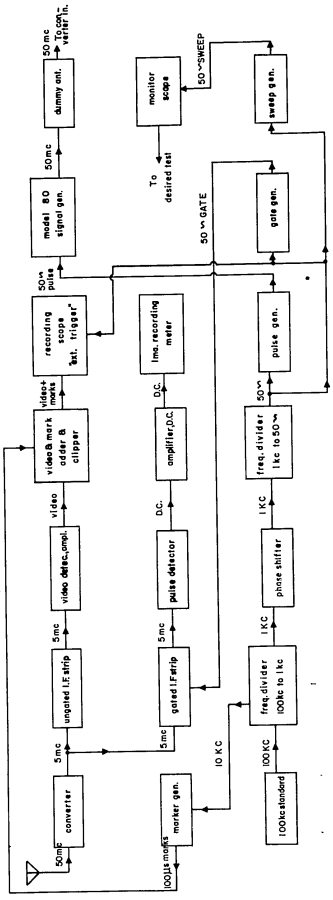

BLOCK DIAGRAM OF RECORDING SYSTEM
FIGURE II-6

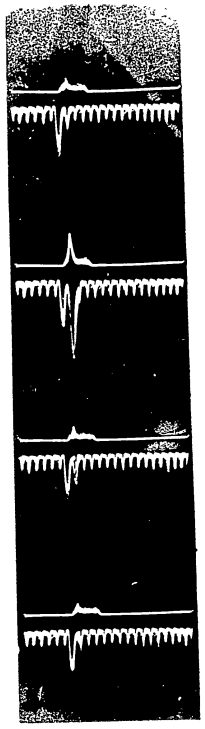

JUL. 15 1953 BETWEEN 09 HRS AND 10 HRS, 75° W TIME. TOP TRACES SHOW THE OUTPUT FROM THE GATED RECEIVER CONTAINING ONLY THE IONOSPHERIC PULSE. THE LOWER TRACES SHOW THE OUTPUT FROM UNGATED RECEIVER CONTAINING BOTH THE TROPOSPHERIC PULSE, FIRST FROM LEFT, AND THE IONOSPHERIC PULSE. TIME MARKERS IN LOWER TRACES ARE AT INTERVALS OF 100 MICROSECONDS. EXPOSURE APPROXIMATELY ONE SECOND PER FRAME AT INTERVALS OF ABOUT 5 SECONDS.

SAMPLES FROM A PHOTOGRAPHIC RECORD OF PULSES RECEIVED AT THE 491 KM SITE

FIGURE II-7

Declassified in Part - Sanitized Copy Approved for Release @ 50-Yr 2014/06/09 : CIA-RDP81-01043R003000180001-4

Declassified in Part - Sanitized Copy Approved for Release @ 50-Yr 2014/06/09 : CIA-RDP81-01043R003000180001-4

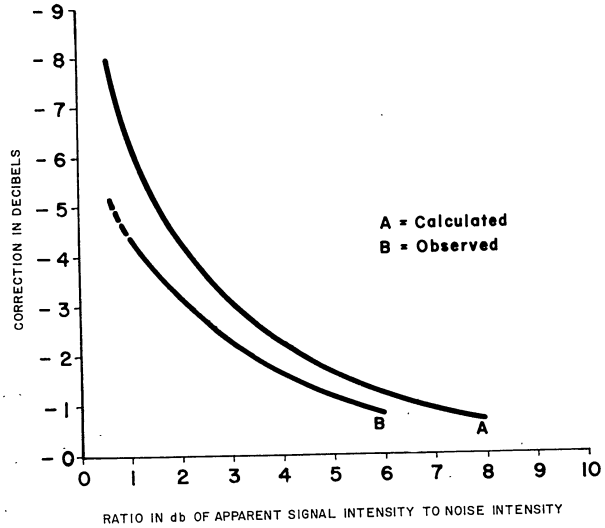

CURVES SHOWING THE CORRECTION IN DECIBELS TO BE APPLIED TO THE RETURNED SIGNAL INTENSITIES TO COMPENSATE FOR NOISE EFFECTS.

FIGURE II-8

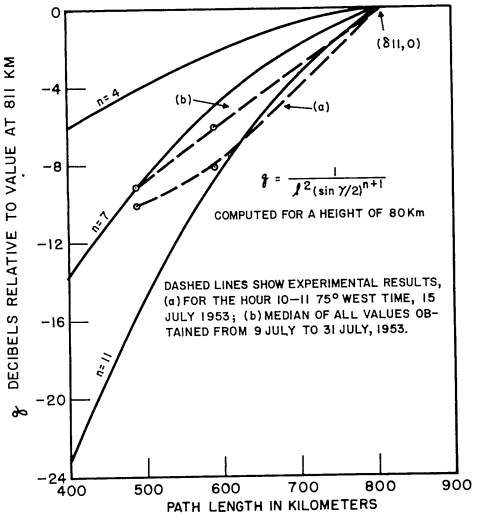

RESULTS OF ANGLE-DEPENDENCE OBSERVATIONS

FIGURE II-9

Declassified in Part - Sanitized Copy Approved for Release @ 50-Yr 2014/06/09 : CIA-RDP81-01043R003000180001-4

Declassified in Part - Sanitized Copy Approved for Release @ 50-Yr 2014/06/09 : CIA-RDP81-01043R003000180001-4

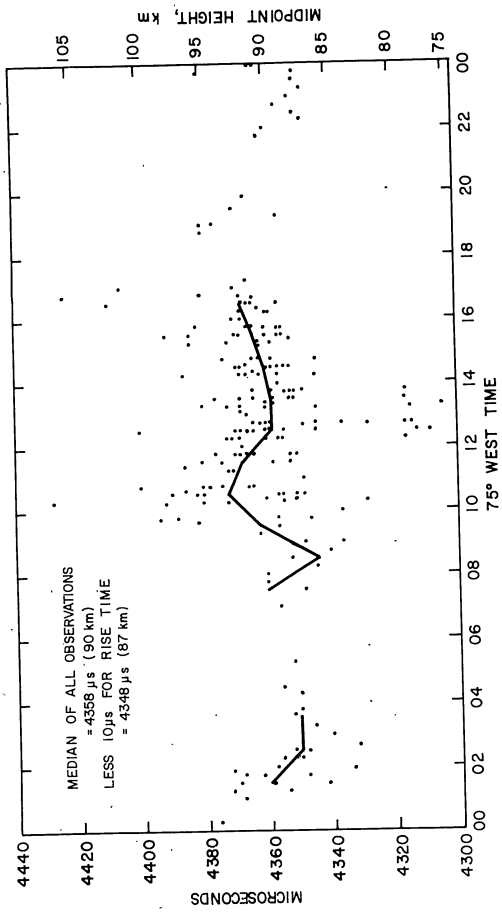

ROUND-TRIP IONOSPHERIC DELAYS OBSERVED DURING DECEMBER, 1954
FIGURE II-10

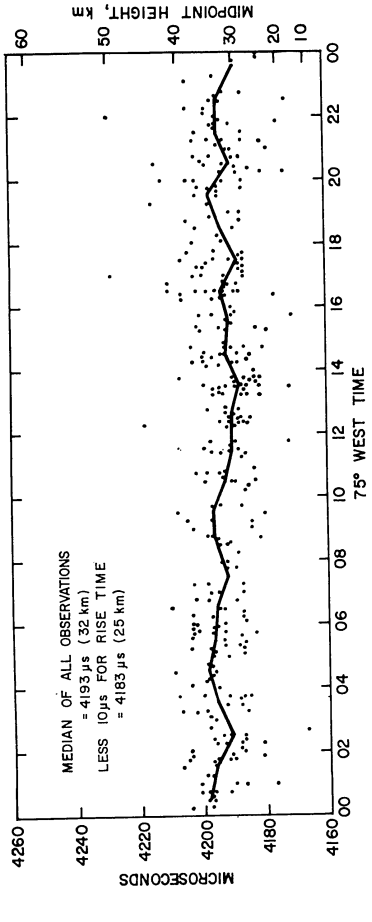

ROUND-TRIP TROPOSPHERIC DELAYS OBSERVED DURING DECEMBER, 1954
FIGURE II-11

Declassified in Part - Sanitized Copy Approved for Release @ 50-Yr 2014/06/09 : CIA-RDP81-01043R003000180001-4

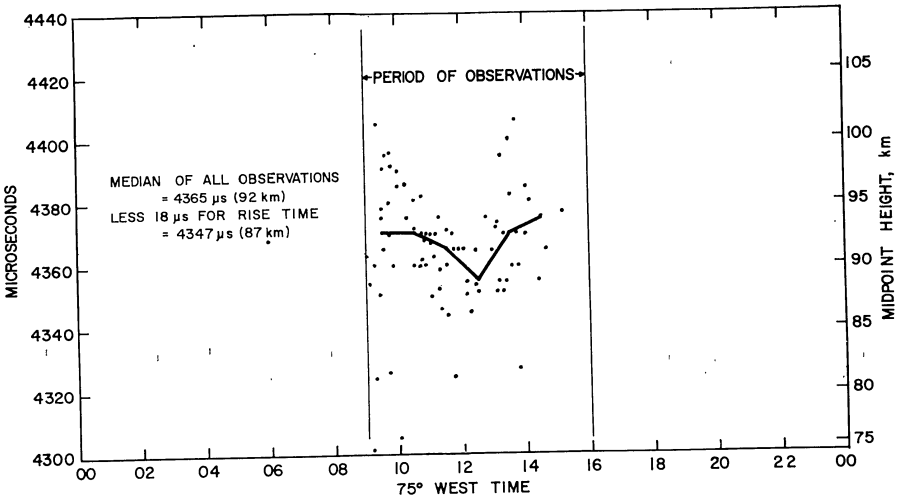

ROUND-TRIP IONOSPHERIC DELAYS OBSERVED DURING THE PERIOD SEPT. 28 TO OCT. 14, 1955

FIGURE 11-12

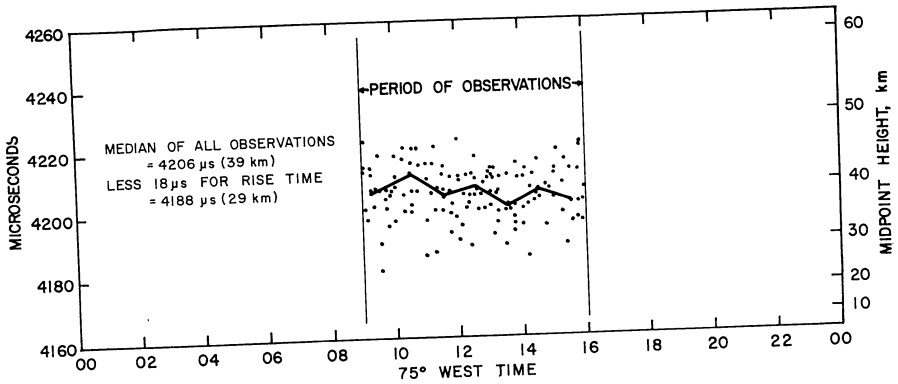

ROUND-TRIP TROPOSPHERIC DELAYS OBSERVED DURING THE PERIOD SEPT. 28 TO OCT. 14, 1955

FIGURE 11-13

Declassified in Part - Sanitized Copy Approved for Release @ 50-Yr 2014/06/09 : CIA-RDP81-01043R003000180001-4
Declassified in Part - Sanitized Copy Approved for Release @ 50-Yr 2014/06/09 : CIA-RDP81-01043R003000180001-4

Declassified in Part - Sanitized Copy Approved for Release @ 50-Yr 2014/06/09 : CIA-RDP81-01043R003000180001-4

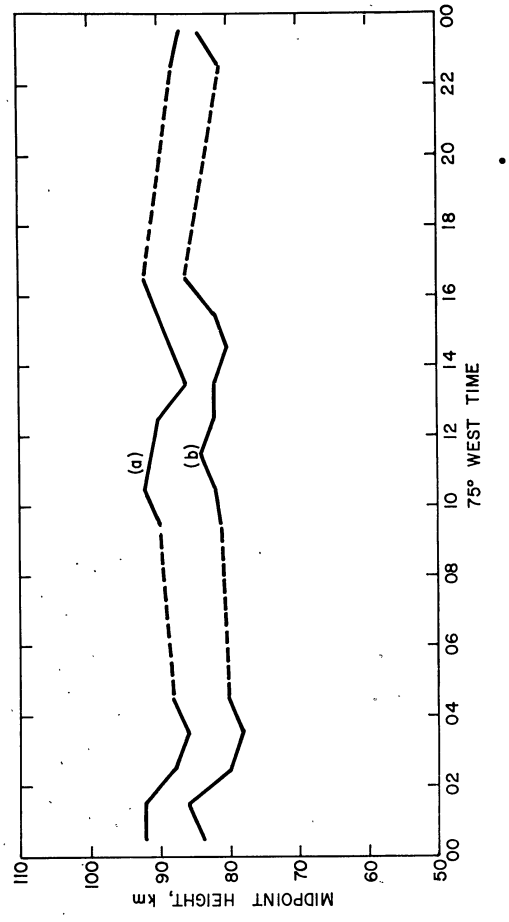

IONOSPHERIC HEIGHTS FROM SIMULTANEOUS MEASUREMENTS OF (a) ROUND-TRIP DELAYS AND (b) IONOSPHERIC vs TROPOSPHERIC DELAYS.

FIGURE II-14

APPENDIX III

PART I

CORRELATION OF VHF SIGNAL INTENSITIES WITH MAGNETIC K-INDICES

H. I. Leighton

In Appendix II of NBS Report 8A117, it was shown that a correlation exists between VHF signal intensities on the Anchorage-Barrow path at 48.87 Mc/s and magnetic K-indices at Fairbanks, Alaska. The possibility of correlation between VHF signal intensities on the Cedar Rapids-Sterling path at 49.8 Mc/s and planetary magnetic K-indices is here considered.

As before, the scale of K runs from 0-9 according to intensity of disturbance. Those K-figures of seven, eight and nine are grouped in one category in making the analysis. The individual VHF signal intensity departures are determined by taking the decibel difference between the numerically central hourly median, for the particular three-hour period, and the monthly median of all the hourly values observed during the month in the three-hour period.

It will be observed from the eight histograms of Figure III-1 and the graph of Figure III-2 that there is no very evident over-all correlation between VHF signal strength on the path observed in the temperate zone and either planetary or Cheltenham magnetic K-indices for the same three-hour periods. There is, however, a tendency toward greater signal strength with the decidedly higher K-figures.

Appendix X and the graphs of Figure 40 in the main text of this report show long-term relationship between signal strengths and planetary K-indices, Kp. The month-to-month correspondence shows a general decrease in both signal strength and magnetic index during the years of decreasing sunspot activity and an increase during the rise in sunspot activity. The correspondence is especially marked for the noontime period.

Declassified in Part - Sanitized Copy Approved for Release @ 50-Yr 2014/06/09 : CIA-RDP81-01043R003000180001-4

Declassified in Part - Sanitized Copy Approved for Release @ 50-Yr 2014/06/09 : CIA-RDP81-01043R003000180001-4

APPENDIX III

PART II

CORRELATION OF VHF SCATTER INTENSITIES WITH H'F RECORDS

R. M. Davis, Jr.

1. INTRODUCTION

This appendix continues and concludes for the present the studies described in previous reports,[1,2] in which a connection was demonstrated between intensities of VHF signals received over the Anchorage to Barrow path and concurrent conditions of the ionosphere as deduced from h'f ionosonde records. VHF signal intensities were shown to exhibit a statistical correspondence with the degree of absorption indicated by the h'f records, both those made at the end points of the transmission path and those made at Fairbanks, Alaska, in the general area of the path midpoint. The period covered by the earlier studies was January through August 1952. The data previously published for the period March through August 1952 are reproduced for the sake of continuity in Figures III-3 through III-10. This appendix presents subsequent data for the autumnal equinox period of 1952, the winter season, 1952-53, and the spring equinox months of 1953.

2. METHOD OF ANALYSIS

The procedure used in analyzing the observations reported in this appendix is the same as that followed in the case of the two earlier reports. It is briefly reviewed below.

Each hour for which VHF signal intensity recordings were available was classified under two headings:

a. The amount of departure of the median signal intensity for the given hour from the monthly median of such intensities.

b. The degree of simultaneous disturbance in the ionosphere indicated on h'f records. The disturbance was evaluated in two ways; first, from the h'f records made at the end points of the transmission path considered together; second, from a single record made at Fairbanks, Alaska.

To facilitate the study the signal intensity departures were grouped in intervals 5 db wide, above and below the median. A positive departure denoted a value of signal intensity above the median, a negative departure a value below the median.

Ionospheric conditions were evaluated by use of a special classification system presented earlier by D. K. Bailey. The system was designed to group the h'f records according to degree of disturbance. Each h'f

record was placed in one of the classes α, β, δ, or ϵ, in order of decreasing absorption and increasing regularity and stability of the ionospheric layers. In this system α represented complete absorption of the h'f trace, corresponding to blackout of HF sky-wave communication. The symbol ϵ stood for stable ionospheric layers and very low D-region absorption. Besides these classifications, there was another, γ, denoting the extremely scattered and fragmented records, with multiple oblique reflections and unusual stratifications, considered to be characteristic of auroral activity. The γ classification was taken to indicate an ionosphere more favorable to HF communication than β, but less favorable than δ. The addition of a star (*) indicated that the minimum frequency returned by the ionosphere was below 1.0 Mc/s. Such records were considered to denote fairly quiet conditions.

In assessing ionospheric conditions for the pair of end-points, the two Greek symbols assigned were replaced by a single figure, 1, 2, 3 or 4. The figure "1" represented the most disturbed average h'f conditions; "4" represented the quietest. Each possible combination of the five Greek symbols was placed in one of the four numbered groups. For Fairbanks, of course, one of the five Greek symbols alone sufficed to describe the ionosphere.

The practice of grouping the observations together for presentation by season is continued in this appendix. Autumnal equinox data are comprised of September and October, winter data of November, December, January and February, and spring equinox of March and April.

3. VARIATION OF VHF SIGNAL INTENSITY WITH H'F OBSERVATIONS

Figure III-11 consists of four normalized histograms depicting for September-October, 1952, distributions of departures of signal intensities from their monthly medians. The histogram at the top refers to category 1, representing extremely disturbed ionospheric conditions at the path end-points. The other histograms present data for increasingly quiet conditions, until the bottom figure illustrates the departures during stable ionospheric conditions when no more than weak absorption was experienced. Figure III-12 presents comparable data for November through February, 1952-53, and Figure III-13 the data for March-April, 1953. Corresponding distributions of departure, referred to the ionospheric conditions recorded at Fairbanks, appear in Figures III-17, III-18 and III-19.

The interesting feature of these figures is the progressive shift in the peaks of the histograms from positive values of departure to negative values as the associated h'f records change from disturbed to quiet. All of the figures, except III-19, exhibit the shift in the peaks of the histograms. It is most clearly shown in the winter figures, III-12 and III-18, in which twice as many observations are incorporated as in other figures. The poor correspondence of signal intensity with h'f condition in Figure III-19 may possibly be explained by the difficulty that

Declassified in Part - Sanitized Copy Approved for Release @ 50-Yr 2014/06/09 : CIA-RDP81-01043R003000180001-4

Declassified in Part - Sanitized Copy Approved for Release @ 50-Yr 2014/06/09 : CIA-RDP81-01043R003000180001-4

was experienced in classifying the April records at Fairbanks. Of the many h'f records classified as α, almost all were doubtful.

4. DIURNAL AND SEASONAL VARIATION OF IONOSPHERIC CHARACTERISTICS

In connection with the above analysis, it is of interest to consider the diurnal and seasonal variations of the occurrence of the four types of ionospheric conditions in the Arctic.

Figures III-14, III-15 and III-16 illustrate the diurnal distribution of the combined Anchorage-Barrow conditions in the fall, winter and spring seasons, respectively. Figures III-20, III-21 and III-22 show how the four ionospheric conditions were distributed at Fairbanks in the same three seasons. Finally there follow two figures describing the ionosphere in the first half of the summer season 1953, for which no study of the signal intensity departures has been attempted. Figure III-23 portrays the ionosphere for Anchorage-Barrow during May-June 1953 and Figure III-24 does the same for Fairbanks.

In general the h'f histograms follow the pattern of the ionospheric characteristics in the late winter, spring and summer of 1952 presented in previous reports. Conditions of total absorption (α) occur mostly in the half-day centered at 1200 hours. The tendency to peak at local noon seems more pronounced at equinox than in winter or summer.

At the other end of the absorption range, the quietest conditions occur predominantly between 1000 hours and midnight, with the afternoon and early evening hours most favored. In winter the quietest conditions are confined to the hours before 2000, and the maximum incidence is about 1400. In summer, on the other hand, the δ-condition occurs most frequently in the evening hours and has a peak about 2000 hours.

The complicated h'f records believed to be associated with auroral activity are about equally frequent at all seasons of the year, according to the Anchorage-Barrow analysis. But at Fairbanks no records of this type were reported in the spring and summer of 1953, in contrast to previous seasons. Fairbanks records also indicate a substantial decrease in the number of γ and δ records in the spring and summer of 1953. Their place was taken for the most part by increased numbers of α's. Some question exists if the augmented number of α's in the spring and summer of 1953 is genuine. As mentioned above most of the α-classifications in April, of which there were many, were considered to be doubtful.

Category 2 is comprised of generally poor conditions. In the Anchorage-Barrow analysis, it is made up of cases of partial absorption at both ends of the path, together with cases of complete absorption at only one end. At Fairbanks the corresponding designation, β, stands for partial absorption of the h'f trace. Category 2 appears to occur with somewhat greater frequency in summer than in winter.

When the distributions of all the characteristics are taken into account, it seems probable that HF conditions in the Arctic are better from 0600 to 1800 in winter than in summer, whereas nighttime conditions (1800 to 0600) are likely to be better in summer than in winter.

Certain of the diurnal variations of the h'f characteristics may be associated with the diurnal pattern of VHF signal intensity. The concentration of both complete and partial absorption in the hours around midday coincides with the high values of signal intensity recorded around local noon on the Anchorage to Barrow path. Furthermore, it is probable that the diurnal minimum of absorption in the early evening hours is associated with the diurnal minimum in VHF signal intensities about 2000 hours.

5. SUMMARY AND CONCLUSION

The relationship between VHF signal intensity and HF propagation conditions, established in the first two reports, has been demonstrated to exist in auroral regions in the autumn and winter seasons as well as in the spring and summer. It has been shown that intensity of VHF scattered signals observed at 50 Mc/s is correlated with degree of ionospheric disturbance, higher signal intensities being observed during conditions of greater absorption.

REFERENCES

1. D. K. Bailey, R. Bateman and R. C. Kirby, "Regular VHF Ionospheric Propagation Observable over Long Distances," NBS Report 8A111, June 30. 1952.

2. D. K. Bailey, R. Bateman and R. C. Kirby, "Second Report on Regular VHF Ionospheric Propagation Observable over Long Distances," NBS Report 8A117, June 30, 1953.

Declassified in Part - Sanitized Copy Approved for Release @ 50-Yr 2014/06/09 : CIA-RDP81-01043R003000180001-4

Declassified in Part - Sanitized Copy Approved for Release @ 50-Yr 2014/06/09 : CIA-RDP81-01043R003000180001-4

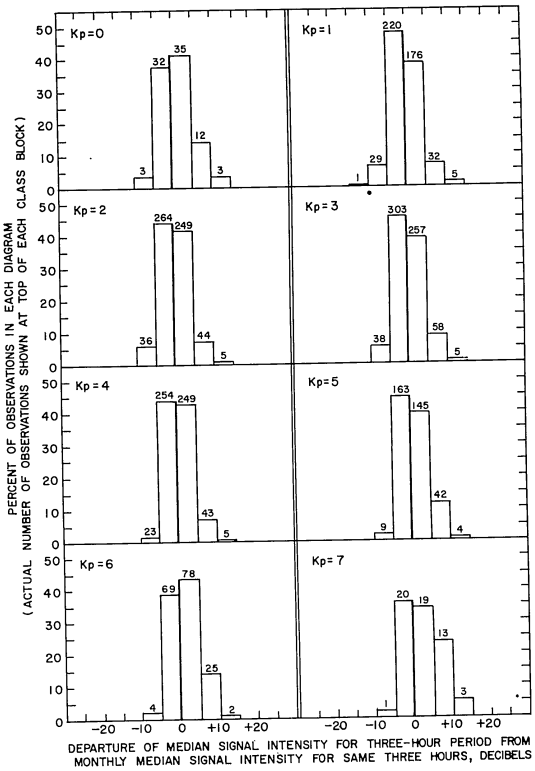

CEDAR RAPIDS—STERLING PATH (49.8 Mc/s)

COMPARISON OF SIGNAL INTENSITY OBSERVATIONS
WITH PLANETARY MAGNETIC K-INDEX

SEPTEMBER 1951 THROUGH SEPTEMBER 1952

FIGURE III-1

Declassified in Part - Sanitized Copy Approved for Release @ 50-Yr 2014/06/09 : CIA-RDP81-01043R003000180001-4

Declassified in Part - Sanitized Copy Approved for Release @ 50-Yr 2014/06/09 : CIA-RDP81-01043R003000180001-4

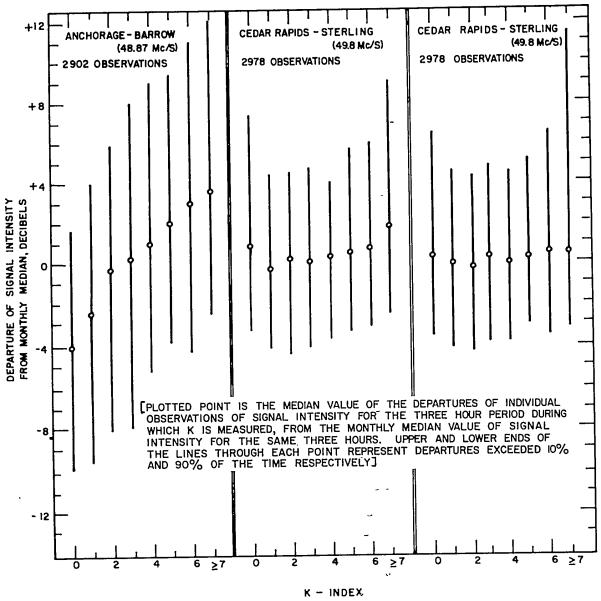
ANCHORAGE - BARROW
(48.87 Mc/S)
2902 OBSERVATIONS
CEDAR RAPIDS - STERLING
(49.8 Mc/S)
2978 OBSERVATIONS
CEDAR RAPIDS - STERLING
(49.8 Mc/S)
2978 OBSERVATIONS
DEPARTURE OF SIGNAL INTENSITY FROM MONTHLY MEDIAN, DECIBELS
+12
+8
+4
0
-4
-8
-12
0 2 4 6 ≥7 0 2 4 6 ≥7 0 2 4 6 ≥7
K - INDEX
[PLOTTED POINT IS THE MEDIAN VALUE OF THE DEPARTURES OF INDIVIDUAL OBSERVATIONS OF SIGNAL INTENSITY FOR THE THREE HOUR PERIOD DURING WHICH K IS MEASURED, FROM THE MONTHLY MEDIAN VALUE OF SIGNAL INTENSITY FOR THE SAME THREE HOURS. UPPER AND LOWER ENDS OF THE LINES THROUGH EACH POINT REPRESENT DEPARTURES EXCEEDED 10% AND 90% OF THE TIME RESPECTIVELY]

COMPARISON OF SIGNAL INTENSITY OBSERVATIONS
WITH MAGNETIC K-INDEX

13 MONTHS DATA, SEPTEMBER 1951 THROUGH SEPTEMBER 1952

FIGURE III-2

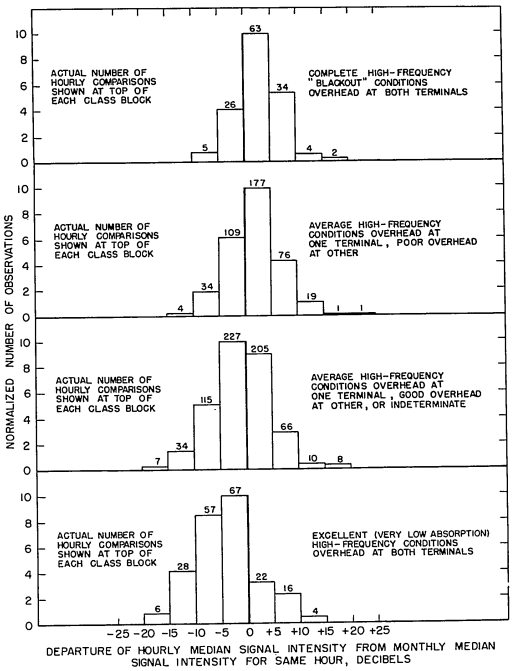
ACTUAL NUMBER OF HOURLY COMPARISONS SHOWN AT TOP OF EACH CLASS BLOCK
COMPLETE HIGH-FREQUENCY "BLACKOUT" CONDITIONS OVERHEAD AT BOTH TERMINALS
5 26 63 34 4 2
ACTUAL NUMBER OF HOURLY COMPARISONS SHOWN AT TOP OF EACH CLASS BLOCK
AVERAGE HIGH-FREQUENCY CONDITIONS OVERHEAD AT ONE TERMINAL, POOR OVERHEAD AT OTHER
4 34 109 177 76 19 1 1
ACTUAL NUMBER OF HOURLY COMPARISONS SHOWN AT TOP OF EACH CLASS BLOCK
AVERAGE HIGH-FREQUENCY CONDITIONS OVERHEAD AT ONE TERMINAL, GOOD OVERHEAD AT OTHER, OR INDETERMINATE
7 34 115 227 205 66 10 8
ACTUAL NUMBER OF HOURLY COMPARISONS SHOWN AT TOP OF EACH CLASS BLOCK
EXCELLENT (VERY LOW ABSORPTION) HIGH-FREQUENCY CONDITIONS OVERHEAD AT BOTH TERMINALS
6 28 57 67 22 16 4
NORMALIZED NUMBER OF OBSERVATIONS
0 2 4 6 8 10
-25 -20 -15 -10 -5 0 +5 +10 +15 +20 +25
DEPARTURE OF HOURLY MEDIAN SIGNAL INTENSITY FROM MONTHLY MEDIAN SIGNAL INTENSITY FOR SAME HOUR, DECIBELS

ANCHORAGE - BARROW PATH (48.87 Mc/s)

COMPARISONS OF SIGNAL INTENSITY OBSERVATIONS WITH HIGH-FREQUENCY PROPAGATION CONDITIONS AS DETERMINED FROM HOURLY IONOSPHERIC SOUNDING OBSERVATIONS MADE SIMULTANEOUSLY AT THE PATH TERMINALS

MARCH AND APRIL 1952

FIGURE III-3

Declassified in Part - Sanitized Copy Approved for Release @ 50-Yr 2014/06/09 : CIA-RDP81-01043R003000180001-4

Declassified in Part - Sanitized Copy Approved for Release @ 50-Yr 2014/06/09 : CIA-RDP81-01043R003000180001-4

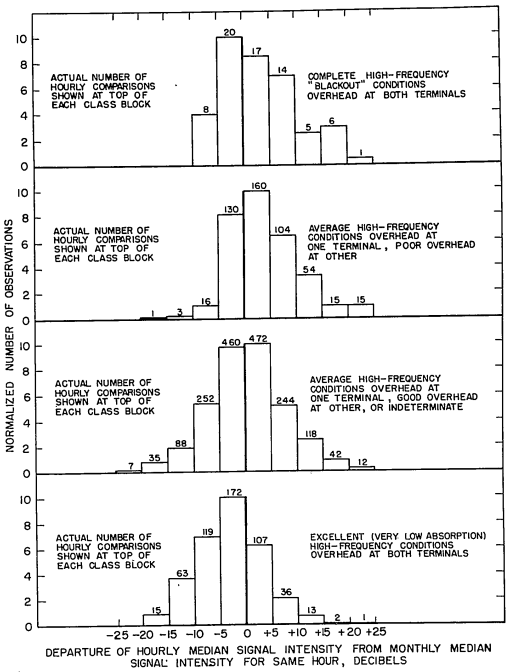
NORMALIZED NUMBER OF OBSERVATIONS
ACTUAL NUMBER OF HOURLY COMPARISONS SHOWN AT TOP OF EACH CLASS BLOCK
COMPLETE HIGH-FREQUENCY "BLACKOUT" CONDITIONS OVERHEAD AT BOTH TERMINALS
8 20 17 14 5 6 1
ACTUAL NUMBER OF HOURLY COMPARISONS SHOWN AT TOP OF EACH CLASS BLOCK
AVERAGE HIGH-FREQUENCY CONDITIONS OVERHEAD AT ONE TERMINAL, POOR OVERHEAD AT OTHER
1 3 16 130 160 104 54 15 15
ACTUAL NUMBER OF HOURLY COMPARISONS SHOWN AT TOP OF EACH CLASS BLOCK
AVERAGE HIGH-FREQUENCY CONDITIONS OVERHEAD AT ONE TERMINAL, GOOD OVERHEAD AT OTHER, OR INDETERMINATE
7 35 88 252 460 472 244 118 42 12
ACTUAL NUMBER OF HOURLY COMPARISONS SHOWN AT TOP OF EACH CLASS BLOCK
EXCELLENT (VERY LOW ABSORPTION) HIGH-FREQUENCY CONDITIONS OVERHEAD AT BOTH TERMINALS
15 63 119 172 107 36 13 2 1
-25 -20 -15 -10 -5 0 +5 +10 +15 +20 +25
DEPARTURE OF HOURLY MEDIAN SIGNAL INTENSITY FROM MONTHLY MEDIAN SIGNAL INTENSITY FOR SAME HOUR, DECIBELS

ANCHORAGE - BARROW PATH (48 87 Mc/s)

COMPARISONS OF SIGNAL INTENSITY OBSERVATIONS WITH HIGH-FREQUENCY PROPAGATION CONDITIONS AS DETERMINED FROM HOURLY IONOSPHERIC SOUNDING OBSERVATIONS MADE SIMULTANEOUSLY AT THE PATH TERMINALS
MAY THROUGH AUGUST 1952

FIGURE III-4

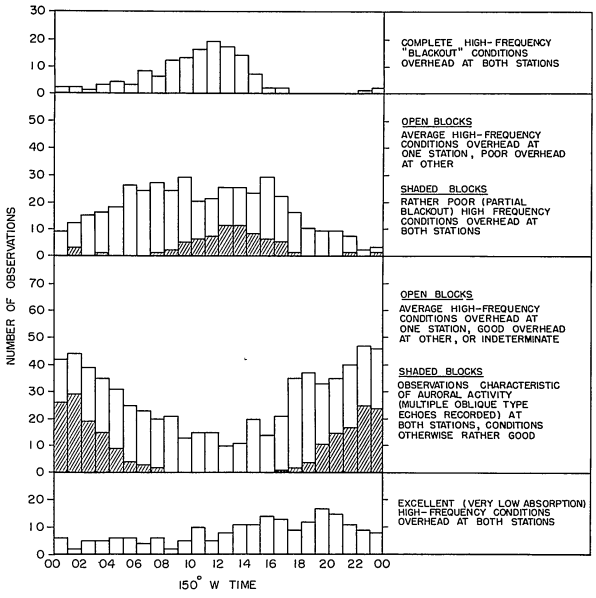
NUMBER OF OBSERVATIONS
COMPLETE HIGH-FREQUENCY "BLACKOUT" CONDITIONS OVERHEAD AT BOTH STATIONS
OPEN BLOCKS
AVERAGE HIGH-FREQUENCY CONDITIONS OVERHEAD AT ONE STATION, POOR OVERHEAD AT OTHER
SHADED BLOCKS
RATHER POOR (PARTIAL BLACKOUT) HIGH FREQUENCY CONDITIONS OVERHEAD AT BOTH STATIONS
OPEN BLOCKS
AVERAGE HIGH-FREQUENCY CONDITIONS OVERHEAD AT ONE STATION, GOOD OVERHEAD AT OTHER, OR INDETERMINATE
SHADED BLOCKS
OBSERVATIONS CHARACTERISTIC OF AURORAL ACTIVITY (MULTIPLE OBLIQUE TYPE ECHOES RECORDED) AT BOTH STATIONS, CONDITIONS OTHERWISE RATHER GOOD
EXCELLENT (VERY LOW ABSORPTION) HIGH-FREQUENCY CONDITIONS OVERHEAD AT BOTH STATIONS
00 02 04 06 08 10 12 14 16 18 20 22 00
150° W TIME

ANCHORAGE AND BARROW IONOSPHERIC CONDITIONS
MARCH AND APRIL 1952

FIGURE III-5

Declassified in Part - Sanitized Copy Approved for Release @ 50-Yr 2014/06/09 : CIA-RDP81-01043R003000180001-4

Declassified in Part - Sanitized Copy Approved for Release @ 50-Yr 2014/06/09 : CIA-RDP81-01043R003000180001-4

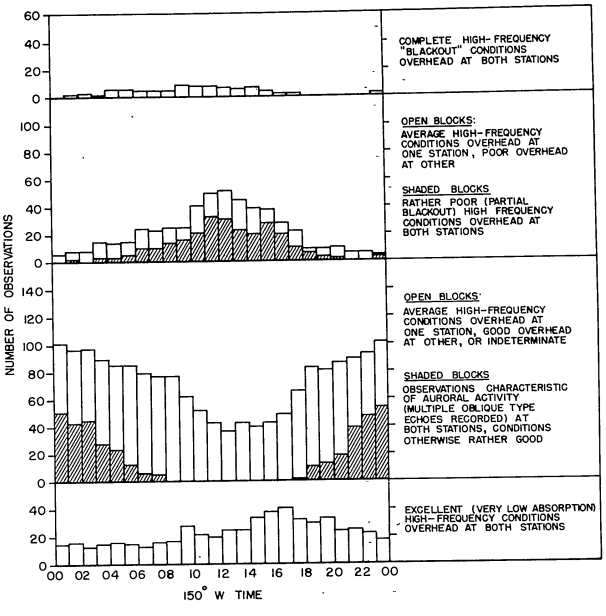
NUMBER OF OBSERVATIONS
COMPLETE HIGH-FREQUENCY "BLACKOUT" CONDITIONS OVERHEAD AT BOTH STATIONS
OPEN BLOCKS: AVERAGE HIGH-FREQUENCY CONDITIONS OVERHEAD AT ONE STATION, POOR OVERHEAD AT OTHER
SHADED BLOCKS RATHER POOR (PARTIAL BLACKOUT) HIGH FREQUENCY CONDITIONS OVERHEAD AT BOTH STATIONS
OPEN BLOCKS: AVERAGE HIGH-FREQUENCY CONDITIONS OVERHEAD AT ONE STATION, GOOD OVERHEAD AT OTHER, OR INDETERMINATE
SHADED BLOCKS OBSERVATIONS CHARACTERISTIC OF AURORAL ACTIVITY (MULTIPLE OBLIQUE TYPE ECHOES RECORDED) AT BOTH STATIONS, CONDITIONS OTHERWISE RATHER GOOD
EXCELLENT (VERY LOW ABSORPTION) HIGH-FREQUENCY CONDITIONS OVERHEAD AT BOTH STATIONS
00 02 04 06 08 10 12 14 16 18 20 22 00
150° W TIME

ANCHORAGE AND BARROW IONOSPHERIC CONDITIONS
MAY THROUGH AUGUST 1952

FIGURE III-6

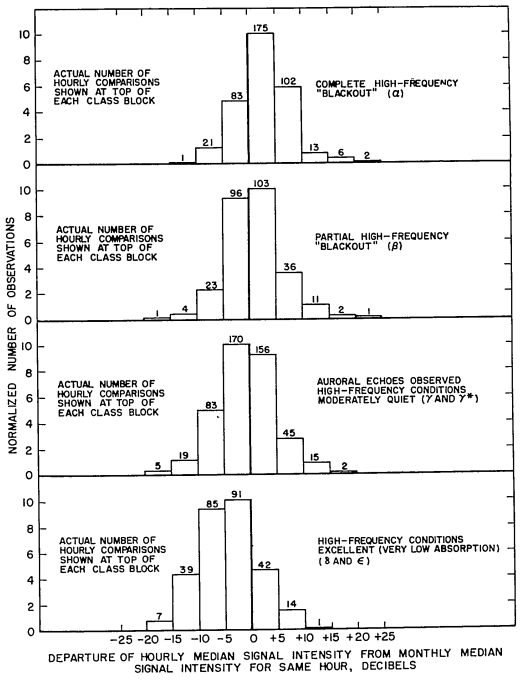
NORMALIZED NUMBER OF OBSERVATIONS
ACTUAL NUMBER OF HOURLY COMPARISONS SHOWN AT TOP OF EACH CLASS BLOCK
COMPLETE HIGH-FREQUENCY "BLACKOUT" (α)
1 21 83 175 102 13 6 2
ACTUAL NUMBER OF HOURLY COMPARISONS SHOWN AT TOP OF EACH CLASS BLOCK
PARTIAL HIGH-FREQUENCY "BLACKOUT" (β)
1 4 23 96 103 36 11 2 1
ACTUAL NUMBER OF HOURLY COMPARISONS SHOWN AT TOP OF EACH CLASS BLOCK
AURORAL ECHOES OBSERVED HIGH-FREQUENCY CONDITIONS MODERATELY QUIET (γ AND γ*)
5 19 83 170 156 45 15 2
ACTUAL NUMBER OF HOURLY COMPARISONS SHOWN AT TOP OF EACH CLASS BLOCK
HIGH-FREQUENCY CONDITIONS EXCELLENT (VERY LOW ABSORPTION) (δ AND ε)
7 39 85 91 42 14 1
-25 -20 -15 -10 -5 0 +5 +10 +15 +20 +25
DEPARTURE OF HOURLY MEDIAN SIGNAL INTENSITY FROM MONTHLY MEDIAN SIGNAL INTENSITY FOR SAME HOUR, DECIBELS

ANCHORAGE - BARROW PATH (48.87 Mc/s)

COMPARISONS OF SIGNAL INTENSITY OBSERVATIONS WITH HIGH-FREQUENCY PROPAGATION CONDITIONS AS DETERMINED FROM HOURLY IONOSPHERIC SOUNDING OBSERVATIONS MADE AT FAIRBANKS - NEAR THE PATH MIDPOINT
MARCH AND APRIL 1952

FIGURE III-7

Declassified in Part - Sanitized Copy Approved for Release @ 50-Yr 2014/06/09 : CIA-RDP81-01043R003000180001-4

Declassified in Part - Sanitized Copy Approved for Release @ 50-Yr 2014/06/09 : CIA-RDP81-01043R003000180001-4

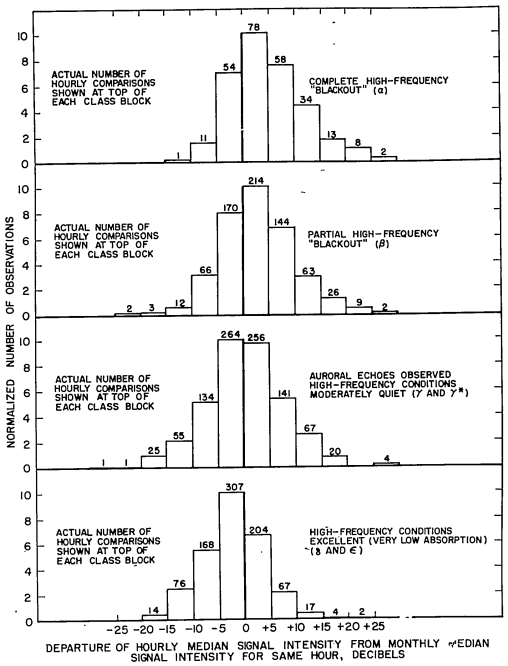
NORMALIZED NUMBER OF OBSERVATIONS
ACTUAL NUMBER OF HOURLY COMPARISONS SHOWN AT TOP OF EACH CLASS BLOCK
COMPLETE HIGH-FREQUENCY "BLACKOUT" (α)
1 11 54 78 58 34 13 8 2
PARTIAL HIGH-FREQUENCY "BLACKOUT" (β)
2 3 12 66 170 214 144 63 26 9 2
AURORAL ECHOES OBSERVED HIGH-FREQUENCY CONDITIONS MODERATELY QUIET (γ AND γ*)
1 1 25 55 134 264 256 141 67 20 4
HIGH-FREQUENCY CONDITIONS EXCELLENT (VERY LOW ABSORPTION) (δ AND ε)
14 76 168 307 204 67 17 4 2
-25 -20 -15 -10 -5 0 +5 +10 +15 +20 +25
DEPARTURE OF HOURLY MEDIAN SIGNAL INTENSITY FROM MONTHLY MEDIAN SIGNAL INTENSITY FOR SAME HOUR, DECIBELS

ANCHORAGE – BARROW PATH (48.87 Mc/s)

COMPARISONS OF SIGNAL INTENSITY OBSERVATIONS WITH HIGH-FREQUENCY PROPAGATION CONDITIONS AS DETERMINED FROM HOURLY IONOSPHERIC SOUNDING OBSERVATIONS MADE AT FAIRBANKS – NEAR THE PATH MIDPOINT

MAY THROUGH AUGUST 1952

FIGURE III–8

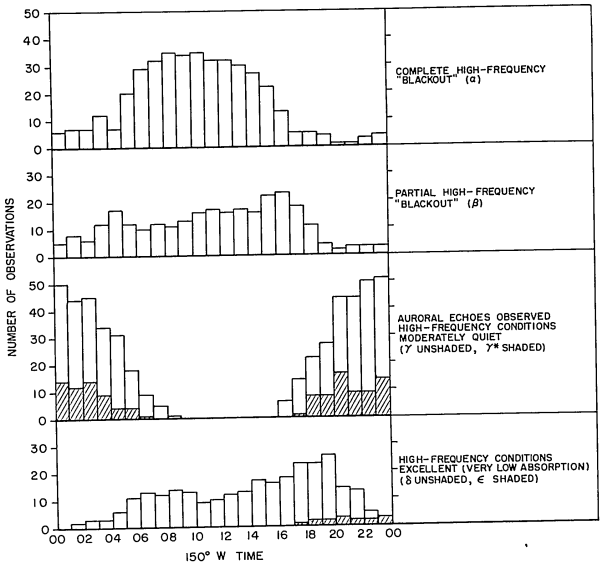
NUMBER OF OBSERVATIONS
COMPLETE HIGH-FREQUENCY "BLACKOUT" (α)
PARTIAL HIGH-FREQUENCY "BLACKOUT" (β)
AURORAL ECHOES OBSERVED HIGH-FREQUENCY CONDITIONS MODERATELY QUIET (γ UNSHADED, γ* SHADED)
HIGH-FREQUENCY CONDITIONS EXCELLENT (VERY LOW ABSORPTION) (δ UNSHADED, ε SHADED)
00 02 04 06 08 10 12 14 16 18 20 22 00
150° W TIME

FAIRBANKS IONOSPHERIC CONDITIONS

MARCH AND APRIL 1952

FIGURE III–9

Declassified in Part - Sanitized Copy Approved for Release @ 50-Yr 2014/06/09 : CIA-RDP81-01043R003000180001-4

Declassified in Part - Sanitized Copy Approved for Release @ 50-Yr 2014/06/09 : CIA-RDP81-01043R003000180001-4

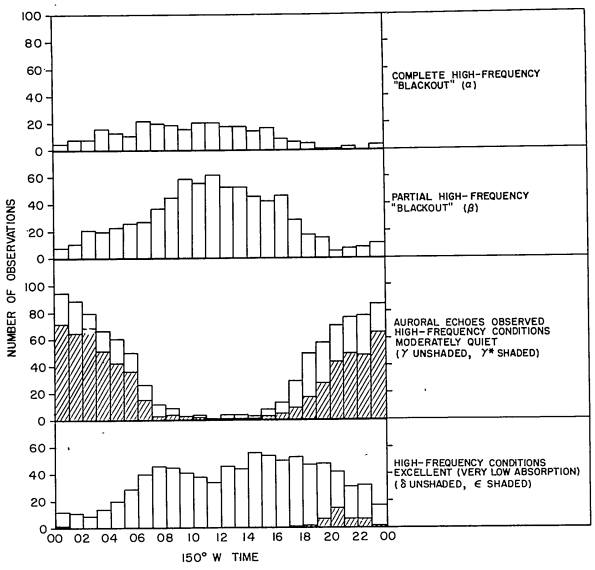
NUMBER OF OBSERVATIONS
COMPLETE HIGH-FREQUENCY "BLACKOUT" (α)
PARTIAL HIGH-FREQUENCY "BLACKOUT" (β)
AURORAL ECHOES OBSERVED. HIGH-FREQUENCY CONDITIONS MODERATELY QUIET (γ UNSHADED, γ* SHADED)
HIGH-FREQUENCY CONDITIONS EXCELLENT (VERY LOW ABSORPTION) (δ UNSHADED, ε SHADED)
00 02 04 06 08 10 12 14 16 18 20 22 00
150° W TIME

FAIRBANKS IONOSPHERIC CONDITIONS
MAY THROUGH AUGUST 1952

FIGURE III-10

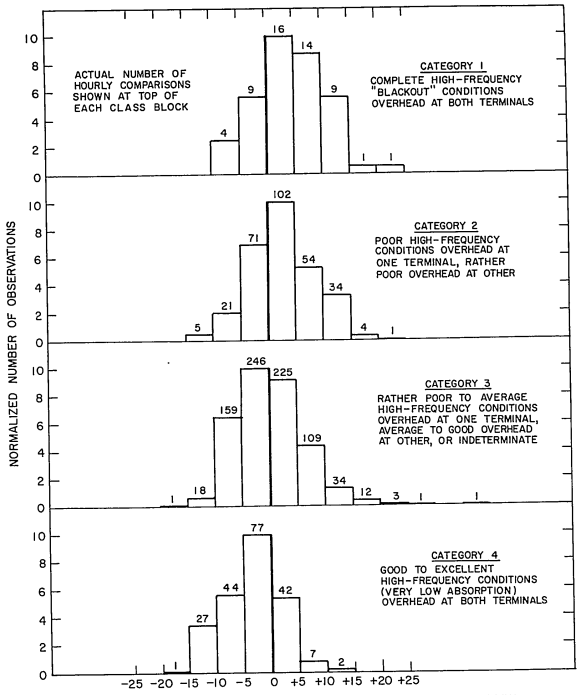
NORMALIZED NUMBER OF OBSERVATIONS
ACTUAL NUMBER OF HOURLY COMPARISONS SHOWN AT TOP OF EACH CLASS BLOCK
CATEGORY 1
COMPLETE HIGH-FREQUENCY "BLACKOUT" CONDITIONS OVERHEAD AT BOTH TERMINALS
CATEGORY 2
POOR HIGH-FREQUENCY CONDITIONS OVERHEAD AT ONE TERMINAL, RATHER POOR OVERHEAD AT OTHER
CATEGORY 3
RATHER POOR TO AVERAGE HIGH-FREQUENCY CONDITIONS OVERHEAD AT ONE TERMINAL, AVERAGE TO GOOD OVERHEAD AT OTHER, OR INDETERMINATE
CATEGORY 4
GOOD TO EXCELLENT HIGH-FREQUENCY CONDITIONS (VERY LOW ABSORPTION) OVERHEAD AT BOTH TERMINALS
-25 -20 -15 -10 -5 0 +5 +10 +15 +20 +25
DEPARTURE OF HOURLY MEDIAN SIGNAL INTENSITY FROM MONTHLY MEDIAN SIGNAL INTENSITY FOR SAME HOUR, DECIBELS

ANCHORAGE TO BARROW - 48.87Mc/s

COMPARISONS OF SIGNAL INTENSITY OBSERVATIONS WITH HIGH-FREQUENCY PROPAGATION CONDITIONS AS DETERMINED FROM HOURLY IONOSPHERIC SOUNDING OBSERVATIONS MADE SIMULTANEOUSLY AT THE PATH TERMINALS
SEPTEMBER AND OCTOBER 1952

FIGURE III-11

Declassified in Part - Sanitized Copy Approved for Release @ 50-Yr 2014/06/09 : CIA-RDP81-01043R003000180001-4

Declassified in Part - Sanitized Copy Approved for Release @ 50-Yr 2014/06/09 : CIA-RDP81-01043R003000180001-4

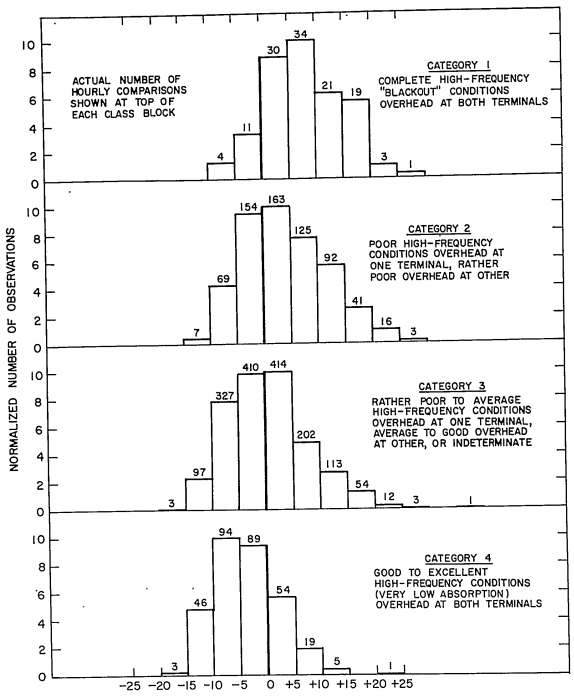
NORMALIZED NUMBER OF OBSERVATIONS
ACTUAL NUMBER OF HOURLY COMPARISONS SHOWN AT TOP OF EACH CLASS BLOCK
CATEGORY 1
COMPLETE HIGH-FREQUENCY "BLACKOUT" CONDITIONS OVERHEAD AT BOTH TERMINALS
4 11 30 34 21 19 3 1
CATEGORY 2
POOR HIGH-FREQUENCY CONDITIONS OVERHEAD AT ONE TERMINAL, RATHER POOR OVERHEAD AT OTHER
7 69 154 163 125 92 41 16 3
CATEGORY 3
RATHER POOR TO AVERAGE HIGH-FREQUENCY CONDITIONS OVERHEAD AT ONE TERMINAL, AVERAGE TO GOOD OVERHEAD AT OTHER, OR INDETERMINATE
3 97 327 410 414 202 113 54 12 3 1
CATEGORY 4
GOOD TO EXCELLENT HIGH-FREQUENCY CONDITIONS (VERY LOW ABSORPTION) OVERHEAD AT BOTH TERMINALS
3 46 94 89 54 19 5 1
0 2 4 6 8 10
-25 -20 -15 -10 -5 0 +5 +10 +15 +20 +25
DEPARTURE OF HOURLY MEDIAN SIGNAL INTENSITY FROM MONTHLY MEDIAN SIGNAL INTENSITY FOR SAME HOUR, DECIBELS

ANCHORAGE TO BARROW – 48.87 Mc/s

COMPARISONS OF SIGNAL INTENSITY OBSERVATIONS WITH HIGH-FREQUENCY PROPAGATION CONDITIONS AS DETERMINED FROM HOURLY IONOSPHERIC SOUNDING OBSERVATIONS MADE SIMULTANEOUSLY AT THE PATH TERMINALS

NOVEMBER 1952 THROUGH FEBRUARY 1953

FIGURE III–12

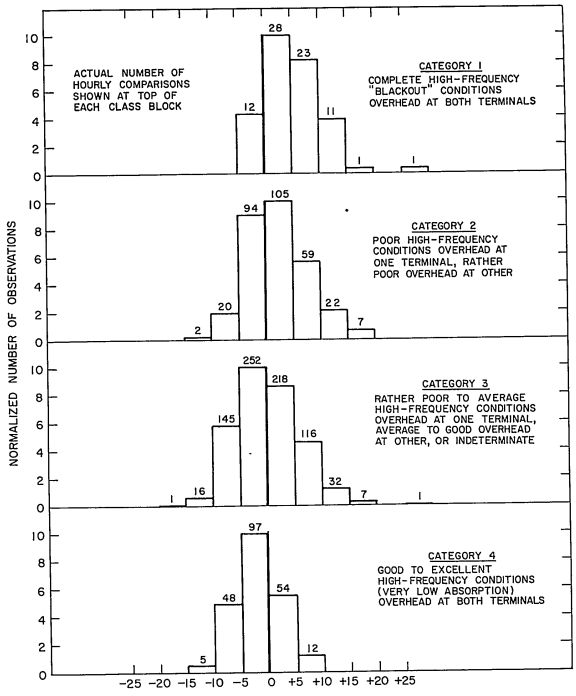
NORMALIZED NUMBER OF OBSERVATIONS
ACTUAL NUMBER OF HOURLY COMPARISONS SHOWN AT TOP OF EACH CLASS BLOCK
CATEGORY 1
COMPLETE HIGH-FREQUENCY "BLACKOUT" CONDITIONS OVERHEAD AT BOTH TERMINALS
12 28 23 11 1 1
CATEGORY 2
POOR HIGH-FREQUENCY CONDITIONS OVERHEAD AT ONE TERMINAL, RATHER POOR OVERHEAD AT OTHER
2 20 94 105 59 22 7
CATEGORY 3
RATHER POOR TO AVERAGE HIGH-FREQUENCY CONDITIONS OVERHEAD AT ONE TERMINAL, AVERAGE TO GOOD OVERHEAD AT OTHER, OR INDETERMINATE
1 16 145 252 218 116 32 7 1
CATEGORY 4
GOOD TO EXCELLENT HIGH-FREQUENCY CONDITIONS (VERY LOW ABSORPTION) OVERHEAD AT BOTH TERMINALS
5 48 97 54 12
0 2 4 6 8 10
-25 -20 -15 -10 -5 0 +5 +10 +15 +20 +25
DEPARTURE OF HOURLY MEDIAN SIGNAL INTENSITY FROM MONTHLY MEDIAN SIGNAL INTENSITY FOR SAME HOUR, DECIBELS

ANCHORAGE TO BARROW – 48.87 Mc/s

COMPARISONS OF SIGNAL INTENSITY OBSERVATIONS WITH HIGH FREQUENCY PROPAGATION CONDITIONS AS DETERMINED FROM HOURLY IONOSPHERIC SOUNDING OBSERVATIONS MADE SIMULTANEOUSLY AT THE PATH TERMINALS

MARCH AND APRIL 1953

FIGURE III–13

Declassified in Part - Sanitized Copy Approved for Release @ 50-Yr 2014/06/09 : CIA-RDP81-01043R003000180001-4

Declassified in Part - Sanitized Copy Approved for Release @ 50-Yr 2014/06/09 : CIA-RDP81-01043R003000180001-4

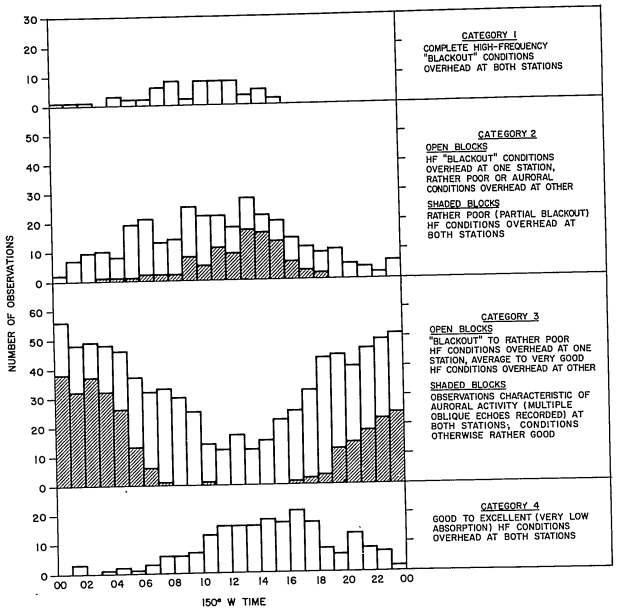
NUMBER OF OBSERVATIONS
CATEGORY 1
COMPLETE HIGH-FREQUENCY "BLACKOUT" CONDITIONS OVERHEAD AT BOTH STATIONS
CATEGORY 2
OPEN BLOCKS
HF "BLACKOUT" CONDITIONS OVERHEAD AT ONE STATION, RATHER POOR OR AURORAL CONDITIONS OVERHEAD AT OTHER
SHADED BLOCKS
RATHER POOR (PARTIAL BLACKOUT) HF CONDITIONS OVERHEAD AT BOTH STATIONS
CATEGORY 3
OPEN BLOCKS
"BLACKOUT" TO RATHER POOR HF CONDITIONS OVERHEAD AT ONE STATION, AVERAGE TO VERY GOOD HF CONDITIONS OVERHEAD AT OTHER
SHADED BLOCKS
OBSERVATIONS CHARACTERISTIC OF AURORAL ACTIVITY (MULTIPLE OBLIQUE ECHOES RECORDED) AT BOTH STATIONS; CONDITIONS OTHERWISE RATHER GOOD
CATEGORY 4
GOOD TO EXCELLENT (VERY LOW ABSORPTION) HF CONDITIONS OVERHEAD AT BOTH STATIONS
00 02 04 06 08 10 12 14 16 18 20 22 00
150° W TIME

ANCHORAGE AND BARROW IONOSPHERIC CONDITIONS
SEPTEMBER AND OCTOBER 1952

FIGURE III-14

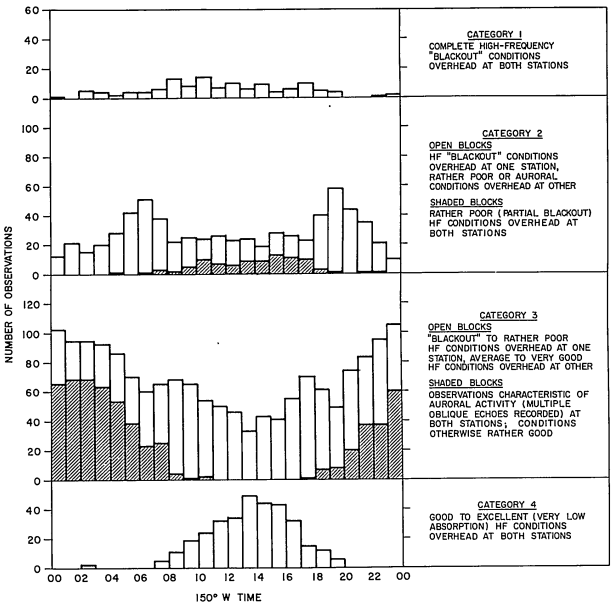
NUMBER OF OBSERVATIONS
CATEGORY 1
COMPLETE HIGH-FREQUENCY "BLACKOUT" CONDITIONS OVERHEAD AT BOTH STATIONS
CATEGORY 2
OPEN BLOCKS
HF "BLACKOUT" CONDITIONS OVERHEAD AT ONE STATION, RATHER POOR OR AURORAL CONDITIONS OVERHEAD AT OTHER
SHADED BLOCKS
RATHER POOR (PARTIAL BLACKOUT) HF CONDITIONS OVERHEAD AT BOTH STATIONS
CATEGORY 3
OPEN BLOCKS
"BLACKOUT" TO RATHER POOR HF CONDITIONS OVERHEAD AT ONE STATION, AVERAGE TO VERY GOOD HF CONDITIONS OVERHEAD AT OTHER
SHADED BLOCKS
OBSERVATIONS CHARACTERISTIC OF AURORAL ACTIVITY (MULTIPLE OBLIQUE ECHOES RECORDED) AT BOTH STATIONS; CONDITIONS OTHERWISE RATHER GOOD
CATEGORY 4
GOOD TO EXCELLENT (VERY LOW ABSORPTION) HF CONDITIONS OVERHEAD AT BOTH STATIONS
00 02 04 06 08 10 12 14 16 18 20 22 00
150° W TIME

ANCHORAGE AND BARROW IONOSPHERIC CONDITIONS
NOVEMBER THROUGH FEBRUARY 1952-53

FIGURE III-15

Declassified in Part - Sanitized Copy Approved for Release @ 50-Yr 2014/06/09 : CIA-RDP81-01043R003000180001-4

Declassified in Part - Sanitized Copy Approved for Release @ 50-Yr 2014/06/09 : CIA-RDP81-01043R003000180001-4

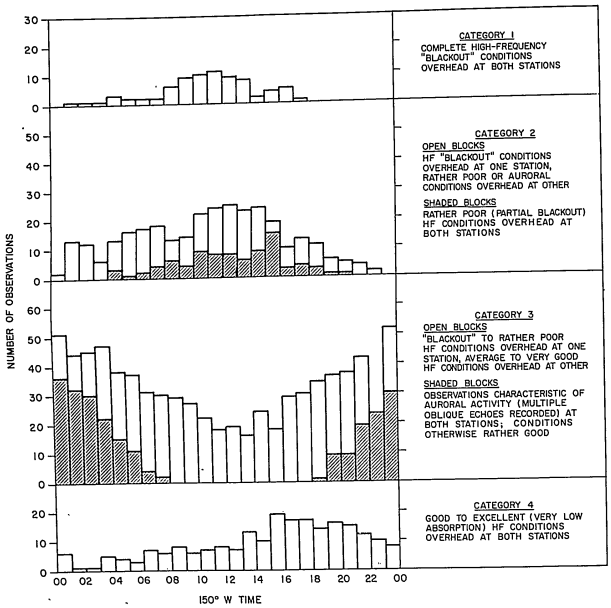
NUMBER OF OBSERVATIONS
CATEGORY 1
COMPLETE HIGH-FREQUENCY "BLACKOUT" CONDITIONS OVERHEAD AT BOTH STATIONS
CATEGORY 2
OPEN BLOCKS
HF "BLACKOUT" CONDITIONS OVERHEAD AT ONE STATION, RATHER POOR OR AURORAL CONDITIONS OVERHEAD AT OTHER
SHADED BLOCKS
RATHER POOR (PARTIAL BLACKOUT) HF CONDITIONS OVERHEAD AT BOTH STATIONS
CATEGORY 3
OPEN BLOCKS
"BLACKOUT" TO RATHER POOR HF CONDITIONS OVERHEAD AT ONE STATION, AVERAGE TO VERY GOOD HF CONDITIONS OVERHEAD AT OTHER
SHADED BLOCKS
OBSERVATIONS CHARACTERISTIC OF AURORAL ACTIVITY (MULTIPLE OBLIQUE ECHOES RECORDED) AT BOTH STATIONS, CONDITIONS OTHERWISE RATHER GOOD
CATEGORY 4
GOOD TO EXCELLENT (VERY LOW ABSORPTION) HF CONDITIONS OVERHEAD AT BOTH STATIONS
00 02 04 06 08 10 12 14 16 18 20 22 00
150° W TIME

ANCHORAGE AND BARROW IONOSPHERIC CONDITIONS
MARCH AND APRIL 1953

FIGURE III-16

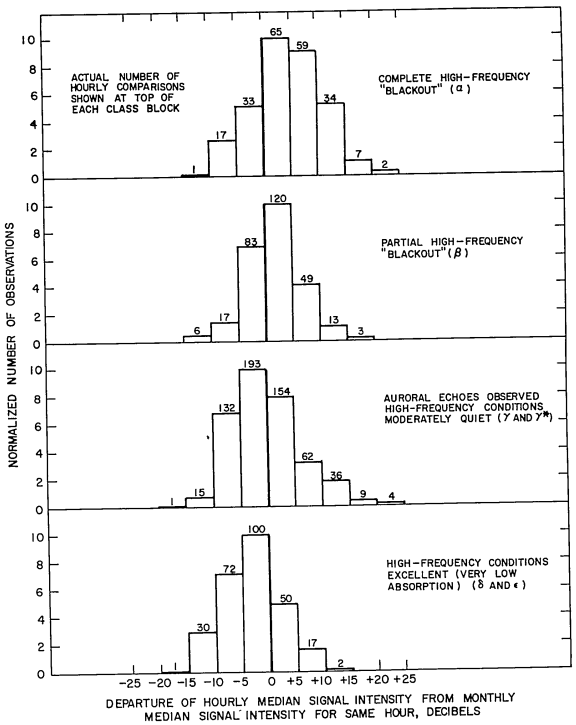
NORMALIZED NUMBER OF OBSERVATIONS
ACTUAL NUMBER OF HOURLY COMPARISONS SHOWN AT TOP OF EACH CLASS BLOCK
COMPLETE HIGH-FREQUENCY "BLACKOUT" (α)
1 17 33 65 59 34 7 2
PARTIAL HIGH-FREQUENCY "BLACKOUT" (β)
6 17 83 120 49 13 3
AURORAL ECHOES OBSERVED HIGH-FREQUENCY CONDITIONS MODERATELY QUIET (γ AND γ*)
1 15 132 193 154 62 36 9 4
HIGH-FREQUENCY CONDITIONS EXCELLENT (VERY LOW ABSORPTION) (δ AND ε)
30 72 100 50 17 2
-25 -20 -15 -10 -5 0 +5 +10 +15 +20 +25
DEPARTURE OF HOURLY MEDIAN SIGNAL INTENSITY FROM MONTHLY MEDIAN SIGNAL INTENSITY FOR SAME HOUR, DECIBELS

ANCHORAGE TO BARROW – 48.87 Mc/s

COMPARISONS OF SIGNAL INTENSITY OBSERVATIONS WITH HIGH-FREQUENCY PROPAGATION CONDITIONS AS DETERMINED FROM HOURLY IONOSPHERIC SOUNDING OBSERVATIONS MADE AT FAIRBANKS, NEAR THE PATH MIDPOINT
SEPTEMBER AND OCTOBER 1952

FIGURE III-17

Declassified in Part - Sanitized Copy Approved for Release @ 50-Yr 2014/06/09 : CIA-RDP81-01043R003000180001-4

Declassified in Part - Sanitized Copy Approved for Release @ 50-Yr 2014/06/09 : CIA-RDP81-01043R003000180001-4

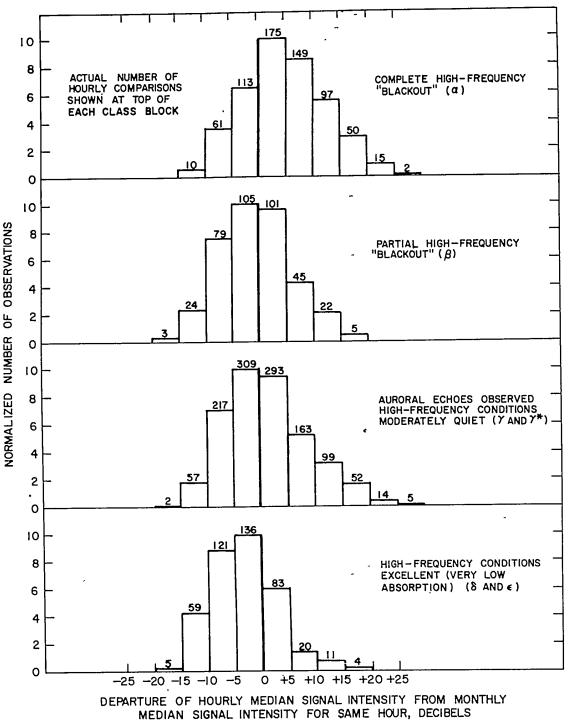
ACTUAL NUMBER OF HOURLY COMPARISONS SHOWN AT TOP OF EACH CLASS BLOCK
COMPLETE HIGH-FREQUENCY "BLACKOUT" (α)
PARTIAL HIGH-FREQUENCY "BLACKOUT" (β)
AURORAL ECHOES OBSERVED HIGH-FREQUENCY CONDITIONS MODERATELY QUIET (γ AND γ*)
HIGH-FREQUENCY CONDITIONS EXCELLENT (VERY LOW ABSORPTION) (δ AND ε)
NORMALIZED NUMBER OF OBSERVATIONS
DEPARTURE OF HOURLY MEDIAN SIGNAL INTENSITY FROM MONTHLY MEDIAN SIGNAL INTENSITY FOR SAME HOUR, DECIBELS

ANCHORAGE TO BARROW – 48.87 Mc/s

COMPARISONS OF SIGNAL INTENSITY OBSERVATIONS WITH HIGH-FREQUENCY PROPAGATION CONDITIONS AS DETERMINED FROM HOURLY IONOSPHERIC SOUNDING OBSERVATIONS MADE AT FAIRBANKS, NEAR THE PATH MIDPOINT

NOVEMBER 1952 THROUGH FEBRUARY 1953

FIGURE III-18

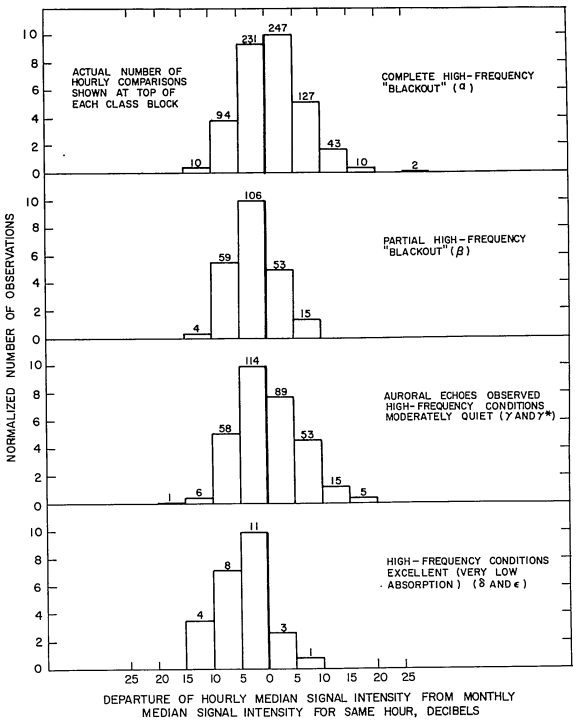
ACTUAL NUMBER OF HOURLY COMPARISONS SHOWN AT TOP OF EACH CLASS BLOCK
COMPLETE HIGH-FREQUENCY "BLACKOUT" (α)
PARTIAL HIGH-FREQUENCY "BLACKOUT" (β)
AURORAL ECHOES OBSERVED HIGH-FREQUENCY CONDITIONS MODERATELY QUIET (γ AND γ*)
HIGH-FREQUENCY CONDITIONS EXCELLENT (VERY LOW ABSORPTION) (δ AND ε)
NORMALIZED NUMBER OF OBSERVATIONS
DEPARTURE OF HOURLY MEDIAN SIGNAL INTENSITY FROM MONTHLY MEDIAN SIGNAL INTENSITY FOR SAME HOUR, DECIBELS

ANCHORAGE TO BARROW – 48.87 Mc/s

COMPARISONS OF SIGNAL INTENSITY OBSERVATIONS WITH HIGH-FREQUENCY PROPAGATION CONDITIONS AS DETERMINED FROM HOURLY IONOSPHERIC SOUNDING OBSERVATIONS MADE AT FAIRBANKS, NEAR THE PATH MIDPOINT

MARCH AND APRIL 1953

FIGURE III-19

Declassified in Part - Sanitized Copy Approved for Release @ 50-Yr 2014/06/09 : CIA-RDP81-01043R003000180001-4

Declassified in Part - Sanitized Copy Approved for Release @ 50-Yr 2014/06/09 : CIA-RDP81-01043R003000180001-4

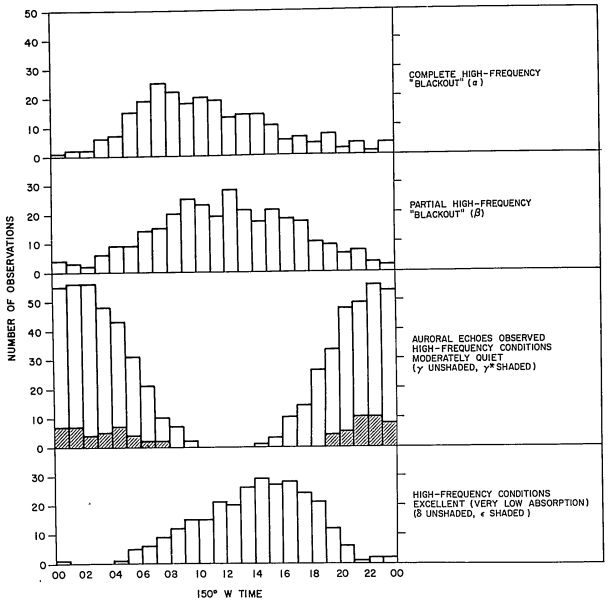
NUMBER OF OBSERVATIONS
COMPLETE HIGH-FREQUENCY "BLACKOUT" (α)
PARTIAL HIGH-FREQUENCY "BLACKOUT" (β)
AURORAL ECHOES OBSERVED HIGH-FREQUENCY CONDITIONS MODERATELY QUIET (γ UNSHADED, γ* SHADED)
HIGH-FREQUENCY CONDITIONS EXCELLENT (VERY LOW ABSORPTION) (δ UNSHADED, ε SHADED)
00 02 04 06 08 10 12 14 16 18 20 22 00
150° W TIME

FAIRBANKS IONOSPHERIC CONDITIONS
SEPTEMBER AND OCTOBER 1952
FIGURE III-20

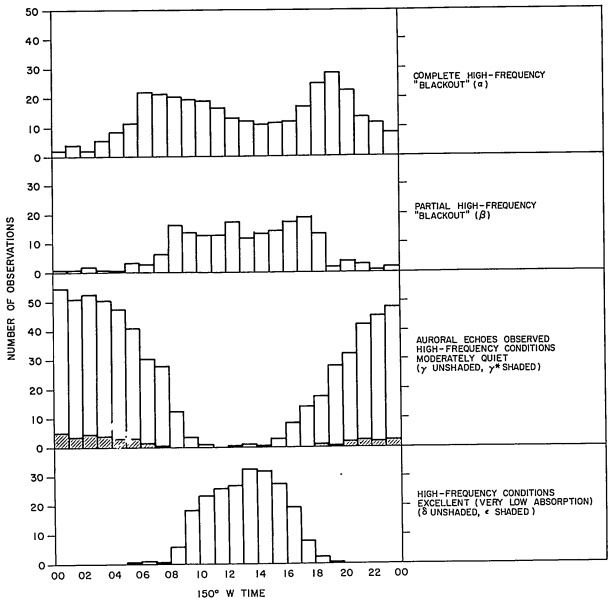
NUMBER OF OBSERVATIONS
COMPLETE HIGH-FREQUENCY "BLACKOUT" (α)
PARTIAL HIGH-FREQUENCY "BLACKOUT" (β)
AURORAL ECHOES OBSERVED HIGH-FREQUENCY CONDITIONS MODERATELY QUIET (γ UNSHADED, γ* SHADED)
HIGH-FREQUENCY CONDITIONS EXCELLENT (VERY LOW ABSORPTION) (δ UNSHADED, ε SHADED)
00 02 04 06 08 10 12 14 16 18 20 22 00
150° W TIME

FAIRBANKS IONOSPHERIC CONDITIONS
NOVEMBER THROUGH FEBRUARY
FIGURE III-21

Declassified in Part - Sanitized Copy Approved for Release @ 50-Yr 2014/06/09 : CIA-RDP81-01043R003000180001-4

Declassified in Part - Sanitized Copy Approved for Release @ 50-Yr 2014/06/09 : CIA-RDP81-01043R003000180001-4

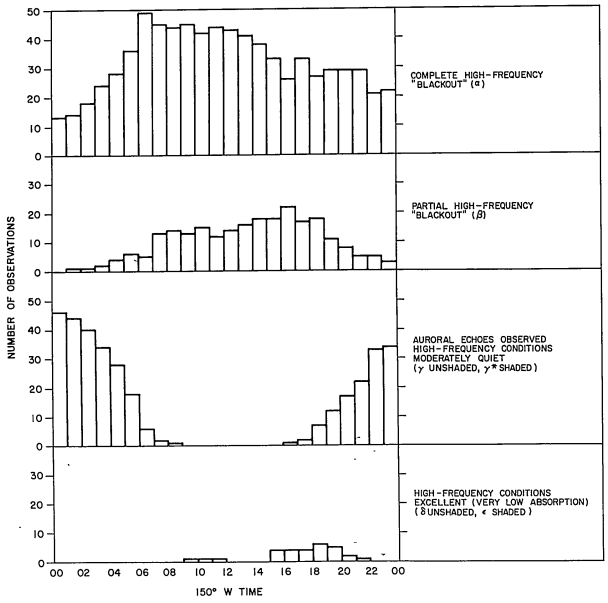
NUMBER OF OBSERVATIONS
COMPLETE HIGH-FREQUENCY "BLACKOUT" (α)
PARTIAL HIGH-FREQUENCY "BLACKOUT" (β)
AURORAL ECHOES OBSERVED HIGH-FREQUENCY CONDITIONS MODERATELY QUIET (γ UNSHADED, γ* SHADED)
HIGH-FREQUENCY CONDITIONS EXCELLENT (VERY LOW ABSORPTION) (δ UNSHADED, ε SHADED)
00 02 04 06 08 10 12 14 16 18 20 22 00
150° W TIME

FAIRBANKS IONOSPHERIC CONDITIONS
MARCH AND APRIL 1953
FIGURE III-22

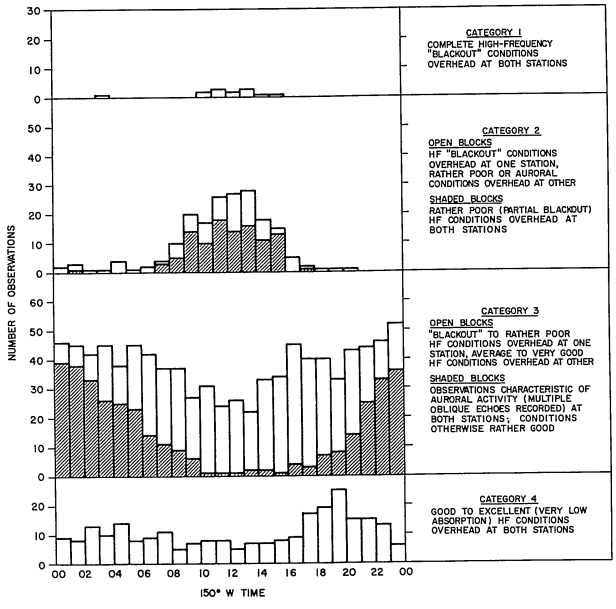
NUMBER OF OBSERVATIONS
CATEGORY 1
COMPLETE HIGH-FREQUENCY "BLACKOUT" CONDITIONS OVERHEAD AT BOTH STATIONS
CATEGORY 2
OPEN BLOCKS
HF "BLACKOUT" CONDITIONS OVERHEAD AT ONE STATION, RATHER POOR OR AURORAL CONDITIONS OVERHEAD AT OTHER
SHADED BLOCKS
RATHER POOR (PARTIAL BLACKOUT) HF CONDITIONS OVERHEAD AT BOTH STATIONS
CATEGORY 3
OPEN BLOCKS
"BLACKOUT" TO RATHER POOR HF CONDITIONS OVERHEAD AT ONE STATION, AVERAGE TO VERY GOOD HF CONDITIONS OVERHEAD AT OTHER
SHADED BLOCKS
OBSERVATIONS CHARACTERISTIC OF AURORAL ACTIVITY (MULTIPLE OBLIQUE ECHOES RECORDED) AT BOTH STATIONS; CONDITIONS OTHERWISE RATHER GOOD
CATEGORY 4
GOOD TO EXCELLENT (VERY LOW ABSORPTION) HF CONDITIONS OVERHEAD AT BOTH STATIONS
00 02 04 06 08 10 12 14 16 18 20 22 00
150° W TIME

ANCHORAGE AND BARROW IONOSPHERIC CONDITIONS
MAY AND JUNE 1953
FIGURE III-23

Declassified in Part - Sanitized Copy Approved for Release @ 50-Yr 2014/06/09 : CIA-RDP81-01043R003000180001-4

Declassified in Part - Sanitized Copy Approved for Release @ 50-Yr 2014/06/09 : CIA-RDP81-01043R003000180001-4

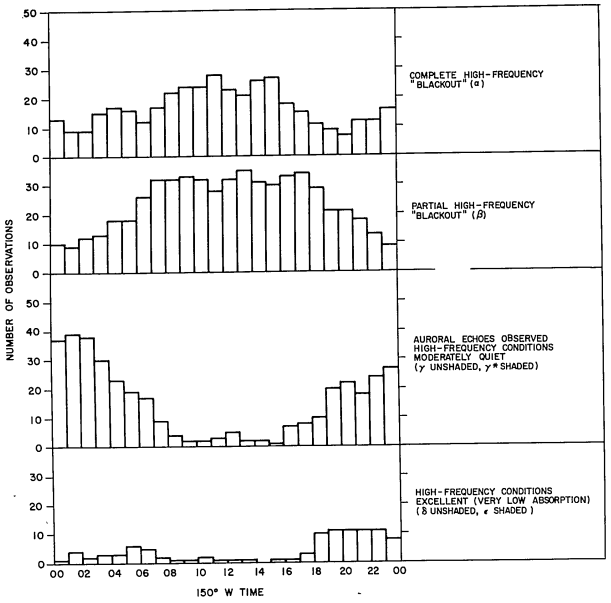
NUMBER OF OBSERVATIONS
COMPLETE HIGH-FREQUENCY "BLACKOUT" (α)
PARTIAL HIGH-FREQUENCY "BLACKOUT" (β)
AURORAL ECHOES OBSERVED HIGH-FREQUENCY CONDITIONS MODERATELY QUIET (γ UNSHADED, γ' SHADED)
HIGH-FREQUENCY CONDITIONS EXCELLENT (VERY LOW ABSORPTION) (δ UNSHADED, ε SHADED)
00 02 04 06 08 10 12 14 16 18 20 22 00
150° W TIME

FAIRBANKS IONOSPHERIC CONDITIONS
MAY AND JUNE 1953

FIGURE III-24

APPENDIX IV

OBLIQUE-INCIDENCE VHF SPORADIC E OBSERVATIONS

R. M. Davis, Jr.

1. INTRODUCTION

Two methods of approach to the study of the phenomenon of sporadic E have been employed under the VHF ionospheric scatter observing program. The first method arose naturally in the analysis of the variations of signal intensity; it consisted of distinguishing the periods in which Es propagation was in effect, and recording the signal intensity. Results of such analyses have been published in earlier reports.[1,2] The second method was simply to measure the duration of Es in each hour by examining the records in the light of certain criteria. Summary of such analyses has also been published.[3]

For each month of the recording program, the records of median signal intensity have been analyzed to determine the intensity levels equalled or exceeded 10%, 50% and 90% of the days at each hour local time. The analysis was made first with enhancements due to Es propagation included, whenever present; second, with the effect of Es propagation eliminated, either by omission of any value for the hour, or by interpolation through periods affected by Es. The two distributions are presented together in Figures 1 - 22 of the main text. Comparison of the solid with the broken lines reveals the relative effect of Es propagation on signal intensity for a given hour, month, path and frequency. The effect of sporadic E is shown in another form in Figures 23-35. Here the cumulative distribution of signal intensity is presented chronologically by season, both including and excluding periods of Es. The hourly value of signal intensity used in these distributions is the value exceeded 50% of the time, or the hourly median.

The second approach to the study of sporadic E was to determine from an examination of the records the periods of time when Es was present. Somewhat severe criteria were applied in deciding whether any part of an hour could be classed as sporadic-E propagation. The criteria were, (1) that the normal scattered signal be obliterated by Es for a minimum continuous period of 12 minutes, and (2) that the signal intensity within this period saturate the record for at least one minute, with the saturation level equivalent to 62 db below the inverse-distance value. Occasionally use of these two criteria had the effect of excluding what appeared to be periods of Es propagation. But the criteria provided the advantage of removing much of the contamination due to meteoric enhancements and other signal increases not due to sporadic E.

Thus, by application of these criteria for sporadic E, the fraction of time that Es was in effect was determined for each hour of recording on each path and each frequency. The observations interpreted

Declassified in Part - Sanitized Copy Approved for Release @ 50-Yr 2014/06/09 : CIA-RDP81-01043R003000180001-4

Declassified in Part - Sanitized Copy Approved for Release @ 50-Yr 2014/06/09 : CIA-RDP81-01043R003000180001-4

as sporadic E do not begin and end abruptly. Because of this, the Es designation was limited to periods having an enhanced signal level that clearly distinguished them from the regular scattered signal and any incidental enhancements. Care was taken to see that consistent practices were followed throughout the program in reading off times of beginning and ending of sporadic E.

The periods of sporadic-E propagation within each hour of recording were finally added and adjusted to bring out various diurnal, seasonal, and annual variations. The paths, frequencies and periods of observation for which these compilations were made are as follows:

Cedar Rapids to Sterling	49.8 Mc/s	1243 Km	Mar 1951-Dec 1955
Cedar Rapids to Sterling	27.775 Mc/s		Apr 1953-Dec 1955
Anchorage to Barrow	48.87 Mc/s	1156 Km	Sep 1951-Jun 1953
Anchorage to Barrow	24.325 Mc/s		Mar 1953-Jun 1953
Fargo to Churchill	49.7 Mc/s	1326 Km	Sep 1951-Mar 1953
Goose Bay to SondreStromfjord	48.02 Mc/s	1608 Km	Apr 1952-Nov 1953

2. RESULTS

2.1 Temperate Latitude - Cedar Rapids-Sterling Path

Figures IV-1, IV-2, IV-3, IV-4 and IV-5 are month-by-month histogram displays of the diurnal variation of total Es duration as recorded on the Cedar Rapids to Sterling path at 49.8 Mc/s. The figures show that each year's sporadic E is concentrated in the summer months, May through August, with the peak of Es incidence in June and July. A secondary, very much smaller, maximum of Es incidence can be discerned in the winter months, November through February. Though very scanty amounts of sporadic E occurred in these months, still there was consistently more than in the intervening equinoctial months. No Es at all on 49.8 Mc/s was recorded in March or April in three out of four years of recordings. In five years of recordings of September and October, there were only three instances of sporadic-E propagation.

In Figures IV-6, IV-7 and IV-8 are shown comparable distributions of sporadic-E incidence on the Cedar Rapids to Sterling recordings at 27.775 Mc/s. Like the histograms for 49.8 Mc/s, they have been adjusted for periods of transmission failure at each hour of the day. The yearly distribution of sporadic E on 27.775 Mc/s resembles in general character that on 49.8 Mc/s. The summer months May through August received the preponderance of Es propagation. On the whole, June and July were more subject to Es than May and August.

A secondary winter maximum can be seen on 27.775 Mc/s, as it was on 49.8 Mc/s. It is obscured to some extent by the substantial amounts of Es recorded in the equinoctial months. But the winter maximum on 27.775 Mc/s is perhaps more significant statistically than the one on

49.8 Mc/s because of the greater number of hours of Es recorded. The month of December contributed the most each year toward the winter maximum on 27.775 Mc/s.

Comparison of the Es histograms for 27.775 Mc/s with those for 49.8 Mc/s reveals more correspondence than simply gross seasonal similarities. Sporadic E on 49.8 Mc/s is invariably accompanied by sporadic E on 27.775 Mc/s, a fact that is often useful in deciding whether a given enhancement is genuine Es. The reverse is not true, for Es on 27.775 Mc/s usually begins earlier and ends later than on 49.8 Mc/s, and there are many occurrences of Es on 27.775 Mc/s at all seasons when the 49.8 Mc/s signal is completely normal. These characteristics show up on the histograms of total Es time. The 27.775 Mc/s values appear to be magnified copies of the 49.8 values, with the condition that every month is marked by some sporadic E on 27.775 Mc/s, even when Es is totally lacking at 49.8 Mc/s.

2.2 Arctic Latitudes

The distribution of Es incidence is presented for three auroral zone paths in the next series of figures. Figure IV-9 shows monthly histograms for Anchorage to Barrow at 48.87 Mc/s and Figure IV-10 represents a four-month sample of Es incidence for the same path at 24.325 Mc/s. Figures IV-11 and IV-12 give the distribution for the Fargo to Churchill path at 49.7 Mc/s, while Goose Bay to SondreStromfjord is shown in Figures IV-13 and IV-14.

Whereas Es incidence on the temperate-zone Cedar Rapids to Sterling path was principally dependent on season of the year, the stronger factor influencing Es on all three auroral paths is hour of the day. The diurnal distribution of sporadic E in the auroral zone is almost the reverse of that in the temperate zone. Sporadic E on the Cedar Rapids to Sterling path occurred mostly during daylight and early evening hours. All the auroral paths show sporadic E concentrated between 1800 and 0600 local time, with very little Es in the hours around noon.

The degree of seasonal influence on Es appears to vary among the three auroral circuits. Fargo to Churchill, with its midpoint at the lowest geomagnetic latitude of any of the three paths, exhibits a marked seasonal variation. Anchorage to Barrow also shows peaking of the seasonal distribution of Es in June and July on 48.87 Mc/s. Es on the Goose Bay to SondreStromfjord path, on the other hand, exhibits considerably less seasonal preference. Every month of the year finds a substantial amount of Es on this path during the period 1600-0000 local time.

None of the auroral-zone circuits exhibits the equinoctial minima and secondary winter maximum in Es incidence, discernible on the Cedar Rapids to Sterling path. Rather a certain amount of sporadic E seems

Declassified in Part - Sanitized Copy Approved for Release @ 50-Yr 2014/06/09 : CIA-RDP81-01043R003000180001-4

Declassified in Part - Sanitized Copy Approved for Release @ 50-Yr 2014/06/09 : CIA-RDP81-01043R003000180001-4

to occur regardless of the season. Anchorage to Barrow is on the whole least subject to sporadic-E propagation, Fargo to Churchill with its high summer incidence shows more Es, and Goose Bay to Sondre-Stromfjord has the most Es. The variation in total occurrence is considered primarily a geographical effect; the differences among the various paths cannot be explained on the basis of simple path-length dependence.

2.3 Temporal Variations

In Figures IV-15, IV-16 and IV-17 the Es-incidence data, displayed for each hour of the day and each month of the year in the foregoing figures, are summarized in monthly totals. The figures thus show the way in which Es duration varied from month to month and from year to year. The Cedar Rapids to Sterling data at two frequencies are displayed together in Figure IV-15, Anchorage to Barrow data at two frequencies are displayed in Figure IV-16, and monthly Es totals on the Fargo to Churchill and Goose Bay to Sondre-Stromfjord paths are shown together in Figure IV-17.

Figure IV-18 represents the diurnal distribution of total Es-incidence, summed over the entire calendar year. Four years of Cedar Rapids to Sterling data for 49.8 Mc/s are displayed in comparison with two years of data for 27.775 Mc/s. Analogous compilations of Anchorage to Barrow data on 48.87 Mc/s, Fargo to Churchill data on 49.7 Mc/s, and Goose Bay to SondreStromfjord on 48.02 Mc/s are presented together in Figure IV-19.

These histograms present in summarized form the contrast between the temperate zone and auroral types of Es incidence. It is seen that the characteristic diurnal pattern for the temperate zone is a diurnal maximum between 1000 and 1200 hours, a second maximum between 1800 and 2100, and relatively high daylight incidence of sporadic E between the two maxima. After 2100 occurrence of Es decreases on both 49.8 Mc/s and 27.775 Mc/s over the temperate zone, Cedar Rapids to Sterling, path. But while Es incidence on 49.8 Mc/s has reached very low values or has vanished by midnight, sporadic E on 27.775 Mc/s continues to be substantial at that hour and only reaches its diurnal minimum between 0400 and 0600. Even then, there is sporadic E on 27.775 Mc/s in an amount of the order of five hours per year. The auroral pattern of Es incidence, on the other hand, is marked by an almost total absence of sporadic E between local hours 0600 and 1600. Added to this is high incidence of Es during the nighttime hours. Sometime between 1600 and 1900, depending on the path, the auroral incidence of Es begins to rise rapidly. It maintains a high level during the first half of the night, then falls to low values sometime between 0000 and 0400, again depending on the path.

An outstanding feature of Figure IV-19 is that Es incidence on the three auroral-zone paths peaks at different local times. Goose

Bay to SondreStromfjord and Anchorage to Barrow, both with path midpoints in regions having aurorae between 90% and 100% of the time, may be best compared in this respect. Es incidence in Figure IV-19 is clearly concentrated at an earlier hour for the Goose Bay to SondreStromfjord path than for the Anchorage to Barrow path. The effect is even more prominent on the monthly diurnal histograms (Figures IV-9 to IV-14). When attention is confined to the summer months May through August, it is found that sporadic-E incidence centers in local hours 2100-2200 for Goose Bay to SondreStromfjord and in hours 0000-0100 for Anchorage to Barrow. The peak takes place an hour earlier on both paths when data for the entire year are considered. But in either case the time difference points to a geographical dependence of the local time of Es incidence. The effect is the same one that was noted by Smith,[4] namely, a shifting of the peak of Es incidence to later time epochs from east to west along the maximum of the auroral zone. A possible explanation of the three-hour difference between the peaks on the Goose Bay to SondreStromfjord and Anchorage to Barrow paths is that Es incidence may depend on geomagnetic time rather than solar time. A geomagnetic time-dependence would make corresponding events 2.5 hours later in local time for Anchorage to Barrow than for Goose Bay to SondreStromfjord. This is of the order of the local time difference noted between Es peaks for the two paths.

Finally, the sporadic-E observations may be considered from the point of view of their year-to-year variation. Do they reveal any relationship to sunspot cycle changes or other long-term variations?

The total annual durations of sporadic E on the Cedar Rapids to Sterling path are summarized in the following table. Parentheses indicate a value estimated from less than a full year's data.

Total Number of Hours of Es

Year	49.8 Mc/s	27.775 Mc/s	Mean Sunspot Number	Mean Magnetic Activity Index (Ap)
1951	(98.1)		69.1	22
1952	86.1		31.4	21
1953	52.7	(518.5)	14.0	16
1954	104.3	616.9	4.8	11
1955	57.4	604.0	37.4	11

It would seem from the table that the total annual duration of sporadic E varies much more widely on 49.8 Mc/s than it does on 27.775 Mc/s. The increase in sporadic E between 1953 and 1954 was 98% on 49.8 Mc/s as against 19% on 27.775 Mc/s.

Declassified in Part - Sanitized Copy Approved for Release @ 50-Yr 2014/06/09 : CIA-RDP81-01043R003000180001-4

Declassified in Part - Sanitized Copy Approved for Release @ 50-Yr 2014/06/09 : CIA-RDP81-01043R003000180001-4

There is no clear relationship apparent in these data between annual Es incidence and mean sunspot activity or magnetic disturbance. The year 1954, when Es incidence was at a maximum, coincided with a period of minimum sunspot activity and relatively low magnetic activity indices. This fact alone would coincide with a negative correlation of Es incidence with sunspot number. The decreasing values of Es incidence from 1951 through 1953, however, suggest a positive correlation with sunspot number, as does the low value for 1955. It must be concluded, therefore, that the limited sample of sporadic-E data presented in this report does not show any simple dependence on the mean sunspot number or the long-term variation of magnetic activity.

3. SUMMARY

Continuous recordings of long-distance VHF transmissions reveal the occurrence of signal enhancements attributable to sporadic-E propagation. A detailed description of the variation of Es occurrence with frequency, time of day, season, sunspot cycle and geographic location is the subject of this report. Additional sporadic-E information and interpretation for the Cedar Rapids to Sterling circuit may be found in another report.[4]

REFERENCES

1. D. K. Bailey, R. Bateman and R. C. Kirby, "Regular VHF Ionospheric Propagation Observable over Long Distances," NBS Report 8A111, June 30, 1952.

2. D. K. Bailey, R. Bateman and R. C. Kirby, "Second Report on Regular VHF Ionospheric Propagation Observable over Long Distances," NBS Report 8A117, June 30, 1953.

3. D. K. Bailey, R. Bateman and R. C. Kirby, "Radio Transmission at VHF by Scattering and other Processes in the Lower Ionosphere," Proc. I.R.E., 43, pp. 1181-1230, October 1955.

4. R. M. Davis, Jr. and E. K. Smith, "The Effect of Sporadic E on VHF Transmission in the U.S.," NBS Report 5547, January 28, 1958.

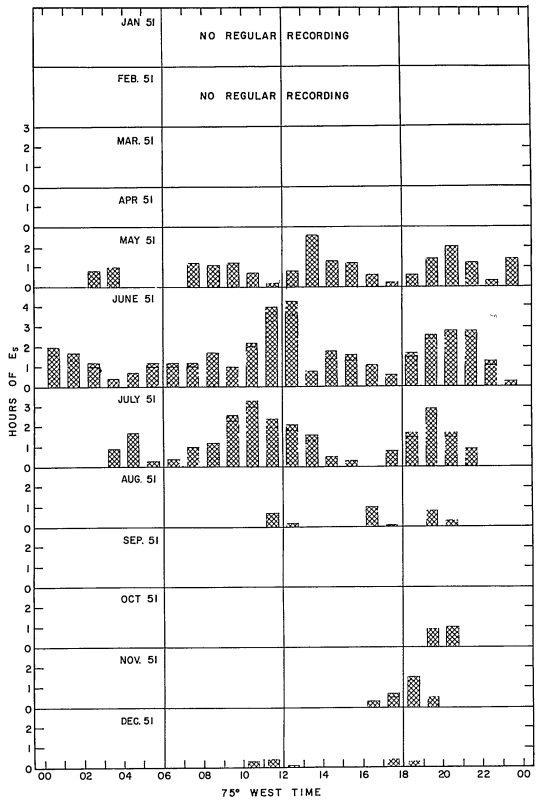

OBSERVED SPORADIC E PROPAGATION
CEDAR RAPIDS TO STERLING — 49.8 Mc/s
JAN—DEC 1951

FIGURE IV-1

Declassified in Part - Sanitized Copy Approved for Release @ 50-Yr 2014/06/09 : CIA-RDP81-01043R003000180001-4

Declassified in Part - Sanitized Copy Approved for Release @ 50-Yr 2014/06/09 : CIA-RDP81-01043R003000180001-4

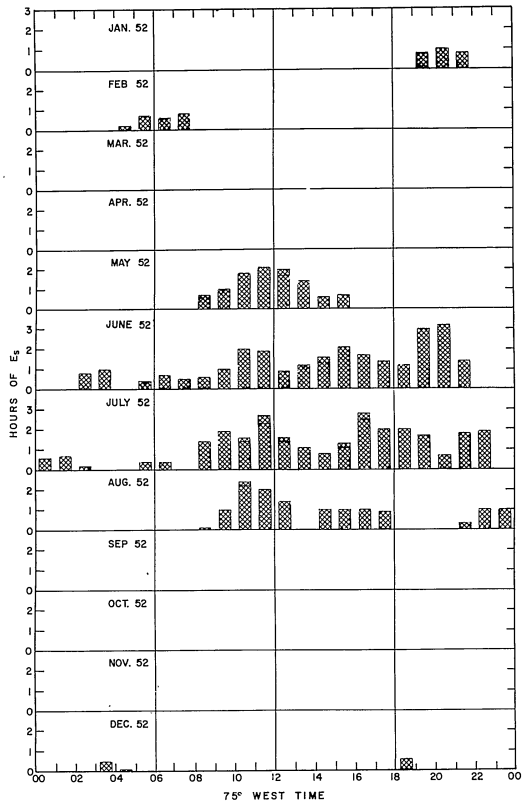

OBSERVED SPORADIC E PROPAGATION
CEDAR RAPIDS TO STERLING – 49.8 Mc/s
JAN – DEC 1952

FIGURE IV-2

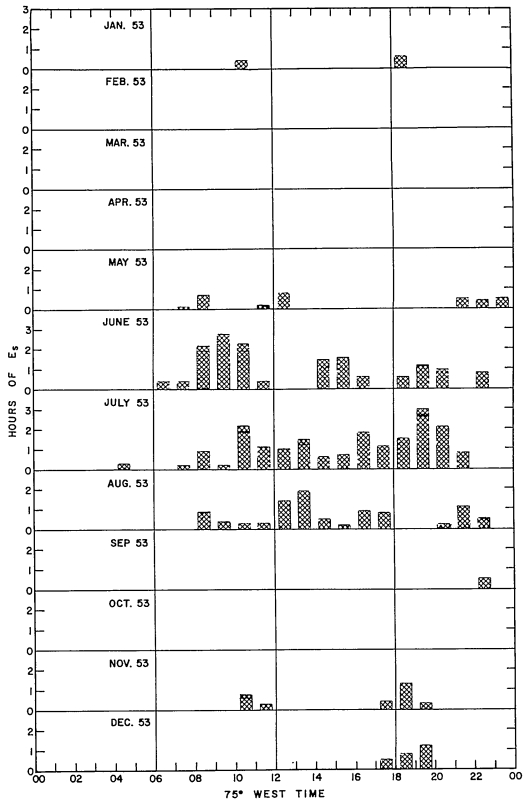

OBSERVED SPORADIC E PROPAGATION
CEDAR RAPIDS TO STERLING – 49.8 Mc/s
JAN – DEC 1953

FIGURE IV-3

Declassified in Part - Sanitized Copy Approved for Release @ 50-Yr 2014/06/09 : CIA-RDP81-01043R003000180001-4

Declassified in Part - Sanitized Copy Approved for Release @ 50-Yr 2014/06/09 : CIA-RDP81-01043R003000180001-4

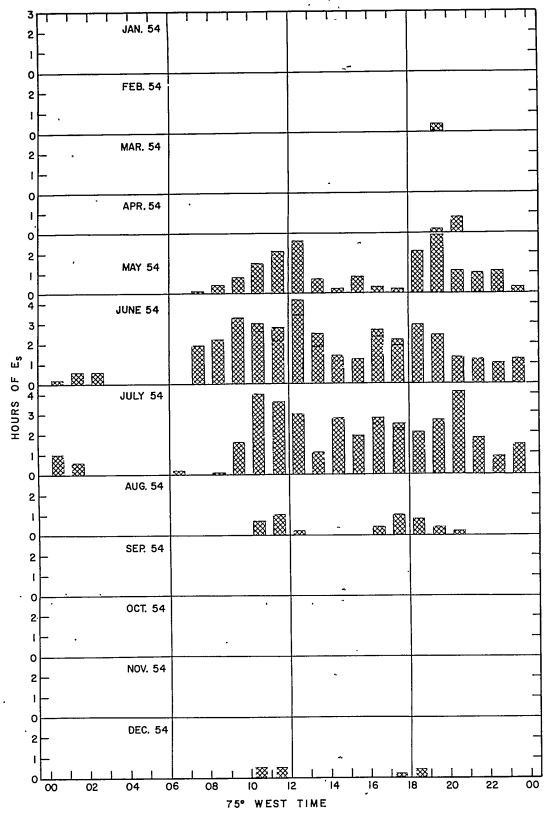

OBSERVED SPORADIC E PROPAGATION
CEDAR RAPIDS TO STERLING – 49.8 Mc/s
JAN – DEC 1954

FIGURE IV-4

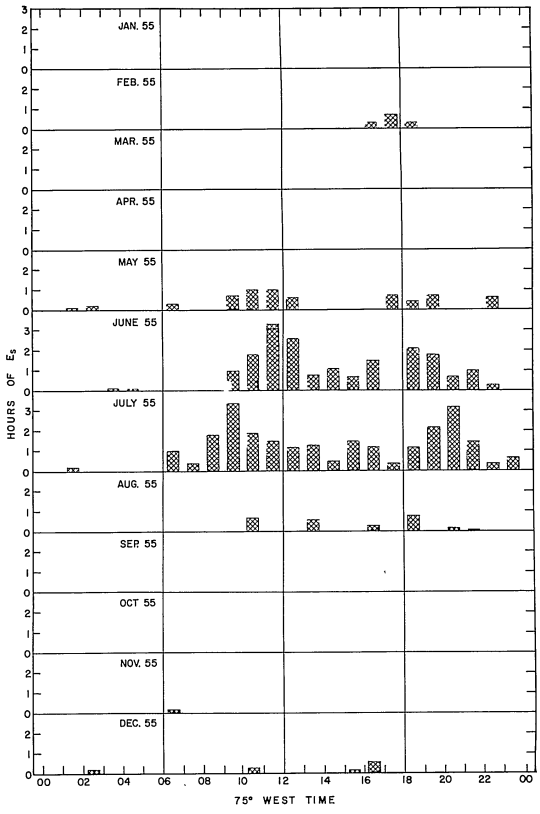

OBSERVED SPORADIC E PROPAGATION
CEDAR RAPIDS TO STERLING – 49.8 Mc/s
JAN – DEC 1955

FIGURE IV-5

Declassified in Part - Sanitized Copy Approved for Release @ 50-Yr 2014/06/09 : CIA-RDP81-01043R003000180001-4

Declassified in Part - Sanitized Copy Approved for Release @ 50-Yr 2014/06/09 : CIA-RDP81-01043R003000180001-4

[ ] INDICATES DATA BASED AT LESS THAN 50% OF HOURS OF MONTH

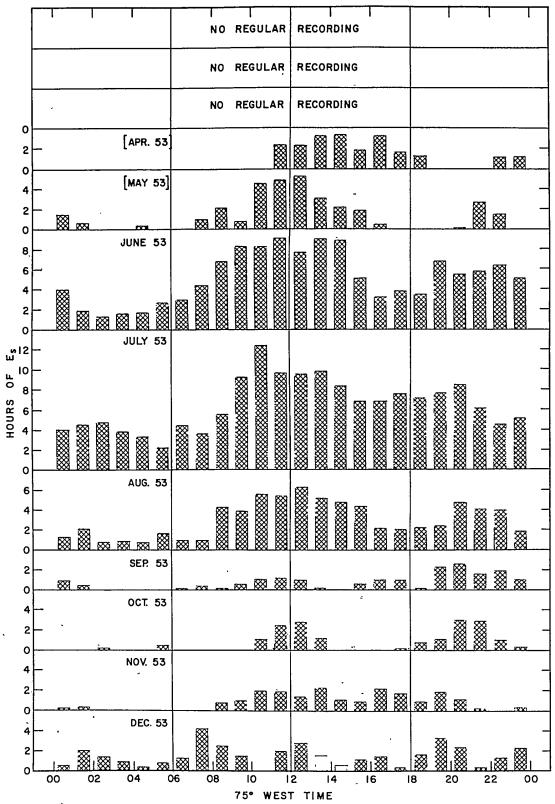

OBSERVED SPORADIC E PROPAGATION
CEDAR RAPIDS TO STERLING—27.775 Mc/s
JAN—DEC 1953

FIGURE IV-6

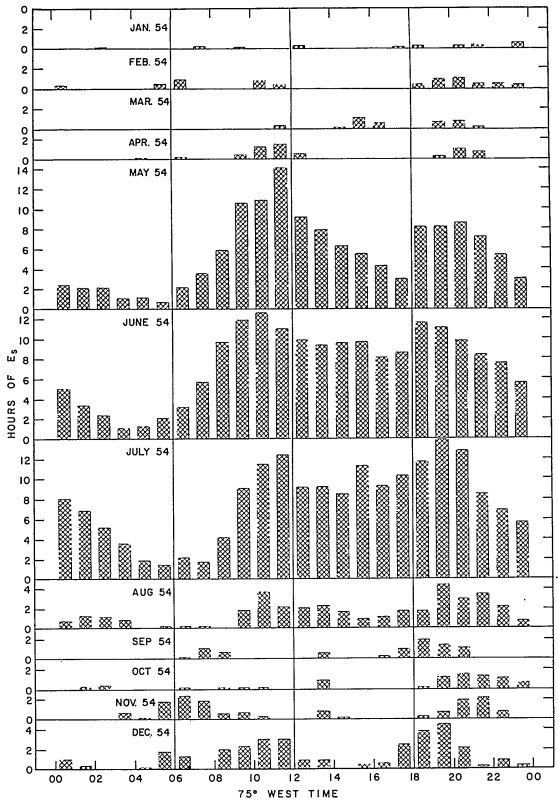

OBSERVED SPORADIC E PROPAGATION
CEDAR RAPIDS TO STERLING—27.775 Mc/s
JAN—DEC 1954

FIGURE IV-7

Declassified in Part - Sanitized Copy Approved for Release @ 50-Yr 2014/06/09 : CIA-RDP81-01043R003000180001-4

Declassified in Part - Sanitized Copy Approved for Release @ 50-Yr 2014/06/09 : CIA-RDP81-01043R003000180001-4

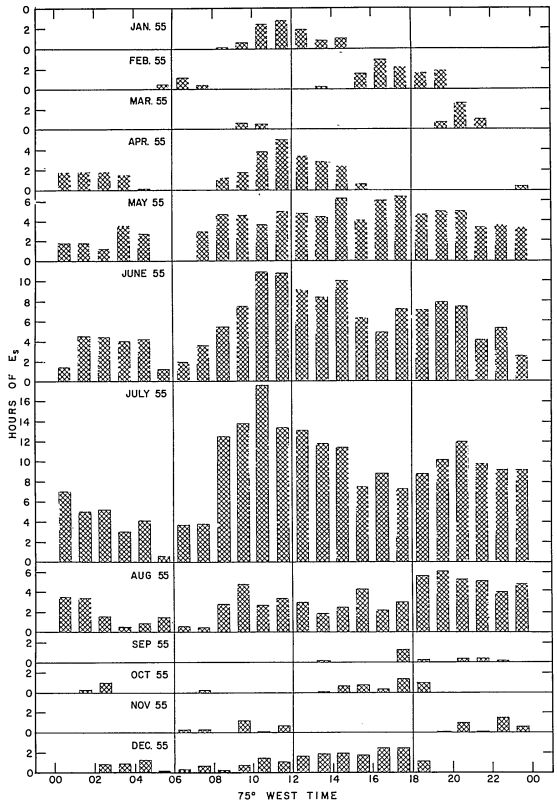

OBSERVED SPORADIC E PROPAGATION
CEDAR RAPIDS TO STERLING – 27.775 Mc/s
JAN – DEC 1955

FIGURE IV-8

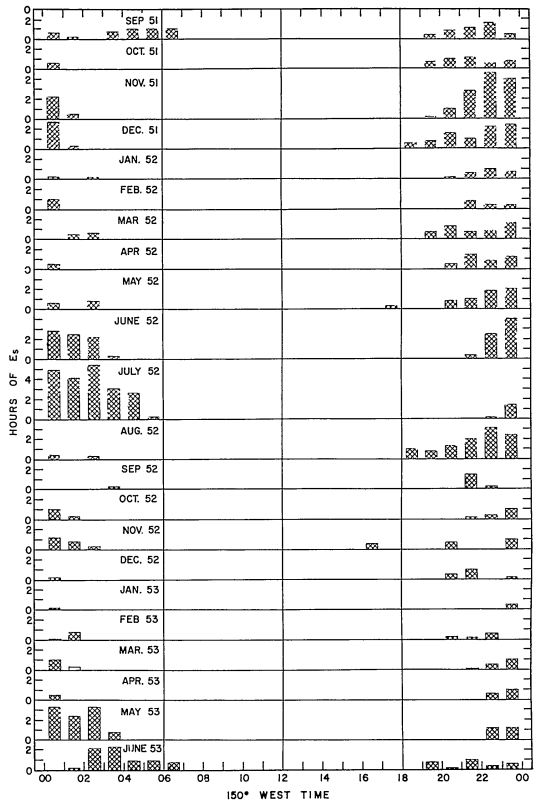

OBSERVED SPORADIC E PROPAGATION
ANCHORAGE TO BARROW – 48.87 Mc/s
SEPT 1951 – JUNE 1953

FIGURE IV-9

Declassified in Part - Sanitized Copy Approved for Release @ 50-Yr 2014/06/09 : CIA-RDP81-01043R003000180001-4

Declassified in Part - Sanitized Copy Approved for Release @ 50-Yr 2014/06/09 : CIA-RDP81-01043R003000180001-4

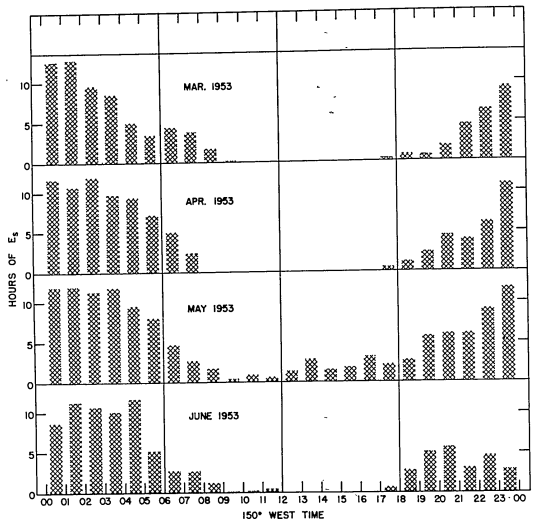

OBSERVED SPORADIC E PROPAGATION
ANCHORAGE TO BARROW — 24.325 Mc/s

FIGURE IV-10.

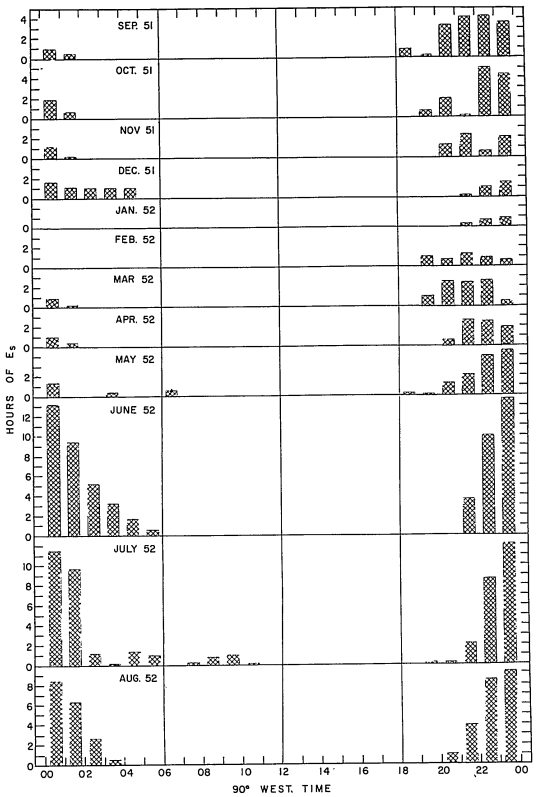

OBSERVED SPORADIC E PROPAGATION
FARGO TO CHURCHILL — 49.7 Mc/s
SEPT 1951 — AUGUST 1952

FIGURE IV-11

Declassified in Part - Sanitized Copy Approved for Release @ 50-Yr 2014/06/09 : CIA-RDP81-01043R003000180001-4

Declassified in Part - Sanitized Copy Approved for Release @ 50-Yr 2014/06/09 : CIA-RDP81-01043R003000180001-4

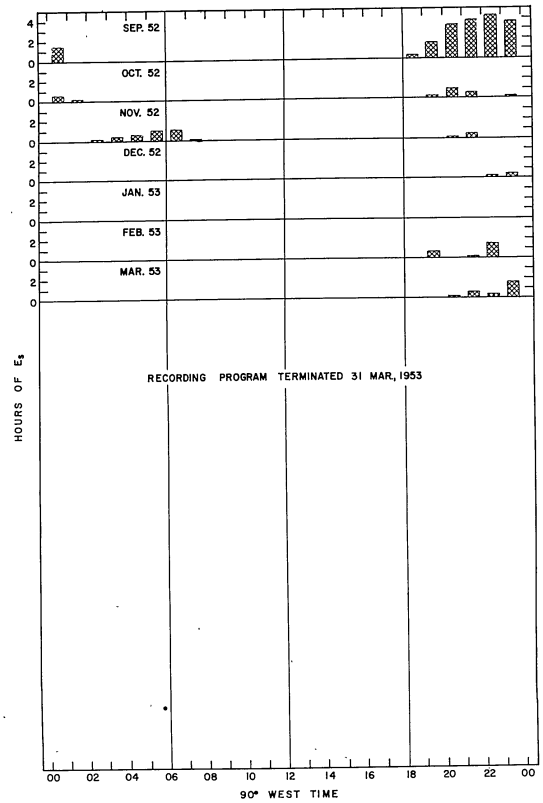

OBSERVED SPORADIC E PROPAGATION
FARGO TO CHURCHILL — 49.7 Mc/s
SEPT. 1952 — MARCH 1953

FIGURE IV-12

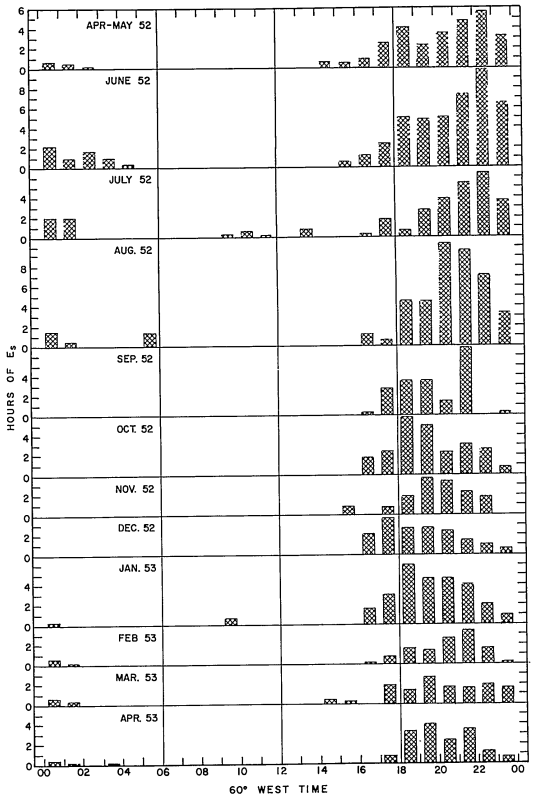

OBSERVED SPORADIC E PROPAGATION
GOOSE BAY TO SONDRE STROMFJORD — 48.02 Mc/s
APRIL 1952 — APRIL 1953

FIGURE IV-13

Declassified in Part - Sanitized Copy Approved for Release @ 50-Yr 2014/06/09 : CIA-RDP81-01043R003000180001-4

Declassified in Part - Sanitized Copy Approved for Release @ 50-Yr 2014/06/09 : CIA-RDP81-01043R003000180001-4

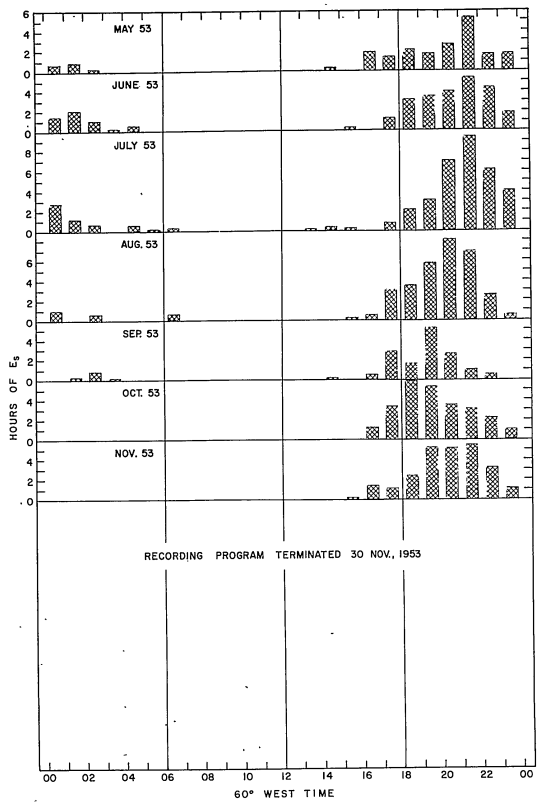

OBSERVED SPORADIC E PROPAGATION
GOOSE BAY TO SONDRE STROMFJORD — 48.02 Mc/s
MAY — NOV. 1953

FIGURE IV—14

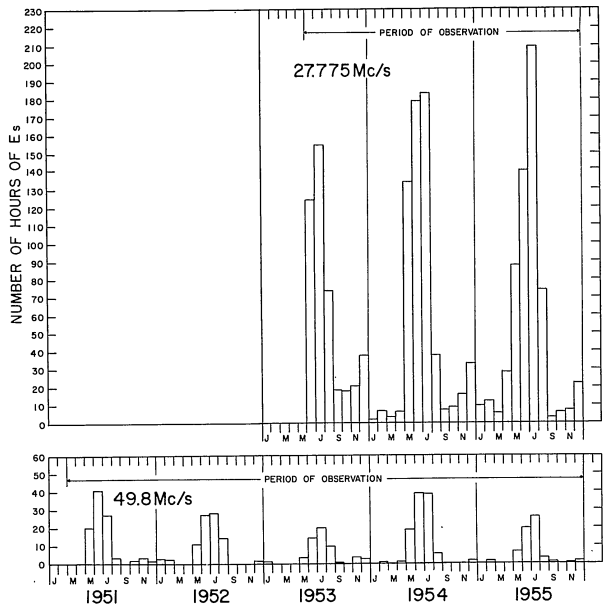
NUMBER OF HOURS OF E_s
PERIOD OF OBSERVATION
27.775 Mc/s
49.8 Mc/s
J M M J S N J M M J S N J M M J S N J M M J S N J M M J S N
1951
1952
1953
1954
1955

SEASONAL AND ANNUAL VARIATION OF OCCURRENCE OF SPORADIC E PROPAGATION
CEDAR RAPIDS TO STERLING

FIGURE IV—15

Declassified in Part - Sanitized Copy Approved for Release @ 50-Yr 2014/06/09 : CIA-RDP81-01043R003000180001-4

Declassified in Part - Sanitized Copy Approved for Release @ 50-Yr 2014/06/09 : CIA-RDP81-01043R003000180001-4

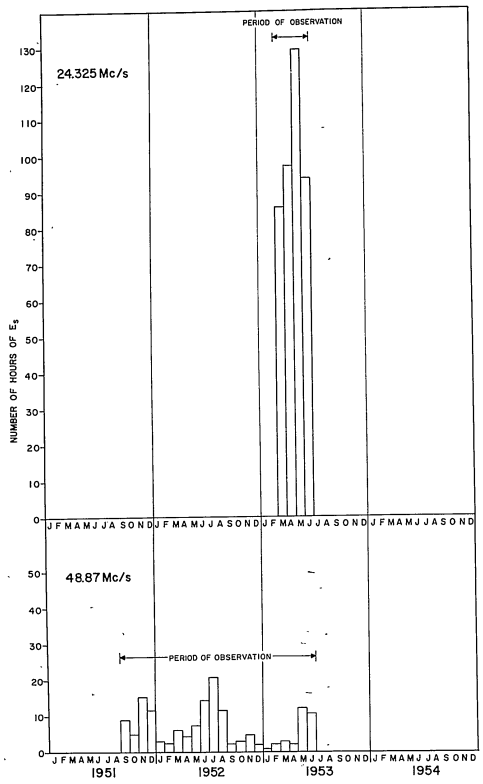
PERIOD OF OBSERVATION
24.325 Mc/s
48.87 Mc/s
PERIOD OF OBSERVATION
NUMBER OF HOURS OF Es
J F M A M J J A S O N D J F M A M J J A S O N D J F M A M J J A S O N D J F M A M J J A S O N D
1951
1952
1953
1954

SEASONAL AND ANNUAL VARIATION OF OCCURRENCE OF SPORADIC E PROPAGATION
ANCHORAGE TO BARROW

FIGURE IV-16

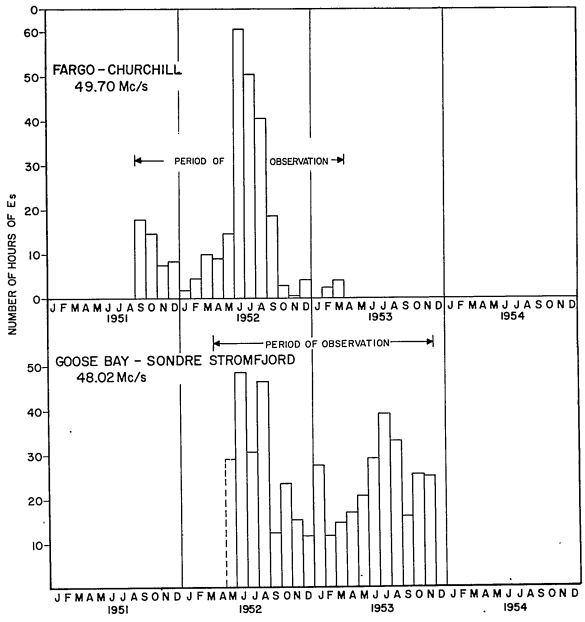
FARGO - CHURCHILL
49.70 Mc/s
PERIOD OF OBSERVATION
GOOSE BAY - SONDRE STROMFJORD
48.02 Mc/s
PERIOD OF OBSERVATION
NUMBER OF HOURS OF Es
J F M A M J J A S O N D J F M A M J J A S O N D J F M A M J J A S O N D J F M A M J J A S O N D
1951
1952
1953
1954

SEASONAL AND ANNUAL VARIATION OF OCCURRENCE OF SPORADIC E PROPAGATION
FARGO - CHURCHILL AND GOOSE BAY - SONDRE STROMFJORD PATHS

FIGURE IV-17

Declassified in Part - Sanitized Copy Approved for Release @ 50-Yr 2014/06/09 : CIA-RDP81-01043R003000180001-4

Declassified in Part - Sanitized Copy Approved for Release @ 50-Yr 2014/06/09 : CIA-RDP81-01043R003000180001-4

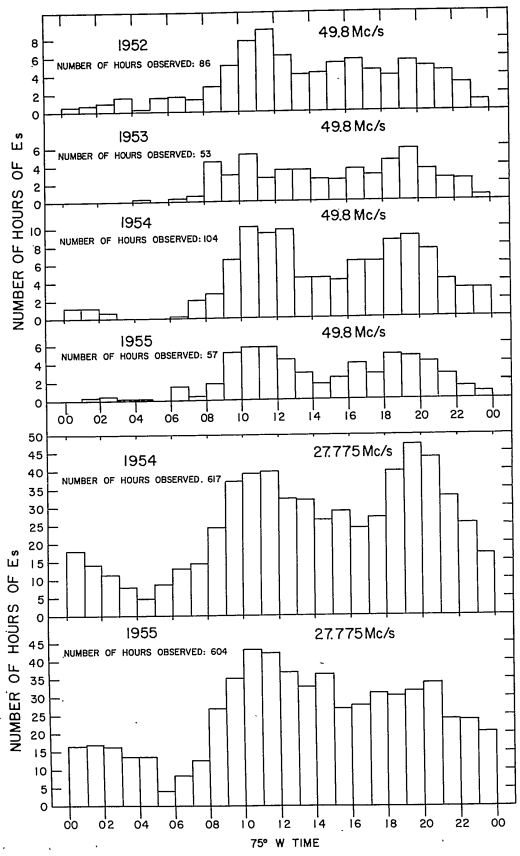

DIURNAL VARIATION OF OCCURRENCE OF SPORADIC E PROPAGATION
CEDAR RAPIDS TO STERLING

FIGURE IV-18

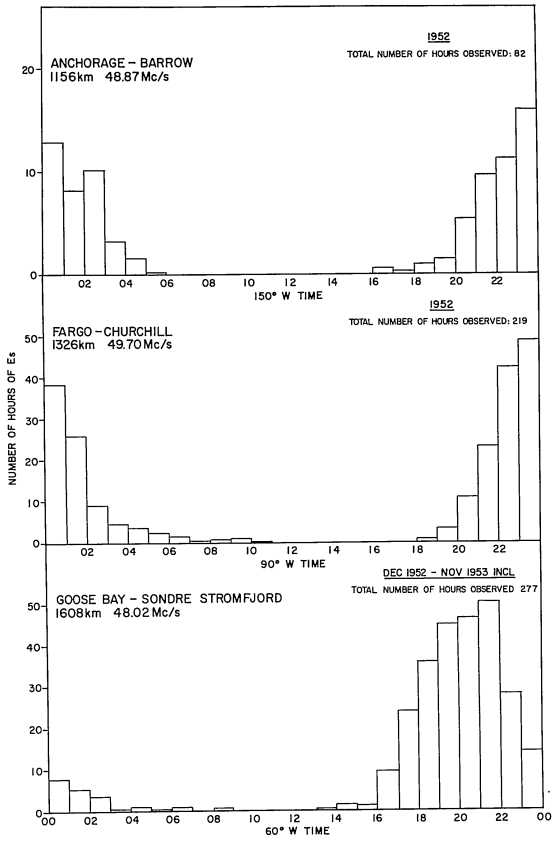

DIURNAL VARIATION OF OCCURRENCE OF SPORADIC E PROPAGATION
FOR ARCTIC PATHS

FIGURE IV-19

Declassified in Part - Sanitized Copy Approved for Release @ 50-Yr 2014/06/09 : CIA-RDP81-01043R003000180001-4

Declassified in Part - Sanitized Copy Approved for Release @ 50-Yr 2014/06/09 : CIA-RDP81-01043R003000180001-4

APPENDIX V

METEOR WHISTLES ON THE CEDAR RAPIDS TO STERLING PATH

E. K. Smith

The program over the Cedar Rapids to Sterling circuit to count meteor Doppler-whistles has been described in the previous report.[1] Briefly, the program consists of counting the number of signals arriving per minute at the receiver of signal strength above some preset level (0.25 or 0.5 microvolt open-circuit voltage at 50 ohms) and Doppler shifted from the carrier frequency (49.8 Mc/s) by more than 200 cps. The requirement that the signals be Doppler shifted at least 200 cycles makes it quite certain that the signals are of meteoric origin. It also restricts the measure to meteor whistles as contrasted to meteor bursts. This, of course, is because the meteor burst occurs when the first fresnel zone of the meteor trail relative to the transmission path is formed. Doppler shifts of the contribution from this zone will be very small (blowing of the trail or differential rate of disappearance of the lagging as contrasted to the leading edge of the zone) and therefore the bursts per se are not recorded. Most bursts are preceded by detectable whistles, but only a small fraction of the whistles recorded here go on to produce bursts. If meteor radiants are assumed to be isotropically distributed, then meteor burst will be proportional to meteor whistles. As such a radiant distribution is demonstrably incorrect, care must be exercised if burst information is to be obtained from whistle data.

Typical diurnal variation of hourly counts was shown in the previous report,[1] and an hourly average count was published in Reference 2.

Figure V-1 shows the smoothed temporal variations in meteor counts recorded over the Cedar Rapids to Sterling circuit between June 1954 and January 1956. The curve parameters are "whistles per minute". At 1000 EST on March 11, 1955, the signal voltage threshold setting was reduced from 0.5 microvolts to 0.25 microvolts and a large increase in recorded whistles immediately followed. The day-by-day averages of recorded counts are shown in Figures V-2 and V-3. The large gaps in the data are due to the requirement that 22 out of every 24 hours of data be available. This rather stringent requirement is necessitated by the large diurnal variation in meteor counts. For instance, if only morning data were available on one day and only evening data on the next, the daily averages might differ by a factor of ten for the same distribution of meteors on the two days.

REFERENCES

1. D. K. Bailey, R. Bateman and R. C. Kirby, "Second Report on Regular VHF Ionospheric Propagation Observable over Long Distances," NBS Report 8A117, June 30, 1953. (See Appendix X.)

2. D. K. Bailey, R. Bateman and R. C. Kirby, "Radio Transmission at VHF by Scattering and other Processes in the Lower Ionosphere," Proc. I.R.E., 43, No. 10, October 1955.

Declassified in Part - Sanitized Copy Approved for Release @ 50-Yr 2014/06/09 : CIA-RDP81-01043R003000180001-4

Declassified in Part - Sanitized Copy Approved for Release @ 50-Yr 2014/06/09 : CIA-RDP81-01043R003000180001-4

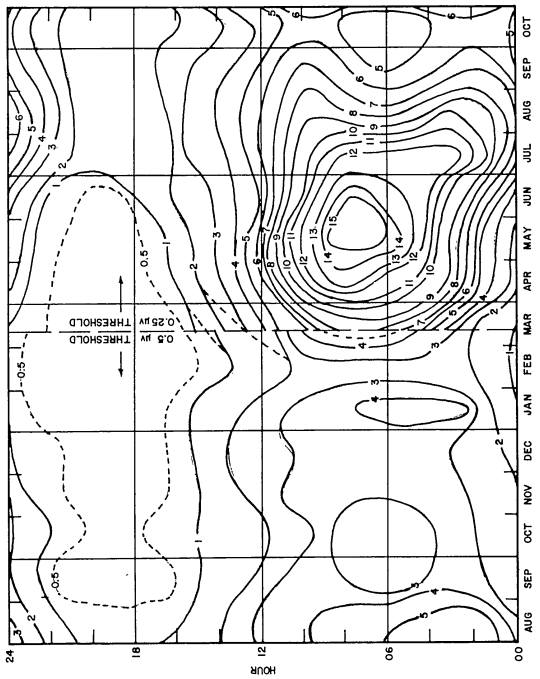

METEOR WHISTLES PER MINUTE, CEDAR RAPIDS TO STERLING, 49.8 Mc.

FIGURE V-1

Declassified in Part - Sanitized Copy Approved for Release @ 50-Yr 2014/06/09 : CIA-RDP81-01043R003000180001-4

Declassified in Part - Sanitized Copy Approved for Release @ 50-Yr 2014/06/09 : CIA-RDP81-01043R003000180001-4

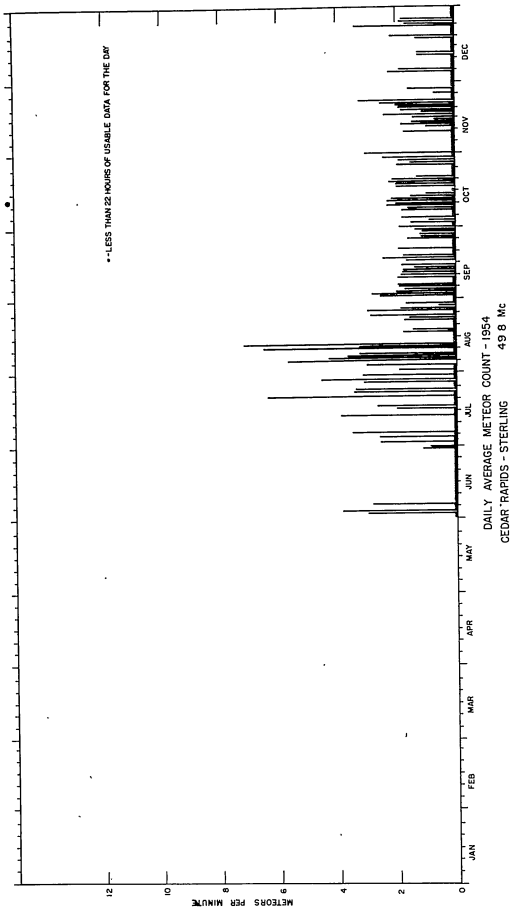

DAILY AVERAGE METEOR COUNT - 1954
CEDAR RAPIDS - STERLING
49.8 Mc

FIGURE V-2

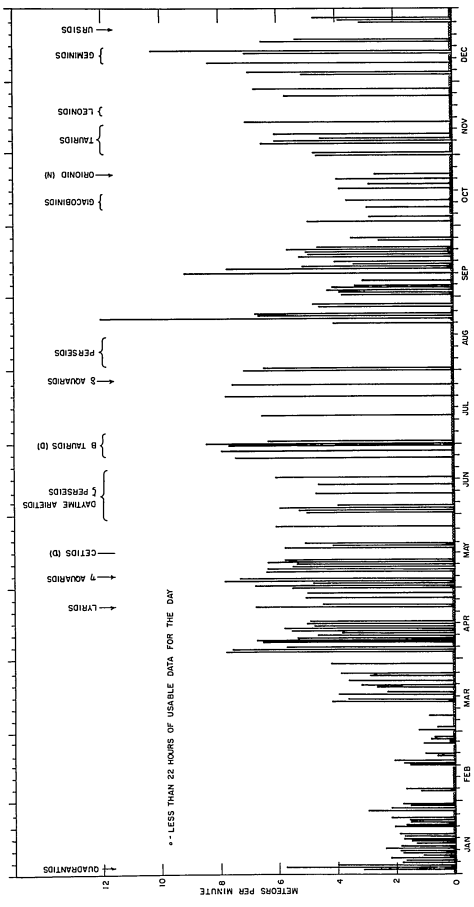

DAILY AVERAGE METEOR COUNT - 1955

FIGURE V-3

Declassified in Part - Sanitized Copy Approved for Release @ 50-Yr 2014/06/09 : CIA-RDP81-01043R003000180001-4

Declassified in Part - Sanitized Copy Approved for Release @ 50-Yr 2014/06/09 : CIA-RDP81-01043R003000180001-4

APPENDIX VI

PART I

OFF-PATH MEASUREMENTS OF AZIMUTH OF ARRIVAL OF 49.8 MC/S SIGNAL

V. C. Pineo

1. INTRODUCTION

This part describes an experimental investigation at 49.8 Mc/s of the relationship between the horizontal radiation pattern of a directional transmitting antenna and the azimuthal pattern for reception of the ionospherically scattered signal.

The purpose was to obtain information about the possibilities of off-path interference to VHF propagation, and, also, to obtain information about the propagation medium. It was of interest whether at a receiving station the apparent direction of arrival of the signal was from an illuminated "scattering volume," defined by the transmitting antenna pattern, or whether the geometry of specular reflections tended to influence the direction of arrival.

Signal intensities of the Cedar Rapids transmissions at 49.8 Mc/s beamed toward Sterling were received at two off-path receiving sites and compared with signal intensities received simultaneously at Sterling. The off-path sites were located so that their distances to Cedar Rapids were as nearly as possible the same as the distance from Cedar Rapids to Sterling. The azimuths from Cedar Rapids to the off-path sites were chosen to be approximately the same as the azimuths of the first and second minima of the horizontal radiation pattern of the transmitting antenna.

2. EXPERIMENTAL DETAILS

The transmitting antenna at Cedar Rapids was a rhombic. Its horizontal radiation pattern had first and second principal minima at angles of 8.6° and 21° respectively, relative to the main lobe direction. The first off-path site was located at Cumberland, Virginia, at a distance of 1243 Km from Cedar Rapids in the direction of the first minimum. The second site was located near Hamlet, North Carolina, at a distance of 1308 Km from Cedar Rapids in the direction of the second minimum.

The geometric arrangement for the experiment is shown in Figure VI-1.

A mobile signal intensity recording unit was used at Cumberland and Hamlet. The equipment in the mobile unit was identical to that used to record reference signal intensities at Sterling. Identical Yagi receiving antennas were used at Sterling and at the off-path sites. The half-power beamwidth of each Yagi was about 65 degrees.

Declassified in Part - Sanitized Copy Approved for Release @ 50-Yr 2014/06/09 : CIA-RDP81-01043R003000180001-4

Declassified in Part - Sanitized Copy Approved for Release @ 50-Yr 2014/06/09 : CIA-RDP81-01043R003000180001-4

The power output of the Cedar Rapids transmitter was about 30 kilowatts.

Signal intensities were recorded at Cumberland May 18 through May 20, and May 24 through May 26, 1954, and at Hamlet from June 3 through June 6 inclusive. Reference signal intensities were recorded continuously at Sterling throughout each of these periods. Signal intensity recording at each site was normally carried on with the Yagi antenna pointed at Cedar Rapids. Direction-of-arrival observations in which the receiving Yagi was rotated back and forth about ± 45 degrees relative to the azimuth of Cedar Rapids were made at Cumberland and Hamlet. The more extensive direction-of-arrival observations were made at Hamlet. The Yagi at Hamlet was rotated in steps of 5° to 25°. Signal intensity was recorded for about 5 minutes at each step. In order to take account of changes in the incident signal intensity occurring during a series of observations, reference signal intensities were recorded with the Yagi pointed at Cedar Rapids for 5 minutes at the beginning and end of each observation.

3. RESULTS

The results of the signal intensity observations of the Cedar Rapids signal made simultaneously at Cumberland and Sterling are shown graphically in Figure VI-2. Signal intensities at Cumberland were 1 db to 3 db stronger than at Sterling from 2300 hours to 1130 hours, and were 1 db to 4 db weaker than at Sterling from 1200 hours to 2230 hours.

Direction-of-arrival observations made at Cumberland by rotating the Yagi antenna seemed to indicate that the signal arrived from the direction of Cedar Rapids. However, the difference between the azimuths to Cedar Rapids and the midpoint of the Cedar Rapids to Sterling path is only about 8 degrees. This is too small a difference in direction of arrival to be detected by swinging a wide-beam antenna.

The results of the signal intensity observations made simultaneously at Sterling and Hamlet are shown in Figure VI-3. Signal intensities at Hamlet relative to Sterling ranged from -4 db during the hour before noon to -10 db during the hours 2100 to 2200.

Direction-of-arrival observations at Hamlet indicated that the signal arrived from the direction of the midpoint of the Cedar Rapids to Sterling path. These observations were repeated several times on different days with nearly identical results each time. The results of the direction-of-arrival observations made at Hamlet are compared in Figure VI-4 with the measured azimuthal radiation pattern of the main lobe of the Yagi receiving antenna. Each of the encircled points shown in Figure VI-4 represents the median value for all the signal intensities observed at that azimuth relative to the signal intensities observed at the azimuth of Cedar Rapids. These experimentally determined points fall very nearly on the curve outlining the radiation pattern of the Yagi.

The azimuthal coverage pattern for midday reception of the Cedar Rapids signal composed from the results of the observations at Sterling, Cumberland and Hamlet are shown in Figure VI-5 in comparison with the azimuthal radiation pattern of the Cedar Rapids rhombic. The dissimilarity between the two patterns is significant.

4. DISCUSSION OF THE RESULTS

The higher, relative to Sterling, signal intensity observed during the morning hours at Cumberland was an unexpected result. However, later analysis of the rate of meteors in long-range propagation at VHF by Eshleman, et al.,[1,2] shows that the contribution to the received signal intensity due to meteor trails maximizes in a region slightly off the great-circle path to the transmitter. This region is north of the midpoint of an east-west path in the morning and south of the midpoint in the evening. Because of the diurnal variation of the geocentric velocities of meteors entering the earth's atmosphere, meteoric effects are greatest in the morning. The approximate locations of the optimum regions for the occurrence of meteoric events observable at Cumberland and Hamlet are shown in Figure VI-1. The Cumberland location was nearly optimum for observing enhanced signal intensity levels due to meteoric events occurring in the region over the midpoint of the Cedar Rapids to Sterling path.

Signal intensities at Hamlet during the morning hours did not show the marked improvement, relative to Sterling, that was observed at Cumberland. This result would have been predicted by the Eshleman model since the optimum region for the occurrence of meteoric events observable at Hamlet was outside of the region illuminated by the Cedar Rapids to Sterling beam.

The differences in diurnal behavior between the signal intensities received at Sterling and Cumberland suggest that two scatter propagation modes were involved. One of these modes may be due to meteoric ionization. The other mode is attributed to solar effects.

These results have a bearing on practical problems of interference and jamming. For example, a transmitter at Hamlet could interfere with reception at Cedar Rapids of a signal being transmitted from Sterling by having its radiation beamed in the direction of the common volume of the Sterling-Cedar Rapids antenna system.

The indicated coverage pattern for reception is of particular importance. It shows that with high transmitter power reasonably good signal intensities can be received at fairly large angles from the direction of the transmitting antenna beam. It is only necessary to point a directional receiving antenna at the scattering region illuminated by the transmitting antenna.

REFERENCES

1. V. R. Eshleman, L. A. Manning, A. M. Petersen and O. G. Villard, Jr., "The Role of Meteors in Extended-Range VHF Propagation," I.R.E. Convention Record, vol. 3, Part I, "Antennas and Propagation," pp. 61-62, 1955.

2. V. R. Eshleman and L. A. Manning, "Radio Communication by Scattering from Meteoric Ionization," Proc. I.R.E., 42, pp. 530-536, March 1954.

Declassified in Part - Sanitized Copy Approved for Release @ 50-Yr 2014/06/09 : CIA-RDP81-01043R003000180001-4

Declassified in Part - Sanitized Copy Approved for Release @ 50-Yr 2014/06/09 : CIA-RDP81-01043R003000180001-4

APPENDIX VI

PART II

EXPERIMENTAL OBSERVATIONS OF THE CONTRIBUTION OF METEORIC IONIZATION TO THE PROPAGATION OF VHF RADIO WAVES BY IONOSPHERIC FORWARD SCATTER

V. C. Pineo

1. INTRODUCTION

The diurnal variation of VHF signal intensities propagated by ionospheric forward scatter has been tentatively interpreted as the resultant of the effect of a solar-related scattering mechanism in the lower E region having a maximum at midday and a meteoric effect having a maximum at about 06 hours and a minimum at about 18 hours local time.[1,2] Other theories have been advanced which attribute this "ionospheric scatter propagation" primarily to reflections and scattering from meteor trails.[3,4,5]

The experiment described in this report was designed to elucidate the relative contributions from these two mechanisms. Another objective of the experiment was to obtain the value of the exponent of angle dependence which appears in various transmission equations[1,2] which has importance in the design of practical communication circuits using the forward scatter mechanism.

In an earlier experiment,[2] signal intensities received over an east-west reference path were compared with signal intensities received simultaneously at a second site located to the south of the reference receiver. The transmitting antenna and both receiving antennas were directed toward the midpoint of the reference path. The value of the off-path angle was chosen in accordance with the model of Eshleman and Manning for maximum contributions from meteoric ionization.[4] The results of that early experiment showed that the off-path geometry had some advantage over the on-path geometry during the morning hours. However, the off-path signal intensities were several decibels lower during the weak signal period which occurred in both cases during the afternoon around 20 hours.

The relatively greater signal intensities observed in the off-path case during the morning hours were presumably due to meteors. O. G. Villard[6] suggested that a similar enhancement might be observed during the afternoon hours by using antennas directed south, rather than north, of the great-circle path between transmitter and receivers.

2. DETAILS OF THE EXPERIMENT

The 1243 Km Cedar Rapids to Sterling path was used as a reference path. Two off-path receiving sites, one to the north and the other to

the south of Sterling were selected for optimum reception of meteoric components.[4] The northerly site was located at Shepherdstown, Pa., and the southerly site at Carysbrook, Va. The geometry of the experiment is shown in Figure VI-6.

Cedar Rapids transmissions at 49.8 Mc/s beamed toward Sterling were received simultaneously at Sterling, Shepherdstown and Carysbrook. At Sterling the rhombic antenna normally used in the signal intensity recording program was employed. Rhombic antennas identical to the antenna used at 49.8 Mc/s at Sterling were installed at Shepherdstown and Carysbrook and directed toward the midpoint of the Cedar Rapids to Sterling path. The computed half-power beamwidths of the antennas were 6° and 7° in the horizontal and vertical planes respectively. The elevation of the maximum of the main lobe in all cases was 7°.

The input power to the rhombic transmitting antenna was 30 Kw. Continuous wave signal intensities at 49.8 Mc/s were recorded simultaneously at the three receiving sites from 17 hours, January 3, to 00 hours, January 27, 75° W time, 1956. The receiver bandwidths were approximately 2.5 Kc/s. The recording time constants were about 13 seconds.

2.1 Cosmic Noise Observations

The receivers at the three sites were calibrated daily by identical signal generators, which themselves were intercompared by a portable substandard several times during the experiment.

It had also been anticipated that cosmic noise might be used as a common reference level between the three receiving stations. Consequently cosmic noise was recorded at each of the three sites during half-hourly two-minute interruptions in transmission. The results are shown graphically in Figure VI-7.

Diurnal minimum values of hourly median cosmic noise intensities were obtained between about 0700 and 0900 hours; and maximum values between about 1700 and 2000 hours at each of the sites. However, it is apparent from the graph that variations of up to 4 db between stations can occur at certain times. These variations from site to site preclude the use of cosmic noise as a reference level. The differences between the cosmic noise effects observed at the various stations are presumed to have been due to differences in noise levels in the galactic areas toward which the antenna beams were directed. The cosmic noise levels are always much smaller in magnitude than the scatter signal intensities, and so need not be taken into account as a correction.

3. ANALYSIS OF THE DATA

In accordance with previously established practices for the whole scatter program, the signal intensity data were adjusted to a reference transmitting antenna power of 40 Kw.

Declassified in Part - Sanitized Copy Approved for Release @ 50-Yr 2014/06/09 : CIA-RDP81-01043R003000180001-4

Declassified in Part - Sanitized Copy Approved for Release @ 50-Yr 2014/06/09 : CIA-RDP81-01043R003000180001-4

The equation for transmission by ionospheric forward scatter can be expressed in simplified form by:

$$\frac{Pr}{Pt} = Kq \qquad \text{Ref. 1}$$

where Pr/Pt is the ratio of received power to transmitted power, K includes all of the terms relating to ionospheric structure, wave frequency, antenna gains, polarization, etc., and q is purely a geometric factor.

In the case of this experiment the point of maximum non-meteoric scattering to any one receiver lies in a plane which is perpendicular to the great-circle path to the transmitter at the midpoint. For this special case the geometric factor,[2] q, may be defined as:

$$q = \frac{1}{\ell^2 \sin \epsilon (\sin \gamma/2)^n}$$

where 2ℓ = the length of the ray path from transmitter to receiver
n = angle dependence exponent
γ = the forward scatter angle
ϵ = the angle between the transmitted ray and the scattering layer. (In this special case $\epsilon = \gamma/2$.)

Incorporating this particular value for ϵ, the following simplified expression for angle dependence is obtained:

$$\left(\frac{E_1}{E_2}\right)^2 = \left(\frac{\sin \gamma_2/2}{\sin \gamma_1/2}\right)^{n+1} \qquad (1)$$

where γ_1 and γ_2 are the forward scatter angles associated with received signal intensities E_1 and E_2.

In the above expression for angle dependence, the assumption that ϵ and ℓ have the same values in the off-path case as they have in the on-path case introduces negligible errors.

In order to deduce the value of the angle dependence exponent, n, from the experimental data, it is necessary to follow the procedure described in the paper by Bailey, Bateman and Kirby.[2] In calculating the angle-dependence exponent, allowance has been made for losses in the off-path case relative to the on-path case due to polarization effects and to the smaller common volume of the antennas. The calculated loss in signal intensity from these two sources was about 2 decibels.

4. RESULTS

4.1 Comparison of 3-Station Signal Intensities

Samples from the 49.8 Mc/s signal intensity records made simultaneously on a typical January day at Shepherdstown, Sterling and Carysbrook are

shown in Figures VI-8 to VI-10 inclusive. The values of the hourly median signal intensities were calculated for each site from records of this type.

The results of these simultaneous signal intensity observations at 49.8 Mc/s are presented graphically in Figure VI-11 and summarized in Table I. These results do not include the 2 db loss calculated above.

TABLE I

SUMMARY OF RESULTS AT 49.8 MC/S

Station	Period during which signal intensity exceeded that of the other two stations (75° W time)
Carysbrook	0400 - 1115
Sterling	1115 - 1715
Shepherdstown	1715 - 0400

It is evident from Figure VI-11 that the great-circle path exhibits a higher signal intensity during the midday hours than either of the off great-circle paths. This result suggests that solar control is predominant at this time.

It is to be noted that the diurnal variation of the 49.8 Mc/s signal intensity was about 6 decibels smaller at Shepherdstown than at either Sterling or Carysbrook.

4.2 Meteoric Effects of 49.8 Mc/s

Individual meteor occurrences can be identified in the CW records as abrupt rises in signal intensity. These were observed to coincide with audio Doppler whistles on the receiver output. Such whistles have long been identified with meteors.

At Carysbrook and Sterling the maximum meteoric effects occurred during the morning hours. The minimum of these meteoric effects occurred during the evening hours. At Shepherdstown the distinction between morning and evening behavior was less pronounced, as great numbers of abrupt rises in signal intensity were observed during both periods. However, the effect on the integrated signal intensity records at Shepherdstown was greatest during the late afternoon and early evening hours.

4.3 Angle Dependence at 49.8 Mc/s

In order to deduce n, the value of the angle-dependence exponent of the solar-related scattering mechanism, from the signal intensity data,

Declassified in Part - Sanitized Copy Approved for Release @ 50-Yr 2014/06/09 : CIA-RDP81-01043R003000180001-4

Declassified in Part - Sanitized Copy Approved for Release @ 50-Yr 2014/06/09 : CIA-RDP81-01043R003000180001-4

it was necessary to choose a time of day when such a mechanism could be expected to exist. It was also necessary to choose a time when the effects of meteoric activity were relatively small. Since the Shepherdstown records exhibited a considerable amount of meteoric activity throughout the day, they were considered unsuitable for angle-dependence calculations. The least amount of meteoric contamination was found in the Sterling and Carysbrook records at about 1530 hours. The difference between the median signal intensities recorded at Carysbrook and Sterling at this time was 6 decibels in favor of Sterling. Assuming a scatter height value of 85 Km^2 enabled the scatter angle to be found, and then from equation 1 the value of the angle-dependence exponent was determined as 6.0. This result strictly applies only for the circuits which have been used to obtain it, but the value is in reasonable agreement with other published results.[1,2,7,8]

4.4 Discussion of the Results

The high signal intensities observed around midday at all three receiving locations indicate dominant solar influence during the daylight hours. The results of the off-path observations suggest that meteoric ionization was the dominant influence during the night and that meteoric influence contributed substantially to the signal intensities observed during the early morning and late afternoon hours. It is worth noting that these results were obtained during midwinter, with minimum hours of sunlight on the path. During other seasons it is likely that meteor influence would be dominant fewer hours of the day; this was illustrated in the earlier summer measurements.[2]

The diurnal variation of the rate of occurrence of meteoric incidences can be explained on the basis of the axial and orbital motions of the earth which result in geocentric velocities having their greatest values around sunrise and their lowest values around sunset. This will in general account for the low signal intensity values observed in the early evening hours.

The behavior of the 49.8 Mc/s signal intensities observed during the morning and afternoon hours at Carysbrook was markedly different from that observed during the same hours at Shepherdstown. This result is attributed to the combined effects of the known specific directivity of meteor radiants,[9,10] which will tend to favor reception in one aerial more than the other at any given time, and of the absolute diurnal variation of the meteor rate.

The use of off-path transmission seems to offer some advantage during the morning and evening hours. Whether or not these advantages could be realized with practical communications circuits would depend on the quality of the received signals.

The apparent advantage of using off-path transmission during these hours, and a practical model, employing antenna beam switching for obtaining these advantages, are shown in Figure VI-7.

5. SUMMARY AND RECOMMENDATIONS

The results of this experiment indicate that there are two principal propagation modes involved in ionospheric scatter propagation at VHF. The prevalent mode during the daylight hours exhibits a dominant solar influence. The daylight mode is most effectively utilized by employing antennas directed along the great-circle path between the transmitter and the receiver. The prevalent mode during the nighttime hours is attributed to meteoric ionization. The influence of the meteoric mode on the received signal intensities can be enhanced by use of off-path transmission.

Other experiments designed to determine whether there are real advantages of off-path transmissions for practical communications circuits should be performed. A properly designed experiment employing pulse techniques to observe the relative delays and the relative amplitudes of the various propagation modes, along with studies of the fading characteristics of the total signal, could yield the maximum amount of information. Another experiment, less rewarding in basic information but having practical value, would be to use radioteletype transmissions and compare off-path performance with on-path performance with respect to error rates.

REFERENCES

1. D. K. Bailey, R. Bateman, et al., "A New Kind of Radio Propagation at Very High Frequencies Observable over Long Distances," Phys. Rev., 86, pp. 141-145, April 15, 1952.

2. D. K. Bailey, R. Bateman, and R. C. Kirby, "Radio Transmission at VHF by Scattering and other Processes in the Lower Ionosphere," Proc. I.R.E., 43, No. 10, October 1955.

3. D. W. R. McKinley, "Dependence of Integrated Duration of Meteor Echoes on Wavelength and Sensitivity," Can. Jour. Phys., 32, pp. 450-467, July 1954.

4. V. R. Eshleman and L. A. Manning, "Radio Communication by Scattering from Meteoric Ionization," Proc. I.R.E., 42, pp. 530-536, March 1954.

5. V. R. Eshleman, L. A. Manning, A. M. Peterson and O. G. Villard, Jr., "The Role of Meteors in Extended-Range VHF Propagation," Proc. I.R.E., 43, No. 10, pp. 1473-1481, October 1955.

6. O. G. Villard, Jr., Scatter Symposium, Washington, D. C., November 1955.

7. F. Villars and V. F. Weisskopf, "The Scattering of Electromagnetic Waves by Turbulent Atmospheric Fluctuations," Phys. Rev., 94, pp. 232-240, April 15, 1954.

Declassified in Part - Sanitized Copy Approved for Release @ 50-Yr 2014/06/09 : CIA-RDP81-01043R003000180001-4

Declassified in Part - Sanitized Copy Approved for Release @ 50-Yr 2014/06/09 : CIA-RDP81-01043R003000180001-4

8. R. C. Kirby, "VHF Propagation by Ionospheric Scattering - A Survey of Experimental Results," I.R.E. Transactions on Communications Systems, CS-4, No. 1, pp. 17-27, March 1956.

9. G. S. Hawkins, Mon. Not. R. Astr. Soc., 116, 92, 1956.

10. C. D. Ellyett and C. S. L. Keay, "Radio Echo Observations of Meteor Activity in the Southern Hemisphere," Aust. J. of Physics, 9, 471, 1956.

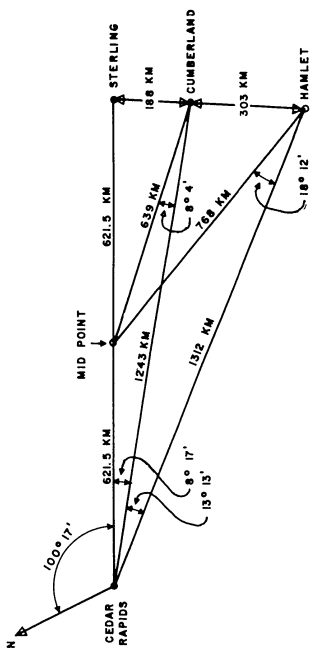

GEOMETRY FOR THE INTERFERENCE EXPERIMENT

FIGURE VI-1

Declassified in Part - Sanitized Copy Approved for Release @ 50-Yr 2014/06/09 : CIA-RDP81-01043R003000180001-4

Declassified in Part - Sanitized Copy Approved for Release @ 50-Yr 2014/06/09 : CIA-RDP81-01043R003000180001-4

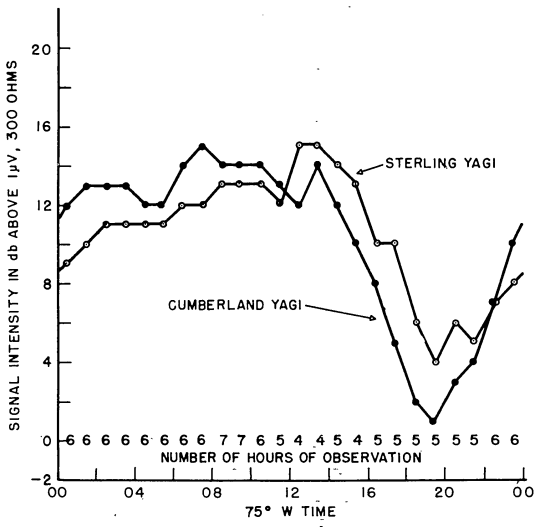

DIURNAL VARIATION OF HOURLY MEDIAN SIGNAL INTENSITIES OBSERVED SIMULTANEOUSLY AT STERLING, VA. AND CUMBERLAND, VA. AT 49.8 Mc/s

FIGURE VI-2

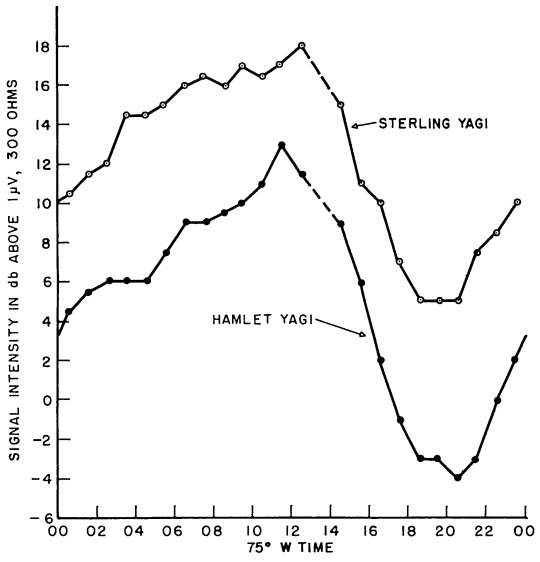

DIURNAL VARIATION OF HOURLY MEDIAN SIGNAL INTENSITIES OBSERVED SIMULTANEOUSLY AT STERLING, VA. AND HAMLET, N.C. AT 49.8 Mc/s

FIGURE VI-3

Declassified in Part - Sanitized Copy Approved for Release @ 50-Yr 2014/06/09 : CIA-RDP81-01043R003000180001-4

Declassified in Part - Sanitized Copy Approved for Release @ 50-Yr 2014/06/09 : CIA-RDP81-01043R003000180001-4

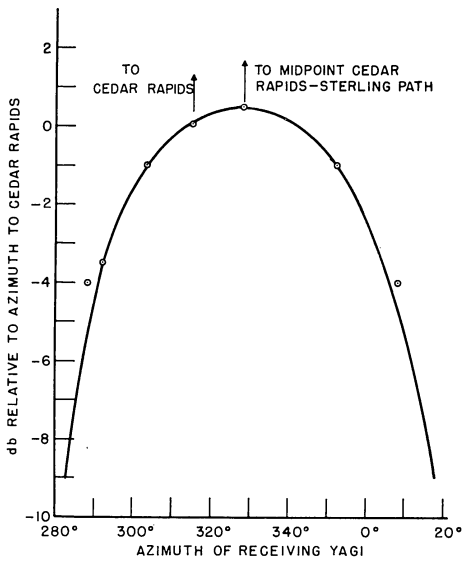

RESULTS OF DIRECTION-OF-ARRIVAL EXPERIMENT AT HAMLET. EXPERIMENTAL RESULTS ARE ENCIRCLED.

FIGURE VI-4

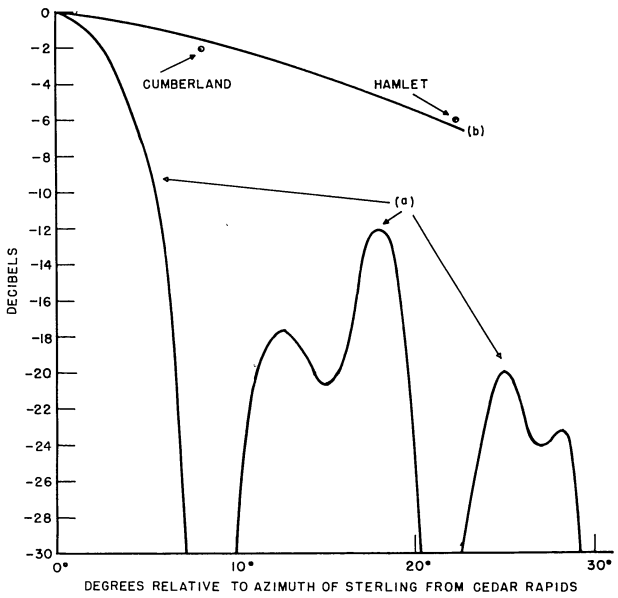

RADIATED POWER IN db RELATIVE TO MAIN LOBE OF TRANSMITTING ANTENNA (a) COMPARED WITH SIGNAL INTENSITIES IN db RELATIVE TO STERLING OBSERVED AT CUMBERLAND VA. AND HAMLET, N.C. (b)

FIGURE VI-5

Declassified in Part - Sanitized Copy Approved for Release @ 50-Yr 2014/06/09 : CIA-RDP81-01043R003000180001-4

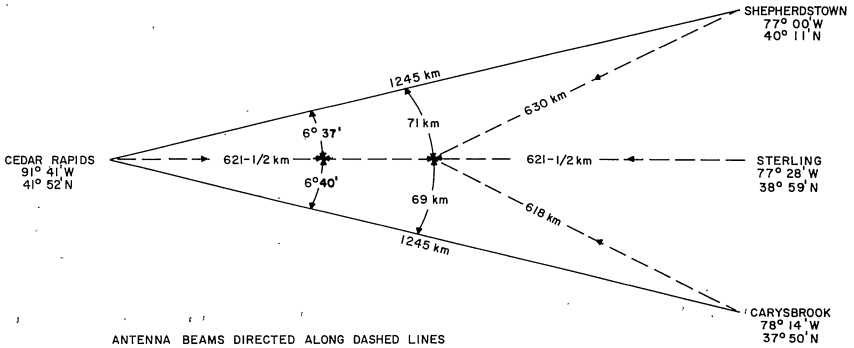

GEOMETRY FOR THE OFF-PATH EXPERIMENT

FIGURE VI-6

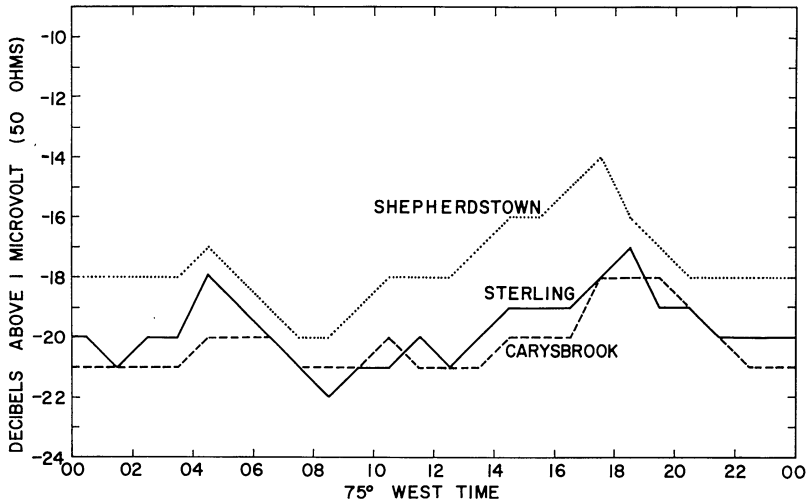

HOURLY MEDIAN VALUES OF COSMIC NOISE RECORDED SIMULTANEOUSLY AT 49.8 Mc/s IN A $2\frac{1}{2}$ Kc/s BANDWIDTH AT STERLING, CARYSBROOK, AND SHEPHERDSTOWN DURING JAN., 1956

FIGURE VI-7

Declassified in Part - Sanitized Copy Approved for Release @ 50-Yr 2014/06/09 : CIA-RDP81-01043R003000180001-4
Declassified in Part - Sanitized Copy Approved for Release @ 50-Yr 2014/06/09 : CIA-RDP81-01043R003000180001-4

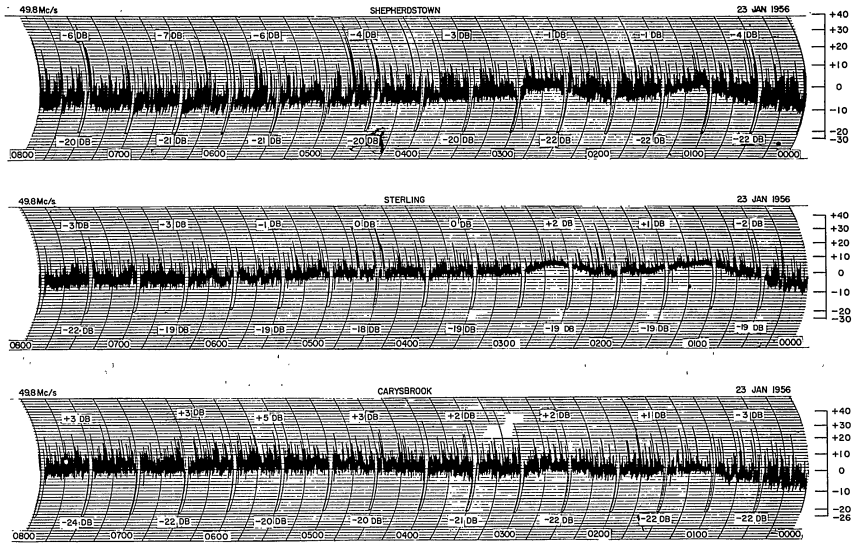

SAMPLE RECORDINGS MADE SIMULTANEOUSLY AT SHEPHERDSTOWN, STERLING, AND CARYSBROOK AT 49.8 Mc/s SHOWING CHARACTERISTIC DIFFERENCES IN BEHAVIOR DURING THE MORNING HOURS.

FIGURE VI-8

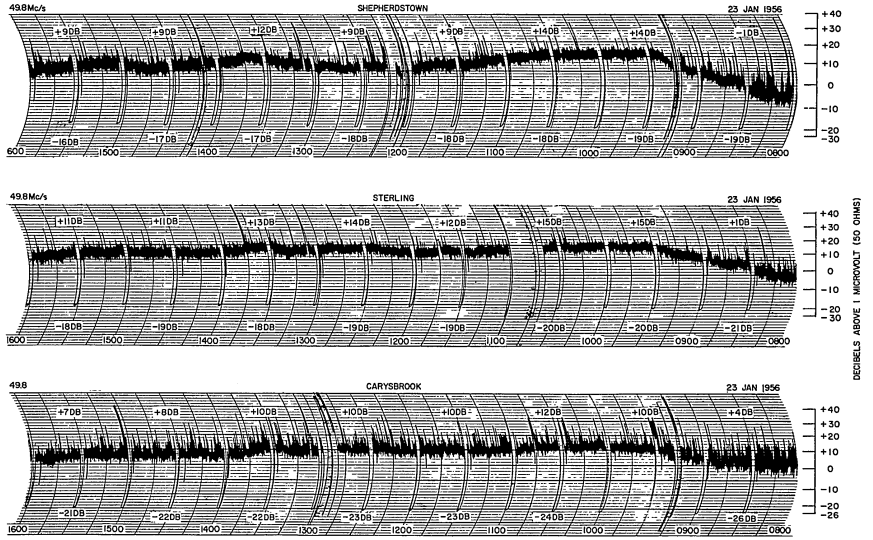

SAMPLE RECORDINGS MADE SIMULTANEOUSLY AT SHEPHERDSTOWN, STERLING, AND CARYSBROOK AT 49.8 Mc/s SHOWING CHARACTERISTIC DIFFERENCES IN BEHAVIOR DURING THE MIDDAY HOURS.

FIGURE VI-9

Declassified in Part - Sanitized Copy Approved for Release @ 50-Yr 2014/06/09 : CIA-RDP81-01043R003000180001-4
Declassified in Part - Sanitized Copy Approved for Release @ 50-Yr 2014/06/09 : CIA-RDP81-01043R003000180001-4

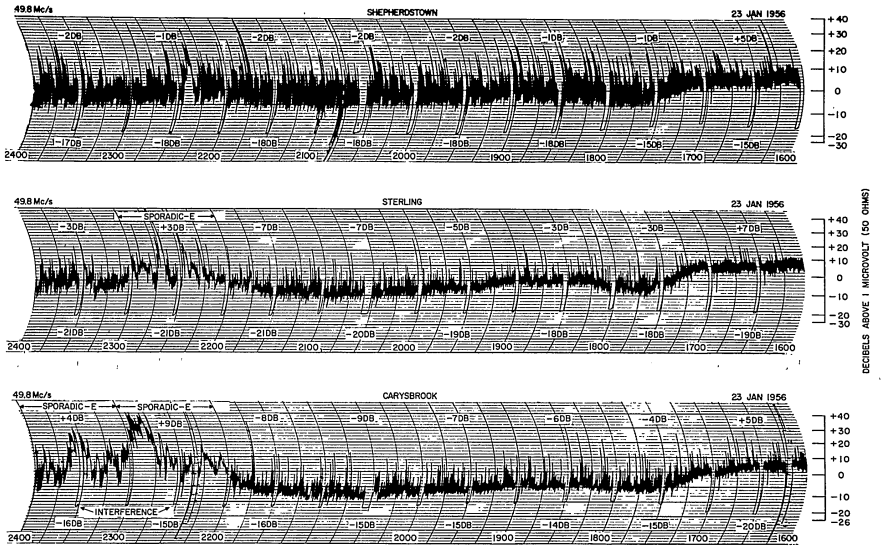

SAMPLE RECORDINGS MADE SIMULTANEOUSLY AT SHEPHERDSTOWN, STERLING, AND CARYSBROOK AT 49.8 Mc/s SHOWING CHARACTERISTIC DIFFERENCES IN BEHAVIOR DURING THE EVENING HOURS.

FIGURE VI-10

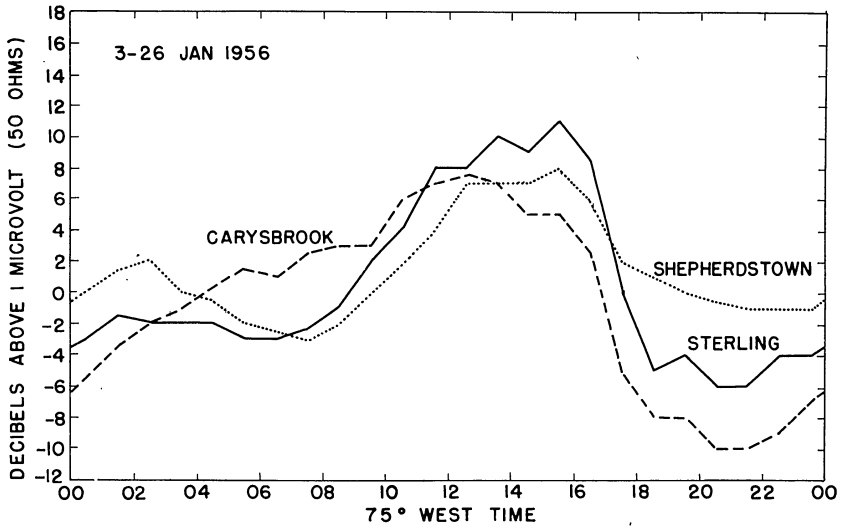

DIURNAL VARIATION OF HOURLY MEDIAN SIGNAL INTENSITIES OBSERVED SIMULTANEOUSLY AT SHEPHERDSTOWN, STERLING, AND CARYSBROOK AT 49.8 Mc/s

FIGURE VI-11

Declassified in Part - Sanitized Copy Approved for Release @ 50-Yr 2014/06/09 : CIA-RDP81-01043R003000180001-4
Declassified in Part - Sanitized Copy Approved for Release @ 50-Yr 2014/06/09 : CIA-RDP81-01043R003000180001-4

Declassified in Part - Sanitized Copy Approved for Release @ 50-Yr 2014/06/09 : CIA-RDP81-01043R003000180001-4

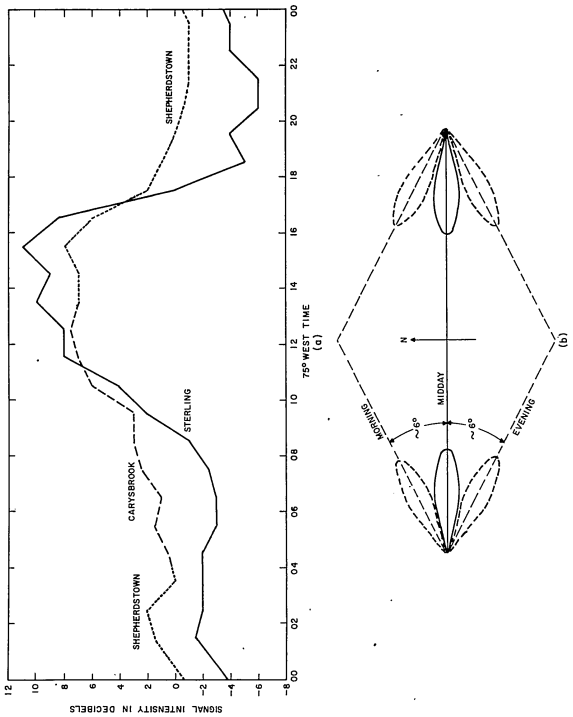

SHOWING (a) COMPARISON OF COMPOSITE OFF-PATH RESULTS INDICATING RELATIVE ADVANTAGE OF OFF-PATH TRANSMISSION DURING MORNING AND EVENING HOURS AND (b) A SUGGESTED PRACTICAL MODEL, EMPLOYING ANTENNA BEAM SWITCHING, FOR REALIZING THE ADVANTAGES OF OFF-PATH TRANSMISSION

FIGURE VI-12

APPENDIX VII

A NARROW-BAND RECORDING RECEIVER

G. Franklin Montgomery

1. INTRODUCTION

This report describes the development of a fixed-frequency narrow-bandwidth receiver for recording the intensity of continuous-wave VHF-scattered signals in the 25 to 60-Mc/s range. The laboratory constructed receivers were designed to operate at 36.0 and 49.8 Mc/s.

In the course of experimental work, it has become necessary to measure the intensity of scatter signals that are considerably weaker than those dealt with previously. To make accurate measurements, the received signal should be as large as possible compared with the background noise, and this requirement is met by using a narrow receiver bandwidth. The ultimate limit in usable pre-detection selectivity for a monochromatic signal depends upon the frequency stability of the transmitter and receiver. Long-term frequency stability of one part in 10^8 is obtainable practically, and for an operating frequency of 50 Mc/s and opposing transmitter and receiver frequency drifts, the maximum frequency difference with this stability is one cycle per second. This figure suggests that a receiver bandwidth of several cycles per second should be usable if the selectivity curve of the receiver is flat-topped. Previous experience has shown, however, that scatter signals are not monochromatic and that at 50 Mc/s the signal bandwidth occasionally may be several tens of cycles per second. Accordingly, it seemed desirable to specify a receiver whose bandwidth could be changed at will from about twenty cps to several hundred cps.

2. DESIGN

Selectivity of the desired order might be attained at the signal frequency by the use of crystal filters in a tuned radio-frequency receiver, but a more practical arrangement is the usual heterodyne technique wherein the signal frequency is reduced before filtering. A superheterodyne receiver would require at least two frequency conversions in order to provide sufficient selectivity and image rejection, and at least two stable frequency heterodyning voltages are needed in such a system. A third possibility is to heterodyne the signal, using one stable heterodyning voltage, directly to the audio-frequency range, where filtering can be accomplished by simple means, and to make special provisions for eliminating the single image response. The receiver to be described uses this principle.

Declassified in Part - Sanitized Copy Approved for Release @ 50-Yr 2014/06/09 : CIA-RDP81-01043R003000180001-4

Declassified in Part - Sanitized Copy Approved for Release @ 50-Yr 2014/06/09 : CIA-RDP81-01043R003000180001-4

A block diagram of the receiver is shown in Figure VII-1. The antenna output is first amplified at signal frequency. It is then fed separately through two radio-frequency tuned circuits whose outputs differ in phase by 90 degrees. The tuned-circuit outputs are applied to two mixers which receive a common heterodyning voltage from the local oscillator. The intermediate-frequency outputs of the mixers, in the 1000-cps range, are modified in phase by two audio-frequency phasing networks and are then added in a common amplifier. The purpose of the twin mixing and the RF and IF phase shifts is to eliminate the receiver image response that lies approximately 2000 cps from the signal frequency in the direction of the local oscillator frequency. The sense of the phase difference produced by the RF and IF networks determines whether the observed signal frequency is above or below the local oscillator frequency. Reversing the sense of the phase change produced by either set of networks reverses this relationship.

The combined intermediate-frequency output is filtered by a bandpass filter whose frequency characteristic is centered at 1000 cps. This filter essentially determines the selectivity of the receiver, and since the control of selectivity is concentrated in one unit, it is convenient to expend as much care in its design as is necessary. The filter units are constructed in plug-in form, so that the receiver bandwidth may be changed easily by substituting a different unit.

The filter output is amplified in a relatively broad resistance-coupled amplifier. The amplifier output is rectified, filtered and fed to a D-C amplifier which operates a recording milliammeter. The filtered D-C output is also available as AVC bias for the first three IF amplifier stages so that the meter indication will be an approximately logarithmic function of average signal amplitude.

Complete circuit diagrams of the receiver RF, IF, and power-supply sections and of the filter units are given in Figures VII-2 through VII-5. Photographs of the receiver unit, except for the frequency control unit, are shown in Figures VII-6 (A) and (B). The stable-frequency local oscillator units were developed separately and are described in Appendix IX.

3. PERFORMANCE

The over-all gain of the receiver, that is, the ratio of D-C detector voltage to open-circuit 50-ohm source voltage, is about 2×10^8 for maximum IF gain in the manual gain position. The maximum gain of the IF amplifier itself is about 3×10^4 at 1000 cps and is 3 db below the 1000-cps gain at 500 and 2000 cps. The open-circuit source voltage for full-scale meter deflection is 0.1 microvolts at maximum gain. With the IF gain reduced, meter deflection remains substantially linear for inputs up to 100 microvolts. In the AVC position, and with maximum meter-circuit gain, full-scale deflection is obtained with an input of 7 microvolts.

With the meter-circuit gain reduced, meter deflection remains substantially logarithmic for inputs up to 200 microvolts. With the 60-cps bandwidth filter, in either the manual or AVC positions, an input of .01 microvolts gives a measurable meter deflection over that due to receiver noise. This figure represents a detectable available power of 5×10^{-19} watts. The receiver noise figure at 50 Mc/s is about 4 db. Image rejection is about 26 db.

4. DISCUSSION

Two problems encountered during the development have not been completely solved. The first is microphonism in the IF amplifier; the second is local oscillator noise.

In operation at maximum receiver gain, the signal level at the IF input is on the order of 100 microvolts, and the signal level at the mixer input is on the order of 3 microvolts. Since the output voltage from the mixer circuit onward is at audio frequency, tubes used for the mixers and succeeding stages should have stable physical structures if microphonics are not to be troublesome. In practice, the worst sources of microphonics have been the first two 6SG7 tubes in the IF amplifier; the 6J6 tubes used in the mixer and combining amplifier stages have been relatively quiet. It is probable that pentodes especially designed for low microphonism would be useful substitutes for the 6SG7 in this application, but none of the available low-noise pentodes has the remote-cutoff grid characteristic that is desirable when AVC is employed. Suitable choice of 6SG7 tubes results in a microphonic level that is not particularly objectionable in normal operation, although vibration from auxiliary equipment must be prevented from reaching the receiver.

Microphonics must also be avoided in the local oscillator. In practice, microphonics have not been a problem in the local oscillator designed for the receiver, but oscillator random noise is of sufficient intensity to require two RF stages ahead of the mixer. The effects of microphonism and local oscillator noise could be reduced still further by using more RF gain and less IF gain. If this modification were made, it would be necessary to apply AVC and manual gain control to one or more RF stages to prevent overloading in the receiver front end.

The oscillator input to the receiver mixers is about one volt. Since the signal level at this same point is about 3 microvolts, modulation of the local oscillator voltage that falls within the IF passband must be considerably less than 10^{-4} percent. Both amplitude and phase modulation of the local oscillator voltage are objectionable, since either results in spurious noise output from the mixers. In general, the random modulation present in the heterodyning voltage obtained by direct frequency multiplication of a stable, low-frequency source is too large to be tolerated. One workable solution is to use a crystal-controlled oscillator, operating directly at the heterodyning frequency, which is locked or otherwise controlled by the output of the stable generator. The noise spectrum of the crystal oscillator is found to be much smaller than that of the controlling source.

Declassified in Part - Sanitized Copy Approved for Release @ 50-Yr 2014/06/09 : CIA-RDP81-01043R003000180001-4

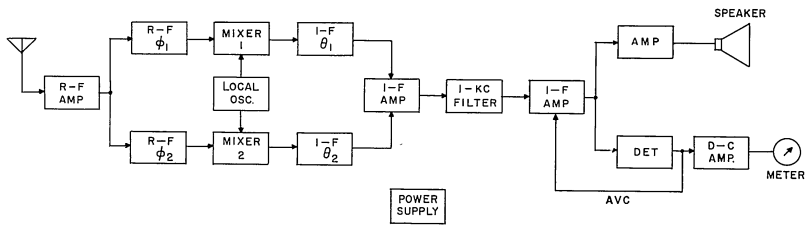

RECEIVER BLOCK DIAGRAM

FIGURE VII-1

Declassified in Part - Sanitized Copy Approved for Release @ 50-Yr 2014/06/09 : CIA-RDP81-01043R003000180001-4

Declassified in Part - Sanitized Copy Approved for Release @ 50-Yr 2014/06/09 : CIA-RDP81-01043R003000180001-4

Declassified in Part - Sanitized Copy Approved for Release @ 50-Yr 2014/06/09 : CIA-RDP81-01043R003000180001-4

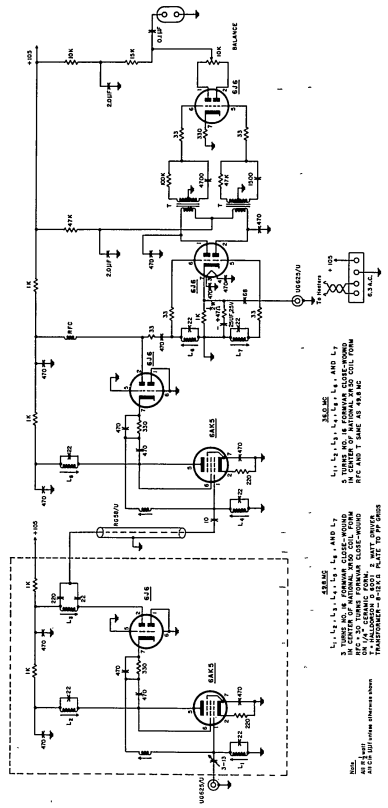

R-F SECTION
FIGURE VII-2

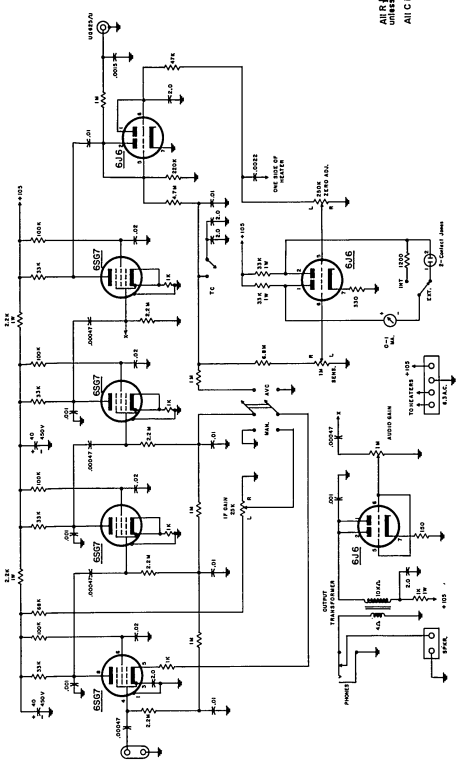

I-F SECTION
FIGURE VII-3

Declassified in Part - Sanitized Copy Approved for Release @ 50-Yr 2014/06/09 : CIA-RDP81-01043R003000180001-4

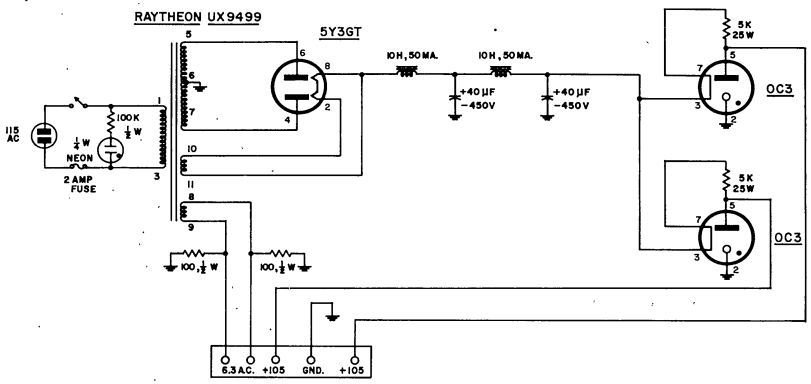

FIG. VII—4 POWER SUPPLY

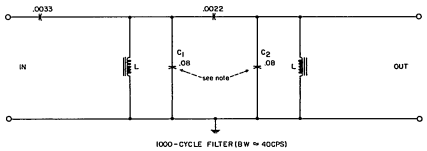

1000-CYCLE FILTER (BW ≈ 40CPS)

Note.
Capacitors in microfarads
L-0.3 Henry (Burnell S-7475)
C1 adjusted for max. voltage across C2 with output shorted. C2 adjusted for min. voltage across C2 with output open

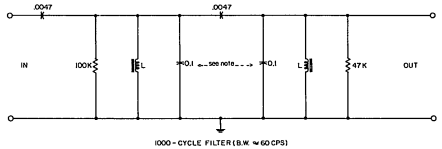

1000-CYCLE FILTER (B.W. ≈ 60 CPS)

Note.
Capacitors in microfarads
L-0.3 Henry (Burnell S-7475)
0.1 capacitors adjusted to resonance at 1000 cps with .0047 capacitors disconnected

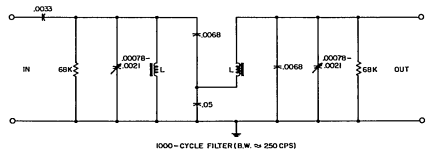

1000-CYCLE FILTER (B.W. ≈ 250 CPS)

Note.
Capacitors in microfarads
L-3 Henry (Burnell S-6762)
Tuning capacitors adjusted to 1000 cps with .05 capacitor shorted.

I-F FILTERS

FIGURE VII-5

Declassified in Part - Sanitized Copy Approved for Release @ 50-Yr 2014/06/09 : CIA-RDP81-01043R003000180001-4
Declassified in Part - Sanitized Copy Approved for Release @ 50-Yr 2014/06/09 : CIA-RDP81-01043R003000180001-4

Declassified in Part - Sanitized Copy Approved for Release @ 50-Yr 2014/06/09 : CIA-RDP81-01043R003000180001-4

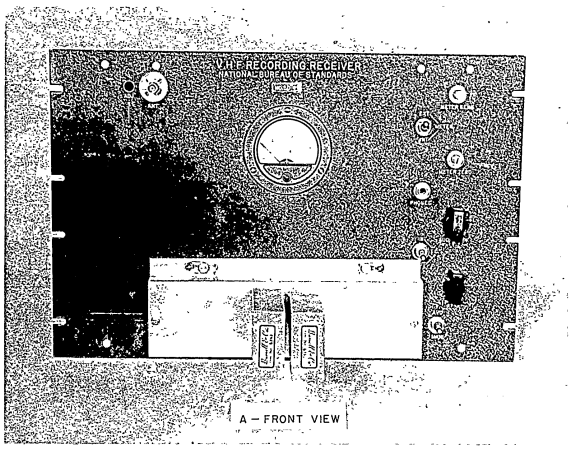

A – FRONT VIEW

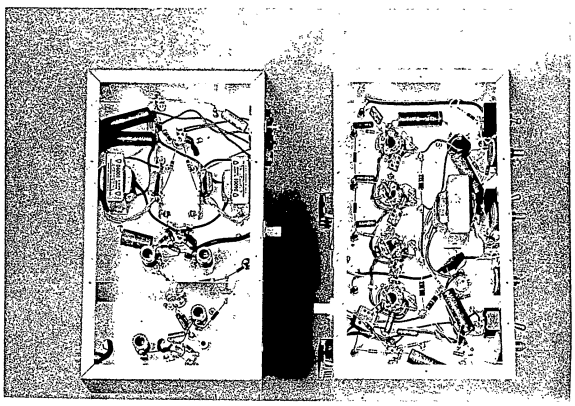

B – BOTTOM VIEW OF IF AND DETECTOR SECTION LEFT, AND RF SECTION, RIGHT, DUST COVERS REMOVED

PHOTOGRAPH OF RECORDING RECEIVER

FIGURE VII–6

APPENDIX VIII

THREE KILOWATT VHF TRANSMITTER FOR RADIO PROPAGATION STUDIES

W. B. Harding and D. C. Whittaker

1. INTRODUCTION

The 3 Kw transmitter is designed to operate at a fixed frequency in the range 30 to 75 megacycles, and is capable of long period, unattended operation. Compactness compatible with ease of servicing was an important design objective, since many of the transmitters are to be installed in small field laboratory buildings or trailers. The single phase power supply design was intended to provide for operation at remote sites where three-phase power is often not available.

One unit has been in substantially continuous operation on 49.80 Mc/s at Cedar Rapids, Iowa, since March 1956. In this service it has operated at a reduced power output of about 2.2 kilowatts as a means of avoiding service calls. Apart from thrice weekly service calls to log the readings of its meters, the transmitter has required replacement of components or tubes on the average less than once every two months.

Additional units have been built in connection with other projects for 30, 36, 40, 50, 54 and 74 Mc/s operation. Application to other frequencies within or beyond this range involves the relatively simple matter of designing appropriate inductors for the tuned circuits.

2. GENERAL DESCRIPTION

A complete setup is shown in Figure VIII-1. A block diagram of the system is shown in Figure VIII-2. The system includes the following separately identifiable units. The 3 Kw Power Amplifier unit includes plate, screen and grid bias power supplies, heater current supply, certain protective circuits, and a VSWR indicator in addition to the amplifier itself. The Driver is a two-stage linear amplifier powered by the Driver Power Supply. The Control Unit contains an automatic Reset Circuit, High VSWR Protector, Off Air Alarm, and forward and back power recording circuits. The reset circuit attempts to return the transmitter to operation if a transient overload occurs. The VSWR Protector interrupts transmissions during periods when the voltage standing wave ratio on the antenna transmission line exceeds a preset limit. The Off Air Alarm is triggered when the transmitted power falls below a preset level. The Recording Circuit facilitates graphic recording of the output voltages from the forward and reverse power diodes in the directional coupler. The Break Keyer interrupts the transmission for an adjustable period of about two minutes each time a one-second pulse is received from a programmer clock. The

Declassified in Part - Sanitized Copy Approved for Release @ 50-Yr 2014/06/09 : CIA-RDP81-01043R003000180001-4

Declassified in Part - Sanitized Copy Approved for Release @ 50-Yr 2014/06/09 : CIA-RDP81-01043R003000180001-4

Identification Keyer provides for the transmission of the station call letters each time the Break Keyer produces a two-minute interruption. The Multiplier-Exciter accepts the approximately 1 Mc/s signal from the Near One Megacycle Standard Oscillator and multiplies its frequency to the desired transmission frequency; this unit amplifies the signal for adequate feed to the Driver. (See Appendix IX for a description of the Standard Oscillator and Multiplier-Exciter.)

The various units are described in the following sections. All units except the 3 Kw power amplifier mount in one standard 19 inch wide by 73 inch high relay rack. The 3 Kw power amplifier unit is housed in a special rack 71 inches high, 29 inches wide and 19.5 inches deep, and weighs 1500 pounds complete. Power required is 60 cycles, 230 volts A-C in a three-wire balanced single phase 50 ampere entrance. The total power consumption is 5.9 Kw.

3. POWER AMPLIFIER

The power amplifier is a completely self-contained unit with bias, screen and high voltage supplies. The output circuit contains a directional coupler and meter to read forward power (power fed to the transmission line from the transmitter), back power (power reflected to the transmitter from the transmission line due to mismatch), Voltage Standing Wave Ratio or "SWR". Output connectors permit recording of both forward and back power voltages generated by the directional coupler. The unit contains all of the conventional protective circuits, such as: time delay for application of high voltage, overload protection, low bias voltage or "under-bias" protection, and chassis interlocks. The amplifier is capable of 3.2 kilowatts output into a 50 ohm load, although an output of 2.0 kilowatts is recommended where reliability is of utmost importance.

Conventional circuit design is used throughout the Power Amplifier and its associated circuits, as shown in the complete schematic wiring diagram, Figure VIII-3. The amplifier proper uses two 4-1000A tetrodes in a grounded cathode, push-pull configuration. The amplifier chassis together with the front upper cabinet panel on which the operating meters are located is hinged and swings forward and outward through 90° for servicing. When in the operating position, the upper part of this unit meets internal shield panelling of the main cabinet so that the 4-1000A tubes and the entire RF part of the plate circuit are completely shielded except for one small opening. This opening is the entry for the adjustable pick-up loop which couples the plate tank power into the directional coupler and hence the antenna. Figure VIII-4 is a rear view showing component arrangement. Figure VIII-5 illustrates the plate tank section as seen from above for a 50 Mc/s unit. Figure VIII-6 shows the bottom view of the 4-1000A sockets with associated grid drive circuits for the 50 Mc/s transmitter, and the fuse and main circuit breaker panel as well as parts of the bottom of the 4-1000A chassis, seen from the rear of the cabinet with the amplifier section swung forward into the servicing position. The Interlock and Protective circuits are described in connection with the Control Unit since the two operate together.

4. DRIVER AND DRIVER POWER SUPPLY

The Driver is a two-stage linear amplifier. The first stage is a 2E26 operated class A. A potentiometer, labelled "Output Level", varies the screen voltage and thereby permits control of the stage gain. The grid and plate circuits are tuned and link coupled. The second stage design depends on the frequency of operation, one model applying to frequencies below about 60 Mc/s, another having been designed for 74 Mc/s. A complete schematic diagram of the Driver, including both forms of the second stage, is presented in Figure VIII-7; the power supply is shown in Figure VIII-8.

The second stage, for frequencies below 60 Mc/s, is a pair of 6146's in push-pull operated class AB2. (For frequencies above 60 Mc/s, the second stage is a single 4X150A operated class AB2.) Link coupling is employed and the second stage is neutralized. All elements of the tubes, with the exception of the second stage plate current, are metered by means of a meter switch and a 0-50 microampere meter. Second stage plate current is metered with a separate 0-300 milliampere meter. In some models there is a relay which is used to break the cathode lead of the 2E26 for keying purposes.

The Driver Power (Figure VIII-8) Supply is of conventional design. (The 4X150A model Driver required 800 volts for the plate, in contrast to the 600 volts required for the 6146's of the lower frequency model, and therefore employs a capacitor input filter. The 4X150A model Power Supply also furnishes 110 volt A-C to operate the blower in the 4X150A air system.)

The lower frequency model furnishes approximately 60 watts of RF power into a 50 ohm load. The higher frequency model furnishes approximately 80 watts of drive into a 50 ohm load. The higher driving power is required for the 4-1000A's as their maximum operating frequency is approached. Any source of RF energy at the operating frequency, which supplies about 2 volts rms to a 50 ohm load, is sufficient to drive the Driver. The multipliers and exciters are discussed in Appendix IX.

5. CONTROL UNIT AND PROTECTIVE CIRCUITS

The Control Unit, used in combination with the Interlock and Protective Circuits of the Power Amplifier cabinet, is described in Figures VIII-9 to VIII-11. The functional block diagram of the complete system (Figure VIII-2) shows the role of the control circuits in relation to the rest of the transmitter.

The Overload circuit interrupts the A-C power supplied to the high voltage supplies when the direct current flowing in the high voltage plate supply exceeds a predetermined amount -- usually about 1.2 amperes. However, it offers no protection against a short circuit in either of the main filter capacitors. When the Overload circuit is tripped, the Overload Reset circuit automatically commences operation, attempting four

Declassified in Part - Sanitized Copy Approved for Release @ 50-Yr 2014/06/09 : CIA-RDP81-01043R003000180001-4

Declassified in Part - Sanitized Copy Approved for Release @ 50-Yr 2014/06/09 : CIA-RDP81-01043R003000180001-4

times within two minutes after the overload to re-close the main A-C contactor. This automatic reset will in general correct a transmission failure caused by a temporary overload, such as might accompany lightning striking a nearby object. If the overload condition persists during the reset cycle, it becomes necessary for the transmitter operator to manually reset the system.

The SWR monitor turns the transmitted carrier off when reflected power from the antenna indicates an excessive standing wave ratio (SWR) on the transmission line. This is intended to protect the transmitter and also to avoid transmissions during periods when the accuracy of measurement of radiated power is under some doubt. High SWR may be the result of weather conditions, ice, snow, rain, or it may be the result of a failure in some component of the antenna system. A portion of the reflected RF power is rectified by a crystal diode, called the "back diode", that is located in the directional antenna coupling unit. The voltage thus produced will be zero under conditions of perfect match and will increase with the degree of mismatch present. At an adjustable preset voltage, representing a standing wave ratio of about 2:1, a relay disables the transmitter and simultaneously starts a 4-RPH motor and cam. After a 15-minute interval, the relay is de-energized, and, depending upon whether conditions have changed, the transmitter will either return to operation or will again be disabled for another 15-minute cycle.

The Off-Air Alarm is triggered when the forward power fed to the antenna transmission line falls below a preset level, usually 75 percent of the desired level. The output of the "forward power" diode in the directional coupling unit is a voltage representing the output power level of the transmitter. When this voltage drops to the predetermined level, due to a malfunction of some component of the transmission system, an alarm sounds and the carrier indicator lamp on the control unit goes out.

In the Recording Circuit the output voltages from the "forward" and "back" power diodes of the Micromatch coupler are amplified and fed during alternate periods of 7½ minutes length to a single 0-1 ma Esterline Angus graphic recorder. Adjustable voltages from the Off-Air Alarm and SWR Protection amplifiers are used for this purpose. Switching circuits permit calibration of the recording in terms of the readings of the directional coupler indicator in the Power Amplifier rack. The recordings are used as a means of standardizing the strength of signals received from the transmitter to one arbitrary level of transmitted power. A typical record is shown in Figure VIII-12.

6. BREAK KEYER AND IDENTIFICATION KEYER

Two keyers are used in the system, the Break Keyer (Figure VIII-13) to make the two-minute noise break on the hour and half hour, and the Identification Keyer (Figure VIII-14) to send the call sign at the beginning of the break. The two-minute half hourly break is required

in the receiving operations this transmitter is meant to satisfy. A programming clock controls both keyers by a pulse sent every half hour. This pulse operates a time constant circuit which opens the keying line for two minutes and starts the identification keyer which repeats the call letters twice in a period of twelve seconds.

Declassified in Part - Sanitized Copy Approved for Release @ 50-Yr 2014/06/09 : CIA-RDP81-01043R003000180001-4

Declassified in Part - Sanitized Copy Approved for Release @ 50-Yr 2014/06/09 : CIA-RDP81-01043R003000180001-4

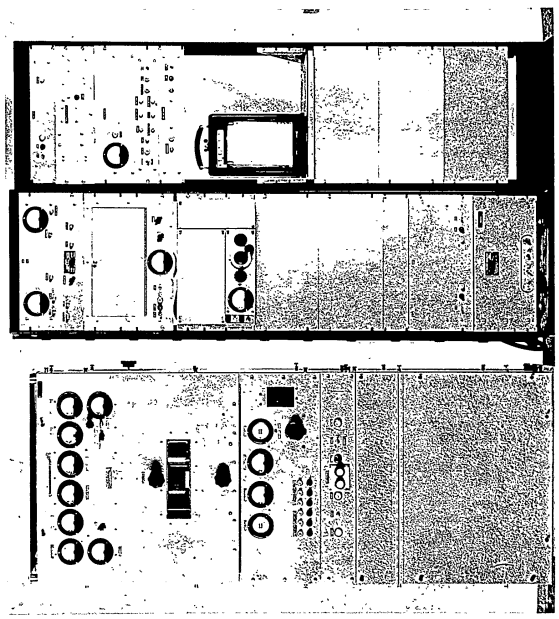

PHOTOGRAPH OF COMPLETE SYSTEM IN A TYPICAL INSTALLATION

FIGURE VIII-1

Declassified in Part - Sanitized Copy Approved for Release @ 50-Yr 2014/06/09 : CIA-RDP81-01043R003000180001-4

Declassified in Part - Sanitized Copy Approved for Release @ 50-Yr 2014/06/09 : CIA-RDP81-01043R003000180001-4

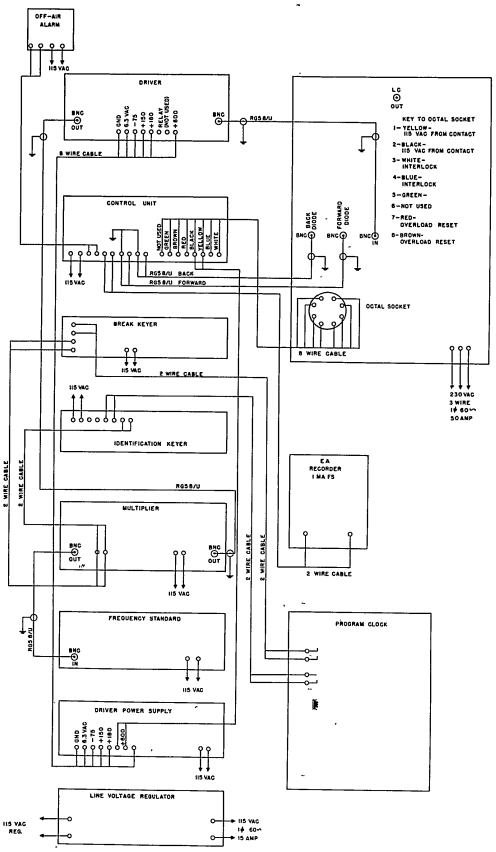

BLOCK DIAGRAM OF COMPLETE TRANSMITTER SYSTEM

FIGURE VIII-2

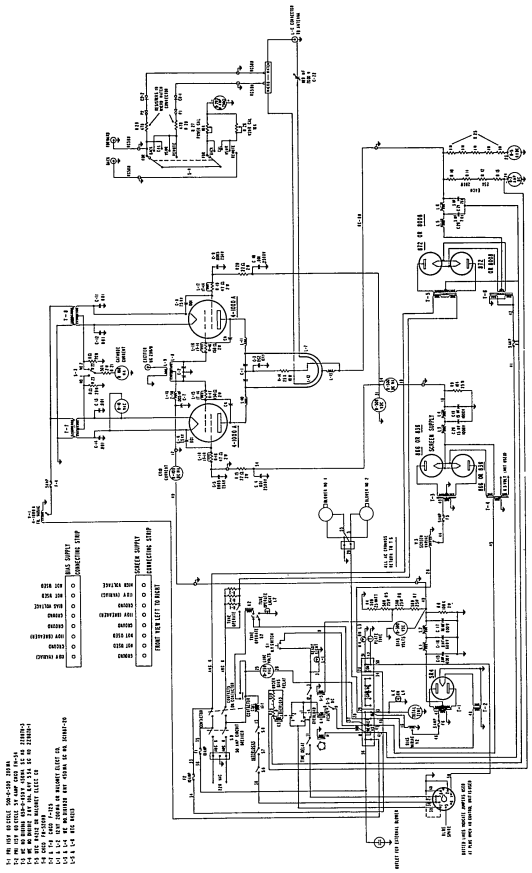

SCHEMATIC WIRING DIAGRAM OF COMPLETE POWER AMPLIFIER (INCLUDING POWER SUPPLIES, PROTECTIVE DEVICES, ETC.)

FIGURE VIII-3

Declassified in Part - Sanitized Copy Approved for Release @ 50-Yr 2014/06/09 : CIA-RDP81-01043R003000180001-4

Declassified in Part - Sanitized Copy Approved for Release @ 50-Yr 2014/06/09 : CIA-RDP81-01043R003000180001-4

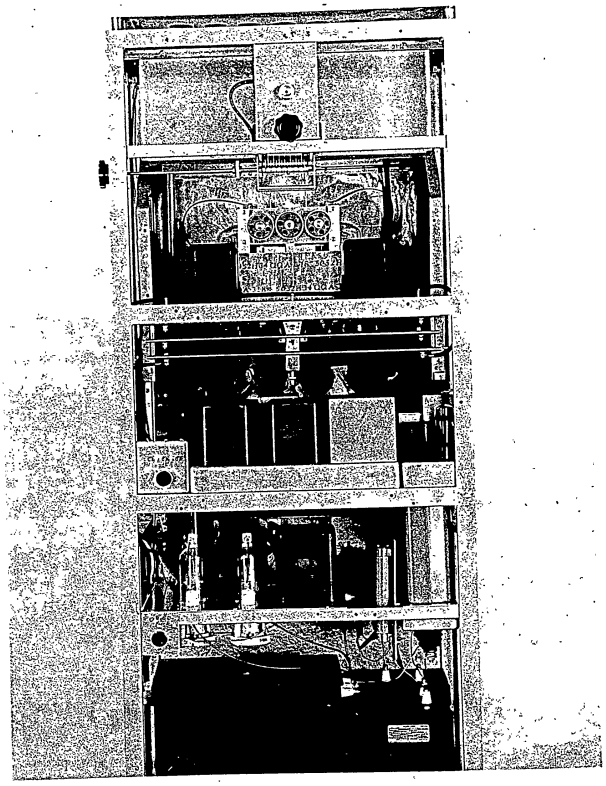

PHOTOGRAPH OF REAR OF POWER AMPLIFIER CABINET WITH PANELS REMOVED
FIGURE VIII-4

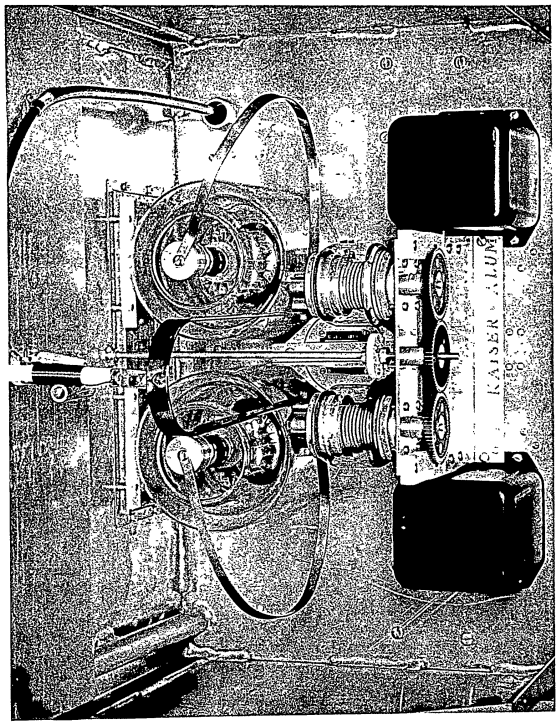

PHOTOGRAPH OF PLATE TANK COMPARTMENT OF 50Mc AMPLIFIER
FIGURE VIII-5

Declassified in Part - Sanitized Copy Approved for Release @ 50-Yr 2014/06/09 : CIA-RDP81-01043R003000180001-4

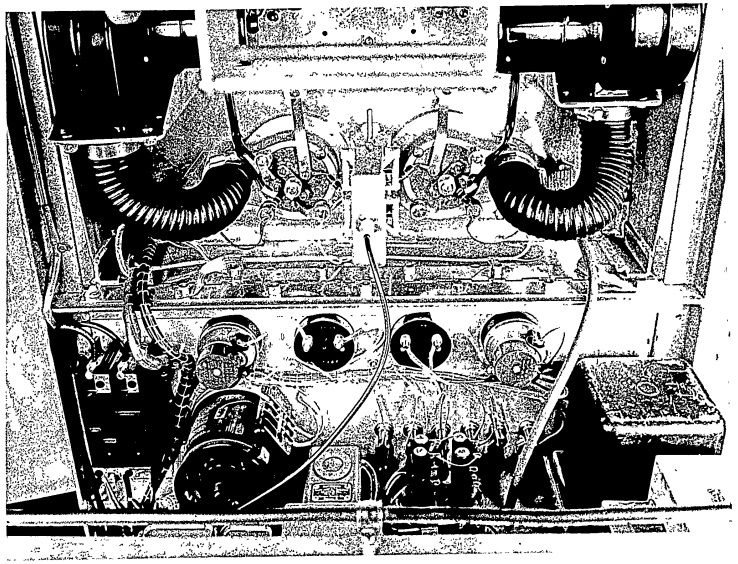

PHOTOGRAPH OF BACK OF FUSE AND BREAKER PANEL IN POWER AMPLIFIER
FIGURE VIII-6

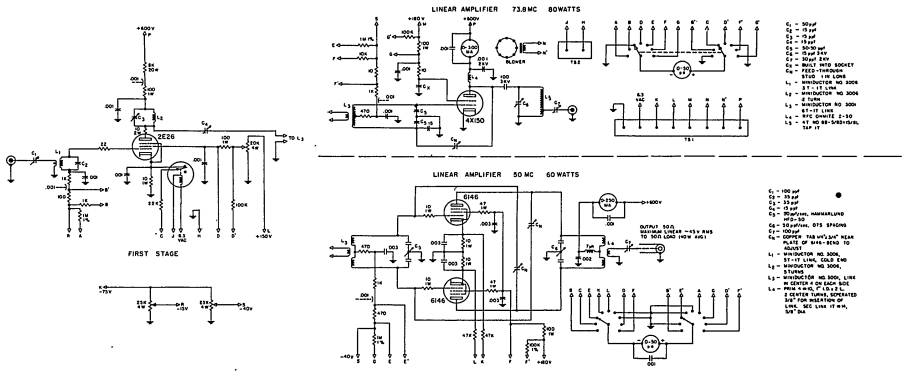

SCHEMATIC WIRING DIAGRAM OF DRIVER
FIGURE VIII-7

Declassified in Part - Sanitized Copy Approved for Release @ 50-Yr 2014/06/09 - CIA-RDP81-01043R003000180001-4
Declassified in Part - Sanitized Copy Approved for Release @ 50-Yr 2014/06/09 - CIA-RDP81-01043R003000180001-4

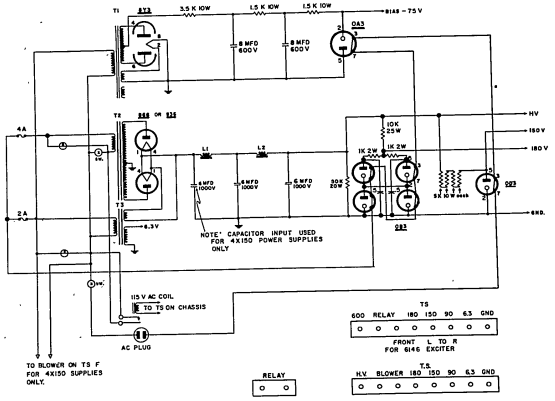

SCHEMATIC DIAGRAM OF DRIVER POWER SUPPLY

FIGURE VIII-8

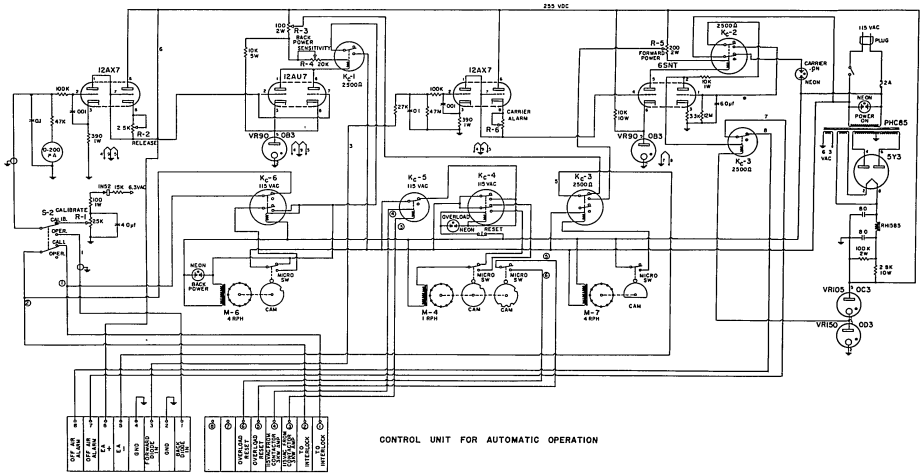

CONTROL UNIT FOR AUTOMATIC OPERATION

SCHEMATIC WIRING DIAGRAM OF CONTROL UNIT

FIGURE VIII-9

Declassified in Part - Sanitized Copy Approved for Release @ 50-Yr 2014/06/09 - CIA-RDP81-01043R003000180001-4
Declassified in Part - Sanitized Copy Approved for Release @ 50-Yr 2014/06/09 - CIA-RDP81-01043R003000180001-4

Declassified in Part - Sanitized Copy Approved for Release @ 50-Yr 2014/06/09 : CIA-RDP81-01043R003000180001-4

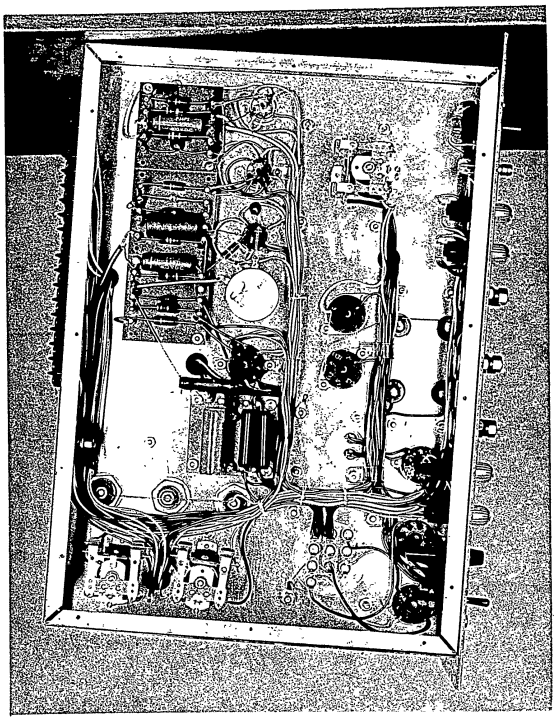

PHOTOGRAPH OF THE CONTROL UNIT FROM THE BOTTOM
FIGURE VIII-10

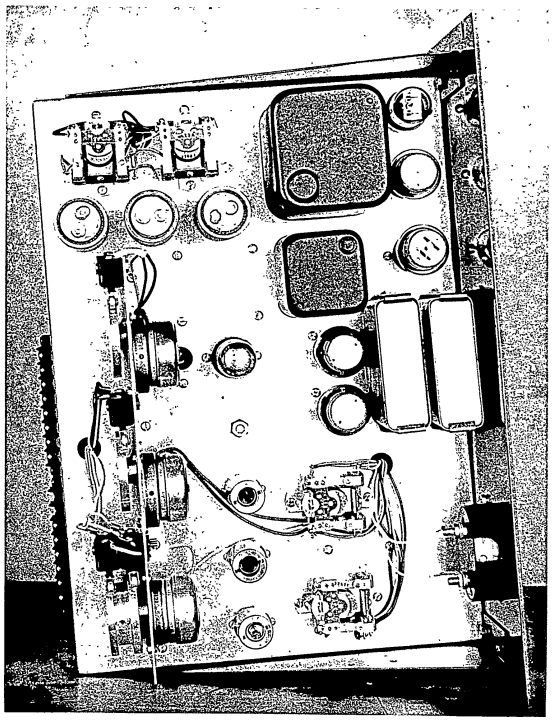

PHOTOGRAPH OF CONTROL UNIT FROM THE TOP
FIGURE VIII-11

Declassified in Part - Sanitized Copy Approved for Release @ 50-Yr 2014/06/09 : CIA-RDP81-01043R003000180001-4

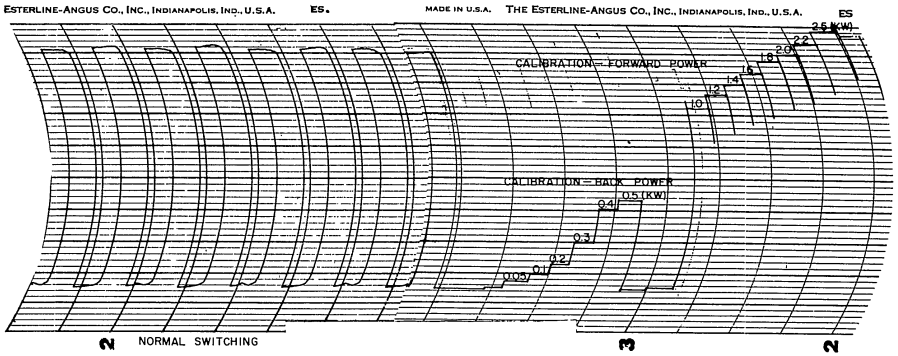
ESTERLINE-ANGUS CO., INC., INDIANAPOLIS, IND., U.S.A.
MADE IN U.S.A.
THE ESTERLINE-ANGUS CO., INC., INDIANAPOLIS, IND., U.S.A.
CALIBRATION — FORWARD POWER
CALIBRATION — BACK POWER
0.5 (KW)
NORMAL SWITCHING

EXAMPLE CHART RECORDING AND CALIBRATION
FIGURE VIII-12

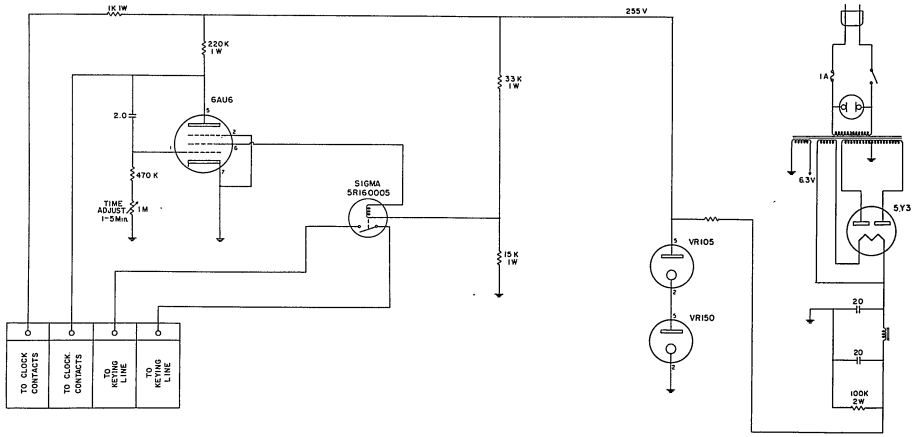

SCHEMATIC DIAGRAM OF THE BREAK KEYER
FIGURE VIII-13

Declassified in Part - Sanitized Copy Approved for Release @ 50-Yr 2014/06/09 : CIA-RDP81-01043R003000180001-4
Declassified in Part - Sanitized Copy Approved for Release @ 50-Yr 2014/06/09 : CIA-RDP81-01043R003000180001-4

Declassified in Part - Sanitized Copy Approved for Release @ 50-Yr 2014/06/09 : CIA-RDP81-01043R003000180001-4

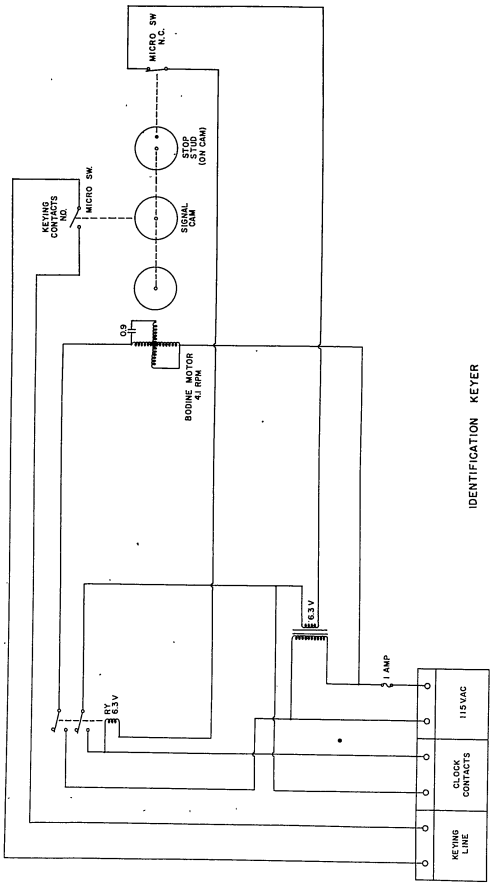

SCHEMATIC WIRING DIAGRAM OF THE IDENTIFICATION KEYER

FIGURE VIII-14

APPENDIX IX

STABLE FREQUENCY CONTROL FOR NARROW-BAND RECORDING RECEIVER AND TRANSMITTER

Peter G. Sulzer

PART I - ONE-MEGACYCLE HIGH-STABILITY FREQUENCY STANDARD

1. INTRODUCTION

The narrow-band recording receiver and transmitter described in Appendices VII and VIII require, for satisfactory stability in recording, frequency control having stability of the order of one part in 10^8 per day.

The oscillator to be described, which employs inexpensive, commercially-available components, has shown a maximum frequency change of a few parts in 10^9 per day, and is expected to have a stability of one part in 10^8 or better in two weeks.

High-frequency stability can be obtained by using a crystal unit to control the frequency of an oscillator. Such a crystal-controlled oscillator can be considered to have three elements: the crystal unit itself, an amplifier or negative-resistance device to supply the losses in the crystal unit and deliver power to a load, and an amplitude control of some kind. The oscillator designer attempts to choose and connect these elements in such a manner that frequency changes caused by tube or component instability are minimized, so that the ultimate stability is nearly that of the crystal itself.

It is understood that any phase shift in the amplifier must be offset by a corresponding, but opposite, phase shift in the crystal unit, thus producing a frequency change. Such a phase shift can be caused by an actual reactance change, resulting, perhaps, from a tube-capacitance change or a drift in the value of an inductor or a capacitor. It can be caused by a variation in the magnitude of a voltage gain, producing a Miller-effect-capacitance change. Phase shifts can also be produced by the electronic component of the input capacitance of a tube, by transit time, and by the effects of non-linearity.

At least three general types of techniques have been used to decrease the effects of amplifier variations: Low reactances can be placed across the amplifier terminals, effectively decoupling the resonator from tube-capacitance changes;[1] phase shifts can be decreased by the use of inverse feedback;[2] or the resonator can be driven by an external oscillator whose frequency is adjusted to resonance by means of a servo system.[3]

Declassified in Part - Sanitized Copy Approved for Release @ 50-Yr 2014/06/09 : CIA-RDP81-01043R003000180001-4

Declassified in Part - Sanitized Copy Approved for Release @ 50-Yr 2014/06/09 : CIA-RDP81-01043R003000180001-4

2. MEACHAM BRIDGE-OSCILLATOR

The second method was chosen here because excellent results can be obtained with a comparatively simple circuit. Although good results can be obtained with the first method, the need for a separate amplitude control usually requires the use of three or more tubes because the amplitude control required for constant crystal drive normally contains a feedback amplifier and rectifier for automatic gain control. The third method can provide extremely high performance, but is too complicated for consideration as a simple oscillator.

The familiar Meacham bridge-oscillator, which can be classified under the second method, is shown in Figure IX-1(a). It is convenient to study the operation of the bridge in terms of positive and negative feedback.[4] Here negative feedback occurs through R_2 and the crystal resistance R_1, while positive feedback occurs through the lamp resistance R_3 and resistor R_4. If the amplifier has sufficient gain, oscillation will start at the frequency of minimum degeneration, which is nearly the series-resonant frequency of the crystal, and the lamp resistance will increase with the amplitude of oscillation until the bridge is nearly balanced. When an equilibrium is reached, the bridge attenuation must equal the amplifier gain.

Considering a small amplifier phase angle ϕ,

$$\phi_f \approx \frac{\phi}{1 + A\beta} = \frac{\phi}{1 + A\,\dfrac{R_1}{R_1 + R_2}},$$

where ϕ is the phase angle of the amplifier without feedback, ϕ_f is the phase angle with feedback, and β is the transmission through the negative-feedback path. Thus good phase stability requires a large voltage-gain A and a maximum transmission β. Unfortunately, however, there are practical limitations to the increase of β. With a given amplifier, the product $A\beta$ cannot be increased without increasing the crystal current or decreasing the lamp voltage, both of which are undesirable. The glass-enclosed, contoured AT-cut crystal chosen for the oscillator has a Q of 5×10^5 and a resistance of 20 ohms, but the crystal current must be kept below one milliampere. However, the A-1 switchboard lamp, which is a suitable amplitude-control element, requires at least 0.7 volt for proper operation. If a crystal current of 0.7 milliampere is specified, R_2 will be approximately 1000 ohms, and $\beta \approx 1/50$ with a 20-ohm crystal. If $A = 1000$, $A\beta \approx 20$, and a 20-fold reduction in effective phase shift is obtained.

Studies of several amplifier designs have shown that sufficient voltage gain for good amplitude stability cannot be obtained with only

one stage. The crystal current must be kept constant because the resonant frequency is a function of current. With two similar stages the voltage gain is square, while the shift is at most doubled, permitting sufficient gain without greatly increased phase shift. Although the use of three stages might appear to be even better by similar reasoning, the requirement for at least three tuned circuits leads to serious difficulties in controlling the sign of the feedback at frequencies far removed from the operating frequency, with a tendency toward parasitic oscillation.

A two-stage amplifier with a voltage gain of 1000 exhibited a maximum phase shift of $\pm$ 10 degrees over a two-to-one supply-voltage range. Using the bridge discussed above, $A\beta \approx 20$, the maximum expected phase change with feedback becomes $\pm$ 0.5 degree. The crystal must experience the same phase shift, and its frequency will be pulled accordingly. A simple calculation shows that if $Q \approx 5 \times 10^5$, the corresponding fractional frequency change is $\pm 1 \times 10^{-8}$. Thus, with reasonably constant supply voltages, the short-term frequency stability can be expected to be somewhat better than this. The long-term stability will depend on these and other factors, however, including the drift of the crystal resonator itself.

Figures IX-1(b) and (c) show the effects of plate-supply and heater-supply variations on the frequency of the oscillator. Figure IX-2 shows the performance of the one-megacycle oscillator over a 24-hour period. The record between the arrowheads shows that the frequency varied less than $\pm$ 2×10^{-9}. The other three records, which are better, were produced by high-stability oscillators using special, 100-kilocycle, GT-cut crystal units.

Figure IX-3 is a schematic diagram of the oscillator (Model A), which employs two type 6AH6 pentodes. This tube type was chosen because it has a high transconductance and a long effective life. Direct-current stabilization, which is accomplished by returning the control grid to a positive supply and using a high value of cathode-bias resistor, helps stabilize the operating point. A tuned circuit including L_1 is used for interstage coupling, while a tuned transformer is used at the output. Although a tuned input transformer would provide more gain, it would be difficult to obtain proper control of the phase shifts in the system. To this end, L_1 has been designed with a high Q, and T_1 with a low Q to decrease the gain rapidly with minimum phase shift outside the passband of the amplifier. The shunting resistor R_5 is also used to keep the phase shift under 180 degrees when the loop gain exceeds unity. This decreases the effective Q of the crystal unit approximately 10 per cent, which is not considered important in the present application. Coil-design data are given in the accompanying paragraphs.

A frequency adjustment of $\pm$ 5 cycles is provided by the variable capacitor C_1. The initial frequency adjustment is made with C_2. If the crystal is series-resonant 20 cycles or more below one megacycle, a capacitor C_2 can be used here. If the crystal unit is higher in frequency,

Declassified in Part - Sanitized Copy Approved for Release @ 50-Yr 2014/06/09 : CIA-RDP81-01043R003000180001-4

Declassified in Part - Sanitized Copy Approved for Release @ 50-Yr 2014/06/09 : CIA-RDP81-01043R003000180001-4

however, an inductor may be required. The crystal unit has an inductive reactance of 10 megohms, and therefore a series reactance of 20 ohms is required to produce a frequency shift of one cycle. The value of capacitance or inductive reactance can be computed accordingly. The inductor, if required, should have high stability and a high Q; a design similar to that of L_1 should be used (see coil data).

Figure IX-4 is a schematic diagram of the oscillator (Model B). The oscillator circuitry is essentially the same in both Models A and B, except for minor modifications in component values. In Model B a buffer amplifier has been inserted between the oscillator circuit and the 1 Mc/s output terminal, and the crystal-oven temperature control circuit has been modified to use a temperature-sensitive bridge as the oven heater current control in place of the thermostat and relay used in Model A. The Model B oven has shown improved stability in laboratory checks of the oscillator output frequency.

3. OVEN DESIGN

The AT-cut crystal should be maintained at a specified, constant temperature to obtain the best frequency stability. The oven used in this oscillator is of the single-stage type, with termperature control provided by a 50-degree centigrade mercury thermostat. Figure IX-5 and IX-6 show the mechanical details of the oven, whose principal feature is the use of a Dewar flask to isolate the controlled chamber from outside temperature changes. Consequently the average-power requirement, 0.4 watt at a temperature difference of 25°C, is very low for an oven of this size.

Detailed performance data cannot be given for the oven itself, as tests have not been completed. It can be stated, however, that with the specified crystal, frequency changes due to oven cycling were less than 10^{-9}, and that the normal (10°C) laboratory-temperature changes were apparently not reflected in crystal-temperature changes.

4. ADJUSTMENT

Proper alignment of the oscillator requires that the tuned circuits L_1 and T_1 be adjusted to exactly one megacycle. This is best accomplished by opening R_2, shorting R_4, and applying a one-millivolt, one-megacycle signal across R_5. One volt should appear across R_3 when the trimmers across L_1 and T_1 are tuned to resonance. The oscillator can then be restored to its original condition, and R_4 should be increased until an output of 0.7 volt is produced. If the output voltage decreases as R_4 is increased, the secondary connections of T_1 should be interchanged.

The amplitude stability of the oscillator should be checked by varying the plate supply from 150 to 300 volts. The output voltage should vary less than 1 percent over this range.

It will take approximately 12 hours for the oven to reach its normal operating temperature of 50°C. After this period it may be necessary to readjust R_4 because the crystal unit resistance is a function of temperature.

Frequency-stability measurements can be made three hours after the oven duty cycle becomes constant. The effects of supply-voltage variations should be approximately as shown in Figure IX-1(b) and (c). Long-term tests with constant supply voltages should be made against WWV or some other time or frequency standard.

It should be pointed out that a buffer amplifier should be used to isolate the oscillator from the effects of load variations. A satisfactory buffer consists of a well-shielded pentode amplifier, preferably with a tuned plate circuit if the maximum output voltage is desired.

5. COIL DATA

L_1: The inductor contains two windings in parallel, each consisting of 28 turns of 90-44 Litz wire, and each covering one-half of the available space on a T-1060-07-A powdered-iron toroidal form. The windings progress in opposite directions so that adjacent leads are connected together, placing high-potential points on the ends of a diameter of the toroid. The Q of the coil with its silvered-mica capacitor is 280 at 1 megacycle.

T_1: The primary contains 120 turns of No. 30 Formex-insulated wire. The secondary contains 14 turns of the same type of wire. Both windings are placed on a T-1060-07-R_2 powdered-iron toroidal form, with the secondary wound over the low-potential end of the primary. The Q of the primary is 25 at 1 megacycle.

As an aid to the duplication of the oscillator, it can be stated that the crystal resonator was supplied by The James Knights Company, Sandwich, Illinois. The toroidal coil forms were supplied by the Lenkurt Electric Sales Company, San Carlos, California. The Litz wire was supplied by the New England Electrical Works, Inc., Lisbon, New Hampshire; and the mercury thermostat was supplied by the Precision Thermometer and Instrument Company, 1434 Brandywine Street, Philadelphia, Pennsylvania. It should also be stated that the mention of these manufacturers does not constitute a specific endorsement of their products by the National Bureau of Standards. These particular components were used because they were available when the oscillator was built. It is quite probable that the products of other manufacturers would be equally satisfactory.

Declassified in Part - Sanitized Copy Approved for Release @ 50-Yr 2014/06/09 : CIA-RDP81-01043R003000180001-4

Declassified in Part - Sanitized Copy Approved for Release @ 50-Yr 2014/06/09 : CIA-RDP81-01043R003000180001-4

PART II - FILTER-TYPE EXCITER

1. DESCRIPTION

The exciter produces an output at 49.8 megacycles from a one-megacycle input. The percentage accuracy of the output frequency is the same as that of the input frequency. The unit furnishes an output of at least one volt to a 50 ohm load.

A block diagram is shown in Figure IX-7. Reference to the schematic diagram of Figure IX-8 will show that the one-megacycle input is amplified and multiplied to 50 megacycles in four stages, V_1 - V_4. A double-tuned interstage is used at 5 megacycles to suppress spurious frequencies. The one-megacycle input is also divided by five in V_6, which is a locked-oscillator cathode-coupled frequency divider. The 200-kilocycle output of V_6 is mixed with the 50 megacycle output of V_4 in a balanced mixer, V_5. The difference frequency, 49.8 megacycles, is filtered in the crystal circuit associated with L_7 and L_8, and amplified by V_7. A second crystal filter is associated with the output amplifier V_8.

The shielding and decoupling have been designed to minimize feed-through at other than the desired frequency. When the balanced mixer and the two crystal filters are adjusted properly, all spurious outputs are at least 100 decibels below the 49.8 megacycle output.

2. OPERATION

The exciter should be connected to a source capable of supplying at least two volts at one megacycle to a high-impedance load. After a suitable warm-up period, the test-point microamperes should be checked with the meter provided on the panel. The normal indication for each point should be determined when the equipment is functioning properly with relatively new tubes. A subsequent deviation of more than ±20 percent from these values indicates possible trouble, and the tube associated with the stage in question should be checked.

In aligning the equipment, L_1, L_2, L_3, L_4, and L_5 should be adjusted to produce the maximum voltage at each indicated frequency. It is desirable to use a tuned voltmeter such as a grid-dip oscillator in the non-oscillating condition for this purpose; if a selective voltmeter is not used, a response may be obtained at the wrong frequency.

The frequency divider V_6 is adjusted by tuning L_6 to 200 kilocycles. A beat will be detected with headphones at the cathode test point of V_6 if the divider is not locked to the one-megacycle input. The trimmer capacitor should be set to the middle of the range over which the beat disappears.

The remaining tuned circuits are best adjusted by connecting a sensitive radio receiver to the output terminal through an 80-decibel attenuator. Tuned circuits L_7 through L_{11} should be adjusted for the maximum output at 49.8 megacycles. At this point it is desirable to

be certain that all of the shields are fastened securely. The receiver should then be tuned to 50.0 megacycles and the potentiometer in the cathode of V_5, the type 12AV7 balanced mixer, should be adjusted to produce the minimum output.

The receiver should then be tuned to 50.2 megacycles, and the two 1-7 micromicrofarad capacitors associated with the crystal filters should be adjusted to produce minimum output. It may be necessary to decrease the attenuation at the receiver input tc obtain sufficient sensitivity.

After following this procedure it is desirable to check the magnitudes of all spurious outputs with respect to the 49.8 megacycle signal. Some readjustment may be required to keep them all 100 decibels down.

3. SERVICING

The servicing of the equipment should consist principally of the replacement of defective tubes. The adjustments of most of the tuned circuits are not critical, and should not require attention when tubes are replaced. This does not apply to the cathode potentiometer of V_5, which must be readjusted whenever V_5 is replaced. It is also desirable to check this potentiometer and the 1-7 micromicrofarad crystal-filter trimmer capacitors at intervals of two or three weeks.

PART III - PHASE-LOCKED-OSCILLATOR EXCITER

1. DESCRIPTION

The phase-locked-oscillator exciter produces an output of approximately one volt at 49.8 megacycles to a 50 ohm load. The percentage accuracy of the output frequency is the same as that of the one-megacycle input frequency.

A block diagram of the equipment is shown in Figure IX-9. The one-megacycle input is amplified and multiplied to 50 megacycles in four stages. The one-megacycle input is also divided by five in a locked oscillator, producing a frequency of 200 kilocycles, which is used as a reference. A crystal-controlled oscillator with a reactance tube operates at 49.8 megacycles and drives two buffer amplifiers, one of which supplies power to the external load. The other buffer amplifier excites a pentagrid mixer which also receives an input at 50 megacycles. The difference frequency at the output of the mixer is compared with the 200-kilocycle output of the frequency divider in a crystal-diode phase detector. If the frequencies are nearly the same, the slowly varying output of the phase-sensitive detector will excite the reactance tube and produce a phase lock between the mixer output and the 200-kilocycle reference frequency. If a phase lock is maintained, the crystal-oscillator frequency will be 49.8 times the input frequency.

Declassified in Part - Sanitized Copy Approved for Release @ 50-Yr 2014/06/09 : CIA-RDP81-01043R003000180001-4

Declassified in Part - Sanitized Copy Approved for Release @ 50-Yr 2014/06/09 : CIA-RDP81-01043R003000180001-4

The decoupling and shielding of the 49.8 megacycle oscillator, reactance tube, and amplifiers have been designed to prevent the feed-through of other frequencies. Although a 50 megacycle output can be detected, as well as various sums and differences of 50 megacycles and 200 kilocycles, these components are thought to be at least 100 decibels below the 49.8 megacycle output.

2. OPERATION

The exciter should be connected to a source capable of supplying at least two volts at one megacycle to a high-impedance load. After the equipment has been operating for a few minutes the test-point microamperes should be checked with the meter provided on the panel. The normal indication at each test point is given in the attached table. A deviation of more than ± 20 percent from these values indicates possible trouble, and the tube associated with the stage in question should be checked. The adjustment of the circuit associated with test-point 10 is discussed below.

The proper functioning of the equipment requires that two oscillators operate at the correct frequencies. The first of these, at 200 kilocycles, is checked by connecting headphones to the front-panel jack marked "Divider Test". The presence of a beat note at this point indicates that the oscillator is not operating at one-fifth of the input frequency, and requires that the compression-mica trimmer marked "200 Kc Osc" be adjusted to the middle of the range producing zero beat.

The second oscillator, which operates at 49.8 megacycles, is aligned with the aid of the meter and test-point 10, which indicates the output of the phase-sensitive detector. The output of the phase-sensitive detector will be a direct voltage only if the crystal oscillator is operating at exactly 49.8 times the input frequency. Under this condition the polarity and magnitude of the phase-detector output will depend upon the phase angle of the 200-kilocycle mixer output with respect to the output of the 200-kilocycle frequency divider. If these two voltages are 90 degrees out of phase, the phase-detector output will be nearly zero. For other phase angles, a positive or negative voltage will be obtained; the maximum value will occur at 0 and 180 degrees. Thus, if the microammeter is deflected one way or the other, the crystal oscillator must be locked to 49.8 megacycles, assuming an input at one megacycle. Adjustment of the tuning slug marked "49.8 Mc Osc" will move the test-meter indication through zero and over the range ± 10 microamperes if the system is locked. The best adjustment is that producing zero deflection.

If the 49.8 megacycle oscillator is so far out of adjustment that a phase lock is not obtained, the phase detector will be driven with two different frequencies, and its output will consist of the beat between these frequencies. Unfortunately this beat will not be indicated by the microammeter; however, it can be detected at the phone jack marked "Phase-Lock Test".

Thus, if the meter indicates zero for test-point 10, the system may be locked at the optimum adjustment, or it may be entirely out of synchronization. The headphones and test meter should be used together while making an adjustment.

3. SERVICING

The servicing of the equipment should consist principally of the replacement of defective tubes. The adjustments of most of the tuned circuits are not critical, and should not require attention when tubes are replaced. This does not apply to the two oscillators discussed above, which should be checked from time to time.

Figure IX-10 is a schematic diagram of the complete equipment.

PART IV - DIRECT MULTIPLIER EXCITER

For applications where the operating frequency is a direct multiple of the crystal frequency, a composite unit was constructed giving output at VHF. Figure IX-11 is a schematic diagram of the unit constructed for 36.0000 Mc/s transmission, which is used with the slight modification indicated in the crystal bridge circuit to obtain output at 36.0010 Mc/s for use as the receiver local oscillator signal.

REFERENCES

1. J. K. Clapp, "An Inductance-Capacitance Oscillator of Unusual Frequency Stability," Proc. I.R.E., pp. 356-359, March, 1948.

2. L. A. Meacham, "The Bridge-Stabilized Oscillator," Proc. I.R.E., pp. 1278-1295, October, 1938.

3. T. A. Pendleton, "Underneath Quartz-Crystal Resonators," Proc. I.R.E., pp. 1612-1614, November, 1953.

4. E. J. Post and H. F. Pit, "Alternate Ways in the Analysis of a Feedback Oscillator and its Application," Proc. I.R.E., pp. 169-174, February, 1951.

Declassified in Part - Sanitized Copy Approved for Release @ 50-Yr 2014/06/09 : CIA-RDP81-01043R003000180001-4

Declassified in Part - Sanitized Copy Approved for Release @ 50-Yr 2014/06/09 : CIA-RDP81-01043R003000180001-4

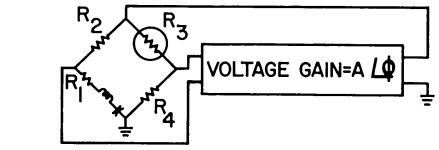

A

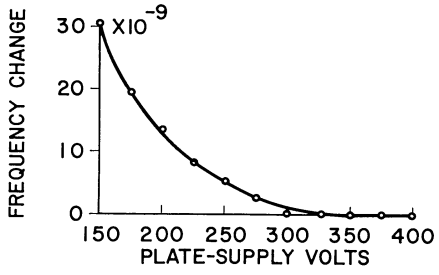

B

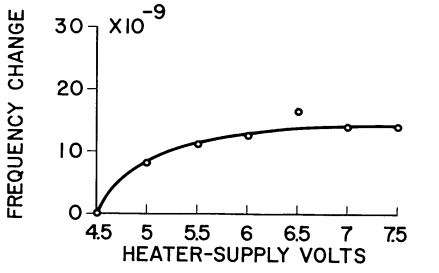

C

PERFORMANCE OF THE ONE-MEGACYCLE MEACHAM-BRIDGE OSCILLATOR WITH SUPPLY-VOLTAGE CHANGES.

FIGURE IX-1

Declassified in Part - Sanitized Copy Approved for Release @ 50-Yr 2014/06/09 : CIA-RDP81-01043R003000180001-4

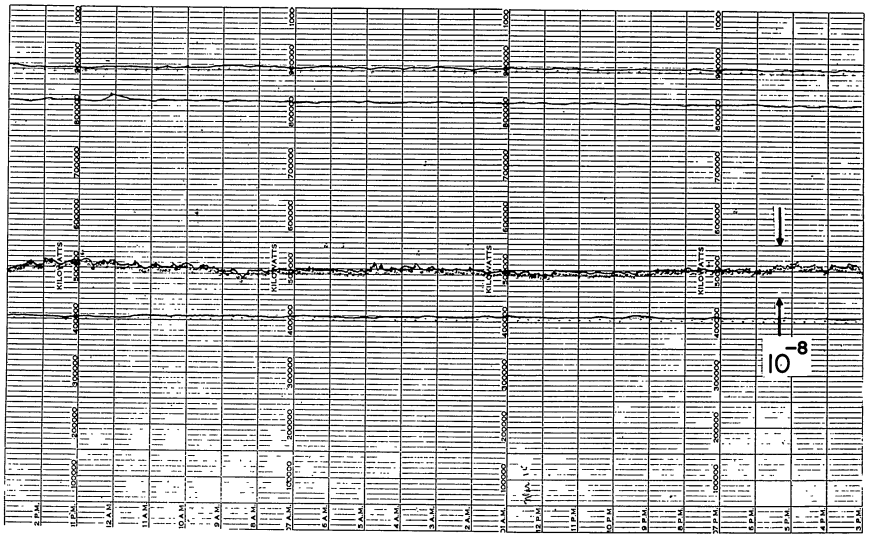

PERFORMANCE OF THE MODEL A ONE-MEGACYCLE OSCILLATOR OVER A 24-HOUR PERIOD

FIGURE IX-2

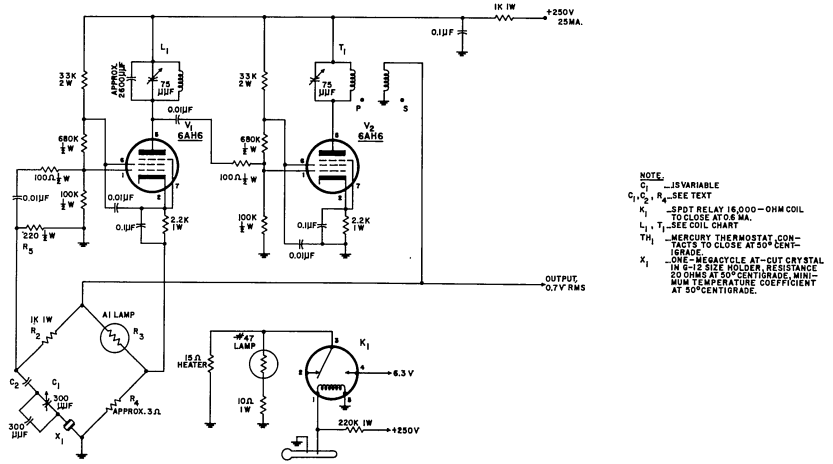

NOTE.
C_1 — IS VARIABLE
C_1, C_2, R_4 — SEE TEXT
K_1 — SPDT RELAY 16,000-OHM COIL TO CLOSE AT 0.6 MA. SEE COIL CHART
L_1, T_1 — SEE COIL CHART
TH_1 — MERCURY THERMOSTAT, CONTACTS TO CLOSE AT 50° CENTIGRADE.
X_1 — ONE-MEGACYCLE AT-CUT CRYSTAL IN G-12 SIZE HOLDER, RESISTANCE 20 OHMS AT 50° CENTIGRADE, MINIMUM TEMPERATURE COEFFICIENT AT 50° CENTIGRADE.

SCHEMATIC DIAGRAM OF THE ONE-MEGACYCLE MEACHAM-BRIDGE OSCILLATOR MODEL A

FIGURE IX-3

Declassified in Part - Sanitized Copy Approved for Release @ 50-Yr 2014/06/09 : CIA-RDP81-01043R003000180001-4
Declassified in Part - Sanitized Copy Approved for Release @ 50-Yr 2014/06/09 : CIA-RDP81-01043R003000180001-4

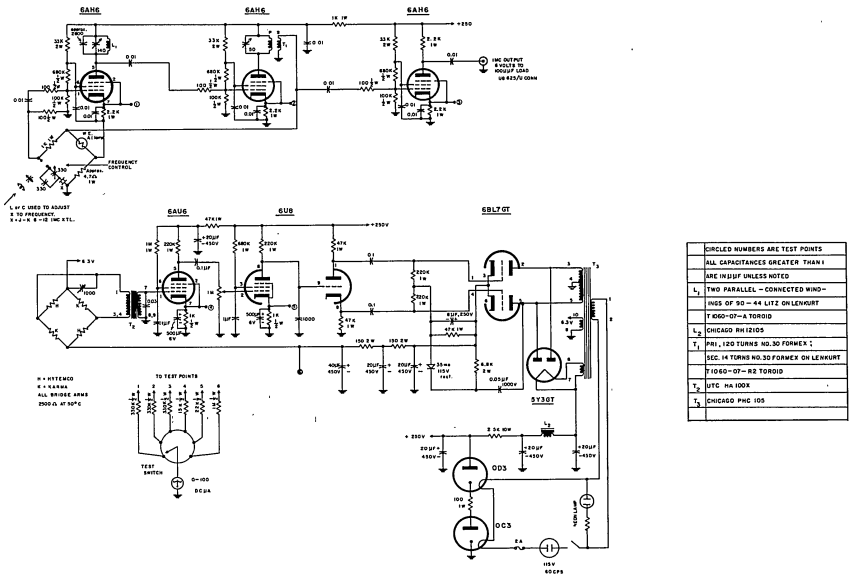

SCHEMATIC DIAGRAM OF THE ONE—MEGACYCLE MEACHAM—BRIDGE OSCILLATOR MODEL B

FIGURE IX-4

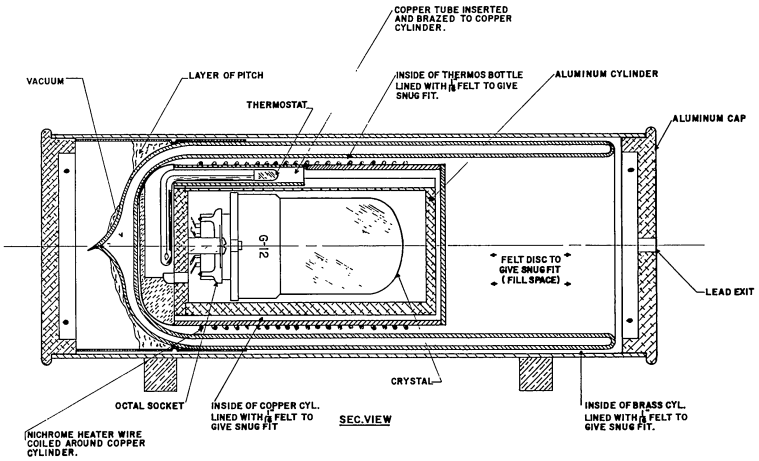
COPPER TUBE INSERTED AND BRAZED TO COPPER CYLINDER.
VACUUM
LAYER OF PITCH
THERMOSTAT
INSIDE OF THERMOS BOTTLE LINED WITH 1/4 FELT TO GIVE SNUG FIT.
ALUMINUM CYLINDER
ALUMINUM CAP
G-12
FELT DISC TO GIVE SNUG FIT (FILL SPACE)
LEAD EXIT
CRYSTAL
OCTAL SOCKET
INSIDE OF COPPER CYL. LINED WITH 1/4 FELT TO GIVE SNUG FIT
SEC. VIEW
INSIDE OF BRASS CYL. LINED WITH 1/4 FELT TO GIVE SNUG FIT.
NICHROME HEATER WIRE COILED AROUND COPPER CYLINDER.

CRYSTAL OVEN

NOTE:
CRYSTAL OCTAL SOCKET AND THERMOSTAT NOT SHOWN AS SECTION VIEW.

Scale
0 1 2

CROSS-SECTION VIEW OF CRYSTAL OVEN

FIGURE IX-5

Declassified in Part - Sanitized Copy Approved for Release @ 50-Yr 2014/06/09 : CIA-RDP81-01043R003000180001-4
Declassified in Part - Sanitized Copy Approved for Release @ 50-Yr 2014/06/09 : CIA-RDP81-01043R003000180001-4

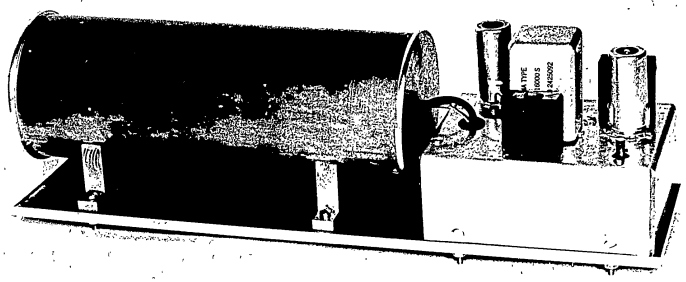

PHOTOGRAPH OF THE OSCILLATOR AND OVEN
FIGURE IX–6

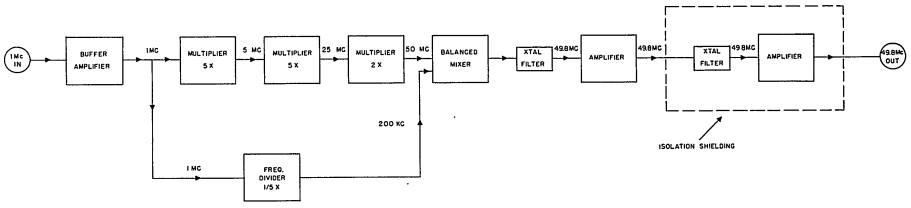

FILTER-TYPE EXCITER
FIGURE IX–7

Declassified in Part - Sanitized Copy Approved for Release @ 50-Yr 2014/06/09 : CIA-RDP81-01043R003000180001-4
Declassified in Part - Sanitized Copy Approved for Release @ 50-Yr 2014/06/09 : CIA-RDP81-01043R003000180001-4

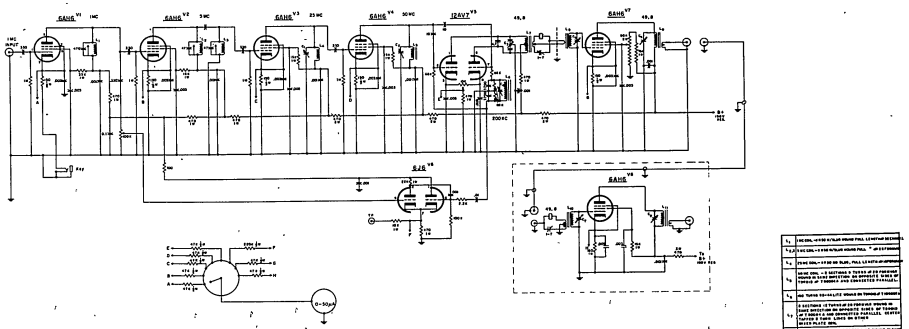

SCHEMATIC DIAGRAM OF FILTER-TYPE EXCITER
(MULTIPLIER & MIXER FOR 49.8 Mc MIXER)

FIGURE IX-8

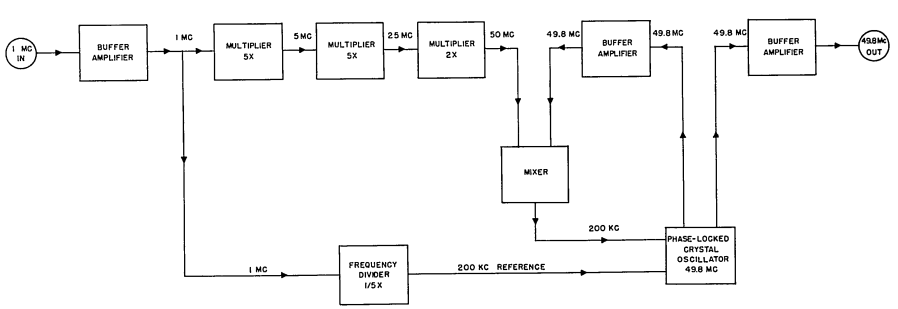

PHASE-LOCKED-OSCILLATOR EXCITER

FIGURE IX-9

Declassified in Part - Sanitized Copy Approved for Release @ 50-Yr 2014/06/09 : CIA-RDP81-01043R003000180001-4
Declassified in Part - Sanitized Copy Approved for Release @ 50-Yr 2014/06/09 : CIA-RDP81-01043R003000180001-4

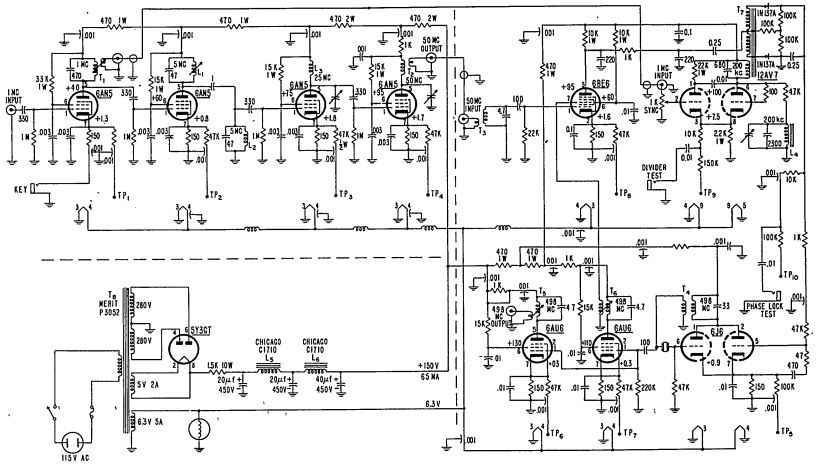

TEST POINT DATA

TEST POINT	1	2	3	4	5	6	7	8	9	10
MICROAMPERES	25	30	35	35	20	12	10	25	40	0

COIL DATA

T_1: PRI XR-50 FORM WOUND FULL WITH NO. 32 ENAM
SEC 5-TURN LINK
T_2 PRI: 7 TURNS NO. 16 ENAM. ON XR-50 FORM
SEC: 1-TURN LINK
T_3 PRI 1-TURN LINK
SEC 7-TURNS NO. 16 ENAM. ON XR-50 FORM
T_4 PRI: 4 TURNS NO. 16 ENAM. ON XR-50 FORM
SEC 1-TURN LINK
T_5 PRI 7 TURNS NO. 16 ENAM. ON XR-50 FORM
SEC: 1-TURN LINK
T_6: PRI: 7 TURNS NO. 16 ON XR-50 FORM
SEC: 2-TURN LINK
T_7: PRI: 50 TURNS NO. 34 ENAM. ON CROWLEY R4227 TOROID
SEC: 50 TURNS C.T. NO. 34 ENAM.
T_8: 280-280V C.T. AT 90 MA. DC, 5V AT 2A, 6.3V AT 5A.; MERIT P3052
L_1, L_2: XR-50 FORM WOUND FULL WITH NO 28 ENAM.
L_3: 14 TURNS NO. 16 ENAM. ON XR-50 FORM
L_4: 150 TURNS 90-44 LITZ ON LENKURT 1106007A TOROID
L_5, L_6 TH., 150 MA., CHICAGO C1710

SCHEMATIC DIAGRAM FOR PHASE-LOCKED-OSCILLATOR TYPE EXCITER

FIGURE IX-10

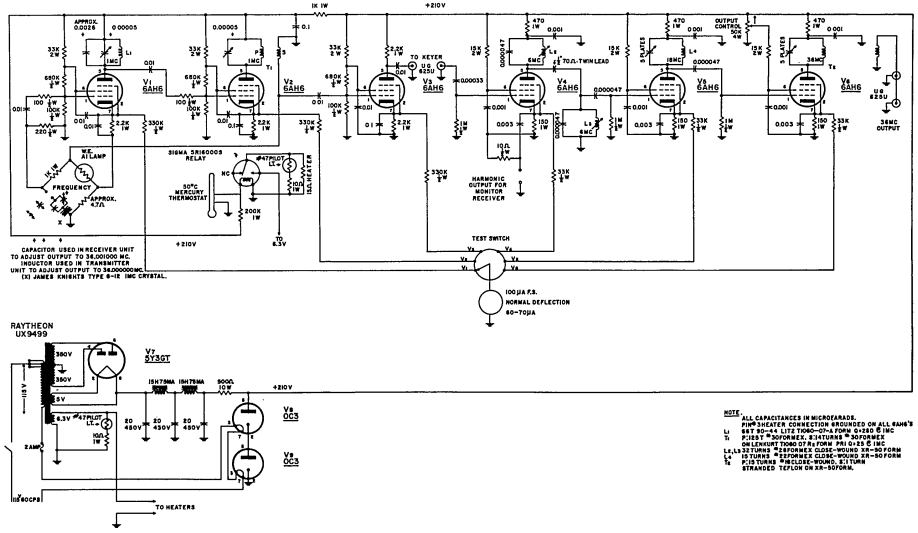

NOTE
ALL CAPACITANCES IN MICROFARADS.
PIN 9 HEATER CONNECTION GROUNDED ON ALL 6AH6'S
L_1: 6 T. #24 LITZ TOP-COUPLED TO L_2 @ 2 MC
T_1: PRI: 8 T. #24 LITZ TOP-COUPLED TO L_1 @ 2 MC
SEC: LENKURT 70060 OT R6 FORM PRI 01-25 @ 2 MC
L_2, L_3: 32 TURNS #30 FORMEX CLOSE-WOUND XR-50 FORM
L_4: 10 TURNS #30 FORMEX CLOSE-WOUND XR-50 FORM
T_2: P 10 TURNS #16 CLOSE-WOUND, 8 T. TURN STRANDED TEFLON ON XR-50 FORM.

SCHEMATIC DIAGRAM OF OSCILLATOR-MULTIPLIER CIRCUIT FOR 36.00 Mc OPERATION

FIGURE IX-11

Declassified in Part - Sanitized Copy Approved for Release @ 50-Yr 2014/06/09 - CIA-RDP81-01043R003000180001-4
Declassified in Part - Sanitized Copy Approved for Release @ 50-Yr 2014/06/09 - CIA-RDP81-01043R003000180001-4

Declassified in Part - Sanitized Copy Approved for Release @ 50-Yr 2014/06/09 : CIA-RDP81-01043R003000180001-4

APPENDIX X

SOLAR CYCLE INFLUENCE ON THE LOWER IONOSPHERE AND ON VHF FORWARD SCATTER

C. Ellyett* and Hope Leighton**

SUMMARY

A brief survey of published literature indicates that the electron concentration in the D region of the ionosphere changes with the solar cycle. Such changes should also be apparent in VHF forward scatter signal intensities.

Analyses have therefore been made of seven years results, at 49.8 Mc/s, from the Cedar Rapids, Iowa, to Sterling, Va., forward scatter path. (1243 km.) On an annual basis, it is found that the monthly median received signal intensity, for the noon and afternoon period only, follows the same trend as the mean monthly sunspot number. The effect is still more pronounced when comparison is made with magnetic disturbance indices.

When, however, the comparison with magnetic indices is made using a direct comparison in each 3-hour period, and eliminating long-term trends, no observable increase of the signal intensity is found as the magnetic conditions become disturbed. This is in sharp contrast to the behaviour of such circuits in auroral regions. Further analysis shows that a weak increase in signal intensity with rising magnetic index does occur if the analysis is confined to the mid-day period.

It is concluded, therefore, that any magnetic influence is smaller on middle than on high latitude scatter circuits, but an effect can be clearly discerned by studying the magnitude of the received signal through a solar cycle. The idea that the whole of a VHF forward scatter signal is due to reflection from meteor trails is thus disproved.

*University of Canterbury, Christchurch, New Zealand
Temporary Consultant, National Bureau of Standards, Boulder, Colorado

**National Bureau of Standards, Boulder, Colorado

Declassified in Part - Sanitized Copy Approved for Release @ 50-Yr 2014/06/09 : CIA-RDP81-01043R003000180001-4

Declassified in Part - Sanitized Copy Approved for Release @ 50-Yr 2014/06/09 : CIA-RDP81-01043R003000180001-4

1. INTRODUCTION

It is well known that the lower ionosphere, below the E region, can partially reflect or scatter both vertical and oblique radio signals. Several direct experiments at medium frequencies have shown the existence of low layer ionospheric stratification. [1-5] Reflection coefficients of the various layers, and the height variation of the layers with time, have been obtained.

Many reports have also now been made of determinations of the height of reflection of oblique transmissions at various frequencies ranging from VLF right through to VHF. [6-8] Although variations occur, the predominant night-time height, for signals transmitted by a lower ionospheric mechanism, is about 85-90 km.; with a fall during daylight hours to approximately 70 km. evident from VLF oblique and MF vertical experiments.

The close similarity of heights obtained on both vertical and oblique transmissions led Bailey, Bateman and Kirby [8] to suggest that the same region was operative in both cases. Wheelon [9] has reviewed the evidence for such a correspondence in some detail, and strongly concludes that the scatter regions are identical. Still more recently, Gregory [10] has shown that an almost perfect correspondence exists between VHF forward scatter height and time variations, as obtained by Pineo [11] in America; and vertical echoes at 1.75 Mc/s, measured in New Zealand. It can therefore be concluded with some certainty that the regions causing both vertical MF reflections and oblique VHF scattering are identical.

If this premise is accepted, then variations in the occurrence and strength of the ionospheric D-region during a solar cycle should be matched by variations in oblique VHF signal intensities. The first purpose of the present paper is to review any evidence for a solar cycle effect in the D-region ionization.

Nearly seven years of continuous signal intensity results are now available on the Cedar Rapids, Iowa, to Sterling, Va., VHF forward scatter circuit, operated at 49.8 Mc/s. by the National Bureau of Standards. Results over this period of time, covering, as they do, both a minimum and a maximum of the sunspot cycle, might be expected to show some solar influence, unless the causitive agent of the layers is entirely meteoric. It has already been established in America, [12-14] in Canada, [15] and in England, [16] as a result of off-great circle path studies of forward scatter, that meteors play a large part in scatter communication. Solar influences do seem necessary, however, to explain the simultaneous broad maxima observed on various paths through the midday and early afternoon period. [14] It seems worthwhile, therefore, to search the Cedar Rapids to Sterling results for a possible solar cycle influence.

Correspondence between long-term variations of the solar cycle and the magnetic K-index has long been known. If a solar influence is established for scatter circuits, they might also be expected to be sensitive to long-term magnetic variations.

Again, it has been known for several years, as a result of the work of Bailey, Bateman and Kirby [8] on Arctic region circuits, that increasing K-index, indicating increasing magnetic disturbance, causes an improvement in the scattered signal intensity. (This behaviour is contrary to that of other communication systems which use conventional refraction from the upper ionospheric layers. Reliability in periods of magnetic disturbance is one of the major advantages of scatter propagation in the Arctic.) It is therefore of considerable interest to see whether lower latitude scatter circuits are influenced in a similar manner by magnetic behaviour. This study concludes the paper.

2. SOLAR CYCLE INFLUENCE ON D-REGION IONIZATION

The D-region of the ionosphere has long been recognized as the principle region of absorption of electromagnetic waves. This has required the presence of at least a weak free-electron concentration.

For many years, in addition to the absorption evidence, discrete echoes at heights below the normal E region have been reported, but these reports have been most conflicting. [17] It is only in the last five years, largely through improved techniques, that unequivocal evidence has been obtained of partial reflection from stratified regions in the virtual height range lying between 50 and 100 km. [1-5] Such echoes, particularly for the main 85 km. layer, but sometimes also for the 70 km. region, persist throughout the day and night. [18] No evidence of a D-region solar cycle effect is therefore likely to be obtained from other than absorption data, solar radiation data, and experiments specifically carried out in the past five years to measure the low-layer stratification.

2.1. Absorption Data

It has been known for at least a decade that absorption follows the sunspot cycle. The absorption of HF radio waves passing through the D-region increases by a factor of approximately 1.5 between sunspot number zero and 100. [19] This work is supported by more recent absorption work at Dakar, French West Africa, [20] from which it is again concluded that the D-layer electron density increases proportional to the sunspot cycle.

(Absorption at VHF is very much reduced, compared to HF, and any 11-year cycle effect in absorption would almost certainly be masked by other variations. [19])

Declassified in Part - Sanitized Copy Approved for Release @ 50-Yr 2014/06/09 : CIA-RDP81-01043R003000180001-4

Declassified in Part - Sanitized Copy Approved for Release @ 50-Yr 2014/06/09 : CIA-RDP81-01043R003000180001-4

2.2. Solar Radiation Data

Direct rocket data on the very low electron concentrations likely to be encountered in the D-region do not yet appear to have been obtained, but there are now available many rocket measurements of the incident solar flux of both hydrogen Lyman-α radiation, and X-rays below 20A. Both these radiations penetrate into the D-region, creating ionization at least down to 75 km.

Values of the solar X-ray flux have been reported from one flight in 1949, three in 1952, three in 1953, and one each in 1955 and 1956. When the summary table [21] is compared with the sunspot curve a reasonable correspondence by years is apparent.

The evidence for a solar cycle variation of Lyman-α radiation is still quite weak. Some 12 intensity measurements are available, [21-22] comprising one in 1949, one in 1950, three in 1952, one in 1954, four in 1955, and two in 1956. The distribution of flights during the solar cycle is good, and a flux decline, agreeing with the cycle, is evident from 1949 through 1952. Values in 1955 and 1956 have increased with the solar cycle rise, but a change in instrumentation introduces some uncertainty into the values. This section can be summarized by stating that direct measurements of the radiations likely to be responsible for D-region ionization are in reasonable agreement with the hypothesis of a solar cycle invluence, without being conclusive.

2.3. Radio Data

Here evidence is meagre indeed. The few papers available on vertical incidence observations are as yet largely qualitative, although two recent papers give values for reflection coefficients. [3-5] Continued observation over a period of several years, with controlled parameters, should now be straightforward, and should give a direct answer to this problem.

Considering the three subsections together, there is quite strong evidence of a definite parallel movement of the electron concentration of the lowest regions of the ionosphere and the 11-year cycle of sunspot numbers.

3. SOLAR CYCLE INFLUENCE ON VHF FORWARD SCATTER

If solar cycle behaviour exerts an influence on the 85 km. region, it should also influence oblique VHF signal intensities, since such signals are observed to be scattered from this height.

Median signal intensity values on an hourly basis are available from the Cedar Rapids to Sterling oblique path from 1 January 1951 to 30 November 1957. Some 3-1/2 years of falling sunspot cycle are thus covered, including the minimum in April, 1954, followed by a steep rise to, or very near, the maximum at the end of 1957. The records of received intensity, following previous practice, [8] have been grouped into four separate median values for each month for the 3-hour periods centered about 00, 06, 12 and 18 hours local time at the path midpoint.

The strongest solar control during the day would be expected in the 3-hour period around noon. The graph of monthly median signal intensity covering this period is given in Fig. 1, together with the curve of final monthly sunspot numbers. Some general correspondence is apparent, but the forward scatter values are strongly influenced by a semi-annual period. To overcome the effect of this period, comparison of the two curves in Fig. 1 has been made for the same month in each year. At the months of peak signal intensity, as shown for June and December in Fig. 2, an excellent trend comparison is evident. Other months are not so clear-cut.

Twelve indices were next obtained from Fig. 1--one for each month of the year--by simply noting whether the trend between the two curves was in parallel or opposition as the same month was followed from year to year. Some cases occurred where the median signal intensity was the same value on the same month in adjacent years. These cases were excluded from the total. Proceeding in this manner for each month, and totalling the indices, it was found for all months combined that the trend was in opposition in 21 cases, and in parallel in 46. It has already been noticed on this circuit that the diurnal peak of the signal intensity is displaced to the afternoon side of noon. [8] Consequently it could be predicted that if the present method of analysis is significant the departure of the curves from random movement should be greatest in the noon period, present in the period centered on 18 hours, very weak in the 06 hour period, and lost--possibly by obscuring meteor activity--in the 00 hour period. The results of the analysis are given in Table 1, where it is evident that the exact behaviour predicted is occurring.

Table 1

Comparison of Trend Between Forward Scatter Signal Intensity and Sunspot Number

Three-hour period centered about	Similar-month movement of values 1951-1957		Percentage of total cases favouring parallel movement (random = 50%)
	In opposition	In parallel	
06 hrs.	25	27	52%
12 hrs.	21	46	69%
18 hrs.	22	39	64%
00 hrs.	32	23	42%

Declassified in Part - Sanitized Copy Approved for Release @ 50-Yr 2014/06/09 : CIA-RDP81-01043R003000180001-4

Declassified in Part - Sanitized Copy Approved for Release @ 50-Yr 2014/06/09 : CIA-RDP81-01043R003000180001-4

Twelve-month running averages of the signal intensity for each of the four daily periods examined are given in Fig. 3 (a). Some similarity is evident between the curves. The noon curve is always the strongest, and is the only one of the four which has not shown a fall from May 1956 to May 1957 when the sunspot curve has been rising sharply. Various tentative explanations could be suggested to account for the rough similarity of the four curves. Probably all that is worth saying in the present state of the information is that a change in the incoming meteoric flux provides the least likely explanation of the causitive agent for the trend over the years, exhibiting some similarity at all hours of the day.

The noon signal intensity curve has been redrawn in Fig. 3 (b), together with the 12-month running means of the final monthly sunspot numbers, and the monthly magnetic indices. It appears at once that the signal intensity follows the magnetic index much more closely than the sunspot curve. The well-known lag of the magnetic figures on the sunspot numbers is evident, [23] and the signal intensity parallels the magnetic figures. These curves could indicate that smoothed sunspot numbers are not necessarily a particularly good measure of the Sun's long-term effect on the lower ionsophere, at least when the sun is in a very active condition.

This section can be summarized by saying that some solar control of the daytime forward scatter signal on a temperate latitude path is undoubtedly present, as evidenced by intercomparison with the solar cycle.

4. SHORT PERIOD MAGNETIC INFLUENCE ON VHF FORWARD SCATTER

The method of obtaining a comparison between magnetic indices and signal intensities is somewhat involved. The procedure was as follows:

(1) A single value of the median received signal intensity level was obtained by inspection for each hour of every day from the continuous pen recording.

(2) A single median value was next obtained for each 3-hour period in the day, agreeing in time with the 3-hour intervals on which world magnetic activity figures are based.

(3) Eight monthly median signal intensity values were obtained for the eight 3-hour intervals of the day.

(4) The departure of each separate 3-hour unit signal intensity value from the monthly median covering the same time was next recorded.

(5) The values of these departures were then collected, for 13 consecutive months of observations, for all cases where the accompanying planetary magentic K-index had zero value (quietest magnetic conditions.) The median of these values then expresses the integrated departure of the signal intensity from the median monthly values over the whole period.

This grouping was repeated for each magnetic index up to 6, with a final group for index 7 and above (most disturbed conditions.)

This process was originally carried out for the Anchorage to Barrow circuit, where the mid-point was in the zone of maximum auroral occurrence. [8] The correlation then obtained, with the K-indices observed at Fairbanks, Alaska, is reproduced in Fig. 4 (a). This result was used by Bailey et. al. [8] to establish the very significant fact that VHF Arctic communications via scatter improve during periods of auroral and magnetic disturbance. (The limits of the vertical lines in the figure give the upper and lower decile values.)

Results for the temperate latitude Cedar Rapids to Sterling circuit, with an identical observing period, and planetary K-indices, are shown in Fig. 4 (b). There is no correlation. This unexpected result was checked by repeating the analysis with the Cheltenham, Maryland, local K-indices --these being the nearest magnetic observations to the Cedar Rapids circuit. Again, as shown in Fig. 4 (c), correlation is non-existent. As a final check, the analysis was repeated for the 1954 signal intensity values against the Cheltenham K-indices (Fig. 4 (d)), with an even more certain absence of any effect.

The method adopted in the above analysis is particularly designed to eliminate any possible long-period trends--such as seasonal or 11-year cycle effects--in the signal intensity records. The comparison of each 3-hourly signal intensity value is made with the magnetic index recorded for the same period, and all parts of the day and night are given equal weight. It can therefore be concluded from this section of the analysis that in temperate latitudes, in contrast to the auroral zone, there is no appreciable instantaneous relation between the forward scatter signal intensity and the magnetic disturbance figure.

It is possible, however, that the scatter component of meteoric origin is a relatively larger part of the total signal in temperate latitudes during the night and morning, so that it swamps any small magnetic effect being looked for on a 24-hour basis. Consequently the comparison analysis was again repeated with a restriction to the period 10-13 hours local time. This period was the nearest to noonday which could be selected to fit the unit period of the magnetic indices. It has already been established from the sunspot cycle study in Section 3. above that the scatter circuit is most affected by solar influence around mid-day.

Declassified in Part - Sanitized Copy Approved for Release @ 50-Yr 2014/06/09 : CIA-RDP81-01043R003000180001-4

Declassified in Part - Sanitized Copy Approved for Release @ 50-Yr 2014/06/09 : CIA-RDP81-01043R003000180001-4

Magnetic indices are related to sunspot values, so if a "same-time" comparison is to show any relationship between the two phenomena, the probability is greatest around the noon period. The result is given in Fig. 4 (e), where a small trend is indeed now apparent. High magnetic indices, if they occur in the noon period, are thus accompanied by a slight increase in signal intensity.

5. LONG PERIOD MAGNETIC INFLUENCE ON VHF FORWARD SCATTER

By using mean monthly values of the planetary K-index, and comparing the trends between identical months in consecutive years with the trends in monthly median signal intensity--in exactly the same way as was done with the monthly sunspot numbers in Section 3.--it becomes possible to identify long-period effects. Table II has been prepared in this way.

Table II

Comparison of Trend Between Forward Scatter Signal Intensity and Planetary Magnetic Index

Three-hour period centered about	Similar-month movement of values 1951-1957		Percentage of total cases favouring parallel movement (random = 50%)
	In opposition	In parallel	
06 hrs.	17	35	67%
12 hrs.	14	47	77%
18 hrs.	17	44	72%
00 hrs.	25	30	55%

The similarity of trends is more marked than in Table I. The signal intensity over the years definitely parallels the magnetic index in the afternoon period, and, in comparison with the sunspot results, now appears to show some parallelism even in the fairly early morning. Once again the midnight value shows no significant correlation.

The conclusion from these magnetic index studies is that there is a small instantaneous relation between the forward scatter signal intensity and the accompanying weaker magnetic effects of the temperate latitudes. The effect has become so slight, compared with auroral path circuits, that it is only noticeable on integrated noon values. There is however a marked daytime correlation on a monthly basis.

6. CONCLUSIONS

It has been established fairly definitely from a review of absorption results and rocket experiments that the electron concentration in the D-region of the ionosphere changes with the 11-year solar cycle. Evidence for this change is strongly supported by a trend comparison of the temperate latitude forward scatter signal intensity values with the sunspot cycle values, and still more strongly by comparison with the magnetic disturbance indices.

It is obvious, from off-great circle path studies, that aspect-sensitive reflections from meteor trails must play a considerable part in forward scatter, [12-15] but the present work shows, contrary to the ideas of McKinley, [24] and of Villard, Eshleman, Manning and Peterson, [25] that solar influences are definitely contributing, especially for the mid-day period, to the magnitude of the received signal. The latter authors [25] qualify their idea of exclusive meteoric ionization by considering that the general background excitation level may affect the extent of ionization produced by small meteors. This concept, if applied only to non-aspect sensitive reflections, cannot be ruled out, [14] but it can still definitely be said that the sun exerts a specific effect on the magnitude of the daytime scatter signal.

* * * * * *

NOTE: Since the work was done on this paper, new measurements have been made of antenna gain at the Cedar Rapids and Sterling stations. The gain at each station was found to have deteriorated relative to that measured earlier in the course of the experiment. It may be expected that this change has caused the apparent rise in signal strengths, shown in figures in this paper during years of rising sunspot cycle, to be somewhat less than actually occurred.

Declassified in Part - Sanitized Copy Approved for Release @ 50-Yr 2014/06/09 : CIA-RDP81-01043R003000180001-4

Declassified in Part - Sanitized Copy Approved for Release @ 50-Yr 2014/06/09 : CIA-RDP81-01043R003000180001-4

REFERENCES

[1] S. Gnanalingan and K. Weekes, "Weak echoes from the ionosphere with radio waves of frequency 1.42 Mc/s.," Nature, vol. 170, pp. 113-114, 1952.

[2] W. Dieminger, "On the causes of excessive absorption in the ionosphere on winter days," J. Atmos. Terr. Phys., vol. 2, pp. 340-349, 1952.

[3] F.F. Gardner and J.L. Pawsey, "Study of the ionospheric D-region using partial reflections," J. Atmos. Terr. Phys., vol. 3, pp. 321-344, 1953.

[4] J.M. Watts and J.N. Brown, "Some results of sweep-frequency investigations in the low frequency band," J. Geophys. Res., vol. 59, pp. 71-86, 1954.

[5] J. Gregory, "Ionospheric reflections from heights below the E region," Aust. J. of Phys., vol. 9, pp. 324-342, 1956.

[6] R.N. Bracewell, K.G. Budden, J.A. Ratcliffe, T.W. Straker, and K. Weekes, "The ionospheric propagation of low and very-low-frequency radio waves over distances less than 1000 km.," Proc. I.E.E., Pt. III, vol. 98, pp. 221-236, 1951.

[7] R. Naismith and E.M. Bramley, "Time-delay reasurements on radio transmission," Wir. Engin., vol. 28, pp. 271-277, 1951.

[8] D.K. Bailey, R. Bateman and R.C. Kirby, "Radio transmission at VHF by scattering and other processes in the lower ionosphere," Proc. I.R.E., vol. 43, pp. 1181-1230, 1955.

[9] A.D. Wheelon, "Diurnal variation of signal level and scattering heights for VHF propagation," J. Geophys. Res., vol. 62, pp. 255-266, 1957.

[10] J. Gregory, "The relation of forward scattering of VHF radio waves to partial reflection of MF waves at vertical incidence," J. Geophys. Res., vol. 62, pp. 383-388, 1957.

[11] V.C. Pineo, "Oblique-incidence measurements of the heights at which ionospheric scattering of VHF radio waves occurs," J. Geophys. Res., vol. 61, pp. 165-169, 1956.

[12] V.R. Eshleman and R.F. Mlodnosky, "Directional characteristics of meteor propagation derived from radar measurements," Proc. I.R.E., vol. 45, pp. 1715-1723, 1957.

[13] M.L. Meeks and J.C. James, "On the influence of meteor-radiant distributions in meteor-scatter communication," Proc. I.R.E., vol. 45, pp. 1724-1733, 1957.

[14] V.C. Pineo, "Off-path propagation at VHF," in publication.

[15] P.A. Forsyth, E.L. Vogan, D.R. Hansen and C.O. Hines, "The principles of Janet--a meteor-burst communication system," Proc. I.R.E., vol. 45, pp. 1642-1657, 1957.

[16] "Report of the Radio Research Board for 1956," H.M. Stationary Office, Great Britain, pp. 17-21.

[17] C.D. Ellyett, "Echoes at D-heights with special reference to the Pacific Islands," Terr. Mag. and Atmos. El., vol. 52, pp. 1-13, 1947.

[18] J. Gregory, Private communication.

[19] "Ionospheric Radio Propagation," National Bureau of Standards, Circular No. 462, p. 112, 1948.

[20] W. Dieminger, Report No. 192 of the German National Committee of URSI presented to the URSI General Assembly, 1957.

[21] T.A. Chubb, H. Friedman, R.A. Kreplin, and J.E. Kupperian, "Lyman Alpha and X-ray emissions during a small solar flare," J. Geophys. Res., vol. 62, pp. 389-398, 1957.

[22] E.T. Byrem, T.A. Chubb, H. Friedman, and J.E. Kupperian, "Observations of the intensity of solar Lyman-Alpha emission," Astrophys. J., vol. 124, pp. 480-482, 1956.

[23] S. Chapman and J. Bartels, "Geomagnetism," Oxford Univ. Press, 1940, p. 371.

[24] D.W.R. McKinley, "Dependence of integrated duration of meteor echoes on wavelength and sensitivity," Canad, J. Phys., vol. 32, pp. 450-467, 1954.

[25] O.G. Villard, V.R. Eshleman, L.A. Manning and A.M. Peterson, "The role of meteors in extended range VHF propagation," Proc. I.R.E., vol. 43, pp. 1473-1481, 1955.

Declassified in Part - Sanitized Copy Approved for Release @ 50-Yr 2014/06/09 : CIA-RDP81-01043R003000180001-4

Declassified in Part - Sanitized Copy Approved for Release @ 50-Yr 2014/06/09 : CIA-RDP81-01043R003000180001-4

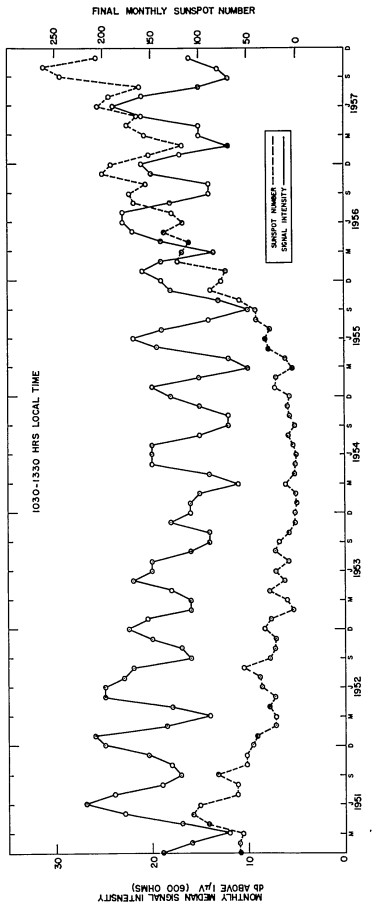

CEDAR RAPIDS TO STERLING, FORWARD SCATTER AT 49.8 Mc/s

FIGURE X-1

Declassified in Part - Sanitized Copy Approved for Release @ 50-Yr 2014/06/09 : CIA-RDP81-01043R003000180001-4

Declassified in Part - Sanitized Copy Approved for Release @ 50-Yr 2014/06/09 : CIA-RDP81-01043R003000180001-4

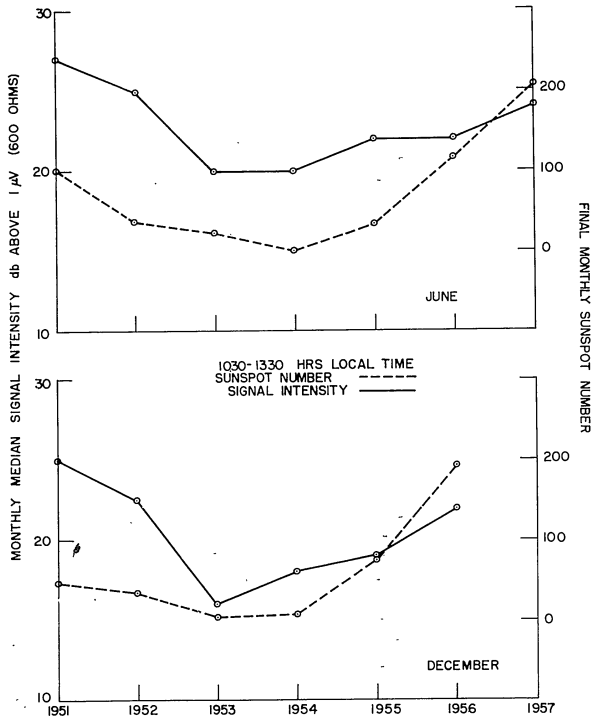

CEDAR RAPIDS TO STERLING, FORWARD SCATTER AT 49.8 Mc/s

FIGURE X—2

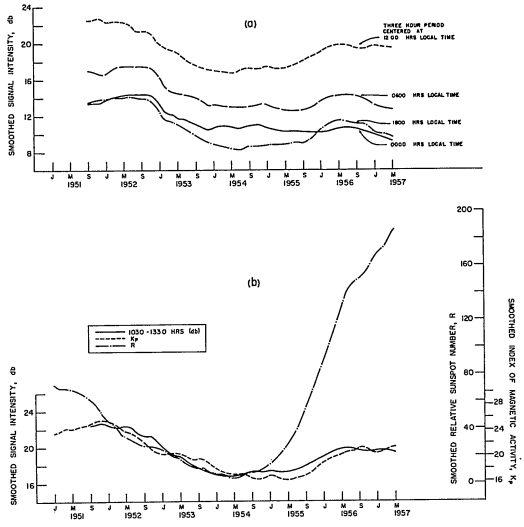

COMPARISON OF SUNSPOT NUMBER AND MAGNETIC ACTIVITY WITH CEDAR RAPIDS TO STERLING SIGNAL INTENSITIES.

FIGURE X-3

Declassified in Part - Sanitized Copy Approved for Release @ 50-Yr 2014/06/09 : CIA-RDP81-01043R003000180001-4

Declassified in Part - Sanitized Copy Approved for Release @ 50-Yr 2014/06/09 : CIA-RDP81-01043R003000180001-4

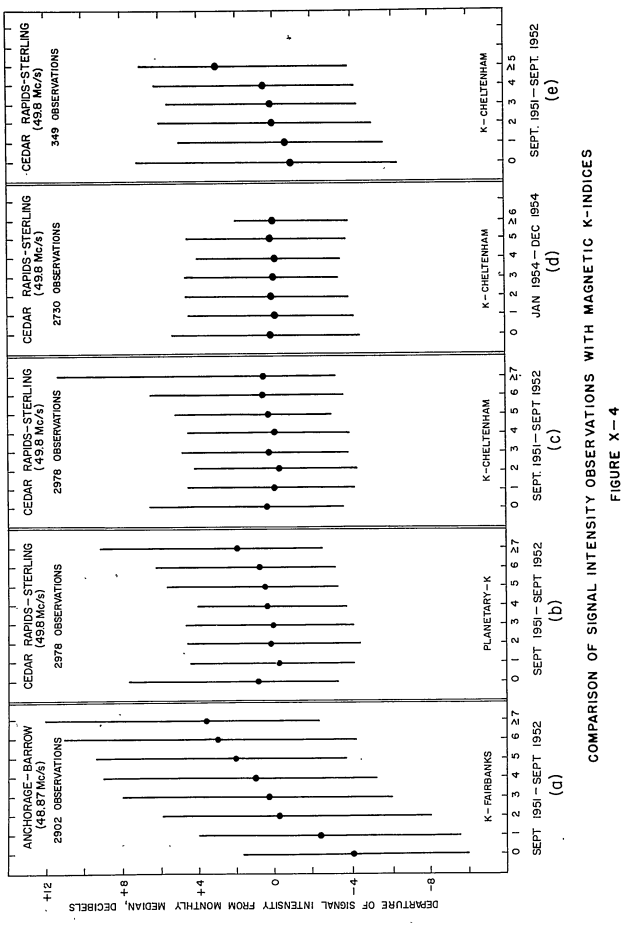

COMPARISON OF SIGNAL INTENSITY OBSERVATIONS WITH MAGNETIC K-INDICES

FIGURE X-4

APPENDIX XI

TABULATED MONTHLY MEDIAN AND DECILE VALUES OF HOURLY MEDIAN SIGNAL INTENSITY RECORDED IN THE ROUTINE RECORDING PROGRAMS

The tables in this appendix give the upper and lower decile and median values, for each month, of the hourly median values of received signal intensity. Values shown are received open-circuit antenna voltage in decibels above one microvolt, for a reference antenna impedance of 600 ohms and an estimated power of 30 kilowatts to the transmitting antenna.

The conditions of the experiment, i. e. antennas, and other details are given in Table 1 of the main text. Table 1 also gives conversion factors which relate the zero decibel level of the tables of this appendix to corresponding values of transmission loss and loss relative to inverse distance attenuation.

The values shown in the table represent signal intensity levels equalled or exceeded for the per cent of days (of the month) indicated by the column heading. Second (right hand) entries in double entry columns represent values obtained by interpolating through periods of Es-type propagation. The extreme right-hand column (N) gives the number of observations available for the month.

Appendix XX of the previous report describes the detailed methods for measuring, analysing and reporting the data.

A list of the tables follows:

CEDAR RAPIDS TO STERLING 27.775 Mc/s:

TABLE XI-1, April, May, 1954
" XI-2, June, July, "
" XI-3, August, September, 1954
" XI-4, October, November, "
" XI-5, December, January, 1954-55

CEDAR RAPIDS TO STERLING 49.8 Mc/s:

TABLE XI-6, October, November, 1952
" XI-7, December, January, 1952-53
" XI-8, February, March, 1953
" XI-9, April, May, "
" XI-10, June, July, "
" XI-11, August, September, "
" XI-12, October, November, "
" XI-13, December, January, 1953-54
" XI-14, February, March, 1954

Declassified in Part - Sanitized Copy Approved for Release @ 50-Yr 2014/06/09 : CIA-RDP81-01043R003000180001-4

Declassified in Part - Sanitized Copy Approved for Release @ 50-Yr 2014/06/09 : CIA-RDP81-01043R003000180001-4

TABLE XI-15, April, May, 1954
" XI-16, June, July, "
" XI-17, August, September, 1954
" XI-18, October, November, "
" XI-19, December, January, 1954-55

CEDAR RAPIDS TO STERLING 107.8 Mc/s:

TABLE XI-20, October, November, 1952
" XI-21, December, January, 1952-53

FARGO TO CHURCHILL 49.7 Mc/s:

TABLE XI-22, October, November, 1952
" XI-23, December, January, 1952-53
" XI-24, February, March, 1953

ANCHORAGE TO BARROW 24.325 Mc/s:

TABLE XI-25, March, April, 1953
" XI-26, May, June, "

ANCHORAGE TO BARROW 48.87 Mc/s:

TABLE XI-27, October, November, 1952
" XI-28, December, January, 1952-53
" XI-29, February, March, 1953
" XI-30, April, May, "
" XI-31, June, 1953

TABLE XI-1

CEDAR RAPIDS TO STERLING 27.775 Mc/s (1954)

Hour 75°W	April				May			
	90%	50%	10%	N	90%	50%	10%	N
00-01	18	22	27	28	19	26	30	28
01-02	18	22½	27	30	22	28	40	28
02-03	20	23	27	30	23	28	34	28
03-04	21	24	28	30	23	29	32	28
04-05	23	26	30	30	25	29	32	26
05-06	23	26	30	30	26	28	36	27
06-07	23	27½ 27	31	30 30	27	30	37	35
07-08	25	29	33	30	26	31 30½	> 68	27
08-09	25	29	34	30	28	33 32	> 68	27
09-10	25	30	36	30	29	35 33	> 68	27
10-11	28	31 30½	36 34	27 26	30	37½ 34	> 68	26
11-12	27	30	36 35	26 24	32	40 37	> 68	25
12-13	27	32	39 35	26 26	30	39 38	> 68	25
13-14	27	31	37	27	26	38 37	> 68	26
14-15	26	31	35	24	28	36 35½	> 68	26
15-16	25	28	31	26	25	34 32½	> 68	25
16-17	20	26	30	30	20	31 30	61	27
17-18	17	23	34	29	20	29½ 28	59	28
18-19	15	22	30	29	19	27	> 68	28
19-20	14	18	25	27	19	25½ 22½	> 68	28
20-21	15	18	24 23	30 29	19	24 21	> 68	28
21-22	16	19	26 25	29 28	18	23 22	> 68	28
22-23	18	21	28	30	18	24 23	29	28
23-00	17	21½	26	30	18	24½ 24	33	28

Declassified in Part - Sanitized Copy Approved for Release @ 50-Yr 2014/06/09 : CIA-RDP81-01043R003000180001-4

Declassified in Part - Sanitized Copy Approved for Release @ 50-Yr 2014/06/09 : CIA-RDP81-01043R003000180001-4

TABLE XI-2

CEDAR RAPIDS TO STERLING 27.775 Mc/s (1954)

Hour 75°W	June 90%	June 50%	June 10%	June N	July 90%	July 50%	July 10%	July N
00-01	24	30 29	56 36	30 26	26	34 31	>68 36	28 24
01-02	25	31 30	68 35	30 27	28	33½ 32	>68 39	28 24
02-03	27	31	45 40	30 28	28	33½ 33	>68 40	28 25
03-04	27	32 31½	50 36	30 28	30	34 32½	48 42	28 26
04-05	27	31½ 31	43 37	30 29	27	33 32	41 40	28 27
05-06	29	32	45 37	30 29	28	33	40	27
06-07	28	33 32	39 37	30 29	28	33	39 37	27 27
07-08	29	34½ 33	>68 36	30 25	29	34 33	39 36	27 27
08-09	29	36 33	>68 37	30 21	28	35 34	50 37	28 26
09-10	32	39 35	>68 39	29 18	30	38 35	>68 41	29 25
10-11	33	40½ 37	>68 42	24 16	28	38 35	>68 42	29 21
11-12	33	39 37	>68 41	23 14	31	42 36	>68 42	29 19
12-13	29	39 37½	>68 42	23 16	33	38 37	>68 41	29 20
13-14	30	38 37	>68 43	21 14	33	39 37½	>68 43	29 22
14-15	33	42 38	>68 42	21 15	29	37 35	>68 41	28 23
15-16	27	40 37	>68 41	23 17	30	38 33½	>68 38	28 20
16-17	27	36 32	>68 37	28 21	26	33½ 30	>68 38	28 23
17-18	25	32 30	>68 36	27 21	24	31 27½	>68 34	28 22
18-19	24	33½ 26½	>68 34	30 22	23	30 26	>68 34	28 22
19-20	23	31½ 26	>68 30	30 21	23	29½ 25½	>68 31	28 20
20-21	22	27 25	>68 31	30 23	23	26½ 25	>68 32	28 21
21-22	22	27½ 25	>68 29	30 24	22	26½ 26	>68 37	28 23
22-23	23	28 26	>68 29	30 25	25	28 27	>68 31	28 24
23-00	22	28	>68 31	30 24	24	30	>68 32	28 25

TABLE XI-3

CEDAR RAPIDS TO STERLING 27.775 Mc/s (1954)

Hour 75°W	August 90%	August 50%	August 10%	August N	September 90%	September 50%	September 10%	September N
00-01	23	30	36	30 29	23	26	36	29
01-02	26	31	37 30	30 29	23	26	33	28
02-03	27	32	38	30 29	22	26	31	28
03-04	26	31 30½	36	30 30	22	26	30	28
04-05	25	30	35	30	22	25	29	29
05-06	25	30	35	30	22	25	28	29
06-07	27	31 30	35	30 30	23	25	31 30	29 29
07-08	27	31	37 34	30 30	23	25	31	29
08-09	25	32	36 34	30 29	24	27	32	29
09-10	28	32½ 32	49 35	30 29	24	28	34	28
10-11	27	36 34	>68 41	31 29	24	30	34	28
11-12	28	34 33½	45 41	31 30	25	30	38	27
12-13	27	34	52 41	31 30	25	30½	37	28
13-14	28	34	50 44	31 30	26	30	39 37	29 29
14-15	27	33 32	42	31 31	24	28	37	29
15-16	25	32	43 38	31 31	24	27	34	28
16-17	24	29	36	31	20	25	38	29
17-18	23	28½ 27	41 33	30 29	20	24	31	29
18-19	21	25½ 25	40 35	30 29	19	22	29 28	29 29
19-20	18	25 23	61 33	30 28	19	22	29	29
20-21	19	24	52 31	30 29	19	22	32 29	29 29
21-22	19	25 24½	>68 29	30 28	19	23	29	29
22-23	21	24	41 31	30 28	20	25	35	29
23-00	21	28	35 34	30 29	22	28	39	29

TABLE XI-4

CEDAR RAPIDS TO STERLING 27.775 Mc/s (1954)

Hour 75°W	October 90%	50%	10%	N	November 90%	50%	10%	N
00-01	21	25	28	29	20	24	32	29
01-02	22	25	28 27	29 29	22	26	30	29
02-03	23	24	27	29	23	27	30	29
03-04	22	25	27	28	22	27	31 30	28 28
04-05	22	25	28	28	23	26	30	29
05-06	23	25	31	28	22	25½ 25	30	28 27
06-07	23	26	31	28	22	25	29 28	29 27
07-08	24	27½	31	28	22	25	34 28	28 26
08-09	23	28½	33	28	23	29	33 32	28 27
09-10	24	30 29	34	29 29	23	29	33 32	28 27
10-11	26	31 30	38 37	29 29	28	31	40	27
11-12	24	32	38	29	28	34	44	27
12-13	23	33	39	29	30	33	44	27
13-14	24	31½	39	30	30	35	48 47	28 27
14-15	25	30	37	28	28	35½	45	28
15-16	23	29½	38	28	26	35½	46	28
16-17	21	27	39	28	25	33½	44	28
17-18	21	28	37	29	22	29	40	29
18-19	20	27	39	29	21	27	39	29
19-20	21	27	38 37	29 29	19	26	33	29 28
20-21	21	27 26	36 34	29 28	19	26 25½	33	29 28
21-22	21	24	34 33	29 28	20	25	33 32	29 28
22-23	21	26	30	29 28	20	24	29 28	29 29
23-00	21	26	31	29 28	20	24	31	29

TABLE XI-5

CEDAR RAPIDS TO STERLING 27.775 Mc/s (1954-55)

Hour 75°W	December 90%	50%	10%	N	January 90%	50%	10%	N
00-01	20	29 28	38 37	27 26	25	29	41	19
01-02	19	27½	35	28	24	29½	37	18
02-03	23	28½	36	28	23	29	34	18
03-04	21	27	34	27	24	28	32	18
04-05	21	26	34	27	24	27	32	17
05-06	21	26	33	27	22	27	31	16
06-07	20	25	34 32	27 27	23	27	30	18
07-08	21	26	33	27	22	27	33	18
08-09	21	30	41 39	29 29	25	28½	38	18
09-10	25	34	42	28	26	32½	41	20
10-11	29	37½ 36	60 41	28 26	28	35½ 35	52 44	22 21
11-12	31	39 37½	61 45	29 26	30	38 37	>68 46	22 20
12-13	29	38	51	29 28	33	38	47 45	23 22
13-14	31	37	46	27	30	37	45	23 22
14-15	29	35	41	26	27	35 34½	45	23 22
15-16	27	35 33	45 44	29 29	24	32	45	22
16-17	28	32	46	28	26	32	40	22
17-18	19	28 25	38	27 27	21	29	41	19
18-19	17	26 24	41 35	27 27	18	27	31	19
19-20	18	24	39 31	27 27	18	22	29	19
20-21	16	23 22	34 33	27 27	18	23	31	19
21-22	16	23	35	27	20	24	30	19
22-23	17	26	37	27	22	25	39	19
23-00	18	27	36	27	23	27	39	19

Declassified in Part - Sanitized Copy Approved for Release @ 50-Yr 2014/06/09 : CIA-RDP81-01043R003000180001-4
Declassified in Part - Sanitized Copy Approved for Release @ 50-Yr 2014/06/09 : CIA-RDP81-01043R003000180001-4

TABLE XI-6

CEDAR RAPIDS TO STERLING 49.8 Mc/s (1952)

Hour 75°W	October 90%	50%	10%	N	November 90%	50%	10%	N
00-01	10	12	16	29	8	11	18	29
01-02	9	13	17	29	9	12	17	29
02-03	10	13	18	29	9	12	19	27
03-04	10	13	16	29	9	13	20	27
04-05	10	13	17	29	10	13	18	28
05-06	10	14	16	29	9	13	18	28
06-07	10	13	17	29	9	13	20	28
07-08	10	14	19	29	10	13½	19	28
08-09	12	15	22	29	10	16	22	29
09-10	13	16	20	30	13	18	23	27
10-11	13	16	20	29	13	19½	25	28
11-12	13	17	21	29	14	20	27	28
12-13	13	17½	23	30	15	20	29	27
13-14	12	17	23	29	14	20	28	28
14-15	11	16	22	30	13	20	29	27
15-16	11	15	20	28	12	18	26	29
16-17	9	14	19	27	12	18	24	29
17-18	8	11	16	29	11	15	23	29
18-19	6	11	17	29	10	14	24	29
19-20	7	10½	19	28	9	13	21	29
20-21	8	11	17	29	8	12	20	29
21-22	8	10	16	29	7	12	18	29
22-23	9	12	17	29	7	12	18	29
23-00	9	13	17	29	8	11	16	29

TABLE XI-7

CEDAR RAPIDS TO STERLING 49.8 Mc/s (1952-53)

Hour 75°W	December 90%	50%	10%	N	January 90%	50%	10%	N
00-01	9	12½	22	26	9	12	19	31
01-02	8	12½	21	26	10	13	18	31
02-03	10	13	20	26	10	14	21	31
03-04	11	14	22 20	25 25	10	14	20	31
04-05	11	13	20	25	11	14	18	31
05-06	10	13	18	25	11	14	18	31
06-07	10	12	18	25	11	13	19	31
07-08	10	12	19	25	11	13	19	31
08-09	10	14	22	25	12	15	20	31
09-10	13	19	30 27	25 25	13	17	23	31
10-11	15	20	26	23	15	20	32	30
11-12	15	23	28	24	14	20	31	31
12-13	16	24	32	25	15	21½	29	30
13-14	15	22	30	25	14	20	28	31
14-15	13	21	27	25	15	20	28	31
15-16	12	21	26	24	13	18½	25	30
16-17	10	19	24	26	10	18	23	30
17-18	10	15	20	26	9	12½	20	30
18-19	9	12½	20 19	26 26	7	11	22	30
19-20	7	11½	20	26	6	10	19	31
20-21	6	10½	21	26	6	9	18	31
21-22	5	10	20	26	7	10	18	30
22-23	5	11	21	26	6	10	19	31
23-00	9	12	21	26	7	12	16	31

Declassified in Part - Sanitized Copy Approved for Release @ 50-Yr 2014/06/09 : CIA-RDP81-01043R003000180001-4
Declassified in Part - Sanitized Copy Approved for Release @ 50-Yr 2014/06/09 : CIA-RDP81-01043R003000180001-4

TABLE XI-8

CEDAR RAPIDS TO STERLING 49.8 Mc/s (1953)

Hour 75°W	February 90%	50%	10%	N	March 90%	50%	10%	N
00-01	6	10	14	27	8	10	14	29
01-02	7	11	14	27	8	11	13	28
02-03	8	12	14	27	9	11	14	30
03-04	9	12	15	27	9	11	15	29
04-05	9	13	16	27	9	12	14	29
05-06	10	13	15	27	10	12	14	29
06-07	10	12	14	26	10	11	14	29
07-08	11	12	14	26	11	13	15	29
08-09	11	13	15	25	11	13	17	30
09-10	11	13	19	26	12	13	17	30
10-11	10	14½	20	26	11	14	19	31
11-12	12	16	21	27	12	14	22	31
12-13	13	16	25	27	12	16	22	31
13-14	14	16	25	27	13	16	23	30
14-15	13	18	26	27	12	16	23	31
15-16	11	17	26	27	10	15	23	30
16-17	11	16	24	27	8	13	20	31
17-18	9	16	23	26	7	11	20	30
18-19	5	10	16	26	5	10	16	29
19-20	3	8½	16	26	5	8	16	29
20-21	4	7½	16	26	5	8	13	30
21-22	3	6½	13	26	5	9	12	31
22-23	4	7	14	27	5	9	11	31
23-00	5	8	14	27	7	9½	14	30

TABLE XI-9

CEDAR RAPIDS TO STERLING 49.8 Mc/s (1953)

Hour 75°W	April 90%	50%	10%	N	May 90%	50%	10%	N
00-01	8	11	16	29	10	13½	17	28
01-02	9	11½	16	30	11	14½	19	28
02-03	9	12½	16	30	12	15	20	28
03-04	10	13	17	30	14	15	19	29
04-05	10	13½	18	30	13	15	19	29
05-06	11	14½	18	30	14	16	20	28
06-07	12	16	24	30	14	17	22	28
07-08	13	17	25	30	14	20	23	27
08-09	14	18½	27	30	14	20 18	24	29 29
09-10	15	19	28	30	14	19	26	30
10-11	14	19	27	29	14	18	27	26
11-12	15	18	26	29	13	20½	25	26
12-13	14	18½	26	28	13	22	30 28	28 28
13-14	13	18	25	29	14	22	27	25
14-15	13	16	21	28	14	18	26	25
15-16	10	14½	20	28	12	16	24	28
16-17	9	13	18	27	11	14	23	30
17-18	6	10	14	28	10	14	21	31
18-19	4	8	14	30	7	13	20	31
19-20	3	6	13	30	6	10	18	29
20-21	2	6½	15	30	5	10	16	29
21-22	3	7	14	30	6	10	15	29
22-23	5	9	14	30	8	11	16	29
23-00	6	10	16	30	8	13	16	29

Declassified in Part - Sanitized Copy Approved for Release @ 50-Yr 2014/06/09 : CIA-RDP81-01043R003000180001-4
Declassified in Part - Sanitized Copy Approved for Release @ 50-Yr 2014/06/09 : CIA-RDP81-01043R003000180001-4

TABLE XI-10

CEDAR RAPIDS TO STERLING 49.8 Mc/s (1953)

Hour 75°W	June 90%	June 50%	June 10%	June N	July 90%	July 50%	July 10%	July N
00-01	10	14	17	28	9	14	18	29
01-02	13	15	17	27	10	15	19	29
02-03	13	16	19	28	12	16	19	28
03-04	12	17½	19	28	13	17	20	28
04-05	13	18	20	28	13	16½	19	28
05-06	14	18	21	27	13	17½	20	28
06-07	15	18	22 21	27 27	13	18	21	28
07-08	14	19	23 22	27 27	12	17	23	28
08-09	14	19	26 23	26 26	14	18 17	24 23	28 27
09-10	14	19	27 24	26 24	13	18	24	29
10-11	14	21	44 25	24 23	13	18	29 23	27 26
11-12	14	21	30	23	14	17	27 26	28 27
12-13	15	19	27	23	12	20 19	28 27	28 26
13-14	15	20	27	23	14	20	26	26
14-15	14	20 19½	27 26	22 22	14	19 18	22	27 27
15-16	12	18	30 24	23 22	13	19 17	24 23	28 28
16-17	9	15 14½	20	25 24	12	17 16½	30 24	29 28
17-18	8	13½	20	26	10	16	26 24	30 29
18-19	7	11½	17	26	8	14 13	28 23	29 28
19-20	6	11 10	17 14	25 25	7	11 10	42 20	29 27
20-21	6	9	12	26	4	9	24 15	29 27
21-22	6	9	11	27	5	9	15 14	30 29
22-23	7	10	14	27	7	9	15	29
23-00	9	12	15	27	8	13	17	29

TABLE XI-11

CEDAR RAPIDS TO STERLING 49.8 Mc/s (1953)

Hour 75°W	August 90%	August 50%	August 10%	August N	September 90%	September 50%	September 10%	September N
00-01	7	11	20	31	6	10	13	29
01-02	8	13	20	31	7	10	12	29
02-03	9	14	19	31	5	10	12	29
03-04	10	15	20	31	6	10	13	29
04-05	10	15	20	31	6	11	14	29
05-06	11	14½	20	30	6	10	13	29
06-07	12	15	22	30	5	11	14	29
07-08	11	15	22	30	6	11	16	29
08-09	10	14½ 14	22	30 30	9	12	19	29
09-10	10	14½	23	30	9	12	17	29
10-11	10	14½	23	30	10	14	20	28
11-12	10	16	27 25	31 31	9	14	22	28
12-13	10	16	29 24	31 31	9	14	20	28
13-14	10	15	28 24	31 31	9	13	21	28
14-15	8	14½	26	30	7	11	18	25
15-16	8	14 13½	23	30 30	7	10	16	25
16-17	8	11	23	29	7	9½	14	28
17-18	7	10½	23 20	30 30	4	8	14	29
18-19	5	9	17	31	4	8	13	29
19-20	5	8	14	31	3	8	13 12	29 29
20-21	4	7	12	31	2	8	15 14	29 29
21-22	5	7	14 11	31 31	3	7	13	29
22-23	5	9	13 12	31 31	6	9	12	29
23-00	6	10	15	31	6	9	13	29

Declassified in Part - Sanitized Copy Approved for Release @ 50-Yr 2014/06/09 : CIA-RDP81-01043R003000180001-4
Declassified in Part - Sanitized Copy Approved for Release @ 50-Yr 2014/06/09 : CIA-RDP81-01043R003000180001-4

Declassified in Part - Sanitized Copy Approved for Release @ 50-Yr 2014/06/09 : CIA-RDP81-01043R003000180001-4

TABLE XI-12

CEDAR RAPIDS TO STERLING 49.8 Mc/s (1953)

Hour 75°W	October				November			
	90%	50%	10%	N	90%	50%	10%	N
00-01	6	8	12	28	2	7	14	30
01-02	6	8	11	28	3	8	13	30
02-03	6	9	11	28	4	9	13	30
03-04	7	9	11	27	5	9	13	29
04-05	6	9	12	27	6	10	13	29
05-06	7	9	12	27	5	9	13	29
06-07	7	9	13	27	5	8½	12	28
07-08	8	10	15	27	4	9	13	28
08-09	8	12	16	27	6	11	16	28
09-10	9	14	22	27	9	13	18	27
10-11	9	17	23	26	9	16 15½	22	24 24
11-12	9	14½	20	26	9	18½ 18	24	22 22
12-13	9	13½	21	26	10	18	24	22
13-14	9	14	20	26	11	18	23	22
14-15	8	11	20	26	12	17	23	22
15-16	7	9	19	25	11	16	23	23
16-17	5	11	16	25	6	13	23	23
17-18	3	7	16	27	4	11 10	21 18	29 29
18-19	3	7	21	29	2	10	21 16	30 30
19-20	2	7	13	29	3	7½	18	30
20-21	2	7	18	29	3	6	16	30
21-22	2	6	12	29	2	6	14	29
22-23	3	7	11	29	3	7	14	28
23-00	3	8	12	29	2	7½	14	30

TABLE XI-13

CEDAR RAPIDS TO STERLING 49.8 Mc/s (1953-54)

Hour 75°W	December				January			
	90%	50%	10%	N	90%	50%	10%	N
00-01	5	9	13	30	4	8½	13	28
01-02	6	10	14	30	6	10	13	27
02-03	6	11	14	30	7	10	13	27
03-04	7	10	15	30	7	10	12	27
04-05	6	10	14	30	7	9	10	27
05-06	6	9½	13	30	6	9	11	27
06-07	7	9½	12	30	6	8	10	27
07-08	7	10	13	29	6	8	11	27
08-09	9	12	17	29	7	8	12	26
09-10	11	13	23	29	8	10	15	25
10-11	11	14	23	29	10	13	22	23
11-12	11	15	22	26	9	17	24	21
12-13	13	17	28	29	9	16	25	23
13-14	12	16½	25	28	11	16	25	24
14-15	10	16	24	29	9	15	21	24
15-16	9	14½	23	28	9	14	22	25
16-17	8	14	25	29	7	11	19	28
17-18	4	10½	23	30	3	6½	12	28
18-19	3	11 10½	24 18	30 30	1	3½	9	28
19-20	1	9½ 9	20 19	30 29	-1	3	18	28
20-21	3	7½ 7	20 13	30 29	0	3	14	28
21-22	1	7	11	30	1	4	10	28
22-23	3	7½	12	30	2	6	12	28
23-00	4	8½	12	30	2	7½	12	28

TABLE XI-14

CEDAR RAPIDS TO STERLING 49.8 Mc/s (1954)

Hour 75°W	February 90%	50%	10%	N	March 90%	50%	10%	N
00-01	4	7½	12	28	3	6	8	30
01-02	5	8	11	28	4	6½	9	30
02-03	6	9	12	28	4	7	11	30
03-04	7	10	12	28	5	7½	11	30
04-05	8	9½	12	28	6	8	11	30
05-06	8	9½	12	28	6	9	13	30
06-07	7	9	11	28	7	10	13	30
07-08	6	9	12	28	9	11	15	30
08-09	8	10	17	27	8	11	17	30
09-10	8	11	19	27	8	11	15	30
10-11	9	12	18	28	8	11	15	30
11-12	11	14	18	28	8	11	19	28
12-13	12	15½	20	26	7	11	16	29
13-14	13	15	23	26	8	12	16	28
14-15	11	15	23	26	7	11	19	28
15-16	10	14½	24	26	5	10	17	29
16-17	7	13	22	27	3	10	19	30
17-18	6	9½	20	28	2	7	13	31
18-19	3	7	13	27	-1	4	10	31
19-20	2	6 5½	12 9	28 28	-2	3	8	29
20-21	2	6	9	28	-2	3	6	29
21-22	2	6	10	28	-1	3	6	29
22-23	2	6	11	28	0	4	6	29
23-00	2	6	13	28	3	5	7	29

TABLE XI-15

CEDAR RAPIDS TO STERLING 49.8 Mc/s (1954)

Hour 75°W	April 90%	50%	10%	N	May 90%	50%	10%	N
00-01	5	7	13	30	7	11	14	31
01-02	5	8	13	29	8	13	16	31
02-03	6	9	13	29	10	14	17	31
03-04	6	10	14	29	10	14	17	31
04-05	7	10	14	29	11	15	18	30
05-06	9	11	15	29	10	15	18	31
06-07	8	11	16	29	12	15	21	31
07-08	8	11	17	29	13	17	22	31
08-09	9	12	19	29	13	17	23 22	31 30
09-10	9	13	19	29	12	18	27 20	31 29
10-11	9	13	20	28	15	19 18½	23	30 30
11-12	10	13	22	27	12	21 19½	39 25	29 26
12-13	9	14	21	26	11	21 20	28 26	29 27
13-14	9	15	21	27	10	20½	26	28
14-15	8	13½	16	26	9	20	22	28
15-16	6	11	16	27	7	17½ 17	23	28 27
16-17	4	9	15	30	7	14½	20	30
17-18	1	7	15	30	7	13	18	31
18-19	1	4	16	30	3	11	38 15	31 29
19-20	-2	3	8	29	3	7	26 11	31 29
20-21	1	2	7 6	29 29	4	7 6	12 9	31 29
21-22	2	4½	7	28	5	7	13 10	31 30
22-23	3	6	11	29	5	9	14 12	31 30
23-00	5	7	11	29	6	10	13	31

Declassified in Part - Sanitized Copy Approved for Release @ 50-Yr 2014/06/09 : CIA-RDP81-01043R003000180001-4
Declassified in Part - Sanitized Copy Approved for Release @ 50-Yr 2014/06/09 : CIA-RDP81-01043R003000180001-4

TABLE XI-16

CEDAR RAPIDS TO STERLING 49.8 Mc/s (1954)

Hour 75°W	June 90%	June 50%	June 10%	June N	July 90%	July 50%	July 10%	July N
00-01	10	14	17	30	11	16	21 20	30 30
01-02	11	15	19	30 29	12	17	20	30
02-03	11	16	20	30	14	18	22	30
03-04	12	16	20	30	13	17	21	30
04-05	13	16	19	30	12	17½	21	30
05-06	15	17	21	30	12	17	21	30
06-07	15	16½	20	30	13	18	22	30
07-08	14	17½ 17	32 22	30 30	13	17	22	30
08-09	14	18 17½	37 22	29 28	12	17	23	31
09-10	15	19 18	42 22	27 25	12	18	28 24	30 30
10-11	16	20½ 20	38 23	26 24	12	18	>60 24	31 30
11-12	12	21 20½	41 24	24 22	13	20	52 28	30 29
12-13	12	22 21	>60 25	24 21	13	21 20	46 28	30 29
13-14	14	20 19	54 25	22 20	12	20 19	29 28	30 29
14-15	13	19 18½	27	24 24	10	19	60 26	30 29
15-16	11	17½ 16½	25	26 26	9	17½ 17	28 15	30 30
16-17	9	17½ 15	22 21	26 25	10	14	26 21	29 29
17-18	8	14	19 18	26 25	11	13 12	31 20	29 29
18-19	7	12	56 15	29 27	6	11	22 19	29 29
19-20	7	9	25 14	30 30	6	10	20 14	29 29
20-21	6	9 8	12	30 30	6	10	60 14	29 29
21-22	7	10	12	30 29	6	10	17 13	29 29
22-23	8	11	14 13	30 29	8	12	17 16	29 29
23-00	8	12½ 12	16 15	30 29	10	14	22 17	29 29

TABLE XI-17

CEDAR RAPIDS TO STERLING 49.8 Mc/s (1954)

Hour 75°W	August 90%	August 50%	August 10%	August N	September 90%	September 50%	September 10%	September N
00-01	7	12	17	27	6	9	14	30
01-02	8	13	18	26	7	10	13	30
02-03	10	14½	18	26	7	10	13	30
03-04	11	13	17	26	8	10	13	30
04-05	11	13	16	26	8	10	12	30
05-06	10	13	15	26	8	9	12	30
06-07	11	13	16	25	8	10	13	30
07-08	10	14 13	19 18	25 25	8	10	13	30
08-09	8	13½	17	28	8	10	12	30
09-10	9	13½	18	28	7	10	15	30
10-11	9	13	22	27	8	10	14	29
11-12	9	14	22	29	8	12	16	29
12-13	9	15½	25	30	8	12	16	29
13-14	10	15	22	30	8	10	18	29
14-15	10	14	20	30	7	10	16	29
15-16	10	13	18	30	6	8	12	29
16-17	8	11	17	29	5	8	12	30
17-18	6	9½	16	28	4	7	10	30
18-19	5	8	13	28	4	6	9	30
19-20	4	7	11	28	4	6	8	30
20-21	4	7	11 10	28 28	3	5½	9	30
21-22	5	7	10	28	2	6	10	30
22-23	6	7	11	28	4	7	12	30
23-00	6	9½	14	28	5	8½	14	30

Declassified in Part - Sanitized Copy Approved for Release @ 50-Yr 2014/06/09 : CIA-RDP81-01043R003000180001-4
Declassified in Part - Sanitized Copy Approved for Release @ 50-Yr 2014/06/09 : CIA-RDP81-01043R003000180001-4

TABLE XI-18

CEDAR RAPIDS TO STERLING 49.8 Mc/s (1954)

Hour 75°W	October 90%	50%	10%	N	November 90%	50%	10%	N
00-01	3	7½	11	28	4	7	11	26
01-02	5	7½	10	28	5	8	11	26
02-03	5	8	11	28	6	9	11	26
03-04	4	8	11	27	7	9½	11	26
04-05	4	9	11	27	7	9	12	26
05-06	4	8	11	27	7	9	11	26
06-07	5	9	11	27	5	8½	11	26
07-08	5	10	12	28	7	9½	12	26
08-09	6	11	14	28	6	12	17	26
09-10	6	11	15	29	9	13	19	27
10-11	6	11	18	29	10	15	23	27
11-12	8	12½	20	28	11	14	22	26
12-13	9	12	20	27	11	14½	22	26
13-14	5	12	19	28	11	16	24	27
14-15	4	11	22	28	10	17	24	27
15-16	3	11½	22	28	8	18	24	27
16-17	1	9	20	29	7	12	25	27
17-18	2	7	19	29	5	10	22	27
18-19	3	6	16	29	4	9	19	27
19-20	1	6	15	29	3	8	12	27
20-21	1	6	13	28	2	7	10	27
21-22	1	6½	13	28	4	7	10	26
22-23	0	7	12	28	4	7	10	26
23-00	2	8	11	28	5	7	11	26

TABLE XI-19

CEDAR RAPIDS TO STERLING 49.8 Mc/s (1954-55)

Hour 75°W	December 90%	50%	10%	N	January 90%	50%	10%	N
00-01	2	8	15	29	8	11	21	31
01-02	3	10	15	29	8	12	17	31
02-03	5	10	16	29	9	12	17	31
03-04	6	11	14	29	9	12	15	31
04-05	6	10	14	29	9	12	16	31
05-06	5	10	12	29	9	11	15	31
06-07	6	10	13	29	8	11	13	31
07-08	6	10	14	29	9	11	14	31
08-09	8	10	15	28	8	11	16	31
09-10	9	15	21	29	9	13	20	30
10-11	12	16	23 22	29 29	10	18	24	30
11-12	12	17	24	28	13	20	26	30
12-13	11	18	27	30	16	21	26	29
13-14	12	18	27	30	15	19½	25	30
14-15	10	18	22	29	11	17	25	30
15-16	10	16	22	29	9	15	23	31
16-17	10	13	21	28	9	15½	20	30
17-18	3	7	16	29	5	12	18	30
18-19	2	5	15 14	28 28	3	7	14	31
19-20	0	5	10	28	3	6	13	31
20-21	-1	4	11	29	2	6½	14	30
21-22	1	5	11	29	4	6	11	31
22-23	1	6	16	29	5	9	13	31
23-00	1	8	16	29	7	10	20	31

Declassified in Part - Sanitized Copy Approved for Release @ 50-Yr 2014/06/09 : CIA-RDP81-01043R003000180001-4
Declassified in Part - Sanitized Copy Approved for Release @ 50-Yr 2014/06/09 : CIA-RDP81-01043R003000180001-4

TABLE XI-20

CEDAR RAPIDS TO STERLING 107.8 Mc/s (1952)

Hour 75°W	October 90%	50%	10%	N	November 90%	50%	10%	N
00-01	-20	-17½	-15	22	-19	-15½	-10	12
01-02	-20	-18	-14	22	-17	-15	-11	11
02-03	-19	-16	-13	21	-18	-15	-13	10
03-04	-18	-16	-13	21	-19	-14	-10	10
04-05	-17	-15	-13	21	-16	-14½	-12	10
05-06	-17	-14	-13	21	-16	-14	-12	10
06-07	-17	-14	-12	21	-14	-13	-10	10
07-08	-17	-15	-12	21	-20	-14	-10	11
08-09	-16	-14	-12	20	-20	-14	-12	11
09-10	-17	-15	-13	21	-19	-12	- 6	13
10-11	-16	-13½	-11	22	-17	-12	- 8	15
11-12	-18	-13½	-10	24	-16	-12	- 8	16
12-13	-18	-14	-11	23	-16	-13	- 7	15
13-14	-20	-15	-11	24	-17	-13	-10	17
14-15	-19	-14	-12	22	-20	-13	-10	17
15-16	-19	-15	-14	21	-20	-14	-11	19
16-17	-21	-18	-10	24	-19	-15	-13	20
17-18	-21	-19	-15	23	-19	-15	-13	19
18-19	-22	-19	-15	23	-20	-15	-13	18
19-20	-21	-18	-15	23	-19	-17	-13	17
20-21	-21	-18	-15	23	-20	-18	-13	18
21-22	-21	-19	-14	23	-19	-17½	-14	16
22-23	-21	-19	-15	22	-20	-18	-14	15
23-00	-21	-18	-15	22	-22	-18	-13	13

TABLE XI-21

CEDAR RAPIDS TO STERLING 107.8 Mc/s (1952-53)

Hour 75°W	December 90%	50%	10%	N	January 90%	50%	10%	N
00-01	-19	-15½	-11	28	-21	-17	-12	30
01-02	-20	-15	-12	28	-20	-17	-12	30
02-03	-19	-15	-12	28	-23	-16	-11	29
03-04	-17	-15	-11	28	-20	-16	-12	28
04-05	-19	-15	-11	28	-24	-16	-12	27
05-06	-19	-15	-12	28	-20	-16	-11	26
06-07	-19	-15	-12	28	-19	-16	-13	26
07-08	-18	-15	-12	27	-20	-16	-12	26
08-09	-17	-14	-11	27	-20	-16	-13	26
09-10	-15	-12	- 9	27	-20	-14	- 9	25
10-11	-15	-12	- 8	27	-18	-13	- 9	25
11-12	-15	-12	- 3	25	-17	-12	- 7	28
12-13	-15	-12	- 1	26	-17	-12	- 5	29
13-14	-13	-11	- 3	25	-16	-13	- 7	29
14-15	-16	-12	- 8	27	-17	-13	-11	30
15-16	-16	-13	-10	27	-17	-14	-11	30
16-17	-19	-15	-11	28	-20	-16	-12	30
17-18	-22	-17	-13	29	-24	-19	-14	28
18-19	-20	-18	-13	29	-23	-19	-13	28
19-20	-22	-18	-12	28	-23	-19	-16	28
20-21	-22	-18	-13	29	-24	-20	-14	27
21-22	-21	-19	-12	29	-24	-21	-17	28
22-23	-21	-19	-11	29	-24	-20	-16	29
23-00	-20	-17	-11	29	-24	-20	-15	29

Declassified in Part - Sanitized Copy Approved for Release @ 50-Yr 2014/06/09 : CIA-RDP81-01043R003000180001-4
Declassified in Part - Sanitized Copy Approved for Release @ 50-Yr 2014/06/09 : CIA-RDP81-01043R003000180001-4

Declassified in Part - Sanitized Copy Approved for Release @ 50-Yr 2014/06/09 : CIA-RDP81-01043R003000180001-4

TABLE XI-22

FARGO TO CHURCHILL 49.7 Mc/s (1952)

Hour 90°W	October 90%	October 50%	October 10%	October N	November 90%	November 50%	November 10%	November N
00-01	10	19½	35 33	30 30	8	18½	27	30
01-02	9	19½	32 31	30 30	10	16½	28	30
02-03	8	17	29	30	11	19½	30	30
03-04	9	15½	29	30	13	21½	35	30
04-05	9	16	27	30	12	20	30	30
05-06	10	16	26	30	13	20½	31	30
06-07	12	18	27	30	12	22	33	30
07-08	12	19½	27	30	12	23	31	30
08-09	12	19½	27	30	14	22	30	30
09-10	14	22	31	30	15	24	30	29
10-11	12	21	32	30	18	24	31	29
11-12	11	21	30	30	18	24½	30	30
12-13	14	22	28	29	19	24	31	30
13-14	13	21	27	29	18	26	30	29
14-15	13	21	26	28	18	25½	32	30
15-16	13	19	24	29	15	23	29	30
16-17	11	17	24	30	16	21	29	30
17-18	10	15½	23	30	15	21½	31	30
18-19	10	15	23	30	11	20	28	29
19-20	8	13½	21	30	10	17	28	29
20-21	10	14	22	30	8	16	30	29
21-22	10	15	22	29	11	17 16½	29 28	30 30
22-23	9	19	25	30	9	17½	28	30
23-00	11	19½	28	30	9	17	25	30

TABLE XI-23

FARGO TO CHURCHILL 49.7 Mc/s (1952-53)

Hour 90°W	December 90%	December 50%	December 10%	December N	January 90%	January 50%	January 10%	January N
00-01	11	18	30	31	11	16	24	30
01-02	11	20	31	31	10	18½	28	30
02-03	11	21	32	31	10	20	28	29
03-04	14	23	35 34	31 31	11	19½	28	28
04-05	12	21	33	31	11	23	32	28
05-06	14	22 21	31 30	31 31	13	22½	32	28
06-07	13	21	40 37	31 31	14	24	32	28
07-08	13	20	37	31	11	25	34	28
08-09	15	22	34	31	11	22½	32	28
09-10	17	26	36	31	15	23	32	28
10-11	20	26	38	31	17	25½	30	28
11-12	20	27	34	31	16	25	30	29
12-13	20	28	36	31	18	26	33	29
13-14	19	27	34	31	18	24	31	30
14-15	21	25	32	31	16	23	31	30
15-16	18	26	36	31	14	24	30	30
16-17	14	24	35	31	11	22½	30	30
17-18	13	24	34	30	10	22	30	30
18-19	14	20	32	30	9	21	27	30
19-20	11	18	32	31	8	16	28	30
20-21	10	19	28	31	7	15	23	29
21-22	9	19	28	31	7	14	22	29
22-23	8	21	31	31	7	14	24	29
23-00	9	19	31	31	8	14	23	29

TABLE XI-24

FARGO TO CHURCHILL 49.7 Mc/s (1953)

Hour 90°W	February 90%	50%	10%	N	March 90%	50%	10%	N
00-01	12	18	27	27	7	18	34 31	27 27
01-02	11	20½	31	28	8	18	32	27
02-03	11	22	35	28	7	19 17	26	27 27
03-04	15	24½	34	28	7	19	27	27
04-05	15	24	33	28	7	19	29	27
05-06	15	22	33	28	11	20	32	27
06-07	16	23½	33	28	11	20	27	27
07-08	14	22½	32	28	12	19	26	27
08-09	15	20½	30	28	13	17	27	29
09-10	14	23½	31	28	14	19	25	30
10-11	15	25½	30	28	13	18	25	30
11-12	15	26	32	28	13	19	23	28
12-13	18	26	29	28	13	19	23	29
13-14	19	24	30	28	14	18	25	29
14-15	21	24	29	28	14	19½	27	30
15-16	18	24½	31	28	12	20	27	29
16-17	16	24	31	28	13	20	27	29
17-18	12	20	26	28	9	19	26	29
18-19	12	20½	31	28	10	17 16	26	29 29
19-20	13	19 18½	29	28 28	9	13	25	29
20-21	11	17½	26	28	9	15	21	29
21-22	12	15½	25	28	9	15	24 23	29 29
22-23	9	14	28 27	28 28	8	18	27	27
23-00	11	15½	29	28	9	19	35 27	27 27

TABLE XI-25

ANCHORAGE TO BARROW 24.325 Mc/s (1953)

Hour 150°W	March 90%	50%	10%	N	April 90%	50%	10%	N
00-01	33	49 35½	79 53	31 28	33	52 40	83 50	29 29
01-02	34	60 37	73 53	31 28	35	47 41½	79 50	28 28
02-03	34	50 40	86 60	31 27	36	49 39	80 52	29 29
03-04	33	44 42	84 55	31 30	34	44 40	75 52	29 29
04-05	33	43 39	63 48	31 31	34	41 39	75 52	29 29
05-06	32	37	80 45	31 31	34	39 38	75 48	29 29
06-07	31	37	68 45	31 31	34	37½ 37	65 46	28 28
07-08	32	36 35	57 42	31 31	34	37 36½	43 39	28 28
08-09	28	33	47 41	31 31	29	35	38	28
09-10	24	32	37	31	28	33½	37	30
10-11	21	31½	35	30	28	32	39	29
11-12	18	31	33	31	26	33½	38	28
12-13	19	29½	33	30	26	33	38	29
13-14	19	29	36	31	24	33	37	29
14-15	24	30	37	31	21	32	36	29
15-16	24	29	35	29	23	30½	37	30
16-17	20	29	36	30	25	30	34	30
17-18	23	29	41 40	31 31	24	30	40	30
18-19	27	31	47 40	31 30	26	30½	38	30
19-20	28	33	51	31	27	30½ 30	45 36	30 30
20-21	30	33	56 42	31 31	29	32½ 31½	68 47	30 30
21-22	30	34	75 49	30 30	30	34½ 32½	55 39	30 30
22-23	30	34½ 34	77 44	30 29	31	35½ 33½	78 42	30 30
23-00	31	46½ 34	77 48	30 28	33	45½ 37½	84 52	30 30

Declassified in Part - Sanitized Copy Approved for Release @ 50-Yr 2014/06/09 : CIA-RDP81-01043R003000180001-4

TABLE XI-26

ANCHORAGE TO BARROW 24.325 Mc/s (1953)

Hour 150°W	May 90%	May 50%	May 10%	May N	June 90%	June 50%	June 10%	June N
00-01	33	39 37	85 47	31 26	36	43 41	73 46	30 29
01-02	34	43 37	85 45	31 27	38	47 42	75 47	30 29
02-03	35	39 37	84 42	31 25	38	45½ 41	82 47	30 29
03-04	35	47 39	81 47	31 26	39	47 42	82 48	30 27
04-05	35	47 40	72 49	31 29	40	48 45	83 51	30 29
05-06	38	45 42	75 49	31 29	40	45	75 51	30 29
06-07	38	42 40½	81 48	31 29	40	44	53 49	29 28
07-08	37	41 40½	47 46	31 30	41	44	58 48	29 29
08-09	36	41 40	50 44	31 31	40	44 42½	50 48	30 30
09-10	33	40	46	30	39	42½	48	30
10-11	35	40	49 48	30 30	39	43	48	30
11-12	31	40 39	44	31 31	39	44 43½	49	30 30
12-13	31	39 38	46 43	31 31	37	43	49	30
13-14	26	39	73 44	31 31	36	40½	48 47	30 30
14-15	30	36	45 41	31 31	36	40	47 46	30 30
15-16	30	36 35	50 43	31 31	37	39½	46	30
16-17	29	35 34	58 43	31 30	34	40	48	30
17-18	29	34	41 39	31 30	31	38	45	30
18-19	29	33	49 38	31 30	32	39 38	52 48	30 30
19-20	30	37 33½	68 41	31 30	32	39 38	62 44	30 30
20-21	31	34	61 38	31 29	32	38 37	62 44	30 28
21-22	31	34 33	62 38	31 31	33	39 37	44 42	29 27
22-23	32	37 35	72 42	31 30	34	38 37	72 42	28 27
23-00	34	39 38	77 48	31 29	35	38 37	80 40	30 27

TABLE XI-27

ANCHORAGE TO BARROW 48.87 Mc/s (1952)

Hour 150°W	October 90%	October 50%	October 10%	October N	November 90%	November 50%	November 10%	November N
00-01	6	17	25	31	8	15	31 30	29 29
01-02	9	19	27	31	10	17	32 31	29 29
02-03	12	19	28	31	8	18	36	29
03-04	11	18	30	31	9	17	34	29
04-05	10	17	26	31	10	18	30	29
05-06	12	17	27	31	10	19	29	29
06-07	11	19	26	31	10	19	35	29
07-08	13	20	27	31	9	17	32	29
08-09	13	20	32	31	8	19½	32	30
09-10	12	20½	31	28	7	18	35	30
10-11	13	21	30	29	8	17	32	29
11-12	11	21	29	29	8	17	32	29
12-13	13	19	27	30	9	16	30	29
13-14	13	20	27	30	11	16½	29	28
14-15	13	20	26	29	10	17	28	30
15-16	11	18	27	31	9	19½	30	30
16-17	10	19	27	30	8	19½	34	30
17-18	9	19	26	29	8	18	28	29
18-19	8	16	23	29	7	16	25	30
19-20	7	14	25	29	7	13½	21	30
20-21	6	13	23	28	6	10½	21	30
21-22	6	12	23	29	5	9	19	29
22-23	5	12	32	29	5	12	21	30
23-00	6	14	26	30	5	12	31 30	30 30

Declassified in Part - Sanitized Copy Approved for Release @ 50-Yr 2014/06/09 : CIA-RDP81-01043R003000180001-4
Declassified in Part - Sanitized Copy Approved for Release @ 50-Yr 2014/06/09 : CIA-RDP81-01043R003000180001-4

TABLE XI-28

ANCHORAGE TO BARROW 48.87 Mc/s (1952-53)

Hour 150°W	December 90%	50%	10%	N	January 90%	50%	10%	N
00-01	7	15	26	31	4	11	26	31
01-02	9	19	30	31	7	14	26	31
02-03	12	20½	33	30	4	17	30	31
03-04	10	22½	32	30	4	14	29	31
04-05	13	23½	39	30	5	13	27	31
05-06	14	21	35	31	6	14	33	31
06-07	12	19	36	31	5	14	30	31
07-08	9	15	31	31	5	14	29	31
08-09	8	18	34	30	5	13	33	31
09-10	8	21	32	31	7	20	30	31
10-11	11	23	34	31	8	18	28	30
11-12	10	21½	33	30	7	17	23	29
12-13	11	21	35	30	5	15	28	31
13-14	10	21	36	29	7	14½	27	30
14-15	8	21½	32	30	7	13	26	31
15-16	7	20½	34	30	6	14	31	31
16-17	7	23	35	31	4	14	25	31
17-18	8	21	33	30	4	13	27	31
18-19	8	16	33	31	6	13	25	31
19-20	7	16	29	31	5	12	26	31
20-21	6	13	23	31	3	10	19	31
21-22	3	11	25	31	4	8	18	31
22-23	8	13	24	31	3	9	19	31
23-00	6	14	27	31	3	10	19	31

TABLE XI-29

ANCHORAGE TO BARROW 48.87 Mc/s (1953)

Hour 150°W	February 90%	50%	10%	N	March 90%	50%	10%	N
00-01	8	15	31	28	9	17 15	29	31 31
01-02	8	19½	33	28	8	19	31	31
02-03	10	21½	32	28	11	18	34	31
03-04	11	19½	33	28	11	18	30	31
04-05	10	20½	34	28	10	17	31	31
05-06	10	20	31	28	9	18	31	31
06-07	11	19	33	28	9	20	29	31
07-08	9	18	28	28	10	17	29	31
08-09	11	16	26	28	12	19	30	31
09-10	11	18	28	28	13	20	31	31
10-11	13	19	29	27	12	22	29	31
11-12	11	20	29	28	12	22	31	31
12-13	16	22	32	27	12	20	27	31
13-14	14	24	31	28	13	19½	28	30
14-15	13	24	32	28	14	21	26	31
15-16	13	22	34	27	14	21	30	31
16-17	13	19½	32	28	15	19	27	30
17-18	10	20	31	28	11	19	26	29
18-19	10	18	31	28	11	19	24	31
19-20	9	15	25	28	7	15	22	31
20-21	7	17 16½	23	28 28	7	13	23	31
21-22	5	15 14½	22	28 28	9	16	21	31
22-23	7	16	28 25	28 28	7	13	29 26	31 31
23-00	7	17½	29	28	7	15	30 28	31 31

Declassified in Part - Sanitized Copy Approved for Release @ 50-Yr 2014/06/09 : CIA-RDP81-01043R003000180001-4
Declassified in Part - Sanitized Copy Approved for Release @ 50-Yr 2014/06/09 : CIA-RDP81-01043R003000180001-4

TABLE XI-30

ANCHORAGE TO BARROW 48.87 Mc/s (1953)

Hour 150°W	April 90%	50%	10%	N	May 90%	50%	10%	N
00-01	10	16	27	29	15	23 22	64 35	30 30
01-02	12	20	28	29	16	22½	37 33	30 30
02-03	13	21	30	29	15	22 21½	38 34	30 30
03-04	13	22	31	29	18	24½ 24	35 34	30 30
04-05	14	21	29	30	17	24½	33	30
05-06	13	19	27	29	17	25	36	30
06-07	13	17	29	30	16	25½	33	30
07-08	13	17	27	30	15	22½	37	30
08-09	12	18½	27	30	15	24	32	29
09-10	13	17½	25	30	17	25½	32	30
10-11	13	18	25	30	17	27	34	31
11-12	14	18½	26	30	20	27	37	31
12-13	14	20	24	29	19	26	36	31
13-14	15	20	27	30	17	26	35	31
14-15	14	19	26	29	17	24	29	30
15-16	13	18	25	29	14	26	33	31
16-17	12	18½	23	30	17	25	37	31
17-18	13	19	24	29	15	22	34	31
18-19	12	19	24	29	14	20	31	30
19-20	12	16½	22	28	14	20½	33	30
20-21	11	14	22	27	13	18	32	30
21-22	10	14	21	29	13	18	26	29
22-23	10	14	23 21	29 29	12	19½	32 31	30 30
23-00	11	17	27 26	29 29	15	23½ 23	37	30 30

TABLE XI-31

ANCHORAGE TO BARROW 48.87 Mc/s (1953)

Hour 150°W	June 90%	50%	10%	N
00-01	19	31	46	29
01-02	20	33	48	28
02-03	17	32	51 45	29 29
03-04	17	32	53 42	29 29
04-05	19	30	52 43	29 29
05-06	18	31	44 43	29 29
06-07	16	28	44 42	28 28
07-08	21	31½	42	28
08-09	26	35	46	29
09-10	28	34	48	29
10-11	28	34½	47	30
11-12	26	35	47	30
12-13	26	35	49	30
13-14	24	33	48	30
14-15	24	30	42	30
15-16	22	32	46	30
16-17	23	29½	46	30
17-18	19	28	48	29
18-19	18	26	51	29
19-20	20	28	41	29
20-21	16	29	38	29
21-22	16	29	37	29
22-23	19	29	38	29
23-00	20	30	40	28

Declassified in Part - Sanitized Copy Approved for Release @ 50-Yr 2014/06/09 : CIA-RDP81-01043R003000180001-4
Declassified in Part - Sanitized Copy Approved for Release @ 50-Yr 2014/06/09 : CIA-RDP81-01043R003000180001-4

TABLE XI-30

ANCHORAGE TO BARROW 48.87 Mc/s (1953)

Hour 150°W	April 90%	50%	10%	N	May 90%	50%	10%	N
00-01	10	16	27	29	15	23 22	64 35	30 30
01-02	12	20	28	29	16	22½	37 33	30 30
02-03	13	21	30	29	15	22 21½	38 34	30 30
03-04	13	22	31	29	18	24½ 24	35 34	30 30
04-05	14	21	29	30	17	24½	33	30
05-06	13	19	27	29	17	25	36	30
06-07	13	17	29	30	16	25½	33	30
07-08	13	17	27	30	15	22½	37	30
08-09	12	18½	27	30	15	24	32	29
09-10	13	17½	25	30	17	25½	32	30
10-11	13	18	25	30	17	27	34	31
11-12	14	18½	26	30	20	27	37	31
12-13	14	20	24	29	19	26	36	31
13-14	15	20	27	30	17	26	35	31
14-15	14	19	26	29	17	24	29	30
15-16	13	18	25	29	14	26	33	31
16-17	12	18½	23	30	17	25	37	31
17-18	13	19	24	29	15	22	34	31
18-19	12	19	24	29	14	20	31	30
19-20	12	16½	22	28	14	20½	33	30
20-21	11	14	22	27	13	18	32	30
21-22	10	14	21	29	13	18	26	29
22-23	10	14	23 21	29 29	12	19½	32 31	30 30
23-00	11	17	27 26	29 29	15	23 23	37	30 30

TABLE XI-31

ANCHORAGE TO BARROW 48.87 Mc/s (1953)

Hour 150°W	June 90%	50%	10%	N
00-01	19	31	46	29
01-02	20	33	48	28
02-03	17	32	51 45	29 29
03-04	17	32	53 42	29 29
04-05	19	30	52 43	29 29
05-06	18	31	44 43	29 29
06-07	16	28	44 42	28 28
07-08	21	31½	42	28
08-09	26	35	46	29
09-10	28	34	48	29
10-11	28	34½	47	30
11-12	26	35	47	30
12-13	26	35	49	30
13-14	24	33	48	30
14-15	24	30	42	30
15-16	22	32	46	30
16-17	23	29½	46	30
17-18	19	28	48	29
18-19	18	26	51	29
19-20	20	28	41	29
20-21	16	29	38	29
21-22	16	29	37	29
22-23	19	29	38	29
23-00	20	30	40	28

Declassified in Part - Sanitized Copy Approved for Release @ 50-Yr 2014/06/09 : CIA-RDP81-01043R003000180001-4
Declassified in Part - Sanitized Copy Approved for Release @ 50-Yr 2014/06/09 : CIA-RDP81-01043R003000180001-4

Declassified in Part - Sanitized Copy Approved for Release @ 50-Yr 2014/06/09 : CIA-RDP81-01043R003000180001-4

Reprinted from the PROCEEDINGS OF THE I.R.E.
VOL. 43, NO. 10, OCTOBER, 1955

PRINTED IN THE U.S.A.

Radio Transmission at VHF by Scattering and other Processes in the Lower Ionosphere*

D. K. BAILEY†, R. BATEMAN†, MEMBER, IRE, AND R. C. KIRBY†, SENIOR MEMBER, IRE

Summary—**The results of a program extending over the last four and one-half years to investigate the nature and characteristics of high-loss regular VHF propagation by means of the lower ionosphere are presented. For the most part continuous-wave transmissions are employed, with the result that the effects of the different elements in the propagation are superposed. Three different ionizing agents operating in the lower ionosphere can be distinguished by means of their differing effects on the behavior of the signal, after the exclusion of behavior associated with sporadic-*E *propagation. They are solar radiation, corpuscular radiation presumably of solar origin, and meteors. The part played by each of these is discussed in the account and interpretation of the principal results obtained. Both short- and long-term characteristics of the observed composite signals are described, as well as the results of experiments with spaced and other antenna arrangements. The intensity and nature of the signals are discussed as a function of time of day, season, geographical position of the transmission path, and level of solar activity. The dependence of the strength of the signals on path length, on frequency, and on scattering angle has been studied. In the latter connection, pulse experiments were performed with equipment permitting fairly direct height determinations, which are found to be in satisfactory agreement with earlier less direct height determinations. Attempts to compare the observations with various existing theories designed to account for the propagation as a scattering process have been made. The results are not entirely satisfactory. The role of antennas in determining the behavior of received signals is examined from the point of view of geometrical concepts of scattering beamwidth, effective scattering volume, and signal coherence. Results of measurements of the realized gain of directive antenna systems are interpreted in relation to parameters involved in the scattering geometry, the influence of meteoric ionization, and the existence of large scale inhomogeneities in the ionosphere. A discussion is given of the possibilities for application of this type of propagation to communication systems operating over distances from about 1,000 to 2,300 kilometers. Design considerations for antenna systems including siting, choice of polarization, and space diversity are given. The useful range of frequencies and certain modulation techniques are discussed. Attention is given to multipath effects associated with the scattering process, and with the presence of meteoric and auroral ionization. Reliability of performance of typical systems is estimated.**

Part I. Propagation Studies

Introduction

AN EARLY allusion to the possibility of radio-wave scattering in the lower ionosphere was made by Kennelly in 1913.[1] Little further thought seems to have been given to this matter until high-frequency communication came into general use, when Eckersley[2] began to investigate the possibility that *E*-region scattering from cloud-like electron concentrations could account for certain special effects which he and others had been observing. Eckersley proposed a theory of scattering[3] in the *E* region to account for his observations. The rapid further development of hf communications in the years that followed diverted attention to other matters, including ground scattering, and considerable time elapsed before further systematic propagation studies such as those now reported were undertaken.

In an earlier paper[4] the preliminary results of the experimental radio transmission at 49.8 Mc/s from Cedar Rapids, Iowa, to Sterling, Va., were described. Continuously present signals were found which exhibited interesting and promising behavior during SID's and during ionospheric disturbance. A program for further experimentation was formulated at that time by the National Bureau of Standards. The results of the program, which was subsequently enlarged in various ways, are now presented together with as much interpretation as seems warranted in view of the unresolved position which exists at present in connection with various theories which have been proposed to explain the propagation.

Throughout the investigations comprising the Bureau program there has existed the dual objective of improving understanding of the propagation, and of providing directly the necessary information for the design and construction of communication systems.

Scattering Theories

A limited account of some of the available scattering theories is presented at this time in order to facilitate the discussion and interpretation of certain of the observations and experiments. It is unfortunate that methods of experimentation and observation have not been found which permit a clear-cut separation in the observations of purely propagational effects from effects related to the antenna systems employed. The various theories of scattering which have been proposed to account for the observations express, or can be used to express the scattering cross section. The scattering cross section is defined as the power scattered per unit incident power density per unit solid angle in some direction γ with respect to the direction of incidence, per unit macroscopic element of volume of the scattering medium. In proceeding from expressions for scattering

* Original manuscript received by the IRE, August 8, 1955; revised manuscript released for publication September 6, 1955, by the Director, National Bureau of Standards.

† National Bureau of Standards, Washington, D. C.

[1] A. E. Kennelly, "The daylight effect in radio telegraphy," PROC. IRE, vol. 1, pp. 39–62; July, 1913.

[2] T. L. Eckersley, "An investigation of short waves," *Jour. IEE*, vol. 67, pp. 992–1032; August, 1929.

[3] T. L. Eckersley, "Studies in radio transmission," *Jour. IEE*, vol. 71, pp. 405–454; September, 1932.

[4] D. K. Bailey, R. Bateman, *et al.*, "A new kind of radio propagation at very high frequencies observable over long distances," *Phys. Rev.*, vol. 86, pp. 141–145; April 15, 1952

Declassified in Part - Sanitized Copy Approved for Release @ 50-Yr 2014/06/09 : CIA-RDP81-01043R003000180001-4

Declassified in Part - Sanitized Copy Approved for Release @ 50-Yr 2014/06/09 : CIA-RDP81-01043R003000180001-4

cross section to transmission equations applicable to experimental situations, it has been generally assumed that only the power in the main lobe of the transmitting antenna is useful, and that the power is so sharply beamed at a small scattering volume containing the path midpoint, as shown in Fig. 1, that variations in distance and scattering angle throughout the volume are of negligible importance at the receiving location. This assumption leads to transmission equations which are independent of the transmitting antenna gain or aperture and avoids the difficult practical problem of how to perform the integration, actually required for rigor, over the entire scattering volume visible in common from the receiver and the transmitter. The fact that observed signal intensity behavior differs, and in some respects differs systematically, according to the antenna directivity used, provides observational confirmation of the importance of this difficulty. The various theories, while used to express transmission equations for very sharp transmitting beams, have nevertheless provided valuable assistance in the experimental program.

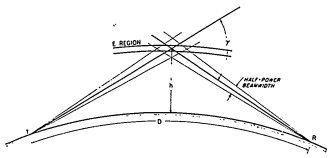

Fig. 1—Geometry of E-region scattering.

The parameters which enter all such transmission equations fall into three broad classes. First there are parameters which describe the scattering region, and with them may conveniently be included a parameter expressing the thickness of the scattering stratum. The thickness is always, and apparently correctly, taken to be small compared with the height at which scattering takes place. The disentanglement and evaluation of the parameters belonging to this class is both difficult and uncertain and has not yet been seriously attempted. In any case such attempts would be of doubtful value if the scattering theories should prove unsatisfactory when tested by means of less difficult experiments involving variation in a known manner of the geometric parameters characterizing the path of propagation. If the frequency used and the plasma frequency corresponding to the mean electron density of the scattering region are included for convenience with the purely geometric parameters such as ray-length and scattering angle, a second class of parameter is defined. Included implicitly in this class is the height at which the scattering takes place. The final class of parameters involves the terminal installations and includes the power radiated, the directivity of the transmitting antenna, the polarization employed, and the aperture of the receiving antenna.

Ideally to evaluate the effect on transmission of a particular parameter in the transmission equation it should be caused or allowed to vary in a known manner while all other parameters are held constant. This is not possible in the case of the parameters descriptive of the ionospheric stratum responsible for the received signals, and knowledge of them is therefore rather difficult to obtain. On the other hand, by making observations and performing experiments with sufficient simultaneity and using whenever possible the same scattering volume, it is possible to investigate the dependence of the scattering on the geometric variables. and the frequency. By using this investigating principle, the effects of the unknown but identical or nearly identical ionospheric parameters are minimized in the ratios of observations which are used. It is through systematic exploitation of this technique that much of the information about the height of the scattering stratum and the dependence of the strength of the received signals on frequency and scattering angle has been obtained.

In examining the various theories available in the literature, which may be called upon in connection with the interpretation of the observations, it is useful first to define the following quantities:

P_r = the received available power,
P_t = the power radiated by the transmitting antenna,
l = the ray distance from the path midpoint in the scattering stratum to the receiver,
f = the frequency of the transmitted wave,
f_N = the plasma frequency corresponding to the mean electron density, N, in the scattering volume,
γ = the scattering angle, defined as the difference in the direction of the incident wave and the received scattered wave,
A = the aperture of the receiving antenna, and
χ = the angle between the incident electric vector and the direction of the scattered wave.

Utilizing these quantities, transmission relations can be indicated. Application of the Booker-Gordon scattering theory[5] to the ionosphere[4] leads to the following:

$$\frac{P_r}{P_t} \propto \left(\frac{f_N}{f}\right)^4 \frac{A \sin^2 \chi}{l^2 \left(\sin \frac{\gamma}{2}\right)^5}. \tag{1}$$

On the other hand an extension of Eckersley's earlier E-region scattering model[3] leads to a transmission relation of the form:

$$\frac{P_r}{P_t} \propto \frac{f_N^4}{f^8} \frac{A \sin^2 \chi}{l^2 \left(\sin \frac{\gamma}{2}\right)^9}. \tag{2}$$

[5] H. G. Booker and W. E. Gordon, "A theory of radio scattering in the troposphere," PROC. IRE, vol. 38, pp. 401–412; April, 1950.

The geometric behavior of these two transmission equations is displayed as a function of path length in Fig. 2, in which the effect of the height of the scattering

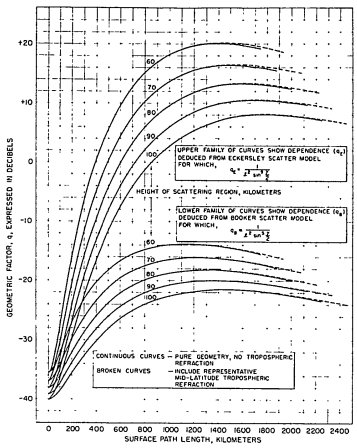
+20
+10
0
-10
-20
-30
-40
60
70
80
90
100
UPPER FAMILY OF CURVES SHOW DEPENDENCE (q_E) DEDUCED FROM ECKERSLEY SCATTER MODEL FOR WHICH, $q_E \propto \frac{1}{f^4 \sin^2 \frac{\gamma}{2}}$
HEIGHT OF SCATTERING REGION, KILOMETERS
LOWER FAMILY OF CURVES SHOW DEPENDENCE (q_B) DEDUCED FROM BOOKER SCATTER MODEL FOR WHICH, $q_B \propto \frac{1}{f^4 \sin^2 \frac{\gamma}{2}}$
CONTINUOUS CURVES — PURE GEOMETRY, NO TROPOSPHERIC REFRACTION
BROKEN CURVES — INCLUDE REPRESENTATIVE MID-LATITUDE TROPOSPHERIC REFRACTION
GEOMETRIC FACTOR, q, EXPRESSED IN DECIBELS
0 200 400 600 800 1000 1200 1400 1600 1800 2000 2200 2400
SURFACE PATH LENGTH, KILOMETERS

Fig. 2—Geometric factor q for midpoint scattering.

stratum is also shown. For this purpose geometric factors, q, are defined as follows:

$$q_B = \frac{1}{l^2 \left(\sin \frac{\gamma}{2}\right)^5}, \tag{3}$$

and

$$q_E = \frac{1}{l^2 \left(\sin \frac{\gamma}{2}\right)^9}. \tag{4}$$

Turning now to that portion of the more recent work of Villars and Weisskopf[6] which applies a theory of homogeneous turbulence to the lower ionosphere, the following approximate transmission relations can be obtained as limiting cases:

$$\frac{P_r}{P_t} \propto \frac{f_N^4}{f^{13/3}} \frac{A \sin^2 \chi}{l^2 \left(\sin \frac{\gamma}{2}\right)^{16/3}}, \tag{5}$$

[6] F. Villars and V. F. Weisskopf, "The scattering of electromagnetic waves by turbulent atmospheric fluctuations," *Phys. Rev.*, vol. 94, pp. 232–240; April 15, 1954.

and

$$\frac{P_r}{P_t} \propto \frac{f_N^4}{f^{11}} \frac{A \sin^2 \chi}{l^2 \left(\sin \frac{\gamma}{2}\right)^{12}}. \tag{6}$$

When f is small (5) applies, and as a practical matter (5) differs but slightly from (1). As f becomes greater the transmission is described by a transition relationship which in the limit for large values of f becomes (6). The meaning of small and large f will be discussed later.

Eq. (1) was developed on the basis of evidence of irregular distribution and irregular motion of ionization in the lower ionosphere taken from such observations as the fading of single reflected waves, the optically observed behavior of long-enduring meteor trails, and the known presence of a strong temperature inversion in the lower E region. The exponential autocorrelation function chosen originally to describe the isotropy of tropospheric turbulence, though not necessarily implausible, is arbitrary and was selected in part for its mathematical convenience. The application to the ionosphere is even more arbitrary and perhaps less plausible. On the other hand the model used for (2) originated many years earlier and was arrived at by means of a wave-mechanical analogy with α-particle scattering. Eq. (2) illustrates nicely what different results can be obtained with different models, a matter which has been pointed out by Staras.[7] Eqs. (1) and (2) predict a constant but different frequency dependence and from them the q-curves of Fig. 2 have been constructed. The exactness implied by them has not been observed, but the difference between them and the results of observation has been a stimulating influence in the interpretation of the observations. Eqs. (5) and (6), based on recent work on the statistical theory of homogeneous turbulence, provide more flexibility in making comparisons with observations since they indicate that both frequency and angle dependence are variable according to the frequency and the state of the scattering region. As will be seen below, it is the latter situation which corresponds more closely albeit nebulously, to the observational results. It is of interest to note that the quantity f_N enters all the transmission equations in the same way. It is this quantity which is supposed to be related directly to the intensity of the solar ultraviolet ionization of the lower E region, and which should respond to long-term changes in the level of solar activity, as well as to such short-term events as SID's.

In addition to the scattering theories discussed above, theories involving partial reflection associated with steep gradients of ionization have been advanced to account for the observations.[8,9] In order for these to

[7] H. Staras, "Scattering of electromagnetic energy in a randomly inhomogeneous atmosphere," *Jour. Appl. Phys.*, vol. 23, pp. 1152–1156; October, 1952.
[8] J. Feinstein and C. Salzberg, private communication, July, 1952.
[9] E. V. Appleton and W. J. G. Beynon, "An ionospheric attenuation equivalence theorem," *Jour. Atmos. Terr. Phys.*, vol. 6, pp. 141–148; March, 1955.

Declassified in Part - Sanitized Copy Approved for Release @ 50-Yr 2014/06/09 : CIA-RDP81-01043R003000180001-4

Declassified in Part - Sanitized Copy Approved for Release @ 50-Yr 2014/06/09 : CIA-RDP81-01043R003000180001-4

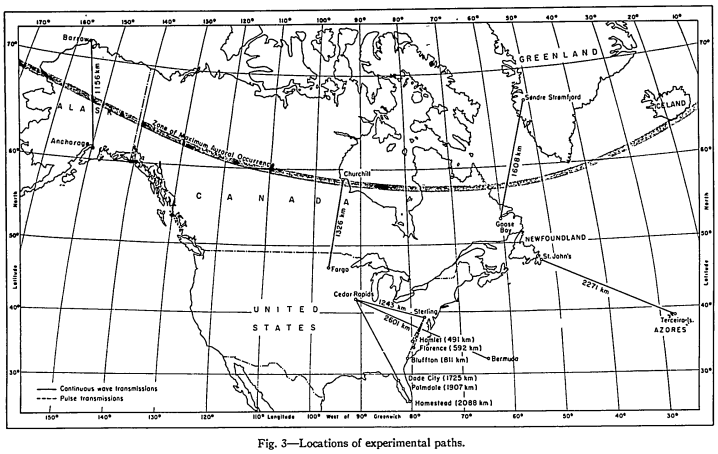

Fig. 3—Locations of experimental paths.

explain the observed fading characteristics, however, it is necessary to introduce either a fine structure of moving and changing irregularities in the gradients or to assign to some of the "constants" of gradient reflection theory an irregular time and space variation. Thus application of partial-reflection theories needs addition of features which can give rise to scattering.

Yet another school of thought exists which accounts for the observations as primarily or entirely the consequence of reflection or scattering at oblique incidence from many meteor trails, in the common volume, overlapping in time.[10–12] Such a view is based on experiments having either very different path geometry or employing much lower frequencies and using less directive antennas. Meteors are one of three major influences on the signals observed and their role will be discussed in due course. The presence of meteoric signals unfortunately adds further complications to the interpretation of the measurements.

As indicated in an earlier paper[4] the received signals are complex and it is certain that meteoric events, at times, and under certain circumstances make an important contribution to the mean signal level. Caution is therefore required in the interpretation of observational results, since none of the above transmission equations is applicable to the more easily recognizable meteoric components of the signal.

Experimental Arrangements

Much of the program has consisted in nearly continuous recording of horizontally polarized continuous-wave transmissions. This has involved several different paths (shown in Fig. 3 above) and operation at several different frequencies. Details are in Table I (facing). For the most part they have been operated at about 40 kilowatts input and all the signal-intensity data presently exhibited have been adjusted for a power level of 30 kilowatts at the transmitting antenna. In general identical rhombic antennas for each path have been used for transmitting and receiving. These antennas, of extreme design, were based on Harper's work.[13] Their plane-wave gains have been of the order of 17 to 20 decibels with reference to horizontal half-wave dipoles at the same height. Exceptions to this arrangement have existed. For the two-frequency comparisons on the Anchorage to Barrow path, horizontal five-element Yagi antennas were employed because of space limitations. For the test path from Goose Bay to Sondre Stromfjord, where vertical polarization was experimented with, vertical half-rhombics, vertical dual corner reflectors, and vertical full rhombics were variously employed.[14] From this latter path, because of the fre-

[10] D. W. R. McKinley, "Dependence of integrated duration of meteor echoes on wavelength and sensitivity," *Can. Jour. Phys.*, vol. 32, pp. 450–467; July, 1954.

[11] V. R. Eshleman, L. A. Manning, A. M. Peterson, and O. G. Villard, Jr., "The role of meteors in extended-range VHF propagation," 1955 IRE Convention Record, Part 1, "Antennas and Propagation," pp. 61–62.

[12] V. R. Eshleman, L. A. Manning, A. M. Peterson, and O. G. Villard, Jr., "The Role of Meteoric Ionization in Extended-Range VHF Propagation," Talk presented at URSI-IRE Meetings, Washington, D. C., May, 1955.

[13] A. E. Harper, "Rhombic Antenna Design," D. Van Nostrand Company, Inc., New York, N. Y., 1941.

[14] R. Bateman, D. K. Bailey, and J. A. Waldschmitt, private communication, August, 1955.

TABLE II
Details of Experimental Paths

	Cedar Rapids–Sterling			Anchorage–Barrow			Fargo–Churchill	Goose Bay–Sondre Stromfjord	St. Johns–Terceira
Frequency, Mc/s	49.800[1]	107.800	27.775	48.870	48.870	24.325	49.700	48.020	36.000
Date of commencement	January 23, 1951	December 4, 1951	May 6, 1953	August 28, 1951	March 2, 1953	February 16, 1953	August 29, 1951	April 1, 1952	October 4, 1954
Date of termination	Continues in operation	January 31, 1953	Continues in operation part time	June 30, 1953	June 30, 1953	June 30, 1953	March 31, 1953	November 30, 1953	September 30, 1955
Transmitter location coordinates of site	Cedar Rapids, Iowa 41°52′N; 91°41′W	←Same	←Same	Anchorage, Alaska 61°7′N; 149°42′W	←Same	←Same	Fargo, North Dakota 46°55′N; 96°46′W	Goose Bay, Labrador 53°17′N; 60°25′W	St. Johns, Newfoundland 47°32′N; 52°42′W
Receiver location coordinates of site	Sterling, Virginia 38°59′N; 77°29′W	←Same	←Same	Barrow, Alaska 71°18′N; 156°45′W	←Same	←Same	Churchill, Manitoba 58°44′N; 94°05′W	Sondre Stromfjord, Greenland 66°58′N; 50°55′W	Terceira Island, The Azores 38°45′N; 27°14′W
Surface path length (great circle)	1,243 km. 773 st. mi.	←Same	←Same	1,156 km. 718 st. mi.	←Same	←Same	1,326 km. 824 st. mi.	1,608 km. 999 st. mi.	2,271 km. 1,411 st. mi.
Geographic coordinates of path midpoint	40°39′N; 84°26′W	←Same	←Same	66°20′N; 152°31′W	←Same	←Same	52°50′N; 95°36′W	60°12′N; 56°39′W	44°51′N; 40°54′W
Geomagnetic latitude of path midpoint	51°38′N	←Same	←Same	65°02′N	←Same	←Same	62°42′N	70°46′N	54°40′N
True azimuth of transmitter from receiver	289°30′	←Same	←Same	160°55′	←Same	←Same	188°56′	203°18′	303°44′
True azimuth of receiver from transmitter	109°17′	←Same	←Same	347°24′	←Same	←Same	6°47′	15°01′	106°07′
Type of antennas	Rhombic-Rhombic	←Same	←Same	←Same	Yagi-Yagi	←Same	Rhombic-Rhombic	Various	Pairs of Yagis Stacked Vertically
Elevation of maximum of main lobe, degrees	7.0	←Same	←Same	5.7[2]	6.4[2]	6.4[2]	5.4	—	T +0.44 R −0.15
Height, feet	41	19	73	50	45	90	52	—	T 880 R 2240
Leg length, feet	500	230	897	500	—	—	500	—	—
Plane-wave gain, relative to dipole at same height, decibels	18	18	18	18	9	9	18	—	12
Attenuation[3] relative to inverse-distance-squared law, represented by received signal intensity of 1.0 microvolt, decibels.	122	115	127	123	105	111	122	—	112

[1] 49.600 Mc/s used from January 17, 1952 through March 31, 1952.
[2] Includes effect of sloping site at Anchorage.
[3] Received open-circuit antenna voltage measured at 600 ohms impedance (−154 dbw). Reference power to transmitting antenna is 30 kw.

Declassified in Part - Sanitized Copy Approved for Release @ 50-Yr 2014/06/09 : CIA-RDP81-01043R003000180001-4

Declassified in Part - Sanitized Copy Approved for Release @ 50-Yr 2014/06/09 : CIA-RDP81-01043R003000180001-4

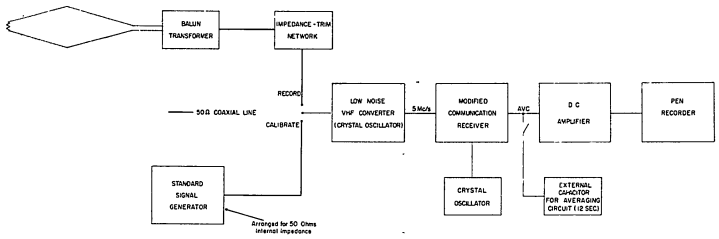

Fig. 4—Routine recording arrangement.

quent changes in the observing arrangements, only sporadic-E transmission data are presented. All antennas used were designed to have their first lobe maxima directed toward the E region at the path midpoint.

Routine reception and recording were performed in accordance with the receiving arrangement shown in Fig. 4, or with an equivalent arrangement. All data are adjusted for an equivalent lossless line impedance of 600 ohms, though later in the program reception was performed at 50 ohms. For the signal-intensity observations the continuous-wave emissions were recorded using a predetection receiver bandwidth of approximately 2 kc/s, and a post-detection RC averaging circuit having a time constant of 12 seconds. The recording receiver arrangement provided an output approximately proportional to the logarithm of the average input signal voltage. The 12-second time constant, while serving to smooth most of the rapid signal fluctuations and thereby facilitate the reduction of the observations, is short enough to allow the more intense meteor reflections or bursts to be indicated as sharp spikes on the record along with all slow variations in signal intensity. A special experiment was performed at Sterling simultaneously on the 49.8 and 107.8 Mc/s signals using an unusual receiving arrangement in order to measure power. This experiment established the validity of interpreting the routine intensity measurements as relative power measurements. Transmissions were interrupted twice each hour to permit the background external noise, mostly cosmic noise, to be recorded. These periodic noise observations provided a valuable check on the performance of the receiving system.

The observations of received signal intensity can be interpreted in terms of transmission loss[15] and loss relative to inverse-distance attenuation. For 30 kilowatts power to the transmitting antenna, a received open-circuit antenna voltage of 1.0 microvolt at 600 ohms impedance corresponds to a transmission loss of 199 decibels. The values of attenuation relative to inverse distance presented in Table I for the experimental paths are based on the assumption that the ground at each of the terminals and the ionosphere are perfectly reflecting planes. Received power for inverse-distance squared attenuation is calculated from the following equation:

$$P_r = \frac{P_t G_t G_r \lambda^2}{(8\pi l)^2}, \qquad (7)$$

where G_r and G_t are power gains of the transmitting and receiving antenna systems, including the effects of perfect ground reflection, relative to an isotropic antenna in free space, and λ is the wavelength.

In addition to the routine observations and measurements, other experiments of relatively short duration having particular objectives in view were performed, for which pulse and other kinds of modulation were employed. Special antennas and receiving arrangements were often used. These experiments and their results are described below.

Characteristics of the Normal Signal

Short-Term Behavior

The characteristics of the normally received signals at about 50 Mc/s are substantially different from those observed over comparable paths at *HF*, *MF*, or *LF*. The signal levels reported in the measurement program are median values of the average open-circuit receiving antenna voltage resulting from reception of a transmitted unmodulated carrier. The instantaneous signal level may be above or below the average value by 20 decibels or more. Observations of signal behavior uninfluenced by the recording time constant lead to the impression that the total signal consists of a continuously present fluctuating component and transient components resulting from reflections or scattering from ionization associated with meteors.

During periods when the received signals are apparently unperturbed by meteor reflections the fading

[15] K. A. Norton, "Transmission loss in radio propagation," PROC. IRE, vol. 41, pp. 146–152; January, 1953.

rates, as observed in the output of a receiver having a bandwidth of two kilocycles, vary in a random manner principally in the range of 0.2 to 5 cycles per second. These variations of the signal level are considered to result from a scattering process in which the contributions of different elements within the effective scattering volume arrive at the receiver with relative phases that have been influenced by motions or changes of ionization. The changing relative phases at the receiver are responsible for the fading characteristics of the received signals. The fluctuation of the signal intensity when not obviously perturbed by meteoric events is adequately described by a Rayleigh distribution. There is thus always a finite probability that the signal intensity will be smaller than any specified value and that it will be smaller than this value for a finite fraction of the time over long periods. More detailed studies of the fading characteristics are presented elsewhere.[16,17]

There are two types of perturbations resulting from meteoric ionization which are easily distinguishable from the fluctuating background signal. First there are the Doppler frequencies which differ appreciably from the transmitted carrier frequency. These give rise to randomly occurring audio heterodyne whistles or beats in the output of a receiver designed for amplitude modulation reception. The heterodyne beats range in frequency from zero to several kilocycles. The Doppler frequency components are produced occasionally by reflections from the heads of ionization accompanying meteors, but much more frequently by scattering from rapidly lengthening meteor ionization trails during the process of their formation.[18,19] Special observations at Sterling have shown that considerably more than 90 per cent of the received Doppler frequencies are higher than the transmitter carrier frequency. It is also observed that most of the audio heterodyne frequencies decrease. Occasionally the Doppler frequencies pass through the carrier frequency from the high side resulting in audio heterodyne frequencies which decrease to zero beat and then increase. Relatively simple geometric considerations indicate that Doppler frequencies above the carrier should occur much more frequently and should be associated with descending audio heterodyne frequencies. Correspondingly the relatively rare ascending audio heterodyne frequencies should be associated with Doppler frequencies below the carrier frequency. A complete analysis of these observations involves much more than pure geometry and has not been attempted. The instantaneous amplitude of the Doppler

[16] G. R. Sugar, "Some fading characteristics of regular vhf ionospheric propagation," p. 1432 of this issue.

[17] R. A. Silverman and M. Balser, "Statistics of electromagnetic radiation scattered by a turbulent medium," *Phys. Rev.*, vol. 96, pp. 560–563; November 1, 1954.

[18] D. W. R. McKinley and P. M. Millman, "A phenomenological theory of radar echoes from meteors," PROC. IRE, vol. 37, pp. 364–375; April, 1949.

[19] L. C. Browne and T. R. Kaiser, "The radio echo from the head of meteor trails," *Jour. Atmos. Terr. Phys.*, vol. 4, pp. 1–4; September, 1953.

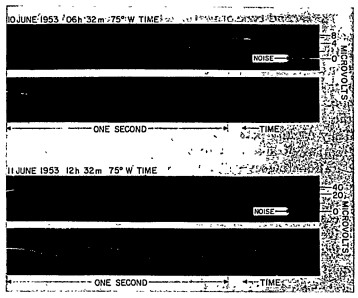

Fig. 5—Oscillograms showing typical short-term signal behavior for the Cedar Rapids to Sterling path at 49.8 Mc/s. System bandwidth is somewhat greater than 1,000 cps. Note in the early morning record interference patterns associated with meteoric reflections.

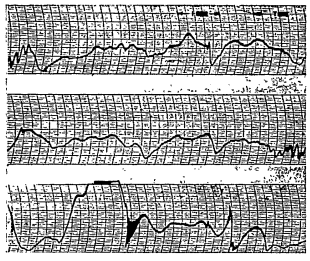

Fig. 6—Record of typical signal fading observed at Sterling at 49.8 Mc/s.

components varies over a wide range relative to the background signal. At 49.8 Mc/s most, but not all, of the Doppler components have intensities which are small relative to the simultaneously received scattered component. An occasional Doppler component will have an intensity greater than that of the scattered component. During periods of high signal intensity such as during the summer day or during strong geomagnetic disturbances the effects of the Doppler components on the composite signal are markedly reduced. In these periods, occurrences of audio-frequency heterodyne whistles may be infrequent or unobserved when conventional receiving techniques are employed. Figs. 5 and 6 (above) show typical short-term behavior of the 49.8 Mc/s signals at Sterling.

Declassified in Part - Sanitized Copy Approved for Release @ 50-Yr 2014/06/09 : CIA-RDP81-01043R003000180001-4

Declassified in Part - Sanitized Copy Approved for Release @ 50-Yr 2014/06/09 : CIA-RDP81-01043R003000180001-4

The second type of perturbation produced by meteors consists of transient but large signal enhancements resulting from reflection from columns of meteoric ionization so oriented as to present first Fresnel zones from which the scattering process more nearly resembles a specular reflection. These enhancements may exceed the fluctuating background signal by many decibels. They usually persist for periods of time ranging from a fraction of a second to several seconds. Occasionally durations of several minutes have been observed. An example occurs in a sample recording shown later in the paper. Drift velocities of meteor ionization trails are small compared to meteor velocities, and the received frequency during meteoric enhancements usually does not differ from the transmitted frequency by more than a few cycles per second.

The characteristics of the received signals are somewhat different at frequencies substantially higher or lower than 50 Mc/s. At the lower frequencies, the observed Doppler components appear to be few and smaller relative to the fluctuating background signal than at 50 Mc/s. Comparisons of recordings at 27.775, 49.8 and 107.8 Mc/s lead to the impression that the intensity of meteoric enhancements decreases more slowly with increasing frequency than does the intensity of the scattered component.

Long-Term Behavior—Middle Latitudes

In order to investigate the long-term behavior of the signals, the original propagation path of 1,243 kilometers from Cedar Rapids, Iowa, to Sterling, Va., operated at 49.8 Mc/s, has been kept in continuous service since early 1951 with routine recording performed as described above. For short periods of time 49.6 Mc/s has been used. Further details of this and other propagation-study paths are given in Fig. 3 and Table I. Over this period it has been found that the signals are always weakest in the evening period represented by about 19 to 21 hours local time at the path midpoint. This characteristic has also been found for all the other paths operated and appears to be a universal characteristic of the propagation. Despite the considerable variations in the hourly medians from day to day, the monthly medians by hours are more nearly the same for a given month from year to year, than are the monthly medians for adjacent months in the same year. Fig. 7 illustrates the diurnal variation of the monthly medians for December, March, June and September together with the upper and lower decile values in order to provide an indication of the day-to-day variation at a given hour. The strongest signals are received in the summer and the weakest at the equinoxes. The winter midday signals are about as strong as the summer midday signals, but are much weaker at other times of day. This behavior appears to be in part associated with the zenith distance of the sun. Fig. 8 (p. 1190) shows variation, by months for a period of several years, of signal intensities representative of three-hour periods centered about 00, 06, 12, and 18 hours local time at the path midpoint. The semi-annual period in the midday intensity is plainly evident, but is absent in the midnight intensities which show an annual period with a maximum in the summer. The winter midday maximum is thought to be closely connected with the winter daytime ionospheric absorption anomaly observed in mid-latitudes.

Fig. 9 (page 1191) shows the diurnal variation of very weak signal intensities observed during the period October, 1951 through September, 1952 as observed at 49.8 Mc/s for the Cedar Rapids to Sterling path. It will be noted that the diurnal minimum for these very low signal intensities also occurs during the period 19 to 21 hours local time at the path midpoint.

Fig. 10(a) (p. 1191) shows the cumulative distribution of the hourly median signal intensities throughout the year from October, 1951 through September, 1952.

Long-Term Behavior—High Latitudes

Following a short period of study of the early results from the Cedar Rapids to Sterling path it was decided to establish two further propagation study paths farther north in regions where hf communication is difficult. The path lengths were chosen to be as nearly the same as practicable as the Cedar Rapids to Sterling path, and similar frequencies were employed. The objective was to determine propagation differences associated with geographical position. The additional paths came into operation nearly simultaneously in late August, 1951 and employed antennas differing only slightly in design from those at Cedar Rapids and Sterling. The recording arrangements were identical. One of these paths, from Fargo, N. D., to Churchill, Manitoba, was somewhat longer than the Cedar Rapids to Sterling path and operated at 49.7 Mc/s. This path is subject to moderately severe auroral zone disturbance as its northern terminal lies practically at the zone of maximum auroral frequency. The other path from Anchorage to Barrow, Alaska, was somewhat shorter than the original path and operated at 48.87 Mc/s. The zone of maximum auroral occurrence crosses this path. For further details about these paths see Fig. 3 and Table I.

These new 50 Mc/s paths were found to exhibit short-term behavior of the kind described for the Cedar Rapids to Sterling path and as at Sterling the signals were found always to be present. With respect to long-term behavior, however, they revealed marked differences. In general the signal intensities were greater, and a number of special effects associated with auroras and severe geomagnetic disturbances were found. The diurnal minima were observed to occur in the evening period as

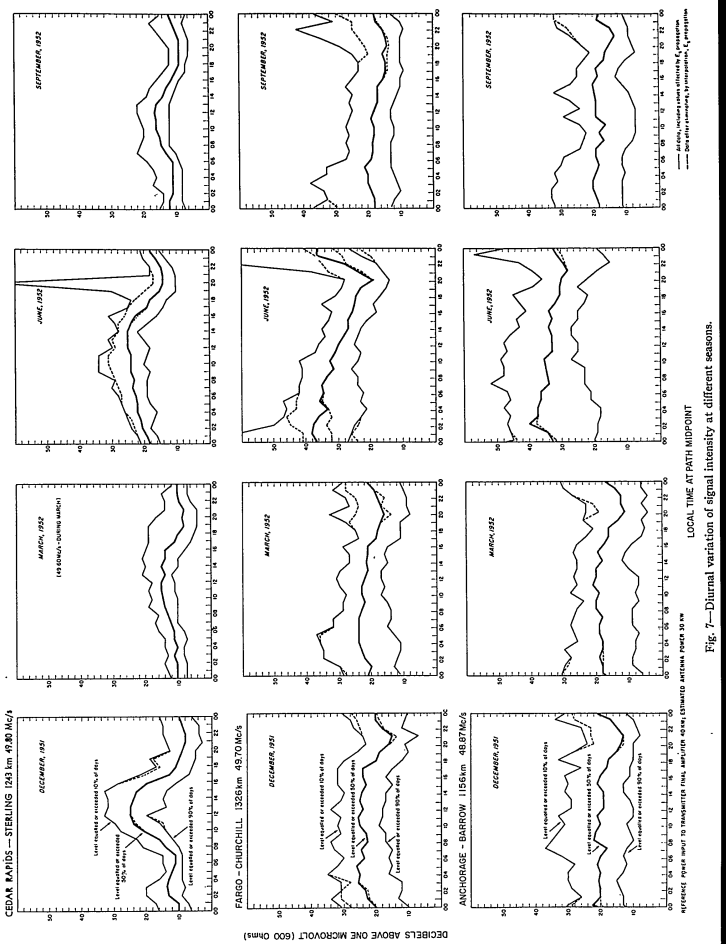
SEPTEMBER, 1952
JUNE, 1952
MARCH, 1952
DECEMBER, 1951
CEDAR RAPIDS — STERLING 1243 km 49.80 Mc/s
FARGO — CHURCHILL 1326 km 49.70 Mc/s
ANCHORAGE — BARROW 1156 km 48.87 Mc/s
DECIBELS ABOVE ONE MICROVOLT (600 Ohms)
LOCAL TIME AT PATH MIDPOINT

Fig. 7—Diurnal variation of signal intensity at different seasons.

Declassified in Part - Sanitized Copy Approved for Release @ 50-Yr 2014/06/09 : CIA-RDP81-01043R003000180001-4

Declassified in Part - Sanitized Copy Approved for Release @ 50-Yr 2014/06/09 : CIA-RDP81-01043R003000180001-4

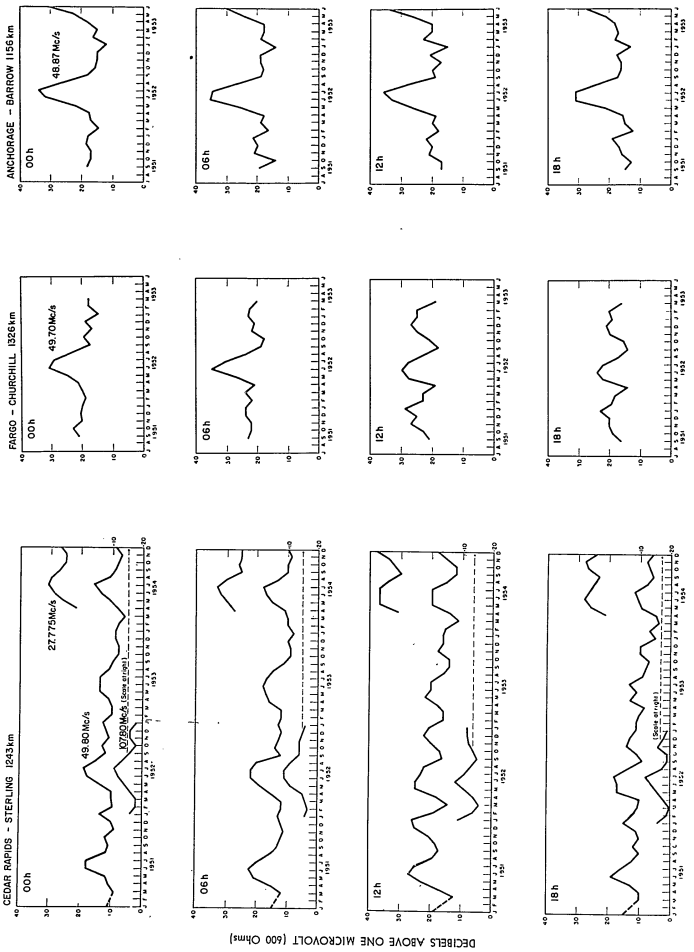

Fig. 8—Seasonal variation of signal intensity at different times of day.

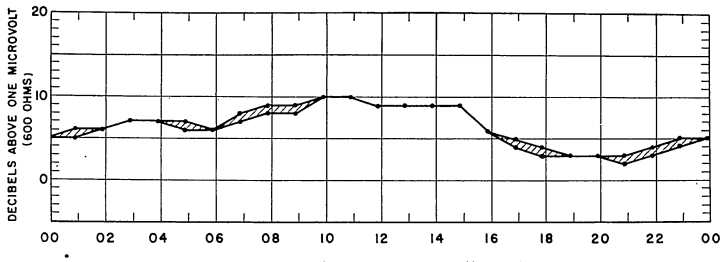

Fig. 9—Diurnal variation of very weak signal intensities observed at Sterling at 49.8 Mc/s for the year October 1951 through September 1952. The shaded areas contain the value of hourly median signal intensity equalled or exceeded 99 percent of the time for the hour shown.

at Sterling, but the hour-to-hour and day-to-day variations in median signal intensity were considerably greater. This is evident in the separation between the upper and lower deciles for December, March, June, and September shown with the corresponding monthly median signal intensities in Fig. 7. For both paths much the strongest signals were found to occur in the summer when the signals were very much stronger than at Sterling. The weakest signals occurred from February through early April, but at these times they were somewhat stronger than the minimum signals at Sterling. The times of day of maximum signal intensity were much less definite than for Sterling. Fig. 8 shows, as for the Sterling signals, the variation by months for the entire period of operation of these paths, of signal intensities representative of 00, 06, 12, and 18 hours local time. In presenting these data for comparison, the influence of sporadic-E propagation has been eliminated by interpolation when possible, and otherwise by omission. Note that the signal behavior of the two arctic paths is quite similar, but very different from that observed at Sterling. In the case of the Churchill observations for noon, some traces of the semiannual period remain.

Figs. 10(b) and 10(c) show for the arctic paths the cumulative distributions of the hourly median signal intensities from October, 1951 through September, 1952.

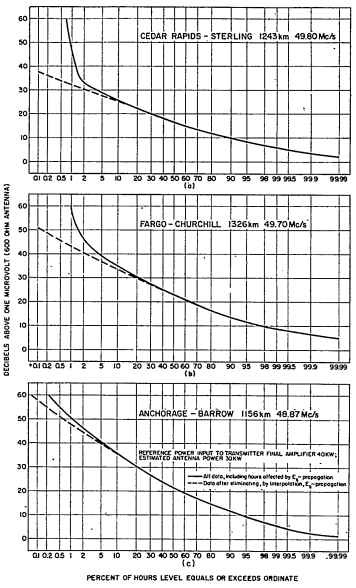
CEDAR RAPIDS – STERLING 1243km 49.80Mc/s
(a)
FARGO – CHURCHILL 1326km 49.70Mc/s
(b)
ANCHORAGE – BARROW 1156km 48.87Mc/s
REFERENCE POWER INPUT TO TRANSMITTER FINAL AMPLIFIER 40KW, ESTIMATED ANTENNA POWER 30KW
All data, including hours affected by E_s – propagation
Data after eliminating, by interpolation, E_s – propagation
(c)
DECIBELS ABOVE ONE MICROVOLT (600 OHM ANTENNA)
PERCENT OF HOURS LEVEL EQUALS OR EXCEEDS ORDINATE

Fig. 10—Cumulative distributions of the hourly median signal intensities for the year from October, 1951 through September, 1952.

Distance Dependence—Ionospheric Heights

The maximum distance over which signals can be observed by means of scattering in the lower ionosphere is a matter of some interest both from the practical viewpoint of communication applications and from the more scientific viewpoint. In the latter connection it is to be noted that the scattering angle is least for the longest paths, and that the actual length of the longest path is determined by the curvature of the earth, the effects of tropospheric refraction on the upgoing and

Declassified in Part - Sanitized Copy Approved for Release @ 50-Yr 2014/06/09 : CIA-RDP81-01043R003000180001-4

Declassified in Part - Sanitized Copy Approved for Release @ 50-Yr 2014/06/09 : CIA-RDP81-01043R003000180001-4

downcoming waves, and the height or range of heights from which the waves are returned. Fig. 11 illustrates for midpoint scattering the relationship of path length, angle of arrival or departure of the waves with respect to horizontal, and height of the scattering region for a range of scattering heights from 60 to 100 kilometers with and without allowance for tropospheric refraction. If very high antenna sites are available the maximum transmission path can be lengthened for a given ionospheric height by use of radiation which departs and arrives horizontally or at slightly negative angles with respect to horizontal.

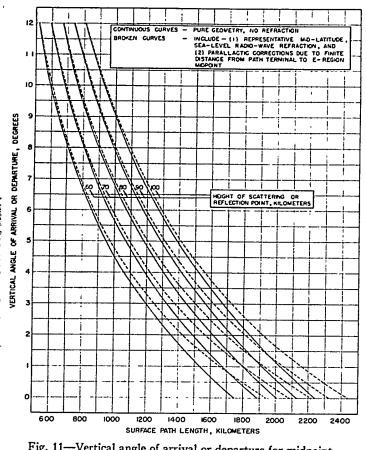
CONTINUOUS CURVES – PURE GEOMETRY, NO REFRACTION
BROKEN CURVES – INCLUDE – (1) REPRESENTATIVE MID-LATITUDE, SEA-LEVEL RADIO-WAVE REFRACTION, AND (2) PARALLACTIC CORRECTIONS DUE TO FINITE DISTANCE FROM PATH TERMINAL TO E-REGION MIDPOINT
HEIGHT OF SCATTERING OR REFLECTION POINT, KILOMETERS
VERTICAL ANGLE OF ARRIVAL OR DEPARTURE, DEGREES
SURFACE PATH LENGTH, KILOMETERS

Fig. 11—Vertical angle of arrival or departure for midpoint scattering.

All distance-dependence tests are closely related to the identification of the height or range of heights above the surface of the earth responsible for returning the waves. From the beginning of observations at Sterling, it was assumed that the heights were ionospheric and specifically that the E region was involved. There were three arguments which supported this view. Firstly, the long- and short-term variations of the signal intensity were inconsistent with the known characteristics of long-distance tropospheric propagation. Secondly, the very early observations of signal enhancement during sudden ionospheric disturbances (SID's) and the less striking evidence at Sterling (subsequently observed to be more striking on the northern paths) that signal intensities tended to be unusually great during periods of severe geomagnetic disturbance, could only be explained in ionospheric terms. The third piece of early evidence was the results of the Bermuda observations of the 49.8 Mc/s signals from Cedar Rapids made during the summer of 1951 using a five-element Yagi antenna for reception. Most of the time no signals whatever were received.

Bermuda lies nearly along the Cedar Rapids to Sterling great circle at about twice the distance of Sterling as is shown in Fig. 3. The distance of Bermuda, 2,601 kilometers, from Cedar Rapids is well beyond any possibility of single-stage propagation from any height in the E region. Furthermore, the main lobe of the transmitting antenna at Cedar Rapids intensely illuminates the F region directly above the general vicinity of Sterling. It was thus possible to compare the occasional cases of weak reception at Bermuda, which could not be related to known cases of sporadic-E propagation between Cedar Rapids and Sterling, with the $h'f$ observations at Ft. Belvoir, Va., about 50 kilometers south of Sterling. No connection was found between Bermuda reception and any unusual conditions in the F region. In particular, no evidence could be found that the cases of "spread" or scattered F-region echoes at vertical incidence which occurred during the period of the Bermuda observations were in any way associated with the occasional weak reception at Bermuda. The occurrence characteristics of the latter could, in fact, be plausibly explained as cases of sporadic-E propagation at the midpoint of the second stage. This result was accepted for the time being as sufficient evidence that the E region was primarily responsible for the propagation observed regularly on the various test paths.

During the first half of 1952 some reception tests at 49.8 Mc/s at extreme range were made in Florida at locations shown in Fig. 3. These involved the occupation, in turn, of several sites along the great circle defined by the direction of the main lobe of a specially constructed long rhombic antenna at Cedar Rapids. This antenna had a plane-wave gain, compared with a half-wave dipole at the same height, of 19 decibels, and its first ground-reflection lobe maximum occurred at an angle of elevation of 2.4 degrees. Both the gain figure and the details of the first lobe were measured by means of an aircraft. At the various stations in Florida two five-element Yagi antennas were used at heights of 40 and 100 feet respectively. The ground-reflection lobe patterns at these two heights could be calculated with adequate precision for the flat and unobstructed Florida sites from earlier laboratory tests of the antenna. At each station observations of height gain for 100 vs 40 feet were made for limited periods, and continuous recording was made on one of the antennas, the 40-foot Yagi antenna at the nearer two of the three principal sites for which data are shown in Fig. 12 (next page), and at 100 feet at the most distant site where signals with the 40-foot Yagi antenna were usually too weak for measurement.

The single available transmitter at Cedar Rapids was connected for alternate half-hourly periods to the special rhombic antenna directed toward Florida, and to the rhombic antenna directed toward Sterling. The Sterling observations thus provided reference signal intensities, and the observed signal intensities in Florida could be expressed as a fraction of the Sterling intensities. This procedure permitted the results shown in Fig. 13 to be interpreted in terms of ionospheric height. The distances from Cedar Rapids to the three principal Florida sites were such that for E-region heights the angles of elevation of the path midpoints were all below the angles of elevation of the first ground-reflection lobes of the transmitting and receiving antennas. As should occur under these conditions for E-region scatter, the received signal power, relative to Sterling signals, decreased rapidly with increasing path length.

By regarding, for purposes of calculation, the received signals as coming from a point scatterer at the path midpoint, it is possible to compute from the known antenna patterns how the relative signal intensity should decrease with increasing path length for a series of trial heights of scatter. Into these calculations a standard inverse-distance squared factor must be inserted, and, in principle, a dependence on scatter angle should be used. Actually the scatter angle varies so little over the range of distances covered by the tests that any reasonable dependence may be used without significantly altering the result. The height is then deduced by comparing the predicted rates of decrease of relative signal intensity with distance, for the assumed heights, with the observed decreases relative to Sterling. This method of height finding, using continuous-wave signals, depends only on comparisons, and is quite insensitive to the form of the scattering transmission equation used. In fact the results are not affected significantly if the simple inverse distance squared term alone is used.

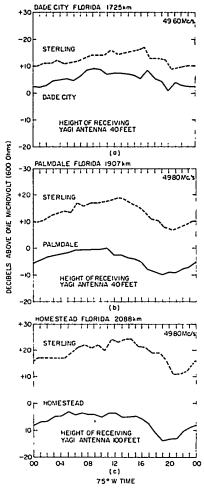

Fig. 12—Distance dependence observations in Florida—(a) Dade City, March 6–18, 1952, inclusive; (b) Palmdale, April 1–30, 1952, inclusive; (c) Homestead, May 21–June 2, 1952, inclusive. Sterling observations shown for corresponding periods.

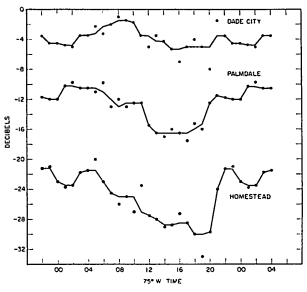

Fig. 13—Smoothed diurnal variation of the ratios of signal intensities received in Florida to those received at Sterling. Ratios shown for the shorter paths are adjusted by observed height gain to permit equivalent comparisons for reception at a height of 100 feet.

The results of these tests are summarized as follows. The heights by day and by night are different. Despite the changing seasons during the tests, the daytime heights lay between 75 and 80 kilometers, and the nighttime heights lay in the range from 85 to 90 kilometers. This day-night height difference received independent confirmation of a still different sort in the systematic differences in the observed height gains between day and night. The daytime height gains, corresponding to the lower height of scatter, were always greater, as would be expected for a smaller common volume associated with the lower midpoint height. At the greatest distance the height gains observed were very close to the theoretical plane-wave result of 8 decibels which would be anticipated if the common volume was small enough to approximate reasonably a point source. Table II summarizes these results. The

TABLE II

Reception Point in Florida	Distance from Cedar Rapids, kilometers	Height Gain, decibels, 100 *versus* 40-foot Yagi	
		Day	Night
Dade City	1,725	3½	3
Palmdale	1,907	5	4
Homestead	2,088	8½	6½

Declassified in Part - Sanitized Copy Approved for Release @ 50-Yr 2014/06/09 : CIA-RDP81-01043R003000180001-4

Declassified in Part - Sanitized Copy Approved for Release @ 50-Yr 2014/06/09 : CIA-RDP81-01043R003000180001-4

[illegible]

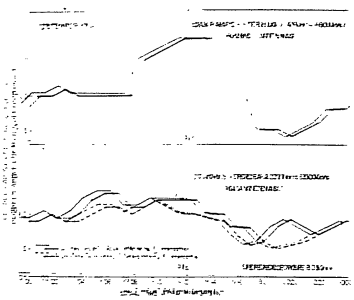

[illegible]

Height Determination by Pulse Methods

[illegible]

[illegible]

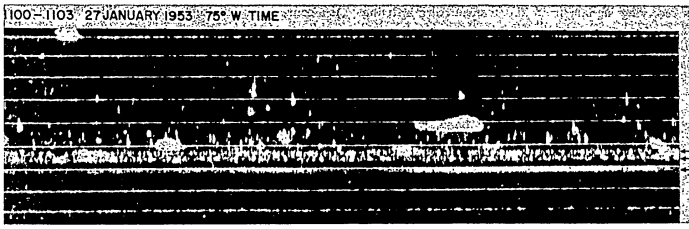

Fig. 15—Oscillogram showing received pulse signals at 49.7 Mc/s on Sterling to Bluffton path, 811 km. T is tropospheric signal, and I_1 and I_2 are ionospheric signals with delays relative to the tropospheric pulses corresponding to heights of approximately 70 and 88 km. Time markers are at 100 microsecond intervals. The transmitted pulses are of approximately 30 microseconds duration, with a repetition rate of 50 per second.

E propagation. Often several strata were simultaneously active. Meteors were not seen at ranges less than that corresponding to the nighttime heights. Fig. 15 is a three-minute sample of the photographic record which shows two active scattering strata, some meteor echoes, and a fairly strong tropospheric signal. This record is typical in most respects for the season and hour except that usually only the lower scattering stratum was observable.

In the summer of 1954 the Bluffton site was reoccupied for ten days for some further height observations. This time the predominant daytime heights were somewhat greater—usually about 80 kilometers. The nighttime heights as in the winter lay mostly between 85 and 90 kilometers.

The agreement between the continuous-wave and pulse methods of height determination is satisfactory, and it only remains to discuss the possible sources of systematic error involved. Of these the most serious is thought to be concerned with the calculation of the travel time of the tropospheric pulses. Some more recent experiments,[22] with round-trip methods for both tropospheric and ionospheric pulses, suggest that the ionospheric heights deduced as described above may be too low by perhaps five kilometers or so. Also some winter observations made on a somewhat more northern path in the winter of 1953 to 1954 indicated that the daytime heights were more like 80 kilometers, though the same nighttime heights were found. This difference may be related to latitude or geographic position, and indicates a need for more extensive height observations. In connection with this work on scattering heights, attention is drawn to the recent work at vertical incidence at about 2 Mc/s by Gardner and Pawsey in Australia[23] which used special new techniques. Their height findings are in some respects so similar to those reported above as to suggest that the same part of the ionosphere is involved.

Angle Dependence

The dependence of the intensity of the signal on the scattering angle has been measured for the case when the transmitting and receiving antennas are directed at the ionospheric midpoint of the path. What has been determined is an approximate value for the exponent of sin $\gamma/2$ which appears in the denominator of the various transmission equations discussed earlier. The experimental arrangement consisted of receiving signals simultaneously from Sterling at 49.7 Mc/s at three receiving stations placed along a single great circle at distances of 491, 592, and 811 kilometers respectively. These distances correspond to a range of path lengths for which the q-curves of Fig. 2 have the greatest difference in slope for different values of the exponent of sin $\gamma/2$. The high-power pulse transmitter, used previously for the height observations, was used and the simultaneously present tropospheric signals were eliminated, by gating, from the measured intensities. The pulse intensities at the short distances used were very weak, and successful observations were only possible on a few summer days when the scattering was strong. The measurements were made during July, 1953.

The experiment was performed as follows. Separate transmitting rhombic antennas designed for each of the three path lengths were erected at Sterling, side by side, with sufficient space between them to avoid interaction. A single rhombic receiving antenna of identical design to the appropriate transmitting rhombic was erected at each of the three observing stations. The pulse transmitter was then connected in turn to each antenna for a period of about fifteen minutes once each hour during the period of the test. The signal intensity recorders were operated simultaneously and continuously at the three receiving locations. For each receiving station a curve was plotted showing the variation from hour to hour, of the received signal intensity when the station

[22] V. C. Pineo and W. G. Abel, private communication; 1955.

[23] F. F. Gardner and J. L. Pawsey, "Study of the ionospheric D-region using partial reflections," *Jour. Atmos. Terr. Phys.*, vol. 3, pp. 321–344; July, 1953.

Declassified in Part - Sanitized Copy Approved for Release @ 50-Yr 2014/06/09 : CIA-RDP81-01043R003000180001-4

Declassified in Part - Sanitized Copy Approved for Release @ 50-Yr 2014/06/09 : CIA-RDP81-01043R003000180001-4

was receiving signals from the transmitting antenna designed for its distance. By interpolation for the remaining periods of each hour at each station, it was possible to arrive at curves which permitted comparison of the intensity of the signals at the different distances.

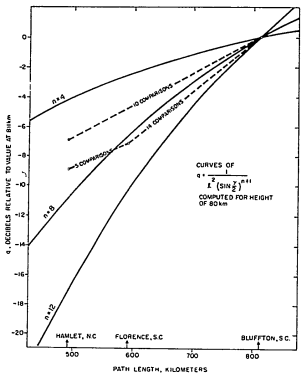

Fig. 16—Results of angle-dependence observations.

The results of these comparisons are given in Fig. 16 which shows comparisons between pairs of receiving stations in order to take account of situations where data are missing from one station. For reference, three q-curves corresponding to exponents of 4, 8, and 12 for a height of 80 kilometers are shown for the appropriate range of distances. It will be seen that the comparison between the two most distant stations indicates that the exponent n in $(\sin \gamma/2)^{n+1}$ is of the order of 8. The other comparisons involving the shortest path for which the observations are thought to be less reliable, indicate a somewhat lower exponent of the order of 4 to 6. All the comparisons are for daytime, and were possible on only three days. Measurements at night and during times of weaker signals will only be possible with much more power. Some further interpretation of these results is given in Part II.

Experiments designed to test the dependence of the intensity of the signals on angle of scatter, for receiving locations off the great circle defined by the principal lobe of the transmitting antenna, have been performed. Their interpretation is complicated by the presence of strong meteoric components which are emphasized in such experiments relative to the scattered signals.[24]

As a consequence the signals observed do not fall off as rapidly as would be indicated by the exponent found in the above experiment. This matter will be discussed further below.

Attention is drawn, at this point in the account, to the relatively limited range of scattering angles available for study by the techniques under discussion. For the longest paths and lowest probable scattering height, values of γ as low as about 18 degrees at the path midpoint may be involved. For the shortest path length considered useful or easy to study, about 1,000 kilometers in length, and highest values of ionospheric scattering height, the largest value of γ at the path midpoint is about 25 degrees. With the extraordinary arrangements of the angle-dependence experiment, signals were occasionally observed at 491 kilometers coming from heights of 80 kilometers or higher. At this distance γ for midpoint scattering is about 40 degrees. If values of γ substantially smaller than 18 degrees were involved, care would be necessary in applying transmission equations of the form given above, since a term in the denominator has been omitted on the grounds that the term involving $\sin \gamma/2$ is always much larger. For very small values of γ the received power does not increase indefinitely, but rather increases to a maximum nearly equal to the free-space value. As a result of the oblique-incidence $h'f$ observing program of the National Bureau of Standards,[25] it now appears that a means for observing ionospheric scattering at angles from zero to 5 degrees or more is available. This technique involves observing signals scattered through a small angle in the E region and subsequently reflected in the classical manner by the E or F region. These observations are possible with moderately directive antennas by using frequencies just a few per cent in excess of the classical F-region (or E-region) maximum usable frequency for the path.[26]

Frequency Dependence

According to the transmission relation originally applied to the Cedar Rapids to Sterling tests of 49.8 Mc/s, and given by (1), the received power should vary inversely as fourth power of operating frequency for constant values of ionospheric and system parameters.

The first opportunity to test the frequency dependence over the Cedar Rapids to Sterling path occurred in the autumn of 1951. The experiment was performed at 418 Mc/s with systems parameters which should just have permitted the successful detection of signal according to the original transmission equation. The systems parameters were as follows:

transmitter output power:	20 kw
transmitting antenna gain over isotropic radiator:	21 db
receiving antenna gain over isotropic radiator:	30 db
receiver noise figure:	4 db
receiver bandwidth:	1 kc/s.

The transmitting antenna was a pyramidal horn tilted to 7 degrees above horizontal in the direction of Sterling. The receiving antenna was a steerable 31-foot paraboloid. The observations made on September 26, September 28–29, and October 17, were disappointing. Only the very strong meteor bursts were observed. They were heard on an average of one every seven or eight minutes in a 24-hour period. This result did not appear sensitive to the angular elevation of the receiving antenna in the range of angles from zero to 30 degrees. At angles much above 30 degrees the burst rate decreased in accordance with expectation considering the beamwidth of the receiving antenna and the path geometry for meteor reflections. It was concluded from these tests that the received power must decline much more rapidly than inversely as the fourth power of frequency.

Routine frequency dependence observations have been made for both the Cedar Rapids to Sterling, and the Anchorage to Barrow paths using frequencies substantially lower than 418 Mc/s. As the results are similar, most of the discussion will deal with the Cedar Rapids to Sterling path, on which two new frequencies have, at different times, been used in addition to 49.8 Mc/s which has always provided a simultaneous reference. For a period of thirteen months continuous-wave transmissions at 107.8 Mc/s were available. Various difficulties with the recording, to some extent associated with the unexpected weakness of the signals, rendered a good part of the observational data of inferior reliability compared with the simultaneous data on 49.8 Mc/s. However, during the summer of 1952 when the signals were strong, good results were obtained, and for the last four months of the program the recording techniques were improved to the point at which it was possible to consider the data of nearly equal reliability to that taken at 49.8 Mc/s. In making comparisons of received signal intensities, representing received available power ratios, the data were adjusted for equal transmitter powers, and equivalent line losses. Also in order that the ionosphere should be illuminated in exactly the same way at the higher frequency, a scaled rhombic antenna was used. This means that the dimensions and height of the new antenna were simply those of the 49.8 Mc/s antenna reduced by the ratio of wavelengths. The 107.8 Mc/s antenna thus had the same lobe pattern and power gain at the maximum of its principal ground-reflection lobe. An identically scaled rhombic antenna was used for receiving at Sterling. In the receiving case, however, it is necessary to remember that the effective area of the 107.8 Mc/s antenna is smaller than that of the 49.8 Mc/s antenna by the wavelength ratio squared. If the frequency dependence is to be expressed on an equal or per unit aperture basis it is necessary to apply this correction before forming ratios. More recently it has been possible to compare 49.8 Mc/s signals with signals received simultaneously from Cedar Rapids at 27.775 Mc/s. Again scaled rhombic antennas have been used, and similar considerations apply.

If it is assumed, in accordance with the various transmission equations, that the received available power varies, after adjustment of the observations to conditions of equal radiated powers, equal apertures, and identical transmitting antenna patterns, as the reciprocal of the frequency to some power n, then a value of n can be obtained by direct comparison of the received signal intensities on two different frequencies. Such comparisons are usually made for simultaneous hourly or half-hourly samples, and the value of n thus determined is referred to as the effective frequency exponent. The word, effective, is intended to qualify the results as applicable only to the comparison of a particular pair of frequencies. In making comparisons, it is of course necessary to eliminate, to the extent possible, observations affected by such things as sporadic-E propagation, individual large meteoric enhancements, tropospheric propagation (very rare), and observations during any malfunctioning of the transmitting or receiving equipment.

With respect to the 107.8/49.8 Mc/s comparisons the following are found:

1. The effective exponent is not constant even when fullest possible allowances are made for experimental error; its extreme range of variation is from about 4 to about 12. (See Fig. 17, next page.)
2. Under conditions of strong signals, particularly in the midday and early afternoon period, as observed at the lower frequency, the median effective exponent tends to be of the order of 8.
3. Under conditions of weak signals, as observed for example at the lower frequency in the evening period and also for somewhat stronger signals in early and midmorning, the median effective exponent is smaller; values of 6 to 7 are typical, as shown in Fig. 18 (next page).
4. These systematic differences in effective exponent are about sufficient to account for certain systematic differences in the diurnal behavior of the median signal intensities observed at the two frequencies, so that no marked correlation can be found between the value of the effective exponent and the strength of the signals at the higher frequency.

This last point in particular is related to the problems of realizable gain and the performance of antennas. The whole question of the meaning of some of the diurnal variations in signal intensity will be discussed below in connection with the role of antennas. In addition to these points, the following special results are noted:

[24] V. R. Eshleman and L. A. Manning, "Radio communication by scattering from meteoric ionization," PROC. IRE, vol. 42, pp. 530–536; March, 1954.

[25] P. G. Sulzer, private communication; 1954.

[26] D. K. Bailey, "The Role of Ionospheric Forward Scatter in Oblique Incidence MUF," Talk presented at URSI-IRE Meetings, Washington, D. C.; May 4, 1955.

Declassified in Part - Sanitized Copy Approved for Release @ 50-Yr 2014/06/09 : CIA-RDP81-01043R003000180001-4

Declassified in Part - Sanitized Copy Approved for Release @ 50-Yr 2014/06/09 : CIA-RDP81-01043R003000180001-4

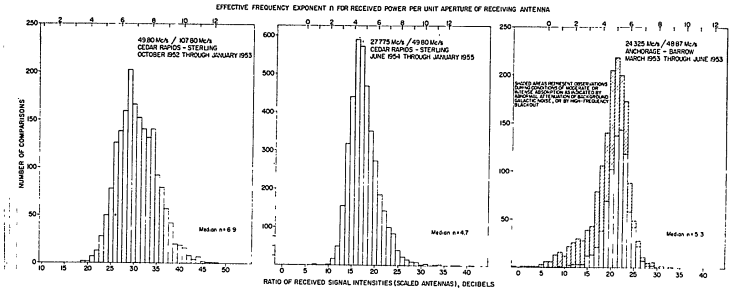
EFFECTIVE FREQUENCY EXPONENT n FOR RECEIVED POWER PER UNIT APERTURE OF RECEIVING ANTENNA
49.80 Mc/s / 107.80 Mc/s
CEDAR RAPIDS - STERLING
OCTOBER 1952 THROUGH JANUARY 1953
Median n=6.9
27.775 Mc/s / 49.80 Mc/s
CEDAR RAPIDS - STERLING
JUNE 1954 THROUGH JANUARY 1955
Median n=4.7
24.325 Mc/s / 48.87 Mc/s
ANCHORAGE - BARROW
MARCH 1953 THROUGH JUNE 1953
Median n=5.3
NUMBER OF COMPARISONS
RATIO OF RECEIVED SIGNAL INTENSITIES (SCALED ANTENNAS), DECIBELS

Fig. 17—Observed dependence of signal intensity on frequency.

5. During moderate or intense sudden ionospheric disturbances, associated with solar flares, and often with solar noise outbursts, approximately equal enhancements occur simultaneously on the two frequencies, so that the effective exponent is not appreciably affected.
6. During major meteor showers, which are readily identified by longer duration meteor bursts, the effective exponent as determined from the routine recordings is not appreciably affected.

Good standardized simultaneous recordings at Sterling of signals from Cedar Rapids at 27.775 Mc/s and 49.8 Mc/s covering a period of several months have been obtained. Again scaled rhombic antennas, directed along the great circle, are used, and all data are adjusted for equal transmitter powers, and equivalent line losses. As required, the data are also corrected for equal apertures. With frequencies as low as 27.775 Mc/s nondeviative D-region absorption may reduce the intensity of the signals as much as three decibels during midday. A correction for nondeviative absorption at 27.775 Mc/s has not been included in the data presented, since evidence that the scattering stratum might lie substantially above the absorbing layer was not obtained until recently. As in the earlier comparisons, the effective frequency exponent seems to vary as shown in Fig. 17. The following different results have been obtained.

1. Under conditions of strong signals as observed at the lower frequency, particularly in the midday and early afternoon period, the median effective exponent tends to be slightly greater than 5; if a rough allowance for absorption at the lower frequency is included, it may be as high as 6 to 6½.
2. Under conditions of weak signals as observed at the lower frequency, the effective exponent is smaller—a value of 4 to 4½ is representative.

A discussion of the 27.775 Mc/s signal behavior during an SID is reserved for another section below. The general long-term behavior observed for the 107.8 Mc/s and 27.775 Mc/s signals is shown in Fig. 8.

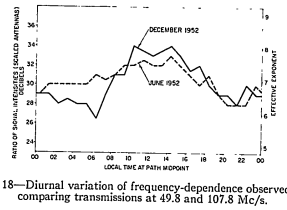

Fig. 18—Diurnal variation of frequency-dependence observed by comparing transmissions at 49.8 and 107.8 Mc/s.

For the last four months of the Barrow operation a second frequency, 24.325 Mc/s, was put on the air at Anchorage. Shortage of space for a scaled rhombic antenna at the Anchorage site led to the adoption of scaled five-element Yagi antennas at both terminals. In order to keep the continuity in the data taken with rhombic antennas at 48.87 Mc/s, the transmitter operating at this frequency was fed alternately for half-hourly periods into the original rhombic antenna and the Yagi. Reception at Barrow was performed simultaneously and separately with both a rhombic and a Yagi antenna. After the usual precautions and adjustments of the data, it was found that the effective frequency exponent was not constant but exhibited characteristics very much like those observed for the 27.775/49.8 Mc/s comparison at Sterling. In Alaska, where severe geomagnetic disturbance is common, the observed value of the effective exponent seemed often to be reduced as a result of nondeviative absorption.

which tended to reduce the intensity of the signals more at the lower frequency. This matter will be further discussed below in connection with special arctic behavior. Fig. 17 presents the results.

Since the effective frequency exponent is not constant for a given pair of frequencies, and differs systematically for a different pair, it would appear to be inappropriate to express the frequency dependence as a constant power of $1/f$. Fig. 19 is presented in an effort to show the frequency dependence in a different way which more directly represents the observations. Still another way of presenting the results is to determine an exponent of $1/f$ which is itself a function of frequency. The tests thus far represent only two substantially different comparisons, and two coefficients, A and B, can therefore be evaluated in an exponent expressed as $A+Bf$.

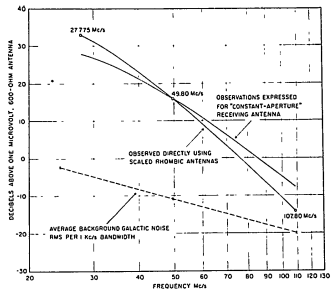
27.775 Mc/s
49.80 Mc/s
OBSERVATIONS EXPRESSED FOR "CONSTANT-APERTURE" RECEIVING ANTENNA
OBSERVED DIRECTLY USING SCALED RHOMBIC ANTENNAS
107.80 Mc/s
AVERAGE BACKGROUND GALACTIC NOISE RMS PER 1 Kc/s BANDWIDTH
DECIBELS ABOVE ONE MICROVOLT, 600-OHM ANTENNA
FREQUENCY Mc/s

Fig. 19—Observed dependence of signal intensity and background galactic noise on frequency. Value plotted at 49.8 Mc/s is median of hourly signal intensity observations during the year from October, 1951 through September, 1952. Remainder of curve plotted through points representing median values of frequency-dependence ratios shown in Fig. 17.

Selected comparisons for constant aperture representing midday and early afternoon periods when the signal intensities appear to show a controlling solar influence, indicate effective frequency exponents of about 8 and 6½ based on comparison of 107.8 and 27.775 Mc/s respectively with 49.8 Mc/s. Allowance has been made for the effect of nondeviative absorption in obtaining these particular effective frequency exponents. The coefficients A and B representing these selected data are found to be:

$$A = 5.3,$$
$$B = 0.0066,$$

for f expressed in megacycles per second.

A further look at the scattering theory of Villars and Weisskopf[8] is indicated. Their limiting cases of the transmission equation are controlled by a transition function $F(x)$ which enters the transmission equation as a factor $[F(x)]^2$ where $x=\lambda/L_s$. λ is the wavelength and L_s is a length describing the smallest eddy—taken to be about 2½ meters. When $x\gg1$ the function is of the order of unity and the transmission equation represented by (5) applies. When $x<1$ however the scattering decreases more rapidly with increasing frequency and scattering angle, and in the limit for $x\ll1$, the transmission is described by (6). Now if λ is fixed as for the 49.8 Mc/s transmissions, the temporal variation in effective exponent must be associated, in the absence of any other mechanism contributing significantly to the net signal, with changes in L_s and therefore with the fine structure of the scattering medium. For a decrease in the exponent, L_s must in fact decrease at a fixed λ, or λ must increase for a fixed L_s. This would explain the lower exponents associated at all times with lower frequencies. It is of some interest to note that for much lower frequencies, the observed exponent would appear to be determined almost solely by the coefficient A and thus be 5.3 for the selected data. The exponent under similar conditions as given by Villars and Weisskopf is 4⅓. It is difficult to say at this time whether the approximate agreement is significant.

Polarization Dependence

Each scatterer in the ionosphere may be thought of as a small radiating dipole oriented according to the direction of the incident electric vector. Its polar diagram is determined by the factor $\sin^2\chi$ shown in the various transmission equations discussed earlier. Thus for midpoint scattering with horizontally polarized transmissions, $\chi=90°$ and $\sin^2\chi=1$. For vertically polarized transmissions for midpoint scattering, $\chi=90°-\gamma$ and $\sin^2\chi=\cos^2\gamma$. A typical value of γ is about 20°, thus a loss of about half a decibel will result. To the extent that the received radiation comes from the general direction of the path midpoint, it will have predominantly the same polarization as the transmitted waves, and various experiments involving receiving antennas of opposite polarization have confirmed this. However signals received from scatterers far removed laterally from the path midpoint will, in general, have components of both polarizations, and complete suppression cannot therefore be effected by the use of receiving antennas which are crossed with respect to the transmitting antenna polarizations. There is room for some interesting investigations of the degree of suppression which can be achieved as a function, for example, of time of day and season, particularly if fairly broad-lobed antennas are used. If both crossed-polarization and split-beam techniques are used simultaneously, most of the scattered signal can be eliminated and other signal components can be isolated and investigated.

Important considerations connected with antennas indicate that horizontal polarization is generally to be preferred. This matter is discussed in more detail below.

Declassified in Part - Sanitized Copy Approved for Release @ 50-Yr 2014/06/09 : CIA-RDP81-01043R003000180001-4

Declassified in Part - Sanitized Copy Approved for Release @ 50-Yr 2014/06/09 : CIA-RDP81-01043R003000180001-4

Observations with Spaced Receiving Antennas

The microscopic structure of the downcoming signal at a receiving site is studied by making simultaneous observations of the signal with spaced receiving antennas. The correlation of the envelopes of scattered signals received on spaced antennas has been investigated at Sterling.[16] The regular transmissions at 49.8 Mc/s from Cedar Rapids were used. Three horizontal five-element Yagi antennas were used for simultaneous reception. The plane-wave gain of each was about 9 decibels with respect to a horizontal half-wave dipole at the same height. The three Yagi antennas were placed at the vertices of a right triangle. The antenna forming the right angle remained fixed and was the reference antenna. The other two were placed at variable spacings from the reference antenna, along the great-circle direction of Cedar Rapids, and normal to the direction of the transmitter respectively. Three voltages, proportional to the envelopes of the signals received by the three antennas, were simultaneously recorded for suitable sampling periods in each of several pairs of spacings. After editing to remove signals obviously strongly influenced by meteoric events, the data were analyzed to determine the envelope correlation coefficients as a function of antenna spacing. Periods of medium and strong signals were somewhat favored. Medians of the results for the different sets of observations made in January and April, 1953 are given in Fig. 20. It will be

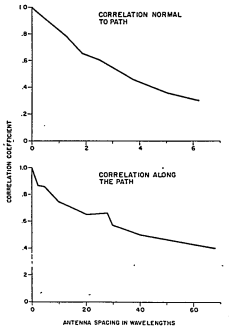

Fig. 20—Observed signal envelope correlation as a function of antenna spacing.

noted that the correlation coefficient falls to 0.5 for spacings of about 3.5 wavelengths normal to the path, and about 40 wavelengths along the path. The interpretation of these results is bound up not only with the scattering mechanism, but also with the beam-width of the transmitting antenna, as discussed in some detail later.

Abnormal Signal Behavior

Meteor Showers

Three well-known meteor showers are recognizable with ease in the routine signal-intensity recordings each year. Doubtless other lesser showers could also be recognized if the records were carefully studied with that objective. The three showers are the Perseids, the Geminids, and the Quadrantids. The shower meteors, which as a class are large meteors compared with the usual ever-present meteors, are recognized on the recordings by the great increase in general spikiness, and by the much longer durations of the bursts which characterize them. Some examples of recordings during a shower and normal recordings with comparable signal intensities are given in Fig. 21 (facing page) for reception at Sterling at 49.8 and 107.8 Mc/s. In these records it should be noticed that spikes associated with a particular meteor are often recognizable at both frequencies. Despite the more frequent and longer duration bursts during the great annual showers, it has not been possible to find any marked general enhancement of the signal intensities. This result is in striking contrast with the result obtained at Ottawa[17] where the signals at 49.8 Mc/s beamed toward Sterling were observed with a much less directive antenna than the rhombic. At Ottawa marked enhancements of the averaged signal intensity are observed during these showers. This result is now better understood as a result of the recent Carysbrook receiving tests which are described below in connection with the discussion of the role of antennas. The position of Ottawa with respect to the region of the ionosphere illuminated by the Cedar Rapids rhombic antenna is such that meteoric signals are enhanced relative to the scatter component. At Sterling the scatter components are greater than the meteoric signals or at times comparable. In the Arctic, events associated with geomagnetic phenomena occasionally lead to considerable enhancements of the scattered signal. If these events, usually having durations of an hour or so, occur during meteor showers or, at times of unusual spikiness in the records, they effectively mask the meteoric signals, as shown in Fig. 22 (facing page).

Sporadic-E Propagation

Occasionally for periods of time varying from a few minutes to several hours very strong signals are received which saturate the normal recorder. These events are considered to be the result of sporadic-*E* propagation, although the field intensities when measured with special auxiliary equipment, generally fall considerably short of inverse-distance values for the paths as shown in Table I. Usually the periods of sporadic-*E* propagation begin gradually and end gradually, though occasionally the beginnings and endings are abrupt. Ex-

[17] P. A. Forsyth and E. L. Vogan, "Forward scattering of radio waves by meteor trails," *Can. Jour. Phys.*, vol. 33, pp. 176–188; May, 1955.

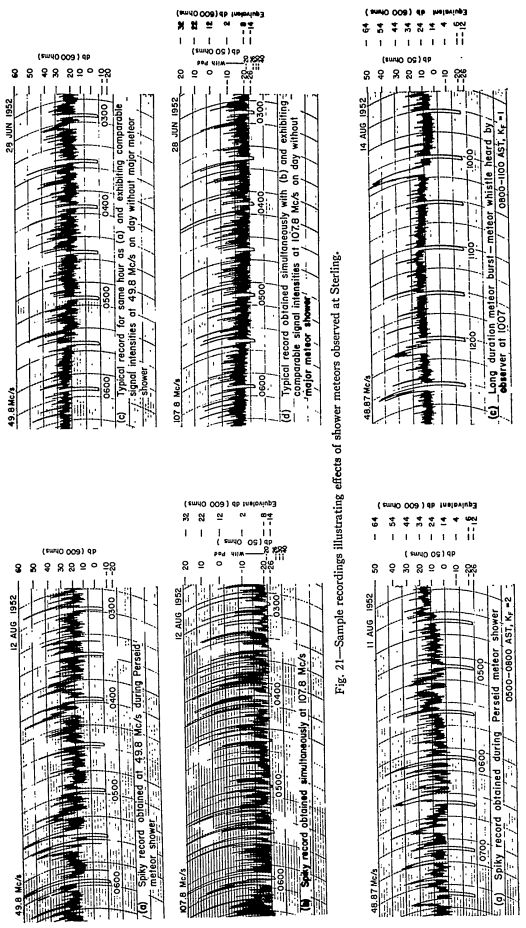
29 JUN 1952
28 JUN 1952
14 AUG 1952
1 AUG 1952
12 AUG 1952
11 AUG 1952
49.8 Mc/s
107.8 Mc/s
(a) Typical record for same hour as (b) and exhibiting comparable signal intensities at 49.8 Mc/s on day without major meteor shower
(b) Typical record obtained simultaneously with (a) and exhibiting comparable signal intensities at 107.8 Mc/s on day without major meteor shower
(c) Long duration meteor burst—meteor whistle heard by observer at 1907 0800–1100 AST, K_p=1
(d) Typical record obtained during same hours as (a) and (b) showing comparable signal levels on day without major meteor shower 0500–0800 AST, K_p=1
(a) Spiky record obtained at 49.8 Mc/s during Perseid meteor shower
(b) Spiky record obtained simultaneously at 107.8 Mc/s
(a) Spiky record obtained during Perseid meteor shower 0500–0800 AST, K_p=2
(b) Meteor spikes masked by strong signal—some hours next day of Perseid shower 0200–0800 AST, K_p=5

Fig. 21—Sample recordings illustrating effects of shower meteors observed at Sterling.

Fig. 22—Sample recordings illustrating effects of shower meteors observed at Barrow.

Declassified in Part - Sanitized Copy Approved for Release @ 50-Yr 2014/06/09 : CIA-RDP81-01043R003000180001-4

Declassified in Part - Sanitized Copy Approved for Release @ 50-Yr 2014/06/09 : CIA-RDP81-01043R003000180001-4

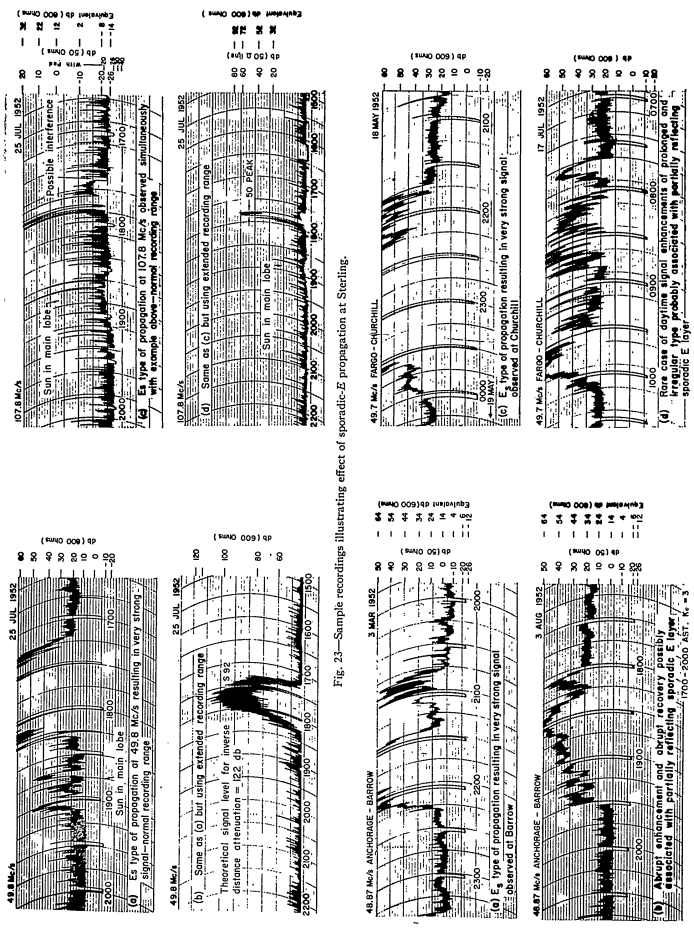
25 JUL 1952
107.8 Mc/s
Possible interference
Sun in main lobe
(a) Es type of propagation at 107.8 Mc/s observed simultaneously with normal, over-water, scatter signal
(b) Some as (a) but using extended recording range
50 PEAK
18 MAY 1952
49.7 Mc/s FARGO - CHURCHILL
(c) E, type of propagation resulting in very strong signal observed at Churchill
17 JUL 1952
(d) Rare case of daytime signal enhancements of prolonged and irregular type probably associated with partially reflecting sporadic E layer
3 MAR 1952
48.97 Mc/s ANCHORAGE - BARROW
(a) Es type of propagation at 49.8 Mc/s resulting in very strong signal—normal recording range
(b) Some as (a) but using extended recording range
Theoretical signal level for diverse distance attenuation = 122 db
(c) Es type of propagation resulting in very strong signal observed at Barrow
3 AUG 1952
(d) Abrupt enhancement and abnormally prolonged sporadic E layer associated with partially reflecting sporadic E layer

Fig. 23—Sample recordings illustrating effect of sporadic-*E* propagation at Sterling.

Fig. 24—Sample recordings illustrating effect of sporadic-*E* propagation on arctic paths.

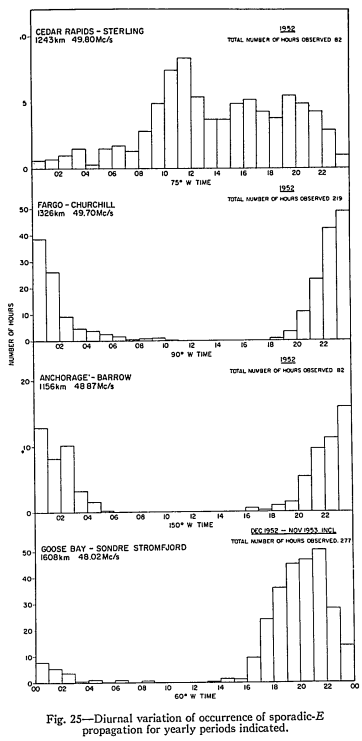

Fig. 25—Diurnal variation of occurrence of sporadic-*E* propagation for yearly periods indicated.

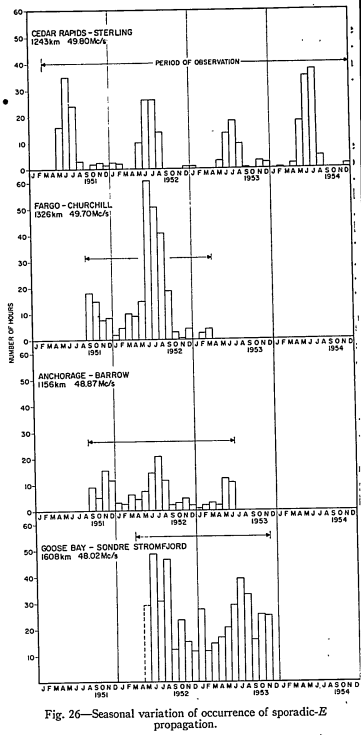
CEDAR RAPIDS - STERLING
1243km 49.80Mc/s
PERIOD OF OBSERVATION
FARGO - CHURCHILL
1326km 49.70Mc/s
ANCHORAGE - BARROW
1156km 48.87Mc/s
GOOSE BAY - SONDRE STROMFJORD
1608km 48.02Mc/s
NUMBER OF HOURS
J F M A M J J A S O N D J F M A M J J A S O N D J F M A M J J A S O N D
1951 1952 1953 1954

Fig. 26—Seasonal variation of occurrence of sporadic-*E* propagation.

amples of routine recordings illustrating such signals are in Figs. 23, 24 at left. Special records of these events have been kept in order to determine their diurnal and seasonal characteristics. Examples are considered in this analysis if, at some time during a period of at least twelve minutes during which the normal signal is masked, the signal levels exceed one millivolt for a reference impedance of 600 ohms. A criterion of this sort is necessary in order to eliminate the occasional long-duration meteor bursts. Whenever possible, interpolation through the sporadic-*E* event is performed in connection with the data analysis of the normal signals.

The sporadic-*E* observations are summarized in Figs. 25 and 26 for the paths operating at about 50 Mc/s. In these summaries are included the observations at 48.02 Mc/s for the experimental communication path from Goose Bay, Labrador, to Sondre Stromfjord, Greenland. For the temperate-zone path from Cedar Rapids to Sterling most of the sporadic-*E* propagation occurs during the summer season. It may occur at any time of day, but is more likely to occur during the daylight hours. A secondary but much weaker maximum occurs during the winter months, which may have somewhat different diurnal characteristics. Sporadic-*E*

Declassified in Part - Sanitized Copy Approved for Release @ 50-Yr 2014/06/09 : CIA-RDP81-01043R003000180001-4

Declassified in Part - Sanitized Copy Approved for Release @ 50-Yr 2014/06/09 : CIA-RDP81-01043R003000180001-4

propagation is not observed at this frequency over this path during the equinox months. These findings agree with other mid-latitude observations by other methods at lower frequencies. The characteristics observed on the arctic paths are totally different. Most of the sporadic-*E* propagation takes place between about 18 hours local time and about 02 hours. On the Goose Bay to Sondre Stromfjord path the diurnal maximum occurs about two hours earlier than on the other arctic paths. Sporadic-*E* propagation is almost completely absent during the late night and the daytime. This diurnal characteristic is observed in all months. There seems to be more sporadic-*E* propagation during the summer season, although the summer of 1953 had less sporadic-*E* propagation than the summer before. Nevertheless it cannot be said that these data show any certain solar cycle influence. The occurrence rates for a particular path were very sensitive to frequency, as would have been expected. At 107.8 Mc/s during the summer of 1952 only two brief occurrences were observed. They coincided with longer events at 49.8 Mc/s. At 27.775 Mc/s more events and a generally longer duration for specific events were observed. A similar result was found in Alaska at 24.325 Mc/s.

A connection between the aurora and sporadic-*E* propagation has long been suggested. At vertical incidence there appears to be a one-to-one correspondence between the zenith or near-zenith appearance of well-defined active auroral forms and *h'f* observations of echoes from about 100 to 120 kilometers. On the other hand, nearly all attempts to associate the strong vhf signals of the type under discussion with the appearance of aurora in the illuminated common volume in the *E* region have proved unsatisfactory. Observations from the terminals of the Anchorage to Barrow path and for a briefer period from Fairbanks, where the path midpoint in the *E* region is more easily examined, failed to establish any significant connection. In the case of the Fargo to Churchill path the results are somewhat less negative though the connection sought is not very definite. Fig. 27 (facing page) shows an example where correlation between *Es*-influenced signal recordings and the presence of active auroral forms in the direction of the path midpoint is fairly direct. In this figure the auroral forms were actually photographed from the receiving hut and some of the poles of the receiving rhombic antenna can be seen. Fading twilight masks the observations at first. The discussion given below in connection with the sputter phenomenon should be borne in mind in any attempt to understand the relationship between *Es*-propagation and auroras.

Sudden Ionospheric Disturbances (SID's)

Signal enhancements at 49.8 Mc/s coinciding with SID's producing sky-wave fadeouts at hf have been observed from the beginning of the program and have already been reported. During 1952 when the 107.8 Mc/s signals from Cedar Rapids were also available at Sterling only a few occurred. They sufficed however to demonstrate that the enhancements were of the same amplitude at the two frequencies and that they occurred simultaneously. Best example obtained is in Fig. 28 (page 1206). Quite recently a moderately strong SID has occurred when signals were being recorded simultaneously at 27.775 and 49.8 Mc/s. In this case a good enhancement was observed at 49.8 Mc/s but the 27.775 Mc/s signal showed at first a trace of enhancement which was followed by a sharp decrease a few minutes after the start of the SID. This is interpreted as indicating that absorption associated with the sharp increase in ionization in the *D* region was more than enough to offset the enhancement once the event had become well developed. It further indicates that most of the scattering takes place in or above the absorbing layer during these events. At minimum the 27.775 Mc/s signal was still many decibels above the background noise level. It is a matter of some interest that the maximum absorption at 27.775 Mc/s occurred several minutes ahead of the maximum enhancement at 49.8 Mc/s. The details of this event are in Fig. 29 on page 1206.

In examining the routine records some care is necessary in identifying SID's. From time to time enhancements or signal variations of very similar appearance are observed which are not associated with unusual absorption. It is also observed that the weaker SID's produce no identifiable enhancement. The simultaneous recording of some distant hf station usually provides an excellent guide. Also whenever the received noise is predominantly cosmic noise and a transmission break occurs during the event, a significant decrease in the cosmic noise level is observed unless a simultaneous burst of solar noise contaminates the observation. The SID behavior is believed to be directly related to an increase in f_N, the plasma frequency corresponding to the mean electron density, N, in the scattering volume.

Polar Blackouts

The term polar blackout has been given to events occurring in regions of high auroral activity which are characterized by periods of very intense nondeviative ionospheric absorption lasting from somewhat less than an hour to six or more hours. These events, unlike SID's which are usually less than an hour in duration and can only occur during daylight, are observed at all hours though they are much less frequent in the evening period from about 18 hours local time to midnight. As with SID's they produce complete fadeouts at hf, but unlike SID's which occur simultaneously all over the sunlit hemisphere, polar blackouts are fairly local. By local it is meant that they occur over an area a few hundred miles wide, outside of which conditions may be fairly normal. They are thought to be associated in some complex way with the corpuscular radiation from the sun. The characteristics of polar blackouts, determined from vertical-incidence *h'f* observations at Fairbanks, are well known.[28]

Polar blackouts are frequently much more intense than SID's. This result is derived from the observations of cosmic noise which show much greater absorption, at times, than has been observed during SID's. At 48.87 Mc/s at Barrow the more moderate blackouts produce signal enhancements, but if the blackout is very intense, the scatter signal may appear normal because the exces-

[28] H. W. Wells, "Polar radio disturbance during magnetic bays," *Terr. Mag.*, vol. 52, pp. 315-320; September, 1947.

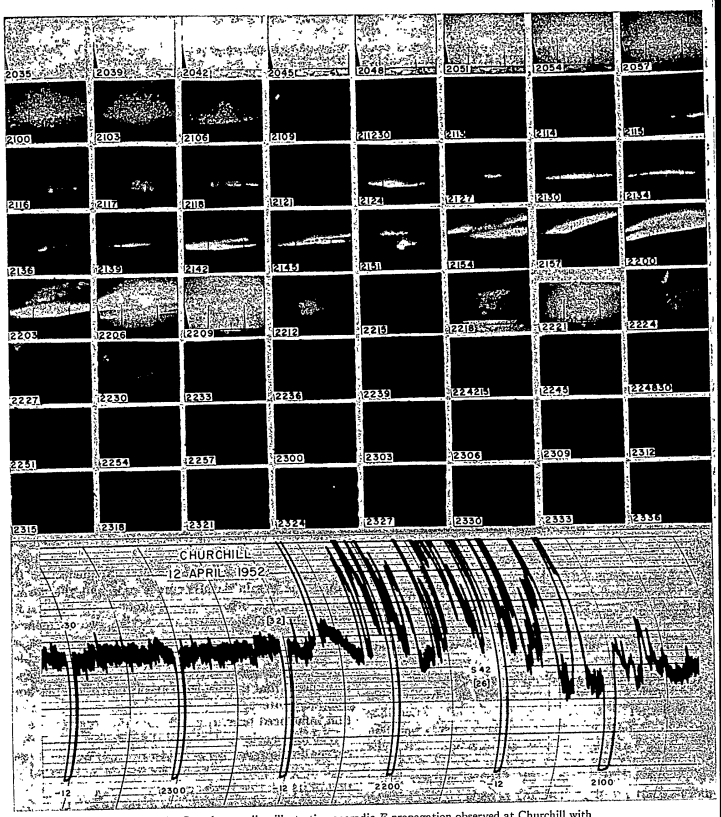

Fig. 27—Sample recording illustrating sporadic-*E* propagation observed at Churchill with accompanying photographs of aurorae in direction of path midpoint.

Declassified in Part - Sanitized Copy Approved for Release @ 50-Yr 2014/06/09 : CIA-RDP81-01043R003000180001-4

Declassified in Part - Sanitized Copy Approved for Release @ 50-Yr 2014/06/09 : CIA-RDP81-01043R003000180001-4

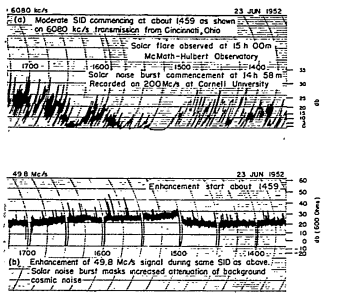
6080 kc/s
23 JUN 1952
(a) Moderate SID commencing at about 1459 as shown on 6080 kc/s transmission from Cincinnati, Ohio
Solar flare observed at 15 h 00m McMath-Hulbert Observatory
1700
1600
1500
1400
Solar noise burst commencement at 14h 58 m Recorded on 200 Mc/s at Cornell University
db above noise
db
49.8 Mc/s
23 JUN 1952
Enhancement start about 1459
db (600 Ohms)
(b) Enhancement of 49.8 Mc/s signal during same SID as above. Solar noise burst masks increased attenuation of background cosmic noise
107.8 Mc/s
23 JUN 1952
Enhancement start about 1458
db (150 Ohms)
Microvolts
Equivalent db (600 Ohms)
(c) Enhancement of 107.8 Mc/s signal during same SID. Solar noise burst activity evident in two-minute transmission breaks commencing with break at 1500

Fig. 28—Sample recordings illustrating simultaneous enhancements of vhf signal intensities observed at Sterling during an SID.

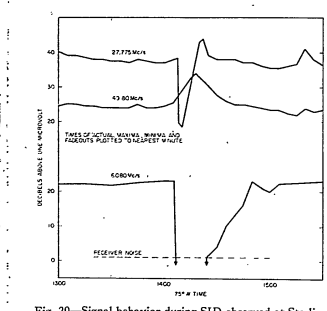

Fig. 29—Signal behavior during SID observed at Sterling on June 18, 1955.

sive absorption has compensated for the enhancement, and the decrease in cosmic-noise level serves as an indicator of the blackout condition. Examples of signal enhancement during intense arctic absorption are shown in Fig. 30.

As no direct pulse observations have been undertaken in high latitudes for height determination, it is of interest to consider what indirect evidence may be adduced about relative height from simultaneous observations on

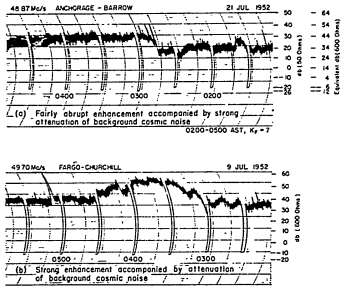
48.87 Mc/s
ANCHORAGE - BARROW
21 JUL 1952
db (150 Ohms)
Equivalent db (600 Ohms)
(a) Fairly abrupt enhancement accompanied by strong attenuation of background cosmic noise
0200-0500 AST, K_p = 7
49.70 Mc/s
FARGO-CHURCHILL
9 JUL 1952
db (600 Ohms)
(b) Strong enhancement accompanied by attenuation of background cosmic noise

Fig. 30—Sample recordings illustrating typical effects of polar blackouts on arctic paths.

the Anchorage to Barrow path at 48.87 and 24.325 Mc/s during an intense and prolonged polar blackout. The basic observational material was obtained during the blackout of May 19, 1953 and it is presented in Fig. 31. The observations were made using scaled Yagi antennas for both transmitting and receiving. Four sets of simultaneous observations are shown. The variation of the scattered signal intensity as a function of time is shown for 24.325 and 48.87 Mc/s, together with a dashed curve representing, for each frequency, the normal behavior of the signal intensity during the same hours. Below these two sets of observations and on the same scale are shown the variations of the recorded background cosmic noise at the same two frequencies at the same time. Again dashed curves represent the normal behavior. The bottom curves cannot safely be used for direct absorption comparisons at the two frequencies because the cosmic noise is recorded from all directions in the sky according to the lobe patterns of the scaled Yagi antennas used, whereas from independent evidence it is known that the low-level absorption of the blackout was more intense to the south of Barrow. The absorption influenced primarily therefore the cosmic noise received in the principal lobes of the antenna. The bottom curves do, however, serve to identify approximately the beginning and end of the blackout, and give an indication of its relative intensity.

Examination of the behavior of the 48.87 Mc/s signal shows that some enhancement appears to have occurred at first, but as the absorption became more intense the strength of the scattered signals dropped to an appearance of normal. As the blackout wore off, the enhancement again appeared temporarily. From the observed signal-intensity and noise-intensity behavior, and judging by the behavior observed during many other blackout enhancements, it is estimated that the peak enhancement, in the absence of the excessive nondeviative absorption, would have resulted in signal intensities some 5 decibels or more above normal. At 24.325 Mc/s

the scattered signals showed a considerable decrease in intensity throughout the blackout. At the height of the absorption, the 24.325 Mc/s signal was about 16 decibels below normal. Now assume, as is reported above in connection with SID observations on higher frequencies, that the actual scattering enhancement is the same on the two frequencies. It then follows that an enhancement of about 5 decibels occurred in the strength of the scattering at 24.325 Mc/s, but that the observed strength of scattering, some 16 plus 5, or 21 decibels lower at the most intense phase of the blackout, was due to the nondeviative absorption occurring below the scattering stratum.

An independent check is available for the argument thus far. The frequencies involved are almost exactly in a one-to-two ratio. The different absorptions deduced for the two frequencies, 21 and 5 decibels respectively, correspond very nearly to an absorption ratio of four-to-one. The absorption in decibels would thus appear to vary inversely as the square of the frequency—a result in accordance with long-established theory, as verified by other kinds of measurements, for nondeviative absorption at frequencies well above the gyro-frequency.

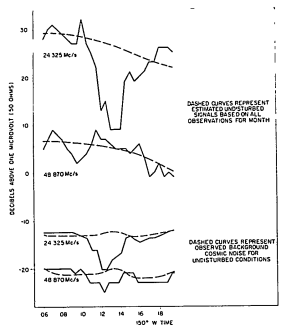

Fig. 31—Signal and background cosmic noise behavior during a polar blackout observed at Barrow on May 19, 1953.

Next observe that the cosmic noise at 24.325 Mc/s decreased some 8 decibels during the maximum of the blackout. This figure represents a conservative estimate, for reasons already given, of the absorption in the direction of arrival of the scattered signals, for a single transit through the absorbing layer. For scattering from heights above the absorbing layer, two transits of the absorbing layer would occur, and the reduction in intensity of the scattered signals during the blackout would be expected to be in excess of 16 decibels. This conclusion is in sufficient accordance with the interpretation of the observations already given, to permit the further deduction that the scattering stratum during a blackout, at any rate, is substantially entirely above the absorbing layer. As with SID's the blackout enhancements are believed to be directly related to an increase in f_N, the plasma frequency indicated in the various transmission equations discussed earlier.

Sputter

Shortly after the commencement of operation of the arctic paths, Fargo to Churchill, and Anchorage to Barrow, occasions were observed when the received signal exhibited fading rates up to two or three hundred cycles per second, or about one hundred times normal. As a result, the signal sounded as if the transmitted wave was being noise-modulated, and the name *sputter* was used to describe the sound. Sputter represents a different propagation mechanism which occurs simultaneously with the regular scattering. If the sputter propagation is of comparable or greater intensity than the normal signal, it can be readily identified in the routine recordings by a characteristic thinning of the trace. Often sputter can be heard, if the audio gain is turned up, when it is too weak to affect the recordings. Since the receiving stations were not continuously manned, it has been necessary to study the occurrence of thinned trace as evidence of occurrence of moderate or strong sputter. Examples of thinned trace resulting from sputter are in Figs. 32 (next page) and 33 (page 1209). A seasonal and diurnal study of the occurrence of thinned trace has been made for Churchill and Barrow with results shown in Fig. 34 (page 1210). Sputter is much more frequent at Barrow. Its diurnal characteristics are similar at both places, and are considerably less distinct than those of sporadic *E*. But, it appears to occur most frequently between 16 hours local time and midnight. At Barrow a secondary maximum seems to occur between the hours of 04 and 08 local time. Sputter was not observed within an hour or so of midday at any season at Barrow and Churchill, nor was it observed during the summer when the normal signal levels were very high. A few cases of sputter at noon have, however, been recorded at Sondre Stromfjord at 48.02 Mc/s. To some extent the summer absence must be regarded as a masking effect, since it has been noticed on occasion when the audio gain has been turned up.

The connection between sputter and aurorae is now fairly well understood. To begin with, the five or six cases of sputter observed at Sterling during the past four and a half years have been associated with known auroral activity and with reports from radio amateurs of weak long-distance vhf communication in the 50 and 144 Mc/s bands. It should not be concluded that all auroras can give rise to sputter. Given suitable seeing conditions, aurora may be seen practically every night at Barrow and Fairbanks, but sputter is relatively infrequent. To produce sputter an aurora must be of the right kind, and must be situated in the correct place with respect to the vhf path. The aurora which can be observed with radar techniques such as those used by Canadian groups, University of Manchester workers,

Declassified in Part - Sanitized Copy Approved for Release @ 50-Yr 2014/06/09 : CIA-RDP81-01043R003000180001-4

Declassified in Part - Sanitized Copy Approved for Release @ 50-Yr 2014/06/09 : CIA-RDP81-01043R003000180001-4

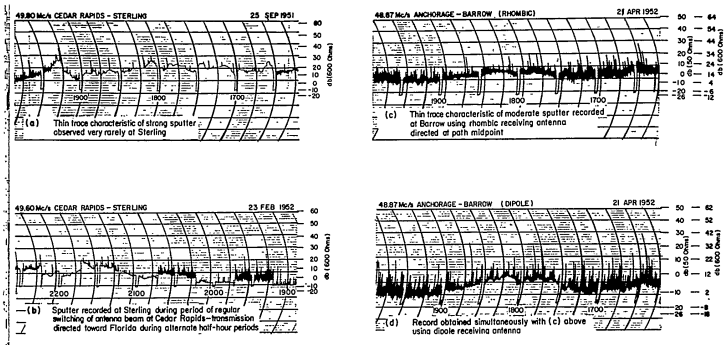
49.80 Mc/s CEDAR RAPIDS - STERLING
25 SEP 1951
(a) Thin trace characteristic of strong sputter observed very rarely at Sterling
48.87 Mc/s ANCHORAGE - BARROW (RHOMBIC)
21 APR 1952
(c) Thin trace characteristic of moderate sputter recorded at Barrow using rhombic receiving antenna directed at path midpoint
49.60 Mc/s CEDAR RAPIDS - STERLING
23 FEB 1952
(b) Sputter recorded at Sterling during period of regular switching of antenna beam at Cedar Rapids—transmission directed toward Florida during alternate half-hour periods
48.87 Mc/s ANCHORAGE - BARROW (DIPOLE)
21 APR 1952
(d) Record obtained simultaneously with (c) above using dipole receiving antenna

Fig. 32—Sample recordings illustrating the effects of sputter propagation.

and the group at Cornell University, has not been identified as the kind capable of giving rise to sputter. A recent paper by Booker, Gartlein, and Nichols[29] reviews the entire problem of radio reflections from the aurorae, and contains a full bibliography of this interesting subject. Chapman has made a thorough study of the geometry of radio echoes from aurora.[30]

A close analogy exists between meteors and aurorae as regards their study by radio techniques employing vhf. In both cases most of the work has been performed with radar techniques. In both cases the requirement for strong echoes has been found to be that the meteoric ionization column or the auroral ionization column should be viewed at normal or nearly normal incidence. In this connection it has been found that the auroral forms giving strong fairly discrete echoes consist of shafts or rays, rather than more diffuse forms. It is also fairly well established that the only part of an auroral ray or shaft capable of giving much of an echo is situated in the height region from about 80 to 120 kilometers—the same region in which meteors produce their ionization. In the case of meteors, the orientation of the ionization column is determined by astronomical considerations involving the orbit of the meteor and the motion of the earth; in the case of aurorae the orientation of the ionization columns is along the lines of the earth's magnetic field. As with meteors, the extension of the radar work to cases where the transmitter and receiver are widely separated leads to considerable geometric complication. In both cases the ionization columns must be so oriented with respect to the path that there exists a plane including the axis of the column of ionization from which the angles of incidence and reflection are about the same. The high rate of fading of the auroral signals is thought to be of Doppler origin and to be associated not only with the corpuscular velocities, which are greater than meteor velocities by factors of 50 to 100, but with rapid changes in the excitation. At any rate the practical effect is to spread a monochromatic transmission into a band two or three hundred cycles wide with weak wings extending much further.

In the light of the geometric conditions required for propagation by way of the aurorae, it is now possible to understand why there is more sputter observed at Barrow than at Churchill. It is also possible to deduce that long paths should exhibit less sputter than short ones. Indirect confirmation of this lies in the observation at Barrow illustrated in Fig. 32 that more sputter is observed when less directive antennas are used. It now seems inappropriate to apply the concepts of frequency and angle dependence, as used for forward scattering, to sputter.

In connection with the analysis of the Barrow observations of sputter, and in connection with studies of the relationship between the strength of the vhf signals and geomagnetic disturbance, many $h'f$ records taken at the same time at Anchorage, Fairbanks, and Barrow were examined. Some of these results are reported in the next section. As a result of this study, however, it is now possible to recognize in regular $h'f$ observations the presence of aurora of the type which gives rise to sputter. Fig. 33 presents examples of the $h'f$ observations at Fairbanks during an event consisting first of a short polar blackout, followed by sputter. As the fadeout wears off, it will be seen that E-region echoes of an unusual type appear. The observation at 04h 15m is particularly typical. As the frequency increases the echo heights are

[29] H. G. Booker, C. W. Gartlein, and B. Nichols, "Interpretations of radio reflections from the aurora," *Jour. Geophys. Res.*, vol. 60, pp. 1–22; March, 1955.
[30] S. Chapman, "The geometry of radio echoes from aurorae," *Jour Atmos. Terr. Phys.*, vol 3, pp. 1–29; January, 1953.

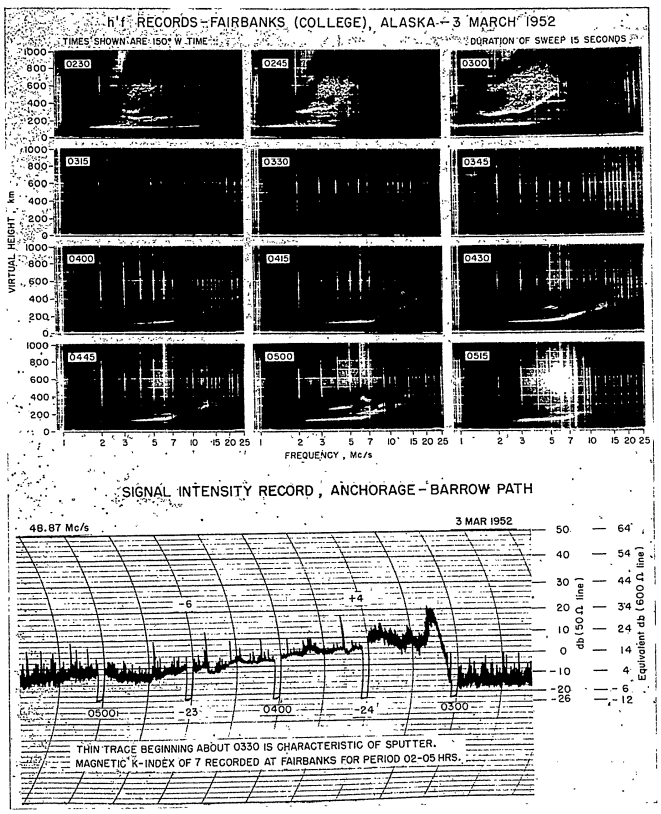

Fig. 33—Sample recording illustrating polar blackout followed by sputter observed at Barrow with accompanying $h'f$ observations made at Fairbanks near the path midpoint.

at first normal, then a steady increase in height with frequency is observed with the echoes disappearing at delays corresponding to heights at vertical incidence of about 450 kilometers. E-layer traces of this type are usually referred to as "slant E." Their interpretation is thought to be about as follows. Until the vertical-incidence critical frequency, about 8 Mc/s in the record cited above, is reached, the E-region trace is normal for the Arctic. At frequencies above the vertical-incidence critical frequency the propagation path is triangular. The first leg is sufficiently oblique for E-layer reflection to take place. The second leg consists of a downcoming

Declassified in Part - Sanitized Copy Approved for Release @ 50-Yr 2014/06/09 : CIA-RDP81-01043R003000180001-4

Declassified in Part - Sanitized Copy Approved for Release @ 50-Yr 2014/06/09 : CIA-RDP81-01043R003000180001-4

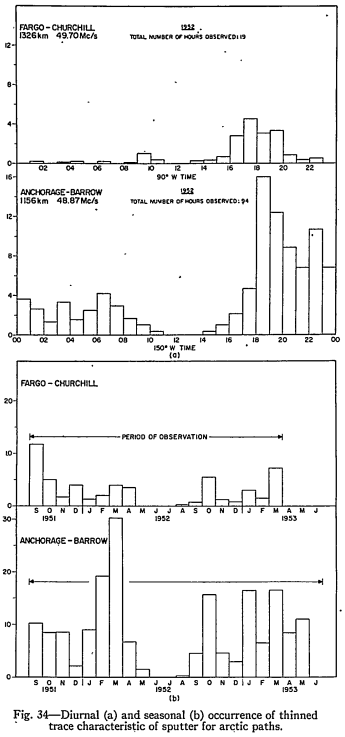

Fig. 34—Diurnal (a) and seasonal (b) occurrence of thinned trace characteristic of sputter for arctic paths.

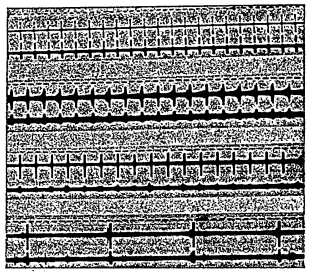

Fig. 35—Reception at Barrow of pulse transmissions from Anchorage at 24.325 Mc/s (upper trace) and 48.87 Mc/s (lower trace), during normal conditions (top frame) and during sputter (lower three frames) showing pulse elongations at either or both frequencies. Pulse duration slightly greater than one millisecond.

ray which impinges on an auroral shaft or part of a shaft lying below the E layer at a particular location such that after reflection at an angle about equal to the angle of incidence, the ray on its third leg is returned to the $h'f$ receiver. Energy may traverse this course in either direction. As the sounding frequency is raised the E-layer reflection becomes more and more oblique; hence different and more distant auroral shafts must be responsible for the echoes observed. Gaps in slant-E records can be due either to an absence of auroral shafts in a suitable position, or to nulls in the antenna patterns in the directions and at the vertical angles required. Systematic observation of slant E at ionospheric stations in the Arctic will thus give much information of the prevalence of aurorae of the type associated with sputter.

As the propagation path for sputter signals is generally quite different from the propagation path of the regular signals, multipath effects can be expected to occur. Systematic observations with millisecond pulses at Barrow showed some elongation during sputter, but the elongations at 48.87 Mc/s even with the Yagi antenna rarely exceeded a millisecond with significant intensity. Elongations at 24.325 Mc/s were more frequent and somewhat greater. Samples are shown in Fig. 35. This is in good agreement with the geometric considerations. Oscillograms of sputter signals were taken at Barrow when the Anchorage transmitter was being keyed with the teletype character R. Examples of these records are given in Fig. 36. A dual-beam oscilloscope was used so that reception on two separate rhombic antennas having a transverse spacing of about 300 feet and other pairs of antennas could be compared. The high-speed fading is clearly uncorrelated.

Correlations with Absorption and Magnetic Activity

The enhancements of the signal intensity observed at 50 Mc/s which occur during SID's and polar blackouts have already been discussed. They represent extreme cases of a more general behavior characteristic which is that departures of the signal intensity from normal, as measured, for example by the monthly medians, are closely correlated with amount of nondeviative absorption relative to the monthly median. This result is demonstrated in Fig. 37 in which absorption conditions at Fairbanks near the middle of the Anchorage to Barrow path have been determined from the $h'f$ observations. The procedure is to divide the $h'f$ observations taken at the middle of each hour for which medians of the vhf signal intensity are taken into four classes according

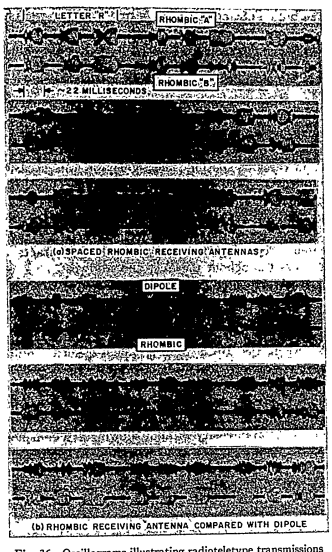

Fig. 36—Oscillograms illustrating radioteletype transmissions observed at Barrow during sputter.

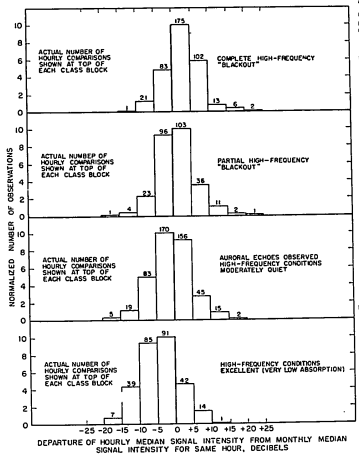
ACTUAL NUMBER OF HOURLY COMPARISONS SHOWN AT TOP OF EACH CLASS BLOCK
COMPLETE HIGH-FREQUENCY "BLACKOUT"
PARTIAL HIGH-FREQUENCY "BLACKOUT"
AURORAL ECHOES OBSERVED HIGH-FREQUENCY CONDITIONS MODERATELY QUIET
HIGH-FREQUENCY CONDITIONS EXCELLENT (VERY LOW ABSORPTION)
NORMALIZED NUMBER OF OBSERVATIONS
DEPARTURE OF HOURLY MEDIAN SIGNAL INTENSITY FROM MONTHLY MEDIAN SIGNAL INTENSITY FOR SAME HOUR, DECIBELS

Fig. 37—Correlation of ionospheric absorption observed at hf with vhf signal intensities observed at Barrow.

to the absorption they indicate. The first class corresponds to a complete hf blackout and no echoes are observed. The second class represents conditions of partial blackout when weak echoes are observed at frequencies well above the normal lower frequency limit. The third class represents fairly quiet conditions when auroral echoes of a type usually not associated with sputter and slant-E are seen.[31] The fourth class corresponds to very quiet ionospheric conditions, when absorption is low, and hf propagation conditions are good. The distributions of departures of the individual hourly medians of the vhf signal intensities from the monthly medians for the same hours are then defined according to the absorption class as shown. In Fig. 38 the diurnal variation in the occurrence of the absorption classes for the same period of time is shown. From these figures it will be seen that as a general rule the signal intensity is stronger than normal when the absorption is greater than normal, and vice versa. It is also of some interest

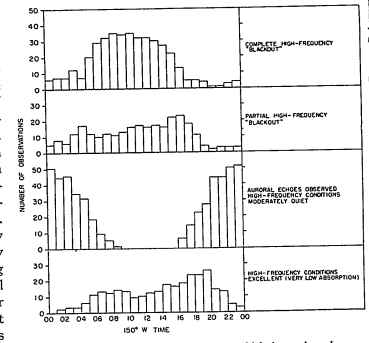
FAIRBANKS IONOSPHERIC CONDITIONS
MARCH AND APRIL 1952
COMPLETE HIGH-FREQUENCY "BLACKOUT"
PARTIAL HIGH-FREQUENCY "BLACKOUT"
AURORAL ECHOES OBSERVED HIGH-FREQUENCY CONDITIONS MODERATELY QUIET
HIGH-FREQUENCY CONDITIONS EXCELLENT (VERY LOW ABSORPTION)
NUMBER OF OBSERVATIONS
150° W TIME

Fig. 38—Diurnal variation of occurrence of hf absorption classes for same period as used for Fig. 37.

to note that the periods of partial and complete blackout occur mostly between about 05 and 17 hours local time, a period corresponding to strong signals according

[31] R. W. Knecht, "Relationships Between Aurorae and Sporadic E Echoes," Talk presented at URSI-IRE Meetings, Washington, D. C.; April 24, 1952.

Declassified in Part - Sanitized Copy Approved for Release @ 50-Yr 2014/06/09 : CIA-RDP81-01043R003000180001-4

Declassified in Part - Sanitized Copy Approved for Release @ 50-Yr 2014/06/09 : CIA-RDP81-01043R003000180001-4

to the monthly medians for the same months. During the universal period of minimum signal intensity in the evening around 20 hours local time, cases of very low absorption were most frequently observed.

A similar sort of analysis has been made in which the departures of the signal intensities observed at Barrow from the monthly median have been compared with the magnetic K-indexes observed at Fairbanks over a period of thirteen months. Result of this analysis is in Fig. 39. Black dots represent the median signal-intensity departures for each class interval in K-index and vertical lines at their limits show upper and lower decile values.

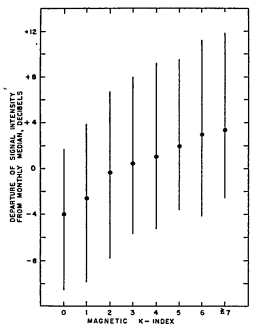

Fig. 39—Correlation of magnetic K-indexes observed at Fairbanks with signal intensities observed at Barrow.

These correlations are not on a one-to-one basis by any means but serve to demonstrate in a definite manner the statistical relationship between the strength of the vhf signals and ionospheric and magnetic conditions. It is the observation that the vhf signals tend to be stronger than normal during periods of heavy hf absorption or complete blackout that makes the vhf propagation attractive for arctic communications.

Tropospheric Propagation

While the various observations of the pulse transmitter located at Sterling have generally shown a "ground wave" even at the greatest distance tried, 811 kilometers, the intensity of the "ground wave" or tropospheric wave was weak, and decreased as the distance increased. There is therefore little reason to suppose that the continuous-wave observations at 49.8 Mc/s at Sterling have been contaminated to any significant extent by tropospheric propagation. This is more especially so because the rhombic antennas used have very poor radiation characteristics at the angles supposed to be of importance for tropospheric propagation. Nevertheless during the late part of the summer of 1952 when both 49.8 and 107.8 Mc/s transmissions were being recorded at Sterling, meteorological conditions were favorable and sufficiently stable for tropospheric ducts to form. During this period the Cedar Rapids transmissions were received for several hours at a time by means of tropospheric propagation with an intensity sufficient to affect and at times dominate the recordings. The most conspicuous sign of the tropospheric propagation was a thinning of the trace, somewhat resembling certain cases of sputter. The signals on this occasion exhibited a rolling type of slow intensity fluctuation characteristic of certain types of tropospheric propagation. Independent evidence of the widespread character of the meteorological situation was received from radio amateurs reporting near record-breaking contacts at 144 Mc/s throughout the East and Midwest.

Tropospheric propagation was observed at that time at both 49.8 and 107.8 Mc/s, though more frequently and conspicuously at the higher frequency. It is suggested that some of the occasions during the summer of 1952 when the 107.8 Mc/s signals seemed unduly strong compared with the 49.8 Mc/s signals, with a resulting small effective exponent for frequency dependence, may have resulted from tropospheric propagation of a type strong enough to affect the measured value of signal intensity without showing as a conspicuous alteration in the character of the trace. Fig. 40 shows simultaneous samples of recordings at 49.8 and 107.8 Mc/s illustrating the influence of tropospheric propagation at 49.8 Mc/s and dominant tropospheric propagation at 107.8 Mc/s.

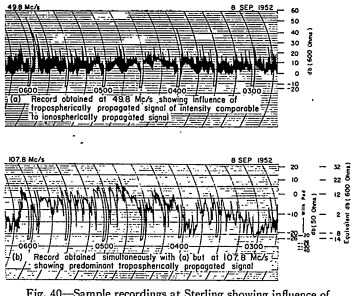

Fig. 40—Sample recordings at Sterling showing influence of unusual tropospheric propagation from Cedar Rapids.

Evidence of tropospheric propagation has not been found again at Sterling, nor has it been found at any time at any of the northern receiving terminals.

Background Noise Observations

Throughout the recording program the transmissions have been interrupted twice each hour in order to observe the level of background noise. Most of these observations have been of cosmic noise. Fig. 41 is a mass plot of the measured noise intensities in a 2 kc/s noise bandwidth at Churchill during December, 1951. The observations are plotted against the right ascension of the direction of the receiving lobe maximum. The declination observed was about 26 degrees south. Two well-defined maxima are observed corresponding to the passage of the plane of the galaxy through the lobe. The greater maximum corresponds closely to the direction of the galactic center. Similar results have been obtained at the other receiving terminals, though they differ in detail owing to the different declinations viewed.

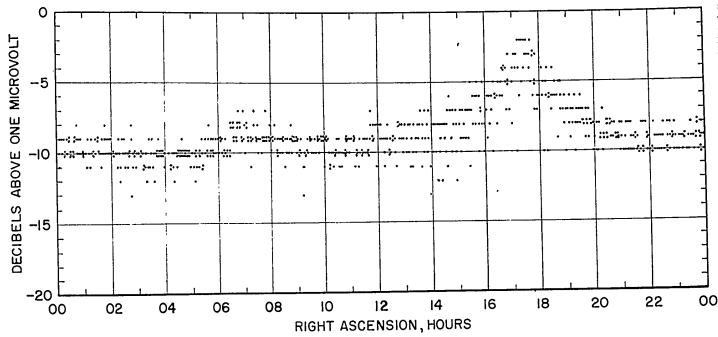

Fig. 41—Cosmic noise intensity observed hourly at Churchill in a 2 kc/s noise band, during December, 1951.

The twice-hourly noise observations soon proved to have definite value in the observing program. In the first place, for most kinds of changes in the receiving antenna or receiving system, drifts or discontinuities in the noise intensities gave a sensitive and valuable warning. Frequently drifts could be compensated for in the data analysis by knowing how much the noise observation was in error. In the second place, the noise levels at 50 Mc/s proved to be moderately sensitive indicators of the presence of unusual ionospheric absorption. A case in point has already been given in connection with the polar blackout illustrated in Fig. 31.

Apart from cosmic or galactic noise, solar noise was occasionally observed. The declination viewed by the Sterling rhombics was about 20 degrees north, and by the Barrow rhombics 11 degrees south. The sun therefore passed directly through these main lobes each day for a period of a few days twice each year. On these occasions solar noise was observed, usually of the quiet background kind, but occasionally of the active outburst kind. The latter was sometimes strong enough to be observed in the side lobes at other times of the year.

At various times noise of terrestrial origin was observed, as for example when active electrical storms were in progress near the receiving locations. Ignition noise, and power line noise have also been observed. At Sterling the precipitation noise levels were frequently high during certain rainstorms. At Churchill and Barrow, snow or drifting ice crystals during blizzard conditions gave rise to high noise levels. In one case at Barrow during a very severe blizzard, the precipitation noise rose to levels exceeding the signal level. During this event the noise level could be closely correlated with the wind velocities as observed at a U. S. Weather Bureau station about a mile away. Fig. 42 illustrates the noise behavior during this blizzard.

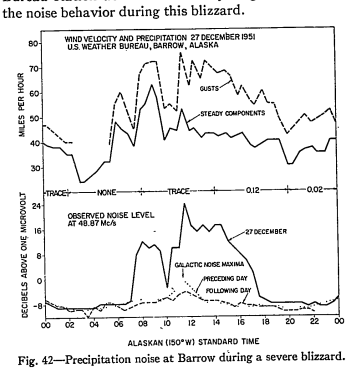

Fig. 42—Precipitation noise at Barrow during a severe blizzard.

If the antennas and receiving equipment are operated correctly and are properly designed, receiver noise is never a limiting factor at 50 Mc/s, though it influences, significantly at times, the observations of background cosmic noise at 107.8 Mc/s.

Declassified in Part - Sanitized Copy Approved for Release @ 50-Yr 2014/06/09 : CIA-RDP81-01043R003000180001-4

Declassified in Part - Sanitized Copy Approved for Release @ 50-Yr 2014/06/09 : CIA-RDP81-01043R003000180001-4

Part II. The Role of the Antennas

Introduction

In the preceding account it has been repeatedly emphasized that the behavior of the observations and the interpretations of this behavior cannot be divorced from consideration of the antennas actually used. In the sections that follow the part played by the antennas in the propagation studies will be examined more closely and from several points of view.

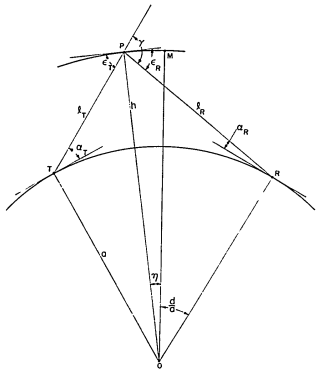

Fig. 43—Geometry for Case I scattering.

Geometric Considerations

Some generalization of the concept of the geometric factors, q, defined in a particular sense by (3) and (4), is indicated. Consider Fig. 43 where P represents the position of an elementary macroscopic volume of the scattering medium which is presumed to be distributed in a shell concentric with the earth, having a thickness b, small compared with its height h above earth. Let

M = midpoint of the path in the scattering medium,
P = a point in the scattering shell displaced from M in the plane containing the transmitter T, receiver R, and center of the earth O,
η = the angular position of P with respect to M measured at the center of the earth,
α_T, α_R = the angular elevation of P as seen from T and R respectively,
l_T, l_R = the ray lengths to P from T and R respectively,
ϵ_T, ϵ_R = the angles between l_T and l_R respectively, and the tangent plane to the scattering shell at P,
γ = the scattering angle,
$2d$ = surface distance from T to R,
a = radius of the earth, and
h = height of the thin scattering stratum.

The following relations may be used to determine the α's, l's, ϵ's, and γ as a function of the displacement of P from M as measured by η according to the conventions of Fig. 43:

$$\tan \alpha_T = \frac{\cos\left(\frac{d}{a} - \eta\right) - \frac{a}{a+h}}{\sin\left(\frac{d}{a} - \eta\right)}, \tag{8}$$

$$\tan \alpha_R = \frac{\cos\left(\frac{d}{a} + \eta\right) - \frac{a}{a+h}}{\sin\left(\frac{d}{a} + \eta\right)}, \tag{9}$$

$$l_T = \frac{(a+h)\sin\left(\frac{d}{a} - \eta\right)}{\cos \alpha_T}, \tag{10}$$

$$l_R = \frac{(a+h)\sin\left(\frac{d}{a} + \eta\right)}{\cos \alpha_R}, \tag{11}$$

$$\cos \epsilon_T = \frac{a}{a+h}\cos \alpha_T, \tag{12}$$

$$\cos \epsilon_R = \frac{a}{a+h}\cos \alpha_R, \tag{13}$$

and finally

$$\gamma = \alpha_T + \alpha_R + 2\frac{d}{a}, \tag{14}$$

or

$$\gamma = \epsilon_T + \epsilon_R. \tag{15}$$

If horizontal polarization is used the angle χ previously discussed is 90°. In vertical polarization $\chi = 90° - \gamma$. Displacements of P from M of the type illustrated by Fig. 43 will be referred to as Case I.

Now consider Case II, as represented by Fig. 44 in which P is displaced from M in a direction forming a right angle at the midpoint with the displacements of Case I. That is to say, P is displaced from M in such a way that $\alpha_T = \alpha_R = \alpha$, $l_T = l_R = l$, and $\epsilon_T = \epsilon_R = \epsilon$. As shown in Fig. 44 let ζ represent the angular position of P with respect to M measured at the center of the earth. It is necessary for Case II to define an azimuth β as the direction of P as seen from T or R with respect to the great-circle path connecting T and R. The following relations may now be used to calculate the principal geometric quantities, as a function of the displacement of P from M as measured by ζ:

$$l^2 = (a+h)^2 + a^2 - 2a(a+h)\cos\frac{d}{a}\cos\zeta, \tag{16}$$

$$\cos \gamma = \frac{2a^2 \sin^2 \frac{d}{a} - l^2}{l^2}, \tag{17}$$

$$\sin \alpha = \frac{(a+h)\cos\frac{d}{a}\cos\zeta - a}{l}, \tag{18}$$

$$\sin \beta = \frac{(a+h)\sin\zeta}{l\cos\alpha}, \tag{19}$$

and

$$\sin \epsilon = \frac{(a+h) - a\cos\frac{d}{a}\cos\zeta}{l}. \tag{20}$$

In Case II if horizontal polarization is used at T, the downcoming signal at R from P will contain both vertically and horizontally polarized components when $\zeta \neq 0$. The power received at R from P with a horizontal antenna is measured by $\sin^4 \chi$, and with a vertical antenna by $\sin^2\chi\cos^2\chi$.

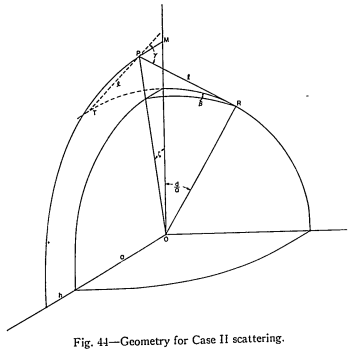

Fig. 44—Geometry for Case II scattering.

To obtain χ the following relationship is used,

$$\cos \chi = \frac{2a}{l}\frac{\sin\frac{d}{a}\cos\frac{d}{a}\sin\zeta}{\sqrt{1 - \cos^2\frac{d}{a}\cos^2\zeta}}, \tag{21}$$

or

$$\cos \chi = \frac{a}{l}\sin\frac{2d}{a}\sin\beta. \tag{22}$$

With the relations above it is possible to compute the geometric quantities required for certain idealized beam swinging transmission arrangements, which are chosen to give further insight into the interpretation of the observations made with less than ideal arrangements.

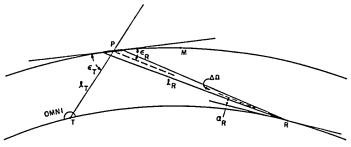

Fig. 45—Geometry for first beam swinging model—"omni to beam."

First Beam Swinging Model—"Omni to Beam"

As a first trial consider Fig. 45, which represents Case I geometry. The transmitter at T is connected to an omnidirectional antenna having an aperture A_0 and the receiver R is connected to a highly directional antenna having a single lobe of solid angle $\Delta\Omega$ which is inversely proportional to its aperture A_D. The receiving antenna is so directive that its beam $\Delta\Omega$ is formed independently of the ground no matter how it is steered as long as the lower edge of the beam is above the horizon. The directivity $\Delta\Omega$ is such that throughout the intercepted elementary macroscopic volume of the scattering medium, the values of the l's and γ may be regarded as constant to a high order of approximation. The position of the intercepted scattering volume may thus be represented by the point P as shown in Fig. 45. The received power is now expressed as a function of the position of P in the plane represented by Fig. 43, that is to say in a Case I manner. In accordance with the definition of the scatter cross section, the following relation can be written

$$P_r \propto \underbrace{\frac{P_t}{l_T^2}}_{(a)} \cdot \underbrace{\frac{bl_R^2\Delta\Omega}{\sin\epsilon_R}}_{(b)} \cdot \underbrace{\frac{\sin^2\chi}{\left(\sin\frac{\gamma}{2}\right)^n}}_{(c)} \cdot \underbrace{\frac{A_D}{l_R^2}}_{(d)}, \tag{23}$$

where

(a) is proportional to the incident power density,
(b) is the macroscopic element of volume illuminated by T seen by the receiving antenna,
(c) is proportional to the scatter function,
(d) is the solid angle intercepted at R,

but $A_D \propto 1/\Delta\Omega$, so that the geometric aspects of the transmission may be expressed by:

$$\frac{P_r}{P_t} \propto \frac{b\sin^2\chi}{l_T^2 \sin\epsilon_R \left(\sin\frac{\gamma}{2}\right)^n}, \tag{24}$$

and a geometric factor, q, generalized in this manner

Declassified in Part - Sanitized Copy Approved for Release @ 50-Yr 2014/06/09 : CIA-RDP81-01043R003000180001-4

Declassified in Part - Sanitized Copy Approved for Release @ 50-Yr 2014/06/09 : CIA-RDP81-01043R003000180001-4

may be defined as

$$q = \frac{1}{l_T^2 \sin \epsilon_R \left(\sin \frac{\gamma}{2}\right)^n}. \quad (25)$$

If the beam $\Delta\Omega$ is swung according to Case II, the analogous generalized geometric factor is:

$$q = \frac{1}{l^2 \sin \epsilon \left(\sin \frac{\gamma}{2}\right)^n}. \quad (26)$$

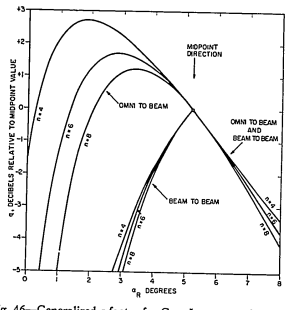

Fig. 46—Generalized q factor for Case I geometry for Cedar Rapids to Sterling distance.

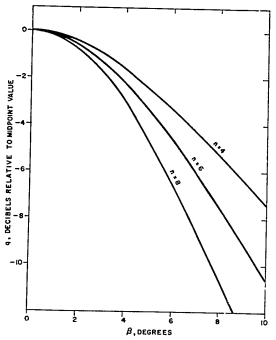

Fig. 47—Generalized q factor for Case II geometry for "omni to beam" model for Cedar Rapids to Sterling distance.

Figs. 46 and 47 illustrate the approximate behavior of (25) and (26) respectively in the vicinity of the path midpoint for the Sterling–Cedar Rapids path for $n=4$, 6, and 8. Fig. 46 shows q as a function of α_R. In Fig. 47 q is plotted as a function of β. For higher values of n the q curves fall more steeply from their maximum values, and the position of the maximum for Case I beam swinging is displaced in the direction of the path midpoint. In Fig. 47 the polarization correction $\sin^4 \chi$ corresponding to horizontal antenna elements at both terminals has been included.

The symmetrical properties of the q for Case I above may be easily established by interchanging T and R and by swinging the beam to a point displaced by an equal value of η in the direction of R.

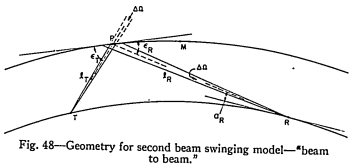

Fig. 48—Geometry for second beam swinging model—"beam to beam."

Second Beam Swinging Model—"Beam to Beam"

For this trial consider Fig. 48 which represents Case I geometry. Both T and R are connected with identical highly directional antennas of the kind used for receiving in the previous example. The two beams are directed toward P. The received power is now expressed as a function of the position of P as it varies in the plane represented by Fig. 43. As before the following relation may be written for P closer to T:

$$P_r \propto \underbrace{\frac{P_t}{l_T^2 \Delta\Omega}}_{(a)} \cdot \underbrace{\frac{b l_T^2 \Delta\Omega}{\sin \epsilon_T}}_{(b)} \cdot \underbrace{\frac{\sin^2 \chi}{\left(\sin \frac{\gamma}{2}\right)^n}}_{(c)} \cdot \underbrace{\frac{A_D}{l_R^2}}_{(d)}, \quad (27)$$

where (a), (b), (c), and (d) have the same meanings as before. Thus:

$$\frac{P_r}{P_t} \propto \frac{A_D b \sin^2 \chi}{l_R^2 \sin \epsilon_T \left(\sin \frac{\gamma}{2}\right)^n}. \quad (28)$$

If P is closer to R, the result corresponding to (28) is:

$$\frac{P_r}{P_t} \propto \frac{A_D b \sin^2 \chi}{l_T^2 \sin \epsilon_R \left(\sin \frac{\gamma}{2}\right)^n}. \quad (29)$$

In both cases the denominator contains the larger l and larger ϵ. If l_l and ϵ_l are written for the larger values of l and ϵ according to the position of P for Case I geometry, the generalized geometric factor q may be defined as:

$$q = \frac{1}{l_l^2 \sin \epsilon_l \left(\sin \frac{\gamma}{2}\right)^n}. \quad (30)$$

If the beams are now swung in azimuth corresponding to Case II geometry, the intersection of one beam with the scattering shell no longer entirely contains the other beam and a further factor is required in the generalized q. Since it is always assumed that the thickness of the scattering shell is small compared with its height, the scattering volume can again be written as the area of the thin shell illuminated multiplied by its thickness. Thus the volume illuminated by the transmitting beam is

$$V = \frac{b l^2 \Delta\Omega}{\sin \epsilon}, \quad (31)$$

and if V_c is defined as that part of the illuminated volume within the receiving beam, then the further factor in the generalized q for Case II geometry is V_c/V, and

$$q = \left(\frac{V_c}{V}\right) \frac{1}{l^2 \sin \epsilon \left(\sin \frac{\gamma}{2}\right)^n}. \quad (32)$$

The factor V_c/V can be approximated as follows. Define 2τ as the exterior angle between the two beam directions projected on a tangent plane at P. τ may be obtained from the following relation:

$$\cos \tau = \frac{\sin \frac{d}{a}}{\sqrt{1 - \cos^2 \frac{d}{a} \cos^2 \zeta}}, \quad (33)$$

or

$$\cos \tau = \frac{\sin \beta}{\sin \zeta} \sin \frac{d}{a}. \quad (34)$$

Then as long as $2\tau \leqq \epsilon$, which includes the region of principal interest:

$$\frac{V_c}{V} \approx 1 - \frac{\sin 2\tau}{\pi \sin \epsilon}. \quad (35)$$

A less convenient approximation for V_c/V which is usable for all possible values of τ is

$$\frac{V_c}{V} \approx \frac{2}{\pi}\left[\arctan\left(-\frac{\cot \tau}{\sin \epsilon}\right) - \arctan\left(\frac{\tan \tau}{\sin \epsilon}\right)\right]. \quad (36)$$

The two arc tangents represent 2nd and 1st quadrant angles respectively. This expression is exact for beams of circular cross section in the limit as $\Delta\Omega \to 0$. Figs. 46 and 47 illustrate the behavior of (30) and (32) respectively for $n=4$, 6, and 8 in the vicinity of the path midpoint for the Cedar Rapids to Sterling path. Fig. 49 includes the polarization correction $\sin^4 \chi$ corresponding to horizontal antenna elements at both terminals. It will be seen that the maximum transmission takes place when the two beams are directed at the path midpoint. The two beams are then matched exactly in the scattering medium. As before if a greater value of n is selected the curves fall away more steeply.

The Beamwidth of the Scattering Mechanism

In general there will be an angular width in azimuth ϕ and an angular width in elevation ψ, which together define the range of directions from which the power received mainly arrives. With the aid of the foregoing beam swinging models it is possible to examine what may be termed the natural beamwidth of the scattering medium. The natural horizontal beamwidth associated with the scatter mechanism is called ϕ_m and is defined by the angular distance between the points three decibels below the maximum q's for Case II geometry. Table III shows values of ϕ_m obtained from Figs. 47 and 49 for typical values of n. It will be noted that ϕ_m

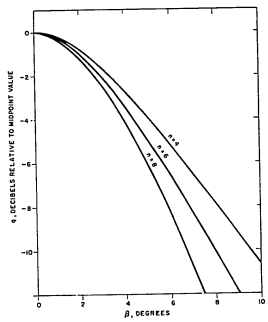

Fig. 49—Generalized q factor for Case II geometry for "beam to beam" model for Cedar Rapids to Sterling distance.

does not vary greatly with extreme variations in the beamwidth of the transmitting antenna. The values in Table III are representative for all practical path lengths. At the greater distances beyond 1,800 kilometers, the ϕ_m's are about one degree narrower, and for the shortest distances of practical interest, about 1,000 kilometers, the ϕ_m's are about one degree wider.

TABLE III

ϕ_m, Degrees, Cedar Rapids to Sterling Path

n	Omni to beam	Beam to beam
4	11.3	8.6
6	9.4	7.5
8	8.0	6.8

In the case of the vertical plane, as represented by Case I geometry, what may be termed the natural beamwidth ψ_m is defined as the angular distance between points three decibels below the maxima shown in Fig. 46. It is to be noted that the transmitting antenna plays a significant part in determining the angular elevation at the receiver of the upper and lower limits

Declassified in Part - Sanitized Copy Approved for Release @ 50-Yr 2014/06/09 : CIA-RDP81-01043R003000180001-4

Declassified in Part - Sanitized Copy Approved for Release @ 50-Yr 2014/06/09 : CIA-RDP81-01043R003000180001-4

of ψ_m. The case of the omnidirectional antenna to beam antenna represents an extreme condition exceeding any found in practice. The beam to beam case comes closer to practice. Table IV shows values of ψ_m obtained from Fig. 46 for typical values of n.

TABLE IV

ψ_m, DEGREES, CEDAR RAPIDS TO STERLING PATH

n	Omni to beam	Beam to beam
4	5.2	4.2
6	5.2	3.9
8	5.0	3.7

These results are discussed below in connection with problems associated with practical antennas.

Effective Volume for Scattering

In practical situations, the transmitting antenna will have considerable directivity. If the transmitting antenna beamwidths, ϕ_a and ψ_a, in azimuth and elevation respectively, are substantially smaller than ϕ_m and ψ_m, ϕ and ψ will be largely determined by ϕ_a and ψ_a. For the longer paths, the common volume geometry shown in Fig. 50 will be the limiting factor in determining ψ.

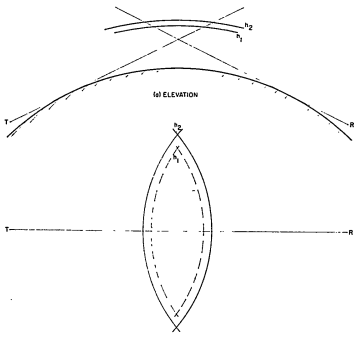

Fig. 50—Common volume geometry.

In this case ψ is approximately determined by the intersection of two planes tangent to the earth at the path terminals with the scattering stratum in the vertical plane passing through the terminals and the path midpoint. ψ thus limited is called ψ_c, and its value is given as a function of path length and scattering height in Fig. 51. For very long paths for which elevated antenna sites must be used ψ_c is greater than the values shown by Fig. 51 approximately by the sum of the dips of the radio horizons at the two terminals. As a practical matter, ϕ will not be limited by common volume geometry effects even for very long paths as can be seen

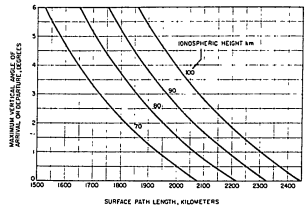

Fig. 51—Limiting effect of common volume geometry on maximum vertical angle of arrival or departure for Case I geometry for antennas at zero height, including effects of representative mid-latitude refraction.

from Fig. 52 and consideration of the influence of path length on ψ_m as discussed earlier. The cone widths ϕ and ψ as influenced by ϕ_m and ϕ_a, and ψ_m, ψ_a, and ψ_c, respectively, determine in a rough way what may be termed an effective volume in the height range over which scattering takes place.

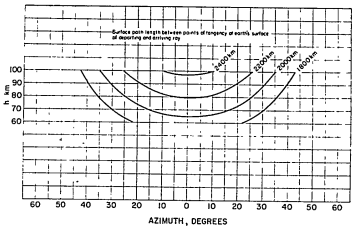

Fig. 52—Limiting effect of common volume geometry on maximum azimuthal angle of arrival or departure for Case II geometry, including effects of representative mid-latitude refraction.

It is useful to consider the influence of the effective volume in the design of antennas for use in transmission by ionospheric scattering. When the transmitting and receiving beamwidths both vertically and horizontally are substantially larger than, and include, the cone of angles associated with the effective volume, the received power will increase as the directivity of the antennas is increased in approximate proportion to the product of the plane-wave gains of the antennas. Under these circumstances increased transmitting directivity produces more intense illumination of the effective volume and, in reception, power from the effective volume is received with a larger aperture resulting in a further increase of received power. If, however, the antenna beamwidths are smaller than the cone of angles determined by ϕ_m, and ψ_m or ψ_c whichever is smaller, the received power will increase more slowly with increasing antenna directivities. For this condition, the power received from the central portion of the effective volume, resulting from the increased intensity of illumination in the maximum of the transmitting antenna beam, and the more effective scattering in the vicinity of the path midpoint, more than offsets the loss of received power resulting from the reduction of the effective volume imposed by the smaller beamwidths. When the antenna beamwidths are approximately equal to ϕ_m, and ψ_m or ψ_c whichever is smaller, the effective volume will just fill the beams and the antenna beamwidths may be said to match the effective volume. The plane-wave gains of transmitting and receiving antennas should in these circumstances be largely realized.

Realized Gains of the Antennas

From early in the experimental program it has been apparent that antenna characteristics have an important influence on the received signal levels and on the diurnal variations of these levels. Fig. 53 shows the computed directivity of the transmitting and receiving

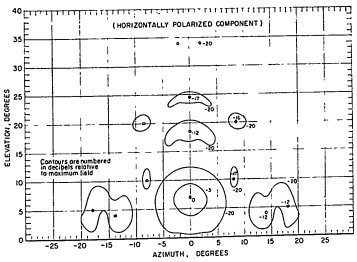
(HORIZONTALLY POLARIZED COMPONENT)
ELEVATION, DEGREES
Contours are numbered in decibels relative to maximum field
AZIMUTH, DEGREES

Fig. 53—Computed directivity of rhombic antennas used for the Cedar Rapids to Sterling path.

rhombics used for the routine signal intensity recording program on the Cedar Rapids–Sterling path. When antennas of lower directivity are used at Sterling for receiving it is found that the average signal intensities available from these antennas are generally lower than those available from the rhombic antenna but that the ratios of the powers received on the rhombic antenna to those received on the less directive antennas vary characteristically with local time. These effects are illustrated in Fig. 54 which displays the received intensities at 49.8 Mc/s on the rhombic antenna and on a five-element horizontal Yagi antenna. The free-space, half-power beamwidths of the Yagi antenna were approximately 65 degrees in the plane of the elements and 52 degrees in the plane normal to the elements. The plane-wave gains of the rhombic and the Yagi antennas in the beam maxima are approximately 18 db and 9 db respectively, relative to a horizontal half-wave dipole at the same height above ground. Comparisons of received

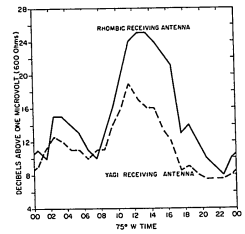

Fig. 54—Median signal intensities observed at 49.8 Mc/s at Sterling with rhombic and Yagi receiving antennas for a 19-day period in December, 1951. Rhombic transmitting antenna used at Cedar Rapids.

signal intensities using rhombic transmitting and receiving antennas and five-element Yagi transmitting and receiving antennas were made on the Anchorage to Barrow path at 48.87 Mc/s in March, 1953. Results of experiment are in Fig. 55. Fig. 56, page 1220, shows

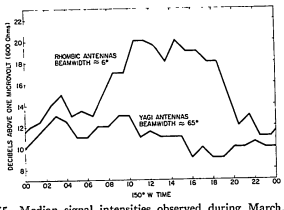

Fig. 55—Median signal intensities observed during March, 1953 at 48.87 Mc/s at Barrow with rhombic to rhombic and Yagi to Yagi antenna arrangements.

distributions of realized gain for rhombic-to-rhombic antenna systems used in the routine recording program as compared with dipole to dipole transmission. The realized gain of an antenna is defined here as the ratio of the signal intensity observed when the antenna is used to that observed when a reference or comparison antenna is used during the same period of time. In stating results of observations of realized gain it is necessary to specify the antenna arrangements used at both terminals. Measurements of realized gain were made on all of the 50 Mc/s test paths by means of alternate half-hourly transmissions on a rhombic antenna and on a reference dipole, with reception performed

Declassified in Part - Sanitized Copy Approved for Release @ 50-Yr 2014/06/09 : CIA-RDP81-01043R003000180001-4

Declassified in Part - Sanitized Copy Approved for Release @ 50-Yr 2014/06/09 : CIA-RDP81-01043R003000180001-4

simultaneously with a rhombic antenna and a dipole. Table V summarizes the results for the Fargo to Churchill path for a three-day period. It is evident that

TABLE V
REALIZED GAIN, DECIBELS

Per Cent of Comparisons in Which Gain Equals or Exceeds Value Shown	Transmitting Rhombic Antenna		Receiving Rhombic Antenna	
	Measured with Receiving Rhombic	Measured with Receiving Dipole	Measured While Transmitting on Rhombic	Measured While Transmitting on Dipole
5	19	14	19	17
10	18	13	18	15
50	14	9	15	10
90	10	4	11	3
95	9	2	10	1

the realized gain of a directive antenna is a function of the directivity of the antenna used at the opposite terminal and is influenced strongly by diurnal variations in the propagation mechanism or mechanisms. It is convenient to discuss this behavior by considering the case of a receiving antenna. The controlling factor in determining the realized gain of a receiving antenna is the angular size of the cone of angles from which power mainly arrives at the receiving location in relation to the angular dimensions of the receiving beam. The observed greater realized gain of the rhombic receiving antenna shown in Fig. 54 during the daylight hours suggests that most of the received power is arriving from a cone of angles determined largely by the directivity of the transmitting antenna or by a highly directive scattering mechanism. On the other hand, the behavior at other times when the realized gain is low suggests that a larger cone of angles exists from which power is effectively receivable. Table V further illustrates these effects.

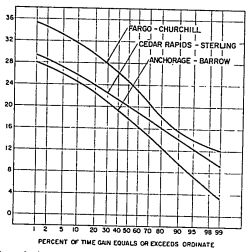

Fig. 56—Cumulative distributions of realized gain at about 50 Mc/s of rhombic to rhombic antenna arrangement over dipole to dipole arrangement, observed for 3-day period for each path.

Factors which can give rise to an increased angular size of the cone during these periods are decreases in the angle dependence of the scattering mechanism, large scale irregularities in the efficiency of scattering over the extent of the common volume, and contributions to from meteor ionization which lies outside the effective volume as determined by ϕ_m, ϕ_a, ψ_m, ψ_a, and ψ_c. The first of these factors, in view of the frequency dependence measurements, and the calculated values of ϕ_m and ψ_m appears to be incapable of producing the observed wide variations in realized gain. Little detailed information is available concerning the nature and behavior of the large scale irregularities in scattering efficiency throughout the common volume, but there is hardly any doubt of their existence. Influence of meteoric ionization is probably most important single factor in causing observed variations in realized gain.

Influence of Meteoric Ionization

Much of the preceding discussion has been based on the assumption that a scattering mechanism is effective in propagating the received signals. To the extent that the received signals are appreciably contaminated by the presence of components resulting from meteoric ionization, the principal influence on the behavior of highly directive antennas will be a reduction in their realized gains as determined by the larger cone of angles associated with the meteoric components. If, however, the contributions from meteoric ionization are dominant, greater signal intensities could be received if different antennas were used.[11,12]

In an earlier paper the[4] possibility was suggested that the diurnal variation of observed signal intensity could be interpreted as the resultant of a solar ultra-violet influence having a maximum at midday, and a meteroic influence having a maximum at about 06 hours and a minimum at about 18 hours local time. To illustrate this suggestion the hourly median signal intensities observed at 49.8 Mc/s at Sterling were shown for April, 1951. Observations of the rate of occurrence of Doppler components differing from the carrier frequency by at least 200 cycles per second have been made at Sterling at 49.8 Mc/s over a long period. The resulting average rates for the month of April, 1955 are shown in Fig. 57

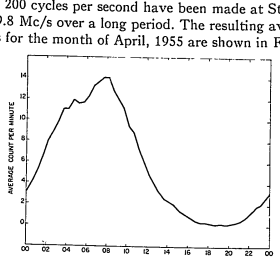

Fig. 57—Diurnal variation of the average rate of occurrence of meteor Doppler components observed at Sterling at 49.8 Mc/s during April, 1955.

for Doppler components having intensities exceeding 0.25 microvolt, open circuit voltage at 50 ohms. The maximum and minimum rates are seen to occur one to two hours later than 06 hours and 18 hours local time at the path midpoint. The secondary maximum at

The principal results of an experiment designed to establish more clearly the relationship between contributions resulting from a scattering mechanism and those resulting from meteoric components are now described. In this experiment, 49.8 Mc/s transmissions beamed towards Sterling, were simultaneously received at Sterling and at a site selected as being nearly optimum for reception of the meteoric components. This

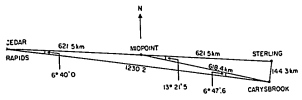

Fig. 58—Geometry for Carysbrook experiment.

site was near Carysbrook, Va., at a distance of 144.3 kilometers from Sterling in a southerly direction as shown in Fig. 58. At Sterling, the rhombic antenna normally used in the recording program was employed. An identical rhombic antenna was erected at Carysbrook, and directed toward the midpoint of the Cedar Rapids to Sterling path. Fig. 59 displays the hourly median signal intensities received simultaneously at Sterling and at Carysbrook during the course of the experiment. The integrated intensities were observed to be higher at Carysbrook between 23 hours and 04 hours local time at the path midpoint. During these hours the results would thus appear to be consistent with the theory that the meteor ionization trails contributing most effectively to the integrated signal intensity occur on one side of the great circle path between the transmitter and the receiver.[24] On the other hand, the existence of greater signal intensities on the Cedar Rapids to Sterling path most of the time provides further support of the view that the observed signals are the result of more than one propagation mechanism.[32] For the conditions under which the experiment was performed, it is concluded that systems designed to work through the universally observed periods of low signal intensity occurring at about 20 hours local time should employ antennas directed along the great circle bearing between the transmitter and receiver. It should be pointed out that the rhombic antennas used on the Cedar Rapids to Sterling path since the beginning of the experimental program were designed for an assumed midpoint height of about 105 kilometers for the scattering region. In the light of the knowledge acquired later concerning the heights at which scattering occurs, it would have been more appropriate to direct the beam maxima toward a midpoint height of about 85 kilometers. Consequently, it is thought that the experimental results throughout the observing program at Sterling including the results presented in Fig. 59 are biased to some extent in favor of the meteoric components.

Further experimentation of the kind above is desirable in order to obtain information on the relative contributions of the scattered components and the meteoric components at other times of year and for other path orientations. Some specific suggestions for related experimentation were made earlier in connection with polarization dependence.

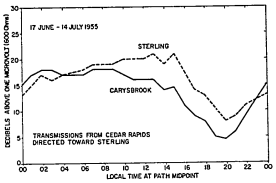
17 JUNE - 14 JULY 1955
STERLING
CARYSBROOK
TRANSMISSIONS FROM CEDAR RAPIDS DIRECTED TOWARD STERLING
DECIBELS ABOVE ONE MICROVOLT/600Ohms
LOCAL TIME AT PATH MIDPOINT

Fig. 59—Diurnal variation of hourly median signal intensities observed simultaneously at Sterling and at Carysbrook, at 49.8 Mc/s.

Diversity Considerations

In an earlier section the measurements of the correlation between the envelopes of signals received on spaced Yagi antennas were described. Fig. 20 illustrates the observed behavior for spacings along and transverse to the path. Envelope correlation coefficients of 0.5 were observed for spacings of about 3.5 wavelengths transverse to the path and about 40 wavelengths along the path. A practical implication of these results is that smaller antenna spacings will suffice for effective diversity action if the diversity antennas are disposed in a line normal to the path rather than along the path.

Gordon[33] has studied the effects of the tropospheric scattering mechanism in relation to the correlation expected between spaced antennas for diversity action. Using somewhat similar, but not identical arguments diversity spacings for transmission by ionospheric scattering can be estimated. While the precise calculations would be involved, important features can be seen from some very simplified considerations. As such consider that the antenna spacing required to produce a low envelope correlation is that necessary to give a difference of one wavelength in the paths of the signals from opposite boundaries of the effective scattering

[32] It is of interest to calculate the expected intensity of the Carysbrook signals relative to the simultaneously observed signal intensities at Sterling on the assumption that propagation is predominantly by a scattering mechanism, as might be expected during the afternoon. Previously given geometric considerations are employed and for angle dependence it is assumed that $n=6$. The loss resulting from the larger scattering angle at Carysbrook is found to be about 4 decibels. In addition a further loss of 1½ to 2 decibels, affecting the Carysbrook observations, is associated with V_0/V as given by (36). Finally there is a loss of about ¾ decibel associated with the use of horizontal polarization, because $\chi=90°$ at Carysbrook. A net loss at Carysbrook relative to Sterling of about 6 decibels is therefore predicted for propagation by scattering uncontaminated by meteoric or other components. This result is seen to be in fair agreement with Fig. 59, during the midafternoon period.

[33] W. E. Gordon, "Radio scattering in the troposphere," PROC. IRE, vol. 43, pp. 23–28; January, 1955.

Declassified in Part - Sanitized Copy Approved for Release @ 50-Yr 2014/06/09 : CIA-RDP81-01043R003000180001-4

Declassified in Part - Sanitized Copy Approved for Release @ 50-Yr 2014/06/09 : CIA-RDP81-01043R003000180001-4

volume. Fig. 60 illustrates the usual diversity arrangement in which diversity action is obtained by spacing the receiving antennas transverse to the great circle path at a constant height. The angle ϕ in Fig. 60 is the width of the cone of angles over which most of the power is received. The diversity distance S_t is defined to be the distance through which a receiving antenna must be moved to produce a change in the difference between the ray path lengths l_1 and l_2 of one wavelength. The ray lengths, l_1 and l_1', and l_2 and l_2', are much greater than S_t so that they may be considered to be parallel.

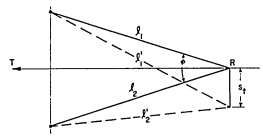

Fig. 60—Geometry for transverse spaced-antenna diversity.

From simple geometrical considerations,

$$l_1' - l_1 = S_t \sin\frac{\phi}{2}, \tag{37}$$

$$l_2' - l_2 = -S_t \sin\frac{\phi}{2}, \tag{38}$$

and the diversity distance is:

$$S_t = \frac{\lambda}{2 \sin\dfrac{\phi}{2}}. \tag{39}$$

The smaller of the cone widths, ϕ_m and ϕ_a is used with (39) for estimating appropriate spacing of the antennas for diversity action.

The diversity distance in a vertical direction at the receiver is, on the basis of similar considerations,[34]

$$S_v = \frac{\lambda}{2 \sin\dfrac{\psi}{2}}. \tag{40}$$

The smallest of the cone angles, ψ_m, ψ_a, and ψ_e, is used for ψ in computing an appropriate diversity distance S_v.

The longitudinal diversity distance S_l along the path and parallel to the tangent plane to the earth under the receiver is influenced by both cone angles ϕ and ψ. It is convenient to state the results separately. For ϕ,

$$S_l(\phi) = \frac{\lambda}{2 \sin^2\dfrac{\phi}{4}}, \tag{41}$$

and for ψ,

$$S_l(\psi) = \frac{\lambda}{2 \sin\dfrac{\psi}{2} \sin\theta}, \tag{42}$$

where θ is the angle between the tangent plane at the receiver and the center of the cone width ψ. When the combined effects of ϕ and ψ are taken into account, the appropriate diversity spacings will be intermediate between the values determined separately. This matter has not been further explored since even the smaller of the diversity distances obtained from the above expressions will, in practice, be many times the diversity distance S_t required for spacings transverse to the path. For this reason longitudinal diversity is not convenient in practice.

As will be discussed in Part III, a useful siting procedure is to align the transmitting and receiving beams on the ionospheric midpoint height by putting the antennas at a height z above a smooth reflecting surface, as determined by,

$$z = \frac{\lambda}{4 \sin\alpha}, \tag{43}$$

where α is the angle of elevation of the path midpoint for the design height of scattering. For the shorter paths in which the antennas are sited in accordance with (43), α will be roughly the same size as ψ. With this in mind, and comparing (43) with (40) it will be seen that for small α and ψ, S_v will be roughly twice as great as $2z$, the distance between the antenna and its image. Accordingly, the correlation between the antenna and its image will be rather poor, and coherent gain will be realized only for the contributions arriving from the central portion of the effective volume. The net increase in signal power resulting from the presence of the image receiving antenna when both transmitting and receiving antennas are thus sited is expected to be about three decibels or slightly greater. An alternative explanation is that the receiving antenna will be receiving power from two poorly correlated sources of approximately equal intensity, the effective volume and its image.

The transverse diversity distance S_t for the Cedar Rapids to Sterling path is 9.6λ on the assumption that $\phi = \phi_a = 6$ degrees. Experimentally observed values of envelope correlation as a function of antenna spacing were given in Fig. 20; extrapolation indicates that the correlation is very small for antennas spaced at the computed distance of 9.6λ.

Height-gain observations made early in the 49.8 Mc/s recording program at Sterling showed that the signal intensities as received on a Yagi antenna were not very sensitive to height over a range of heights from about 35 to about 80 feet indicating poor correlation between the Yagi antenna and its image in the ground. The diversity distance S_v for the Cedar Rapids to Sterling path is 11λ as computed for $\psi = \psi_m = 5.2$ degrees. In the distance-dependence tests, height-gain

[34] In these equations certain cosines have been set equal to unity because of the smallness of the angles.

comparisons at Homestead given in Table II for antennas at heights of 40 and 100 feet showed that the daytime signal intensities observed at a height of 100 feet were greater than those at 40 feet by 8½ decibels. For the path length 2,088 kilometers between Cedar Rapids and Homestead, ψ_e will be the limiting angle in determining cone width ψ. By using values for ψ_e from Fig. 51, for an 80 kilometer height, and making approximate allowances for the effects of the heights of the transmitting and receiving antennas, a cone width ψ_e of about 1.1 degrees is determined for this path, corresponding to a diversity distance S_v of about 1,030 feet. The spacing of 200 feet between the antenna and its image for the upper antenna height is substantially less than the computed diversity distance for this path. At night, however, the observed height gain between the 40 and 100-foot heights was 6½ db indicating a somewhat larger cone width ψ_e. This behavior might be anticipated on the basis of the higher observed heights during the night hours and the contributions from meteoric ionization which occur at the greater heights. Similar observations made at shorter distances during the Florida distance dependence tests showed lower height gains than those observed at Homestead, indicating greater effective values of ψ_e. The observed behavior in the experiments discussed above is thus seen to be in good qualitative agreement with the behavior predicted from diversity considerations.

The Significance of the Frequency and Angle-Dependence Results

In the light of the preceding discussion on the role of the antennas it is of interest to consider the extent to which the frequency and angle dependence measurements may be regarded as providing a basis for judging models of the scattering medium having frequency and angle dependence of the kinds discussed earlier. From the theory of Villars and Weisskopf, or from more elementary physical considerations, it is expected that the angle-dependence as expressed by an exponent of $1/\sin\gamma/2$ will vary with frequency and with conditions in the medium. The medium will scatter with a sharper polar diagram as the frequency is raised confining the downcoming waves at the receiving point to a smaller effective cone. Correspondingly the cone angle at the receiver will decrease with an increase in the effective frequency exponent at a fixed frequency. Thus, measurements of frequency dependence using scaled antennas will not accurately represent the frequency dependence characteristics of the scattering mechanism unless the antenna beamwidths are small relative to the beamwidths associated with the scattering mechanism. The beamwidths of the antennas used for the measurements were, in fact, comparable to the natural beamwidths of the scattering mechanism shown for the second beam swinging model and it would be expected that variations in the characteristics of the mechanism with frequency or with time at a given frequency would influence the measured values of n by no more than plus or minus 0.5. A more serious source of difficulty in interpreting the observations results from the existence of meteoric components having varying intensities relative to the scattered signal. In this connection, the relative behavior of the signal intensities at Sterling and at Carysbrook, suggests that for several hours during the afternoon period, the contributions from meteoric ionization are small in comparison with the scattered components. The frequency dependence observations made during this portion of the day are therefore thought to provide a fairly reliable estimate of the frequency dependence of the scattering mechanism. Correspondingly, the observations made during the early morning hours particularly during the winter months can probably be used to provide a reasonably good estimate of an effective frequency dependence of the integrated signal intensities produced by reflections from meteoric ionization for the experimental arrangements. Considering the various uncertainties including experimental errors associated with the observations and the interpretation of the observations it is thought that the effective exponent n representing frequency dependence of the scattering mechanism is being measured to within about twenty per cent when selected data are used.

The interpretation of the angle-dependence observations is similarly beset with difficulties. First, a relatively small systematic error is introduced by the finite beamwidths of the antennas since the scattering angle γ increases on either side of the midpoint in the scattering region. Thus the effective γ would be expected to be somewhat greater than the midpoint value. Secondly, because of experimental difficulties associated with the measurements of pulse signal intensities over the shorter paths used for this experiment, it was not possible to make measurements except during periods of very high signal intensity and consequently only a limited quantity of data was obtained. On the other hand, the data were taken during periods considered to be relatively free from contamination by reflections from meteoric ionization. On the basis of the preceding discussion it is thought that the exponent n associated with the angle dependence of the scattering mechanism at 50 Mc/s was not greater than nine nor less than six, for the particular periods during which the measurements were made.

Part III. Design Considerations for Communication Applications

Introduction

Sufficient experience has been acquired with the propagation mechanism under study to permit an evaluation of some of the communications possibilities. Experience in the Arctic and middle latitudes has provided evidence of the utility of the propagation mechanism for communication purposes. With systems gains comparable to those used on the test paths, or somewhat

Declassified in Part - Sanitized Copy Approved for Release @ 50-Yr 2014/06/09 : CIA-RDP81-01043R003000180001-4

Declassified in Part - Sanitized Copy Approved for Release @ 50-Yr 2014/06/09 : CIA-RDP81-01043R003000180001-4

greater, and for somewhat lower frequencies, say from 30 to 40 Mc/s, multichannel radio-teletype operation can be realized with a very high degree of reliability. Under these circumstances, radiotelephone communications and transmission of facsimile are also feasible. In the Arctic the known characteristics with respect to magnetic disturbances are of particular value.

Useful Path Lengths

The most useful range of path lengths is from about 1,000 to 2,000 kilometers. Recent experience with the test path between Newfoundland and the Azores has indicated that, subject to the availability of high sites, overlooking the sea for example, path lengths as great as 2,300 kilometers may be used successfully. As discussed earlier in this paper, received signal intensity decreases rapidly with decreasing distance below 1,000 kilometers and for this reason path lengths shorter than about 1,000 kilometers are to be avoided.

Useful Range of Frequencies

The range of frequencies of greatest usefulness is from 25 to 60 Mc/s. Frequencies lower than 25 Mc/s, wherever used, will be subject to and will cause interference to a much greater degree as a result of normal and sporadic ionospheric propagation. The interference will be particularly serious in years of high solar activity, and will be influenced by diurnal, seasonal and geographical factors. Back scatter will be experienced, particularly in middle and low latitudes and in years of high solar activity.

In general, the lower frequencies in the range are less susceptible in high latitudes to the various difficulties described above. The lower frequencies in the range of 25 to 60 Mc/s have other inherent natural advantages. For fixed transmitter power and antenna directivities, use of the lower frequencies will result in greater signal-to-noise ratios, less interference from meteoric effects, and slower fading. Effects of SID's and polar blackouts, although more pronounced on the lower frequencies, will not affect the reliability of communications circuits operating in the lower portion of this range.

It should not be concluded that there is little use for frequencies as high as 50 or 60 Mc/s. In certain seasons, these higher frequencies may be of considerable value. If potential interference from regular-layer propagation and back scatter is to be practically eliminated, the higher frequencies must be used for applications requiring extreme reliability, even at the expense of higher transmitter power.

Bandwidths and Channel Separations

It seems unlikely for some time to come that systems will require bands greater than about 50 kc/s. In many instances substantially smaller bands will suffice. Because of problems associated with slopes of the pass bands in receiving equipment, which may arise during occurrence of very strong signals, it is probably advisable to separate channels about 2 to 3 times the width of the nominally occupied bands. It is also necessary to allow for the effects of sporadic-E propagation, transient meteoric enhancements, and regular ionospheric propagation.

Transmitters and Receivers

In order to take full advantage of the propagational reliability of the mechanism it is important that transmitters of sufficiently high power be used and that the equipment employed at the path terminals be designed to provide a very high degree of reliability.

The transmitters and receivers should be capable of operating in the frequency range 25 to 60 Mc/s. For most applications there is no need to incorporate provisions for continuous "front-panel" frequency changing as large changes in frequency will almost always require careful tuning of new antenna arrangements and need only be provided for within the equipment itself. For some applications, involving low information rates, such as single-channel radio-teletype transmission, transmitter powers of the order of five kilowatts are likely to be found adequate at frequencies of the order of 35 Mc/s, particularly in the Arctic.

In the frequency range 25 to 60 Mc/s external noise will be the limiting factor in communications provided that the receivers have sufficiently low noise figures. A receiver noise figure of two can easily be realized and is adequate.

Multipath Limitations

Various types of multipath propagation have been observed in the experimental program. The most commonly observed multipath effect is produced by reflections from meteoric ionization in the ionospheric volume common to the transmitter and the receiver. Values of maximum multipath delays and corresponding azimuths have been computed from the common volume geometry illustrated in Fig. 50 for the longest and shortest geometrically possible ray paths and are plotted in Figs. 61 and 62. Multipath delays as great as the values derived from Fig. 61 for the shorter paths will be extremely rare since the probability of occurrence of meteor ionization becomes vanishingly small at the points where the tangent planes intersect at meteoric heights. Furthermore, the intensity and duration of received signals will be very low for reflections within the common volume but near the intersections of the tangent planes as a consequence of increased inverse distance attenuation, the decreased obliquity,[24] and the additional directivity discrimination at low angles of elevation resulting from interference between the direct and ground-reflected waves. Observations of such multipath delays were made using pulsed transmission on the 811 kilometer experimental path between Sterling, Va. and Bluffton, S. C. The results summarized

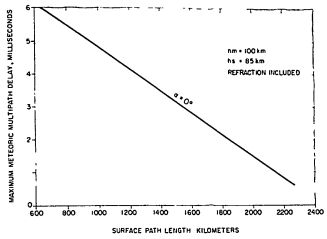

Fig. 61—Maximum meteoric multipath delays for antennas at zero height.

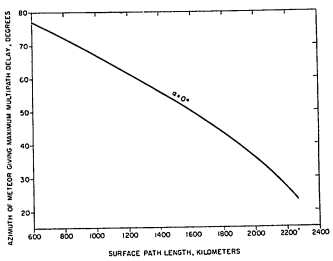

Fig. 62—Azimuth of meteor giving maximum multipath delay for antennas at zero height.

in Fig 63, were obtained from range-time oscillograms of the type shown in Fig. 15.

A second type of multipath effect, associated with sputter, is illustrated in Fig. 35. This type of multipath, characterized by rapid fading is of practical importance as the associated delays may be as much as several milliseconds. It occurs most frequently for paths crossing or near the zone of maximum auroral occurrence, where it may be expected to cause difficulty at times with antennas having typical directivity characteristics. These effects are illustrated by Figs. 35 and 36. Fig. 50 illustrates the common volume geometry associated with this type of multipath as well.

Other possible sources of multipath include off-path reflections from banks of sporadic-E ionization and from ground-scattered energy propagated by $F2$ or E-region reflection for several different types of multipath geometry. The delays associated with multipath arising from back scatter may be as great as 50 milliseconds or more and are potentially capable of seriously limiting the transmission speed. The harmful effects of back scatter may be reduced or eliminated by using antennas designed for suppression of the back lobes.

For transmission by ionospheric scattering, multipath from strong offpath reflections from meteoric ionization is, during its existence, a factor reducing the available radio path bandwidth. The antennas which have been used in the experimental program do not have sufficiently low radiation in the minor lobes, as compared with the main beam, to provide adequate suppression of the off-path meteoric components. Considering the preceding discussion in conjunction with the experimental observations, it seems reasonable to expect that multipath components having delays exceeding half a millisecond will occasionally occur with sufficient intensity to introduce transmission errors on the shorter paths. However, the available radio path bandwidth, as estimated from the reciprocal of the delay, for these shorter paths is greater than 2 kc/s for a large percentage of the time. For the intermediate and longer path lengths the available bandwidths will be

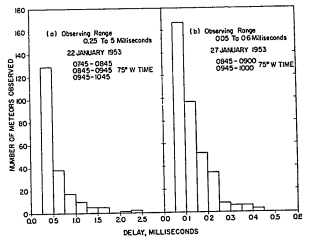

Fig. 63—Distribution of observed meteoric multipath delays observed at Bluffton at 49.7 Mc/s for a transmission path of 811 km from Sterling.

somewhat greater but still largely determined by the minor lobes of the antennas and the reflecting properties of the ground.

With antennas of improved directivity, multipath associated with meteoric ionization will no longer be a problem and the radio path bandwidth will be limited by the antenna beamwidths or the natural beamwidth associated with the scattering process. While the subject of wide-band transmission at vhf by ionospheric scattering has not been extensively analyzed, it is of interest to estimate the inherent bandwidth limitation imposed by the scattering mechanism. Values of generalized q computed for the Cedar Rapids to Sterling path are presented in Figs. 46 and 47. Multipath delays have been derived from the ray paths associated with the ionospheric midpoint and positions in the common volume corresponding to the half power values of q, assuming $n=6$ and the use of an omnidirectional transmitting antenna. With these idealizations, the maximum delay is 21 microseconds and is associated with ψ_m. The available path bandwidth for the assumed conditions is 48 kc/s. For practical situations, the effect

Declassified in Part - Sanitized Copy Approved for Release @ 50-Yr 2014/06/09 : CIA-RDP81-01043R003000180001-4

Declassified in Part - Sanitized Copy Approved for Release @ 50-Yr 2014/06/09 : CIA-RDP81-01043R003000180001-4

of ground reflection will usually be such that the delays associated with ϕ will be greater than those associated with ψ. Assuming sharply beamed antennas ϕ_m is limiting and the delay is 9 microseconds. This corresponds to an available path bandwidth of 110 kc/s. If the transmitting and receiving antenna beamwidths are smaller than bandwidths of the scattering mechanism, still greater bandwidths are in principle available.

Antennas

With the results of the experimental program (Part I) and the discussion of the role of the antennas (Part II), together with the multipath considerations given above, it is possible to establish the characteristics of antenna systems for use in communication applications. For purposes of discussion, Table VI indicates certain desirable characteristics without regard to whether antennas having such characteristics are at present practicable.

TABLE VI
Desirable Antenna Characteristics

Horizontal beamwidth	8 degrees or less
Vertical beamwidth including ground effects	6 degrees or less
Maximum radiation in any minor lobe	At least 40 decibels below radiation in the maximum of the main beam
Radiation efficiency; i.e., ratio of total power radiated to antenna input power	90 per cent or greater
Horizontal orientation of beam	Normally on great-circle bearing between transmitter and receiver
Vertical orientation of beam	85 kilometers above midpoint of great-circle path
Provision for reducing directivity or for varying direction of the beam	For use during periods when scattering is not homogeneous and during periods when scattering from meteoric components will provide higher signal-to-noise ratios
Bandwidth over which characteristics are to be maintained	200 kc/s

Although most of the above set of characteristics are self-explanatory some additional comments are indicated. When a low noise-figure receiver is employed, somewhat lower radiation efficiencies for receiving antennas can be tolerated since the available noise power from galactic sources is much higher than that resulting from internal noise generated in the receiver. For the longer paths, increased vertical directivity is necessary in order to utilize effectively the reduced common scattering volumes. From the common volume point of view, horizontal beamwidths smaller than 8 degrees will not be required for any except the very longest paths. The suggested techniques for varying directivity or for orienting the main beam in directions other than the great circle-bearing have not been tested under operational conditions and a determination of the practical effectiveness of this scheme will require further study and trial. It remains to be seen to what extent antennas having characteristics approaching those envisaged above will find their way into practice.

The use of spaced-antenna receiving diversity is definitely desirable for good communications. From the spaced-antenna observations of envelope correlation between spaced antennas, and from the diversity-distance considerations discussed in Part II, it is concluded that for effective diversity action the component of spacing transverse to the path should not be less than about 10 wavelengths.

The effects of the scattering mechanism with regard to the polarization of the transmitted waves have been considered earlier and it was shown that the scattering losses are somewhat less for horizontal than for vertical polarization. Horizontal polarization is generally to be preferred for additional reasons associated with the reflection characteristics of the ground.[14]

Practical Antenna Siting

A corollary to the observed failure to realize, for a large fraction of the time, antenna gains comparable to the plane-wave gains, is that the additional gain resulting from ground reflection will not be fully realized, even though ideal sites are employed at the transmitter and receiver. The reason for this was discussed in Part II in connection with vertical diversity spacing. Nevertheless there are demonstrable advantages in siting the antennas with respect to a ground surface so that the plane-wave ground-reflection lobe patterns are well formed. In fact, if either antenna is poorly sited, the beams may only partially intersect in the height region where scattering occurs.

For the idealized beam-swinging models discussed in Part II two limiting cases were considered with respect to the transmitting antenna patterns. They were an omnidirectional antenna and an extremely directive antenna. The generalized q-curves representing Case I geometry, in which the effective scattering volume is displaced toward one terminal, are shown in Fig. 46 as a function of α_R. In practice the directivity of the transmitting antenna is intermediate between the two extremes. It is therefore anticipated that slightly greater signal intensities will result if the transmitting and receiving beams are directed toward a point in the scattering stratum slightly displaced in the manner above provided appropriately different directivities are employed at the terminals. While unsymmetrical operation of this kind, employing negligibly increased scattering angles, would represent no disadvantage, it is nevertheless recommended in practice that antenna beams be designed to have their principal lobes directed toward the path midpoint in the ionosphere. The recommended ionospheric height for antenna design and corresponding site selection is 85 kilometers.

Some exceptions to this design recommendation can be made with advantage for paths longer than about 2,200 kilometers. For such extreme path lengths some increase in received signal intensity is likely to be realized with antennas having practical vertical free-space directivities if use is made of heights greater than required to direct the first ground-reflection lobe at the path midpoint in the ionosphere. As the antenna heights increase, ψ_e increases with the increasing depression of the radio horizons. As a consequence the total power radiated into the common volume is increased. Thus, for very long paths greater heights should be used wherever practicable and especially at one terminal if height limitations exist at the other terminal. The design heights indicated for lobe alignment at the path midpoint in the ionosphere should be regarded for paths of extreme length as minimum rather than optimum.

The curves of Fig. 11 show the vertical angle of arrival or departure for various ionospheric midpoint heights as a function of the surface distance between the transmitter and the receiver. They have been found useful in connection with antenna design and siting problems. The values given by these curves have been calculated for elevations near sea level for the assumed condition of no lower atmosphere and for representative radio-wave refraction in mid-latitudes. Some remarks concerning the general applicability of the curves are indicated. First, the refraction corrections decrease with elevation of the terminal above sea level. Secondly, in warm, humid regions, such as many tropical locations, the increase in angle of arrival over that for the case of no lower atmosphere may be about $1\frac{1}{4}$ times the values shown. Thirdly, in polar regions, particularly under winter conditions when the absolute humidity is very low, the increase in angle over that for the case of no lower atmosphere may be only about two-thirds of the values of increase shown. Lastly, the corrections for angles below about one or two degrees may, as a practical matter, be extremely variable, particularly if conditions conducive to superrefraction occur.

In siting an antenna intended to function effectively for small angles of arrival and departure, it is insufficient merely to provide a suitable site on which to perform the construction. Nor is it sufficient simply to have an unobstructed horizon in the desired azimuth for the desired angle of departure or arrival. When the angle of departure or arrival is small, the ground for a considerable distance in front of the antenna plays a critical role in formation of the lobe pattern. The problem of ground-reflection lobes and general requirements for a smooth first Fresnel zone has been given considerable study, particularly with respect to the ground radar siting problem. For the purposes of the following discussion it is assumed that the lowest lobe will be effectively formed when the terrain in front of the antenna is flat and smooth over an area no smaller than the first Fresnel zone. Horizontal polarization only is considered so that lobe formation is not complicated by large variations in the ground-reflection coefficient over the range of angles of interest. Mathematically, the antenna is assumed to be at a point and the ground-reflected wave is assumed to have the same amplitude as the incident wave but to undergo a 180-degree phase change at reflection.

The first Fresnel zone is defined, with the aid of Fig. 64, as the area of ground, assumed smooth and plane, in front of the point antenna A from within which

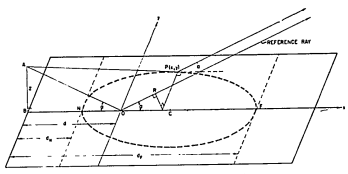

Fig. 64—Geometry of first Fresnel zone.

all secondary wavelets, according to Huygens' principle, contributing to a plane-wave front advancing in the direction of the positive x-axis with an inclination upward of α, differ in phase by 180 degrees or less from a reference ray, obeying strict geometric optics. The origin of the coordinates, O, is situated at the ground-reflection point for the reference ray.

For alignment of the maximum of the first ground-reflection lobe at an angle of elevation α, it is necessary for the point antenna A to be at a height, z, given previously by (43), as follows:

$$z = \frac{\lambda}{4 \sin \alpha},$$

where λ is the wavelength. The distance from the antenna base at B to the geometric ground-reflection point is given by:

$$d = \frac{z}{\tan \alpha}. \tag{44}$$

Now let $P(x, y)$ be a general point obeying the conditions defining the boundary of the first Fresnel zone, so that

$$AP - (AO + OR) = \frac{\lambda}{2}, \tag{45}$$

where R is the point along the reference ray at which the phase comparison is made with the wavelet originating at P.

By using (43) to eliminate λ in (45) and expressing AP, AO, and OR as functions of h, α, and the coordinates x and y, the locus of P is found, after some simplification, to be:

Declassified in Part - Sanitized Copy Approved for Release @ 50-Yr 2014/06/09 : CIA-RDP81-01043R003000180001-4

Declassified in Part - Sanitized Copy Approved for Release @ 50-Yr 2014/06/09 : CIA-RDP81-01043R003000180001-4

$$\frac{\left(x-\frac{2z}{\tan\alpha}\right)^2}{\frac{8z^2}{\sin^2\alpha}}+\frac{y^2}{8z^2}=1. \quad (46)$$

This is seen to be the standard Cartesian form for an ellipse.

As a practical matter it is of interest to know the distance from the antenna base at B to the near edge of the first zone d_N, to the far edge d_F, and the maximum width w, or the minor axis, of the zone. These distances, increased suitably for the finite dimensions of a practical antenna, determine the extent and location of the ground in front of the antenna which must be flat and free of obstructions for effective lobe formation. From (46) when $y=0$,

$$x=\frac{2z}{\tan\alpha}\left(1\pm\frac{\sqrt{2}}{\cos\alpha}\right), \quad (47)$$

so that,

$$d_N=\frac{z}{\tan\alpha}\left(3-\frac{2\sqrt{2}}{\cos\alpha}\right), \quad (48)$$

$$d_F=\frac{z}{\tan\alpha}\left(3+\frac{2\sqrt{2}}{\cos\alpha}\right), \quad (49)$$

and the maximum width of the zone is:

$$w=4\sqrt{2}z. \quad (50)$$

The effect of the curvature of the earth on the first Fresnel zone will be appreciable only if the angle of arrival or departure, α, is very small. The qualitative result of curvature is to cause the elliptical area to be reduced in size and to be altered into an egg shape elongated with the broad end near the antenna. The quantity d_N is almost unaltered, whereas d is somewhat reduced, and d_F is considerably reduced. The maximum width will be slightly reduced and will occur somewhat nearer the antenna. An additional effect of some practical importance is the reduction in the height, z, of the antenna required for the first lobe maximum to be formed at a specified angle α. For the plane-earth case this height was given by (43).

Curves of z and d have been derived, and are plotted in Figs. 65, 66, and 67 as a function of α for plane earth and for the curved earth, for three fixed values of λ corresponding to frequencies of 30, 40, and 50 Mc/s. Some compensation for the effects of tropospheric refraction has been introduced for curved-earth case. Fig. 68 (next page) gives values of d_F as a function of α for the three sample frequencies for a plane earth according to (49). When α is greater than two or three degrees the values for a curved earth will be smaller by a negligible amount.

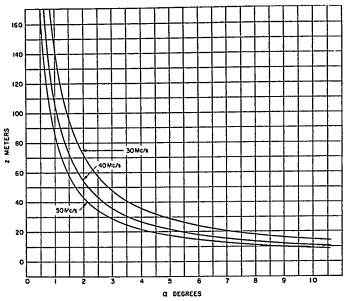

Fig. 65—Antenna heights for aligning first ground-reflection lobe maximum at indicated elevation angle, for horizontal polarization and a plane earth.

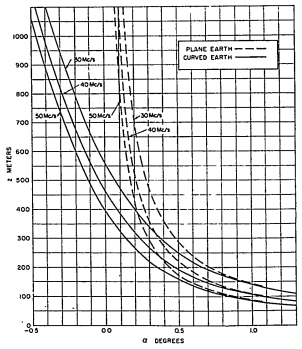

Fig. 66—Antenna heights for aligning first ground-reflection lobe maximum at indicated low elevation angle for horizontal polarization, for plane and curved earth.

When α is less than two or three degrees the curves shown give values of d_F substantially greater than the actual values for a curved earth, and provided they can be satisfied in practice no difficulties can be expected to result from their use.

It is of practical importance to know what sort of departures from the ideal first Fresnel zone may be tolerated. For a well-developed first ground-reflection lobe the entire first zone at least, should be flat, and the horizon from every part of it should subtend less than

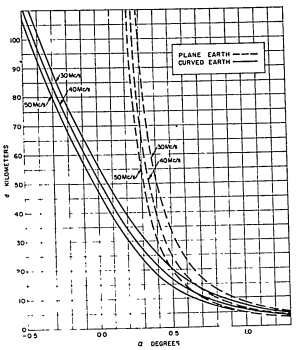

Fig. 67—Distance to ground-reflection point from antenna having first ground-reflection lobe maximum at indicated low elevation angle for horizontal polarization, for plane and curved path.

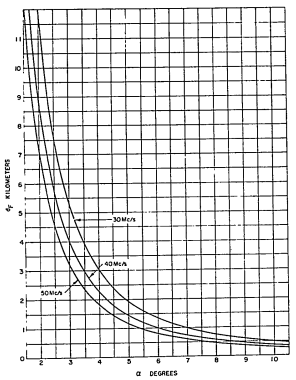

Fig. 68—Distance to far edge of first Fresnel zone from antenna having first ground-reflection lobe maximum at indicated elevation angle for horizontal polarization and plane earth.

the angle α. Norton and Omberg,[35] applying Rayleigh's criterion, state that irregularities in the terrain in the first zone should have a departure from ideal smoothness of not more than one-fourth of the antenna height. As a practical matter, water surfaces make excellent first Fresnel zones, particularly for small values of α.

The ray treatment leading to the results presented above for the curved earth should not be relied upon for values of α less than about 0 degree at which the horizon, for the heights involved, is actually below minus half a degree. For one thing the divergence factor begins to reduce the effectiveness of the ground-reflection in the formation of the lower lobes, though this may be offset by other considerations, as discussed for example by Burrows and Attwood.[36]

Modulation Techniques

In the development of systems utilizing vhf ionospheric propagation it is important that consideration be given to the special behavior characteristics of the received signals in order to realize a system capable of minimizing or eliminating the undesirable transmission effects produced by reflections from meteoric ionization and the fading and multipath characteristics of the normally received signals. Considerations of path geometry and meteor velocities indicate that the difference between the transmitted frequency and the Doppler frequencies should not be greater than about 6 kc/s for the Cedar Rapids to Sterling path at 49.8 Mc/s. This difference in frequency is, for a particular meteoric event, directly proportional to the transmitted frequency.

Estimated System Performance

A considerable body of signal intensity and noise intensity data has been acquired in the experimental program. It is possible, using these data, to estimate the expected reliability of a system employing a typical type of service such as single-channel radioteletype transmission. System reliability estimates are made for several assumed types of service.

Montgomery[37,38] has studied the behavior of several types of modulation for narrow-band transmission of binary-coded messages in the presence of fluctuation noise and has considered the effects of diversity action in the reception of narrow-band frequency-shift transmission. His results will be used for estimating ratios of average signal power to rms noise power required to establish a specified system performance for radiotele-

[35] K. A. Norton and A. C. Omberg, "The maximum range of a radar set," Proc. IRE, vol. 35, pp. 4–24; January, 1947.

[36] C. R. Burrows and S. S. Attwood (Eds.), "Radio Wave Propagation," Academic Press, Inc., New York, N. Y., pp. 80–81, 119–120; 1949.

[37] G. F. Montgomery, "A comparison of amplitude and angle modulation for narrow-band communication of binary-coded messages in fluctuation noise," Proc. IRE, vol. 42, pp. 447–454; February, 1954.

[38] G. F. Montgomery, "Message error in diversity frequency-shift reception," Proc. IRE, vol. 42, pp. 1184–1187; July, 1954.

Declassified in Part - Sanitized Copy Approved for Release @ 50-Yr 2014/06/09 : CIA-RDP81-01043R003000180001-4

Declassified in Part - Sanitized Copy Approved for Release @ 50-Yr 2014/06/09 : CIA-RDP81-01043R003000180001-4

type transmission. The required ratios of average signal power to rms noise power given by Montgomery for specified error probabilities are based on the use of ideal receivers. These ratios will be increased by three decibels as an allowance for the nonideal receivers used in practice. For the examples illustrating radioteletype operation it will be assumed that a binary error probability of 2×10^{-4}, corresponding approximately to a teletype character error probability of 10^{-3} for synchronous radio-teletype transmission, will provide a satisfactory service.

Fig. 69 presents distributions of the values of the ratios of hourly median signal intensity to rms noise power in a 2 kc/s band observed on three experimental

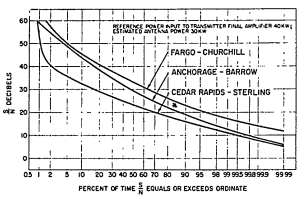
REFERENCE POWER INPUT TO TRANSMITTER FINAL AMPLIFIER 40 KW;
ESTIMATED ANTENNA POWER 30 KW
FARGO – CHURCHILL
ANCHORAGE – BARROW
CEDAR RAPIDS – STERLING
S/N DECIBELS
60
50
40
30
20
10
0
0.5 1 2 5 10 20 30 40 50 60 70 80 90 95 98 99 995 998 999 9999
PERCENT OF TIME S/N EQUALS OR EXCEEDS ORDINATE

Fig. 69—Cumulative distributions of the ratios of hourly median signal intensity to rms background galactic noise observed at about 50 Mc/s in a 2 kc/s noise band for the year from October, 1951 through September, 1952.

paths over a 12-month period. Fig. 19 may be used for estimating systems performance at other frequencies. The assumption will be made that the distributions of the ratios of hourly median signal intensities to noise intensities in a 2 kc/s noise band correspond to the actual distributions of the ratios of average signal power to rms noise power in a 2 kc/s band. This assumption is not expected materially to affect the results, as measurements have indicated small differences between the recorded signal intensities and the rms signal power.

For the first example, an estimate is made of the expected reliability for synchronous single-channel frequency-shift radioteletype operation over the Cedar Rapids to Sterling path at 49.8 Mc/s using dual spaced-antenna diversity and suitable dual-filter receivers arranged for elimination of meteor Doppler errors. In this example, the bandwidth of each of the filters is assumed to be 100 cycles per second.

Required ratio of average signal power to rms noise power (Fig. 6 of ref. 37)	+34 db
Allowance for use of nonideal receivers	+ 3 db
Allowance for diversity gain (Fig. 2 of ref. 38)	−14 db
Allowance for bandwidth ratio (2 kc/s to 0.1 kc/s)	−13 db
Required ratio of average signal power to noise power in a 2 kc/s band	+10 db
Expected propagational reliability (Fig. 69)	99.5 per cent.

For the second example, an estimate is made for synchronous four-channel, time-division, radioteletype operation with dual, spaced-antenna diversity at a frequency of 49.7 Mc/s, using the Fargo–Churchill path. Each of the dual filters in the receivers is assumed to have a bandwidth of 400 cycles. Following the procedure used in the preceding example it is found that the required ratio of average signal power to rms noise power in a 2 kc/s band is 16 decibels. From Fig. 9 a value of 99.6 per cent is obtained for the estimated reliability.

Finally, an estimate is made for the expected reliability using narrow-band frequency modulation radiotelephony on the Fargo to Churchill path at 49.7 Mc/s. Dual, spaced-antenna diversity reception is assumed. It is also a value of 14 decibels for the ratio of hourly median signal intensities to rms noise power in a 2 kc/s band is required for satisfactory radiotelephone service. Reference to Fig. 69 gives a value of 99.9 per cent for the estimated propagational reliability.

Some additional comments are in order with respect to the above derived estimates of propagational reliability. As discussed previously, the controlling noise is usually of galactic origin. There are, however, periods when other kinds of noise, such as atmospherics from local thunderstorms or from thunderstorms located within the beam of the receiving antenna and within optical range, precipitation noise, and man-made noise, have to be reckoned with. No allowances have been made for the effects of noise sources other than galactic and the above estimates are probably optimistic by several tenths of a per cent. Outages resulting from the effects of sputter on paths crossing or near the zone of maximum auroral occurrence are estimated to reduce the reliability by no more than half a per cent. Furthermore other sources of outage, such as equipment failures, power failures, and shutdowns for maintenance are likely to be greater than those resulting from insufficient signal-to-noise ratios. Assuming that outages caused by these and related factors do not exceed three per cent, a systems reliability of about 96 per cent or greater should be realized for the types of service considered in the above examples.

Acknowledgment

It is desired to acknowledge the valuable contributions made by our colleagues at the National Bureau of Standards, and in particular the parts played by V. C. Pineo in the experimental program, and K. W. Sullivan in the observational program. The following organizations have made important contributions to this work. The Massachusetts Institute of Technology, the Rand Corporation, the Collins Radio Company, Engineering Experiment Station of North Dakota Agricultural College, E. C. Page Consulting Radio Engineers, and the Department of Defense.

Declassified in Part - Sanitized Copy Approved for Release @ 50-Yr 2014/06/09 : CIA-RDP81-01043R003000180001-4

Declassified in Part - Sanitized Copy Approved for Release @ 50-Yr 2014/06/09 : CIA-RDP81-01043R003000180001-4

U. S. DEPARTMENT OF COMMERCE
Sinclair Weeks, *Secretary*

NATIONAL BUREAU OF STANDARDS
A. V. Astin, *Director*

THE NATIONAL BUREAU OF STANDARDS

The scope of the scientific program of the National Bureau of Standards at laboratory centers in Washington, D. C., and Boulder, Colorado, is given in the following outline:

Washington, D.C.

Electricity and Electronics. Resistance and Reactance. Electron Devices. Electrical Instruments. Magnetic Measurements. Dielectrics. Engineering Electronics. Electronic Instrumentation. Electrochemistry.

Optics and Metrology. Photometry and Colorimetry. Optical Instruments. Photographic Technology. Length. Engineering Metrology.

Heat. Temperature Physics. Thermodynamics. Cryogenic Physics. Rheology. Engine Fuels. Free Radicals.

Atomic and Radiation Physics. Spectroscopy. Radiometry. Mass Spectrometry. Solid State Physics. Electron Physics. Atomic Physics. Neutron Physics. Nuclear Physics. Radioactivity. X-rays. Betatron. Nucleonic Instrumentation. Radiological Equipment. AEC Radiation Instruments.

Chemistry. Organic Coatings. Surface Chemistry. Organic Chemistry. Analytical Chemistry. Inorganic Chemistry. Electrodeposition. Molecular Structure and Properties. Physical Chemistry. Thermochemistry. Spectrochemistry. Pure Substances.

Mechanics. Sound. Mechanical Instruments. Fluid Mechanics. Engineering Mechanics. Mass and Scale. Capacity, Density, and Fluid Meters. Combustion Controls.

Organic and Fibrous Materials. Rubber. Textiles. Paper. Leather. Testing and Specifications. Polymer Structure. Plastics. Dental Research.

Metallurgy. Thermal Metallurgy. Chemical Metallurgy. Mechanical Metallurgy. Corrosion. Metal Physics.

Mineral Products. Engineering Ceramics. Glass. Refractories. Enameled Metals. Concreting Materials. Constitution and Microstructure.

Building Technology. Structural Engineering. Fire Protection. Air Conditioning, Heating, and Refrigeration. Floor, Roof, and Wall Coverings. Codes and Safety Standards. Heat Transfer.

Applied Mathematics. Numerical Analysis. Computation. Statistical Engineering. Mathematical Physics.

Data Processing Systems. SEAC Engineering Group. Components and Techniques. Digital Circuitry. Digital Systems. Analogue Systems. Application Engineering.

- Office of Basic Instrumentation
- Office of Weights and Measures

Boulder, Colorado
BOULDER LABORATORIES
F. W. Brown, *Director*

Cryogenic Engineering. Cryogenic Equipment. Cryogenic Processes. Properties of Materials. Gas Liquefaction.

Radio Propagation Physics. Upper Atmosphere Research. Ionosphere Research. Regular Propagation Services. Sun-Earth Relationships. VHF Research. Ionospheric Communications Systems.

Radio Propagation Engineering. Data Reduction Instrumentation. Modulation Systems. Navigation Systems. , Radio Noise. Tropospheric Measurements. Tropospheric Analysis. Radio Systems Application Engineering.

Radio Standards. High Frequency Electrical Standards. Radio Broadcast Service. High Frequency Impedance Standards. Electronic Calibration Center. Microwave Physics. Microwave Circuit Standards.

USCOMM-NBS-DL

Declassified in Part - Sanitized Copy Approved for Release @ 50-Yr 2014/06/09 : CIA-RDP81-01043R003000180001-4

Declassified in Part - Sanitized Copy Approved for Release @ 50-Yr 2014/06/09 : CIA-RDP81-01043R003000180001-4

Department of Commerce
National Bureau of Standards
Boulder Laboratories
Boulder, Colorado

Official Business

NBS

Postage and Fees Paid
U. S. Department of Commerce

Declassified in Part - Sanitized Copy Approved for Release @ 50-Yr 2014/06/09 : CIA-RDP81-01043R003000180001-4